OBSERVATOIRE DE PARIS

SYSTÈMES DE RÉFÉRENCE TEMPS-ESPACE
UMR8630 / CNRS

The Celestial Reference Frame for the Future

Vers un futur repère de référence céleste

JOURNÉES 2007 ☆

SYSTÈMES DE RÉFÉRENCE SPATIO - TEMPORELS

☆ PARIS, 17-19 SEPTEMBER

OBSERVATOIRE DE PARIS

SYSTÈMES DE RÉFÉRENCE TEMPS-ESPACE

UMR8630 / CNRS

61 avenue de l'Observatoire, F-75014 Paris
FRANCE

The Celestial Reference Frame for the Future

Vers un futur repère de référence céleste

Actes publiés par
Edited by
N. CAPITAINE

JOURNÉES 2007 ☆

SYSTÈMES DE RÉFÉRENCE SPATIO - TEMPORELS

☆ PARIS, 17-19 SEPTEMBER

ISBN 978-2-901057-59-8

TABLE OF CONTENTS

PREFACE

The Journées 2007 "Systèmes de référence spatio-temporels", with the sub-title "The Celestial Reference Frame for the Future", have been held from 17 to 19 September 2007 at Paris Observatory on its Meudon site. These Journées were the eighteenth conference in this series organized in Paris each year from 1988 to 1992 and then alternately, since 1994, in Paris (in 1996, 1998, 2000 and 2004) and other European cities, namely Warsaw in 1995 and 2005, Prague in 1997, Dresden in 1999, Brussels in 2001, Bucharest in 2002, St. Petersburg in 2003 and again Warsaw in 2005.

For organizing the Journées 2007, we have received financial supports from the Scientific Council of Paris Observatory, the French Ministry of Education and Research, the European "Descartes-nutation" project and the town of Meudon; we are grateful to these bodies or institutions for their support and we also thank the mayor of Meudon for his kind reception at the "Orangerie du Château" of the ancient Palace of Meudon.

The Journées 2007 were focused on the issues related to the recent developments, perspectives of future realizations and scientific applications of the celestial reference frame. There have been presentations and discussions related to the new Division 1 Commission 52 "Relativity in Fundamental astronomy", IAU Working Groups on "Numerical standards in Fundamental astronomy" and "The second realization of the ICRF" that have been established at the 26th IAU GA, and the IERS Working Groups on "The second realization of the ICRF" (joint IERS/IVS WG) and "Prediction". The recent evolution in the concepts, terminology, models and results in fundamental astronomy have been discussed, as well as topics related to the geophysical excitation of Earth rotation. There has been a special session dedicated to nutation in relation both with the "Descartes nutation" project and the 30-year anniversary of the IAU Colloquium No 78 on "Nutation and the Earth's rotation" that was organized in Kiev in 1977. In addition, a session have been devoted to various aspects relative to prediction of the Earth Orientation.

The Journées 2007 were organized in conjunction with the IERS Workshop on Conventions, that have been held on 20-21 September 2007 at BIPM (Sèvres, France).

There were 106 participants from 26 different countries.

The scientific programme of the meeting included 7 invited papers, 37 oral communications and 30 posters. It was composed of the four following sessions:

- Session I: Plans for the new ICRF
- Session II: Models and Numerical standards in Fundamental astronomy
- Session III: Relativity in Fundamental astronomy
- Session IV: Prediction, combination and geophysical interpretation of Earth Orientation Parameters

These Proceedings are divided into four sections corresponding to the sessions of the meeting. The Table of Contents is given on pages iii to v, the list of participants on pages vii and viii and the scientific programme on pages ix to xii. The Postface on page 231 gives the announcement for the "Journées" 2008 that will be held in Dresden on 22-24 September 2008.

I am very grateful to the Scientific Organizing Committee for its valuable contribution to the elaboration of the scientific programme and to all the authors of the papers for their valuable contributions. On behalf of the SOC, I thank the Local Organizing Committee and its Chair, Daniel Gambis, for the very efficient work before and during the meeting. I am also grateful to O. Becker for his efficient technical help for the publication.

Nicole CAPITAINE
Chair of the SOC

April 2008

List of Participants

ALTAMIMI Zuheir, *LAREG, IGN, France*, altamimi@ensg.ign.fr
ANDREI Alexandre Humberto, *Observatorio Nacional/MCT, Brasil*, oat1@on.br
BARACHE Christophe, *SYRTE, Observatoire de Paris, France*, christophe.barache@obspm.fr
BIZOUARD Christian, *SYRTE, Observatoire de Paris, France*, christian.bizouard@obspm.fr
BOBOLTZ David, *U.S. Naval Observatory, USA*, dboboltz@usno.navy.mil
BOEHM Johannes, *Vienna University of Technology, Austria*, johannes.boehm@tuwien.ac.at
BOLOTIN Sergei, *Main Astr. Observ., National Academy of Sciences, Ukraine*, bolotin@mao.kiev.ua
BOLOTINA Olga, *Main Astr. Observ., National Academy of Sciences, Ukraine*, olga@mao.kiev.ua
BOUQUILLON Sébastien, *SYRTE, Observatoire de Paris, France*, sebastien.bouquillon@obspm.fr
BOURDA Geraldine, *Observatoire de Bordeaux, France*, geraldine.bourda@obs.u-bordeaux1.fr
BRZEZINSKI Aleksander, *Space Research Centre, Polish Academy of Sciences, Poland*, alek@cbk.waw.pl
CAPITAINE Nicole, *SYRTE, Observatoire de Paris, France*, n.capitaine@obspm.fr
CHAPANOV Yavor, *Central Laboratory for Geodesy, Bulgaria*, astro@bas.bg
CHARLOT Patrick, *Observatoire de Bordeaux, France*, charlot@obs.u-bordeaux1.fr
COLLILIEUX Xavier, *LAREG, IGN, France*, xavier.collilieux@ensg.ign.fr
DAMLJANOVIC Goran, *Astronomical Observatory, Serbia*, gdamljanovic@aob.bg.ac.yu
DE VIRON Olivier, *IPGP/Paris 7, France*, deviron@ipgp.jussieu.fr
DÉBARBAT Suzanne, *SYRTE, Observatoire de Paris, France*, suzanne.debarbat@obspm.fr
DEFRAIGNE Pascale, *Observatoire Royal de Belgique, Belgium*, p.defraigne@oma.be
DEHANT Véronique, *Observatoire Royal de Belgique, Belgium*, vronique.dehant@oma.be
DELEFLIE Florent, *OCA/GEMINI-GRGS, France*, florent.deleflie@obs-azur.fr
DERMANIS Athanasios, *Aristotle University of Thessaloniki, Greece*, dermanis@topo.auth.gr
DIMARCQ Noël, *SYRTE, Observatoire de Paris, France*, noel.dimarcq@obspm.fr
EFROIMSKY Michael, *U.S. Naval Observatory, USA*, me@usno.navy.mil
ENGLICH Sigrid, *Institute of Geodesy and Geophysics, Austria*, senglich@mars.hg.tuwien.ac.at
ESCAPA Alberto, *Dpto. Matemática Aplicada. Escuela Politécnica Superior, Spain*, alberto.escapa@ua.es
FEY Alan, *U.S. Naval Observatory, USA*, afey@usno.navy.mil
FIENGA Agnes, *Observatoire de Besancon, France*, agnes@obs-besancon.fr
FOLGUEIRA Marta, *Instituto de Astronomia y Geodesia, Spain*, martafl@mat.ucm.es
FRANCOU Gerard, *SYRTE, Observatoire de Paris, France*, gerard.francou@obspm.fr
GAMBIS Daniel, *SYRTE, Observatoire de Paris, France*, daniel.gambis@obspm.fr
GAUME Ralph, *U.S. Naval Observatory, USA*, rgaume@usno.navy.mil
GONTIER Anne-Marie, *SYRTE, Observatoire de Paris, France*, anne-marie.gontier@obspm.fr
GROSS Richard, *Jet Propulsion Laboratory, USA*, richard.gross@jpl.nasa.gov
GUINOT Bernard, *SYRTE, Observatoire de Paris, France*, guinot.bernard@wanadoo.fr
HESTROFFER Daniel, *IMCCE, Observatoire de Paris, France*, hestro@imcce.fr
HILTON James, *U.S. Naval Observatory, USA*, jhilton@usno.navy.mil
HOHENKERK Catherine, *UK Hydrographic Office, United Kingdom*, catherine.hohenkerk@ukho.gov.uk
JOHNSON Thomas, *National Geospatial-Intelligence Agency, USA*, thomas.j.johnson@nga.mil
KALARUS Maciej, *Space Research Centre, PAS, Poland*, kalma@cbk.waw.pl
KLIONER Sergei, *Lohrmann-Observatory, TU Dresden, Germany*, sergei.klioner@tu-dresden.de
KLUEGEL Thomas, *BKG, Wettzell, Germany*, thomas.kluegel@bkg.bund.de
KOLACZEK Barbara, *Space Research Centre, Polish Academy of Sciences, Poland*, kolaczek@cbk.waw.pl
KOOT Laurence, *Observatoire Royal de Belgique, Belgium*, laurence.koot@oma.be
KORBACZ Anna, *Space Research Centre, PAS, Poland*, akorbacz@cbk.waw.pl
KOSEK Wieslaw, *Space Research Centre, Polish Academy of Sciences, Poland*, kosek@cbk.waw.pl
KOVALEVSKY Jean, *OCA, France*, jean.kovalevsky@obs-azur.fr
KRYNSKI Jan, *Institute of Geodesy and Cartography, Poland*, krynski@igik.edu.pl
KUDRYASHOVA Maria, *Astronomical Institute of St. Petersburg University, Russia*, kudryashova@astro.spbu.ru
KUDRYAVTSEV Sergey, *Sternberg Astronomical Institute of Moscow State University, Russia*, ksm@sai.msu.ru
KURDUBOV Sergey, *Institute of Applied Astronomy of Russian Academy of Science, Russia*, ksl@quasar.ipa.nw.ru
LAMBERT Sébastien, *SYRTE, Observatoire de Paris, France*, sebastien.lambert@obspm.fr

LANOTTE Roberto, *Telespazio, Italy*, roberto.lanotte@asi.it
LASKAR Jacques, *IMCCE, Observatoire de Paris, France*, laskar@imcce.fr
LUZUM Brian, *U.S. Naval Observatory, USA*, bjl@maia.usno.navy.mil
MA Chopo, *Goddard Space Flight Center, USA*, cma@gemini.gsfc.nasa.gov
MANCHE Hervé, *IMCCE, Observatoire de Paris, France*, manche@imcce.fr
MARCO Francisco j., *Universidad Jaume I, Spain*, marco@mat.uji.es
MARTINEZ Maria j., *Universidad Politecnica de Valencia, Spain*, mjmartin@mat.upv.es
MASAKI Yoshimitsu, *Geographical Survey Institute, Japan*, ymasaki@gsi.go.jp
MCCARTHY Dennis, *U. S. Naval Observatory, USA*, dennis_mccart57@hotmail.com
MORCOV George, *Faculty of Geodesy Bucharest, Romania*, georgemorcov@yahoo.com
NASTULA Jolanta, *Space Research Centre, Polish Academy of Sciences, Poland*, nastula@cbk.waw.pl
NIEDZIELSKI Tomasz, *Space Research Centre, Polish Academy of Sciences, Poland*, niedzielski@cbk.waw.pl
NIELL Arthur, *MIT Haystack Observatory, USA*, aniell@haystack.mit.edu
NOTHNAGEL Axel, *Institut of Geodesy and Geoinformation, Bonn, Germany*, nothnagel@uni-bonn.de
PASHKEVICH Vladimir, *Central (Pulkovo) Astronomical Observatory, RAS, Russia*, pashvladvit@yandex.ru
PAVLIS Erricos c., *JCET/UMBC and NASA Goddard, USA*, epavlis@umbc.edu
PETIT Gérard, *BIPM, France*, gpetit@bipm.org
PETRACHENKO William, *Natural Resources Canada, Canada*, bill.petrachenko@nrc.gc.ca
PETROV Leonid, *NVI, Inc./NASA GSFC, USA*, leonid.petrov@lpetrov.net
PITJEVA Elena, *Institute of Applied Astronomy of Russian Academy of Science, Russia*, evp@ipa.nw.ru
POLLET Arnaud, *LAREG, IGN, France*, pollet@ensg.ign.fr
POUTANEN Markku, *Finnish Geodetic Institute, Finland*, markku.poutanen@fgi.fi
RICHARD Jean-Yves, *SYRTE, Observatoire de Paris, France*, jean-yves.richard@obspm.fr
ROGOWSKI Jerzy, *Institute of Geodesy and Geodetic Astronomy, Poland*, jbr@gik.pw.edu.pl
RON Cyril, *Astronomical Institute, Czech Republic*, ron@ig.cas.cz
RZESZOTKO Alicja, *Space Research Centre, Polish Academy of Sciences, Poland*, alicja@cbk.waw.pl
SALSTEIN David, *Atmospheric and Environmental Research, USA*, salstein@aer.com
SCHUH Harald, *University of Technology, Vienna, Austria*, harald.schuh@tuwien.ac.at
SEOANE Lucia, *SYRTE, Observatoire de Paris, France*, lucia.seoane@obspm.fr
SKURIKHINA Elena, *Institute of Applied Astronomy of Russian Academy of Science, Russia*, sea@quasar.ipa.nw.ru
SOFFEL Michael, *Lohrmann-Observatory, TU Dresden, Germany*, soffel@rcs.urz.tu-dresden.de
SOHN Bong won, *KVN/KASI, South Korea*, bwsohn@kasi.re.kr
SOKOLOVA Julia, *Central (Pulkovo) Astronomical Observatory, RAS, Russia*, jrs@mars.hg.tuwien.ac.at
SOUCHAY Jean, *SYRTE, Observatoire de Paris, France*, jean.souchay@obspm.fr
SPIRIDONOV Eugene, *Shmidt's Institute for Physics of the Earth, RAS, Moscow, Russia*, spiridonov@ifz.ru
STAMATAKOS Nicholas, *U.S. Naval Observatory, USA*, stamatakos.nick@usno.navy.mil
STEFKA Vojtech, *Astronomical Institute, Czech Republic*, stefka@ig.cas.cz
TEYSSANDIER Pierre, *SYRTE, Observatoire de Paris, France*, pierre.teyssandier@obspm.fr
THIBERGER Reuben, *Ben Gurion University, Beer Sheva, Israel*
TITOV Oleg, *Geoscience Australia, Australia*, oleg.titov@ga.gov.au
TUPIKOVA Irina, *Lohrmann-Observatory, TU Dresden, Germany*, irina.tupikova@googlemail.com
URAS Silvano, *Istituto Nazionale di Astrofisica, Italy*, uras@ca.astro.it
VAN DAM Tonie, *University of Luxembourg, Luxembourg*, tonie.vandam@uni.lu
VARGA Peter, *Geodetic and Geophysical Research Institut, Hungary*, varga@seismology.hu
VONDRAK Jan, *Astronomical Institute, Czech Republic*, vondrak@ig.cas.cz
WALLACE Patrick, *Rutherford Appleton Laboratory, United Kingdom*, p.t.wallace@rl.ac.uk
WANG Wen-jun, *School of Surveying, Henan Polytechnic University, China*, wwj@asch.whigg.ac.cn
WEBER Robert, *University of Technology, Vienna, Austria*, rweber@mars.hg.tuwien.ac.at
WOODEN William, *U.S. Naval Observatory, USA*, wooden.william@usno.navy.mil
YAGUDINA Eleonora, *Institute of Applied Astronomy of Russian Academy of Science, Russia*, eiya@ipa.nw.ru
YATSKIV Yaroslav, *Main Astr. Observ., National Academy of Sciences, Ukraine*, yatskiv@mao.kiev.ua
ZACHARIAS Norbert, *U.S. Naval Observatory, USA*, nz@usno.navy.mil
ZACHARIAS Marion, *U.S. Naval Observatory, USA*,miz@usno.navy.mil
ZERHOUNI Wassila, *SYRTE, Observatoire de Paris, France*, wassila.zerhouni@obspm.fr

SCIENTIFIC PROGRAMME

Scientific Organizing Commitee: A. Brzeziński, Poland, N. Capitaine, France (Chair), P. Defraigne, Belgium, T. Fukushima, Japan, D.D. McCarthy, USA, M. Soffel, Germany, J. Vondrák, Czech, R. Ya. Yatskiv, Ukraine

Local Organizing Commitee: D. Gambis (Chair), P. Baudoin, O. Becker, C. Bizouard, S. Bouquillon, L. Garin, A.-M. Gontier, S. Lambert, J. Souchay

Monday 17 September 2007, 9h00-13h00

Opening of the Journées 2007
Welcome from N. Dimarcq, Director of Department SYRTE of Paris Observatory
Introduction to the Journes 2007 by N. Capitaine (Chair of the SOC) and D. Gambis (Chair of the LOC)

Session I - Plans for the new ICRF
Chair: J. Vondrák, D.D. McCarthy

Ma, C.: *Progress in the 2nd realization of ICRF (Invited)*
Charlot, P. et al.: *Selecting ICRF-2 defining sources based on source structure*
Malkin, Z., Yatskiv, Ya.: *Next ICRF: Single global solution versus combination*
Boboltz, D., Fey, A. & K-Q VLBI Survey Collaboration: *Time Series Analysis of VLBI Astrometric Source Positions at 24-GHz*
Titov, O.: *Reference radio source apparent proper motions*
Bolotin S.: *Influence of different strategies in VLBI data analysis on realizations of ICRF*
Sokolova, J.: *Effect of the reference radio source selection on VLBI CRF realization*
Zacharias, N. et al.: *Extragalactic Optical-Radio Link Research at USNO*
Andrei, A. et al.: *A GAIA oriented analysis of a large sample of quasars*
Bourda, G. et al.: *A VLBI survey of weak extragalactic radio sources for the link with the future GAIA frame*

Monday 17 September 2007, 14h00-18h30

Session II - Models and Numerical standards in Fundamental astronomy
Chair: N. Capitaine

Luzum, B. et al.: *Current Status of the IAU Working Group Numerical Standards of Fundamental Astronomy (Invited)*
Soffel, M., Klioner, S.: *On astronomical constants (Invited)*

Short review of posters *by A.-M. Gontier, J. Souchay, S. Lambert*

Discussion on the 2nd realization of the ICRF and the numerical standards
Chair: B. Luzum, C. Ma, N. Capitaine

POSTER SESSION

Tuesday 18 September 2007, morning, 9h00-13h00

Session II - Models and Numerical standards in Fundamental astronomy (continuation)
Chair: M. Soffel

Capitaine, N.: *Recent progress in concepts, nomenclature and models in fundamental astronomy*
Pitjeva, E.: *Recent models of the planet motion and fundamental constants determined from position observations of planets and spacecraft*
Laskar, J. et al.: *INPOP06. A new numerical planetary ephemeris*
Manche, H. et al.: *INPOP: Adjustments to LLR data*
Hilton, J.: *Prospects for Improving the Masses of Asteroids*
Kudryavtsev, S.: *Harmonic models of tide-generating potential of terrestrial planets*

Session II - Sub-session on nutation
Chair: A. Brzezinski

Dehant, V. et al.: *Recent advances in modeling precession-nutation (Invited)*
Yatskiv, Ya., Korsun, A.: *IAU Symposium 78 "Nutation and the Earth's rotation" (held in Kiev,May 1977)as a first step in the consideration concerning the Non-rigid Earth Nutation Theory"*
Koot, L. et al.: *Estimation of Earth interior parameters from a Bayesian inversion of nutation time series*
Vondrák, J., Ron, C.: *VLBI observations of nutation, its geophysical excitations and determination of some Earth model parameters*
Petrov, L.: *About observability of the free core nutation*
Lambert, S., Dehant, V., Gontier, A.-M.: *Some issues in the Earth's interior exploration with VLBI*
Wallace, P., Capitaine, N.: *Concise algorithms for precession-nutation*

Tuesday 18 September 2007, 14h30-17h45

Session III - Relativity in Fundamental astronomy
Chair: V. Dehant

Klioner, S.: *Relativity in Fundamental Astronomy: solved and unsolved problems (Invited)*
Hestroffer, D. et al.: *Local tests of GR and dynamical reference frame linking with Gaia astrometry of asteroids*
Pashkevich, V., Eroshkin, G.: *Geodetic relativistic rotation of the solar system bodies*
Klioner, S., Soffel, M., Le Poncin-Lafitte, Ch.: *Towards the relativistic theory of precession and nutation*

Session IV - Prediction, combination and geophysical interpretation of Earth Orientation Parameters
Chair: Ya. Yatskiv

Wooden, W.: *Activities of the IERS Working Group on Prediction (Invited)*
Altamimi, Z., Gambis, D., Bizouard, Ch.: *Rigorous combination to ensure ITRF and EOP consistency (Invited)*
Kosek W., Kalarus, M., Niedzielski, T.: *Forecasting of the Earth orientation parameters - comparison of different techniques*
Kalarus, M., Kosek, W., Schuh, H.: *Current results of the Earth Orientation Parameters Prediction Comparison Campaign*

Wednesday 19 September 2007, 9h00-13h00

Session IV - Prediction, combination and geophysical interpretation of Earth Orientation Parameters (continuation)
Chair: H. Schuh, P. Defraigne

Stamatakos, N., Luzum, B., Wodden, W.: *Recent Improvements at the IERS Rapid Service/Prediction Center*
Nothnagel, A. et al.: *GGOS-D: A German Project on the Integration of Space Geodetic Techniques*
Stefka, V., Pesek, I., Vondrák, J.: *Three years solution of EOP by combination of results of different space techniques*
Kluegel, T. et al.: *Advances in inertial Earth rotation measurement - new data from the Wettzell 'G' ring laser*
Pavlis, E.: *ILRS contributions to near-real time EOP series*
Salstein, D. et al.: *Atmospheric excitation of Earth rotation/polar motion at high temporal resolution*
Brzezinski, A.: *On the influence of diurnal atmospheric tides on Earth rotation*
Englich, S., Weber, R., Schuh, H.: *Empirical validation of the conventional model for l.o.d. variations due to zonal Earth tides*
Korbacz, A., Brzezinski, A., Thomas, M.: *Geophysical excitation of LOD/UT1 estimated from the output of the global circulation models of the atmosphere - ERA-40 reanalysis and of the ocean - OMCT*
Kudryashova, M.: *Geophysical excitation of diurnal prograde polar motion derived from different OAM and AAM data*
Seoane, L., Bizouard, Ch., Gambis, D.: *Coherence of satellite gravimetric observations with the polar motion*

Discussion on the prediction of the EOPs
Chair: W. Wooden

Closing of the Journées 2007

LIST OF POSTERS

SESSION I

Fey, A., Boboltz, D.: *Analysis of Astrometric Position Time Series for ICRF-2*
Gontier, A.-M., Lambert, S.: *Selection of stable radio sources to define a new ICRF*
Kurdubov, S., Skurikhina, E.: *Source positions time series generation and analysis*
Martinez, M., Marco F.J., Lopez J.A.: *Precessional parameters obtained from biased data of Hipparcos-FK5 proper motion*
Niell, A. & VLBI 2010 Committee: *VLBI2010: Progress towards the next generation geodetic VLBI system*
Petrachenko, W. et al.: *A Study of VLBI2010 Potential for Source Structure Corrections*
Yagudina, E.: *Connecting the dynamical frame to the ICRF by use of NEA's observations and the historical phenomenon of "fictitious equinox motion"*
Sohn, B.W.: *Korean VLBI Network and its plan for VLBI metrology*

SESSION II

Damljanovic, G.: *Better proper motions accuracy for stars with Hipparcos satellite and ground-based observations*
Dermanis, A. Tsoulis, D.: *On the consistent definition of EOPs in relation to the observed ITRF-ICRF transformation*
Escapa, A., Getino, J., Ferrándiz J.-M.: *Geopotential of a triaxial Earth with rigid inner core in Andoyer canonical variables*
Folgueira, M., Dehant, V.: *Estimation of the topographic torque at the core-mantle boundary on the nutation*
Marco, F.J., Martinez, M.J., Lopez, J.A.: *Considerations about some problems on functional parametrical models implementation from a discrete set of data*
Pashkevich, V.: *Non-rigid Earth rotation series*
Tupikova, I.: *Analytical theory for an asteroid in the gravitational field of a migrating planet*
Zerhouni W., Capitaine, N., Francou, G.: *The use of LLR observations (1969-2006) for the determination of the GCRS coordinates of the pole*

SESSION IV

Bolotina, O.: *Combination of different space geodetic techniques: algorithm of parameters estimation*
Chapanov, Ya., Gambis D.: *Correlation between the solar activity cycles and the Earth rotation;*
Chapanov Ya., Ron C., Vondrák, J.: *Estimation of the short-term zonal tides from UT1 observations*
Gambis, D., Richard, J.-Y., Salstein, D.: *Use of Atmospheric Angular Momentum forecasts for UT1 predictions*
Masaki, Y.: *Meteorological interpretation of transient LOD changes*
Morcov G.: *The polar motion and the draconitic period*
Nastula, J., Kolaczek, B., Salstein, D.: *Comparison of hydrological and GRACE-based excitation functions of polar motion in the seasonal spectral band*
Niedzielski, T., Kosek W.: *Forecasting irregular variations of UT1-UTC and LOD data caused by ENSO*
Poutanen M. et al.: *Status report on the Fennoscandian-Japanese project for near real-time UT1-observations with e-VLBI*
Rzeszotko, A., Kosek, W., Popinski, W.: *The influence of variable amplitudes and phases of the most energetic oscillations in the EOP on their prediction errors*
Spiridonov, E., Tsurkis E., Vinogradonova, O.: *Estimation of coefficients of differential equation modeling the polar motion*
van Dam, T., Gross, R., de Viron, O.: *The impact on EOP predictions of AAM forecasts from the ECMWF and NCEP*
Varga, P. et al.: *Correspondence of EOP and geomagnetic field*
Wang, W.J. et al.: *Frequency Modulation Solution of Earth Rotation*

Session I

PLANS FOR THE NEW ICRF

PROJETS POUR UN NOUVEL ICRF

PROGRESS IN THE 2ND REALIZATION OF ICRF

C. MA[1]
[1] Goddard Space Flight Center
Code 698.0
8800 Greenbelt Road, Greenbelt, Maryland, 20771, USA
e-mail: Chopo.Ma@nasa.gov

ABSTRACT. The ICRF derived from VLBI observations of extragalactic radio sources up to 1995.6 and effective since 1998.0 was a radical change from the FK5 stellar/equinox celestial system. The number of geodetic/astrometric VLBI observations has since tripled and the number of radio sources with astrometrically useful data has quadrupled. A systematic program for monitoring astrometric sources has been established although the available observing capability limits this to only a fraction of all such sources. Advances in modeling, generation of source position times series, and greater availability of source structure information will permit the identification of better "defining" sources. The VLBA Calibrator Survey will provide a large number of additional sources although most are observed at only one epoch. Working groups have been established by the IAU, IERS and IVS with the goal of presenting the second realization of the ICRF at the IAU General Assembly in 2009.

1. INTRODUCTION

The ICRF (International Celestial Reference Frame) was adopted by the IAU in 1997 and became the formal basis for celestial positions from 1 January 1998. The ICRF catalogue was derived from VLBI data and analysis available in mid-1995. The catalogue was extended in ICRF-Ext.2 (Fey et al. 2004) using data through 2002, and the positions of the non-defining sources were improved. See figure 1. The axes of the frame were left unchanged since the positions of the 212 defining sources were retained. Since 2002 the data set and analysis have improved considerably, and several steps have been taken towards the second realization of the ICRF.

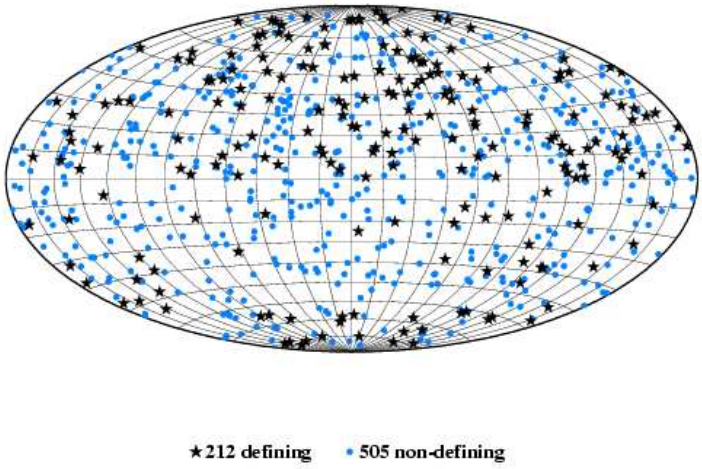

Figure 1: ICRF Ext.2 Sources

2. DATA CONSIDERATIONS

The balance of the global VLBI observing program for geodesy and astrometry has always been heavily weighted towards geodesy, in large part because the geodetic parameters such as EOP (Earth Orientation Parameters) and station positions are constantly changing and require regular monitoring. The radio sources observed for these purposes have changed over time and were selected for being relatively strong, compact, and well distributed at the particular time. However, since geodetic observing sessions generally now use only 50 to 60 sources (the earliest sessions used fewer than 20 very strong sources), the geodetic catalogue has only ∼100 sources, a small fraction of the sources with useful astrometric positions. The geodetic sources do have many epochs of observation, some extending more than 20 years. The geodetic catalogue does not include many defining sources (see Figure 2), and some geodetic sources do not have stable positions according to the analysis by Feissel-Vernier (2003). (See Figure 3). In order to improve the data for the ICRF, a CRF monitoring program was begun in 2004 to observe stable, potential stable, and defining sources at least semi-annually. (See Figure 4). This goal has generally been met for the defining sources. (See Figure 5).

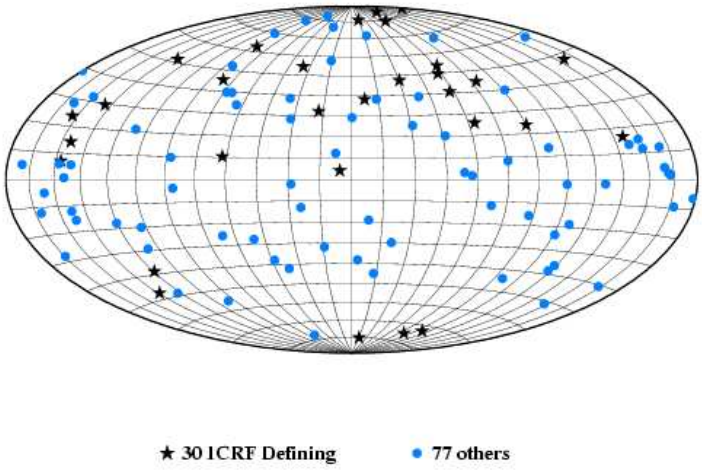

Figure 2: Geodetic sources.

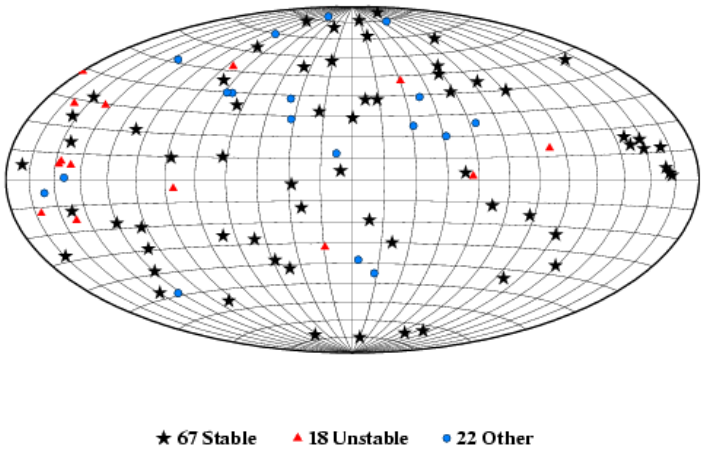

Figure 3: Geodetic source stability.

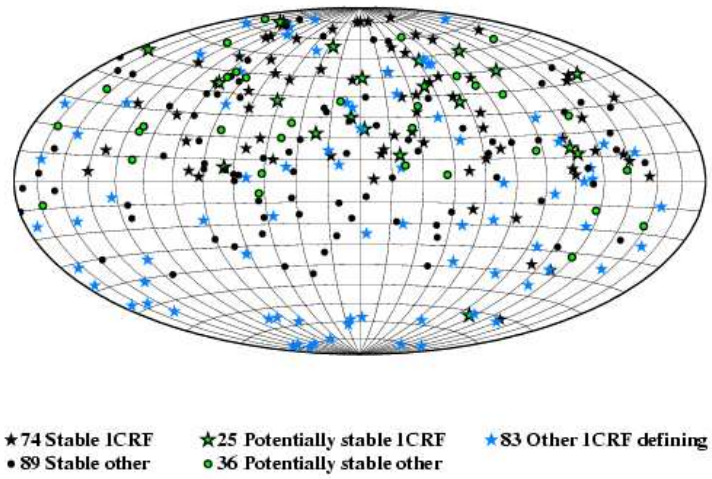

Figure 4: Total CRF monitoring sources.

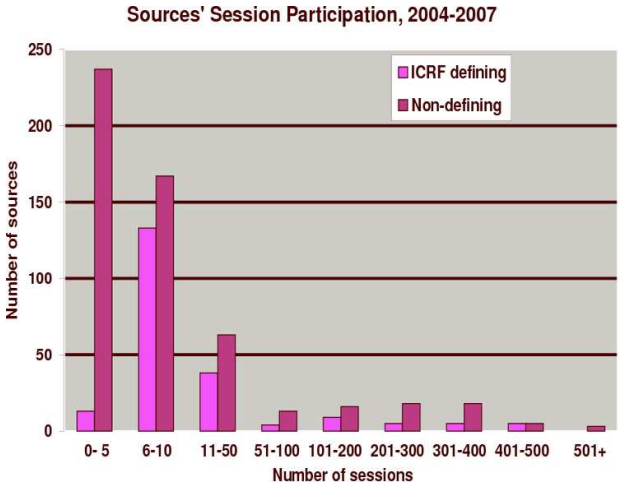

Figure 5: Sources' session participation, 2004—2007.

3. GENERATION OF SOURCE POSITION TIME SERIES

Although radio sources observed for geodesy and astrometry are relatively compact, they are not ideal points. All sources have some degree of structure, which is astrometrically benign if radially symmetric. However, there is clear evidence that some source positions can vary with time at the level of precision achieved with VLBI while others are quite stable. (See Figure 6). The generation and analysis of position time series is therefore an important factor for the analysis of the next realization of the ICRF.

As part of the work of the IERS/IVS working group for the second realization of the ICRF, several VLBI analysis centers have generated source position time series. (See Table 1). Different strategies were used to decide how a source position was defined or estimated at a particular epic, what sources, if any, were adjusted as global parameters, i.e., a single position averaged over the entire data set, and how the reference frame was established. It is impossible to estimate the position of every source in a given session without some type of constraint. For most analyses, some set of sources was estimated globally. Then the position of each of the remaining sources was estimated in the sessions in which it appeared. Alternatively for a single session all positions were estimated with no-net-rotation and no-net-translation conditions. The choice of globally adjusted sources had two variations, either only stable sources or some fraction of all sources chosen for uniform sky distribution. To get time series for all sources it is necessary to treat globally adjusted sources in one solution as non-global sources in another solution. The reference frame for time series was set by the ICRF defining sources or by a set of sources with stable positions.

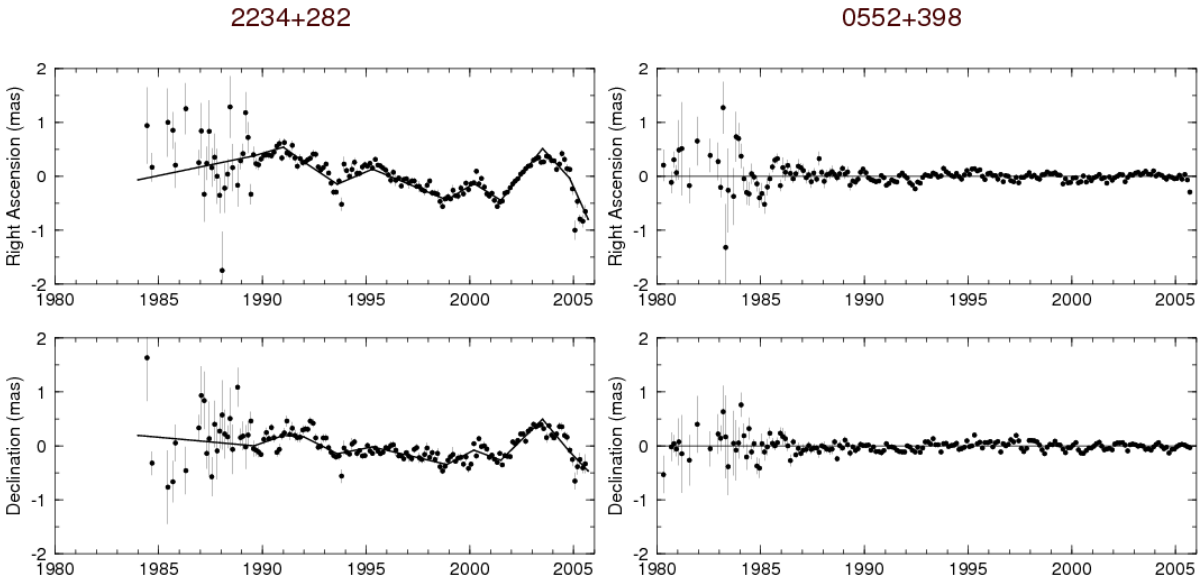

Figure 6: Examples of sources with unstable (left) vs. stable (right) positions.

Table 1: Centers that generated source position time series.

Geoscience Australia
Paris Observatory
BKG (Germany)
DGFI (Germany)
Institute of Applied Astronomy (Russia)
Main Astronomical Observatory (Ukraine)
Goddard Space Flight Center (USA)
U. S. Naval Observatory

Another variable factor was the choice of data. Some series were generated using all data from 1979-2007 while others restricted the data by date (as earlier data are not as good for various reasons) or by minimum network size or number of observations per source in a single session.

4. ANALYSIS OF TIME SERIES

Work has begun in comparing the time series to determine how to generate series that best characterize the actual variability of source positions given the extreme heterogeneity of the overall data set.

The time series will provide basic information to guide analysis for the next ICRF. On one hand, time series will be used to decide which sources have so high a level of systematic or random position variation that they should not be treated as having a single value over the entire time span of the data. On the other hand, defining sources must have small position variations. There are several factors that complicate the analysis. First, there is a wide range of the number of epochs in the time series but only the small number of geodetic sources have dense time series. This disparity is somewhat mitigated by the CRF monitoring program since 2004, but this interval is only a small fraction of the overall time span. Second, the observing sessions are irregularly spaced in time, so measures that require even spacing such as Allan variance are difficult to apply. Third, the quality of the data varies with source declination, a reflection of the dearth of observing stations and time in the southern hemisphere.

Consequently the visual and statistical tests that are applicable to the geodetic sources will need to be carefully adapted to the majority of sources with many fewer points. Likewise the criteria for selecting the defining sources may need to be modified, particularly in mid-southern declinations, in order to have a sufficient number in all parts of the sky.

5. ISSUES FOR THE SECOND RADIO ICRF

The most important point is to improve the selection of defining sources based on time series analysis and supplemented by source structure information. On the other extreme estimating variable positions for some sources should be refined over the method used in the first ICRF in order to extract the most information for the ICRF and for other parameters estimated simultaneously including EOP and TRF. The geophysical and astronomical modeling has improved significantly in the last decade, particularly for the troposphere. These improvements must be included in the ICRF analysis. The effects of station-dependent correlated errors and elevation-dependent errors on CRF parameters need to be studied. Since the intrinsic data quality has improved in terms of instrumental sensitivity and network geometry over time, it may be better to discard some early or small network data that are particularly noisy. However, a significant part of the data for the south is from single baseline or small network sessions, so judicious data selection will be required. Finally it must be decided how the final ICRF catalogue will be derived, e.g., a single solution or a rigorous combination.

6. REFERENCES

Feissel-Vernier, M., 2003, "Selecting Stable Extragalactic Compact Radio Sources from the Permanent Astrogeodetic VLBI Program", A&A , 403, pp. 105–110.

Fey, A.L., Ma, C., Arias, E.F., Charlot, P., Feissel-Vernier, M., Gontier, A.-M., Jacobs, C.S., Li, J., MacMillan, D.S., 2004, "The Second Extension of the International Celestial Reference Frame: ICRF-Ext.2", AJ , 127, pp. 3587–3608.

SELECTING DEFINING SOURCES FOR THE NEXT ICRF BASED ON SOURCE STRUCTURE

P. CHARLOT[1], A. L. FEY[2], A. COLLIOUD[1], R. OJHA[2], D. A. BOBOLTZ[2], J. I. B. CAMARGO[3]
[1] Laboratoire d'Astrophysique de Bordeaux, Université Bordeaux 1 – CNRS
BP 89, 33270 Floirac, France
e-mail: charlot@obs.u-bordeaux1.fr, collioud@obs.u-bordeaux1.fr
[2] U.S. Naval Observatory
3450 Massachusetts Ave., NW, Washington, DC 20392-5420, USA
e-mail: afey@usno.navy.mil, rojha@usno.navy.mil, dboboltz@usno.navy.mil
[3] Observatorio do Valongo, Universidade Federal do Rio de Janeiro
Ladeira do Pedro Antônio, 43, Rio de Janeiro, RJ, Brazil
e-mail: camargo@ov.ufrj.br

ABSTRACT. The intrinsic radio structure of the extragalactic sources is one of the limiting errors in the definition of the International Celestial Reference Frame (ICRF). This paper reports about the ongoing work to monitor the structural evolution of the ICRF sources by using the Very Long Baseline Array and other VLBI telescopes around the world. Based on more than 5000 VLBI images produced from such observations, we have assessed the astrometric suitability of 80% of the ICRF sources. The number of VLBI images for a given source varies from 1 for the least-observed sources to more than 20 for the intensively-observed sources. From this analysis, we identify a subset of 194 sources that are highly compact at any of the available epochs. Such sources are prime candidates to define the next ICRF with the highest accuracy.

1. INTRODUCTION

The International Celestial Reference Frame (ICRF), which has been the official IAU celestial reference frame in use since 1 January 1998, is currently based on the VLBI positions of 717 extragalactic radio sources. Of these, 608 sources are from the original ICRF built in 1995, with a categorization that comprised 212 well-observed *defining* sources (which served to orient the axes of the frame), 294 less-observed *candidate* sources, and 102 *other* sources showing coordinate instabilities (Ma et al. 1998). The accuracy in the individual ICRF source positions has a floor of 250 μas, while the axes of the frame are stable to about 20 μas in orientation. Since then the positions have been improved for the non-defining sources and the frame has been extended by 109 *new* sources in ICRF-Ext.1 and ICRF-Ext.2 using additional data acquired in the period 1995–2002 (Fey et al. 2004).

At the IAU XXVI$^{\rm th}$ General Assembly in Prague (August 2006), the community decided to engage in the realization of the successor of the ICRF, to be presented at the next IAU General Assembly in 2009. The motivation for generating this new celestial frame is to benefit from recent improvements in VLBI modeling (e.g. for the troposphere) and to take advantage of the wealth of VLBI data that have been acquired since 1995 when the ICRF was built. A major issue to be addressed in this new realization is the revision of the source categorization, in particular the choice of the defining sources. Such a revision is necessary because some of the original ICRF defining sources were found to have extended structures (Fey and Charlot 2000) or position instabilities (e.g. MacMillan 2006), and are therefore improper for defining the celestial frame with the highest accuracy.

The selection criteria that are considered by the working group in charge of the realization of the next ICRF for the identification of proper defining sources are based either on source structure information (VLBI images), to evaluate the compactness and astrometric suitability of the sources, or on time series of source coordinates, to assess the source position stability. In this paper, we discuss only the former. There are now more than 5000 VLBI images available to evaluate source quality, while there were less than a hundred at the time the ICRF was built, thereby permitting considerable progress. In Sect. 2, we present the observational data and analysis method used in this work. Our results are discussed in Sect. 3 with emphasis on statistics of source quality for each ICRF source category and for the entire ICRF. We

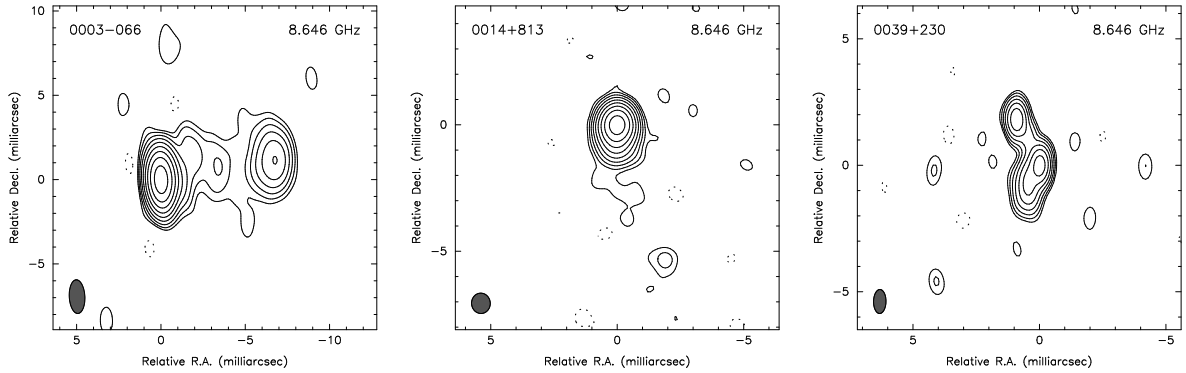

Figure 1: VLBI images at X band (8 GHz) for three ICRF sources (0003−066, 0014+813, 0039+230) as derived from the data of a RDV session conducted on 2003 December 17. The three sources were selected randomly according to increasing right ascension starting at RA=00h.

also draw prospects for further improvements in assessing the source quality before the next ICRF is generated.

2. OBSERVATIONAL DATA AND ANALYSIS METHOD

The VLBI maps used in our analysis were produced from a total of 38 VLBI sessions conducted between 1994 and 2007, which were imaged either at USNO or at Bordeaux Observatory. These comprise:

- 8 dedicated dual-frequency (8 GHz/2 GHz) imaging sessions conducted with the Very Long Baseline Array (VLBA) between July 1994 and January 1997 (Fey et al. 1996, Fey and Charlot 1997, Fey and Charlot 2000);
- 23 dual-frequency (8 GHz/2 GHz) Research & Development VLBA (RDV) sessions conducted between January 1997 and June 2007; these sessions include the 10 VLBA stations and up to 10 additional geodetic telescopes;
- 5 dedicated southern-hemisphere 8 GHz imaging sessions conducted between July 2002 and April 2004 with the Australian Long Baseline Array, augmented by radio telescopes in South-Africa, Hawaii, and Japan (Ojha et al. 2004, Ojha et al. 2005);
- 2 VLBA sessions at 2 GHz/8 GHz/24 GHz and 8 GHz/24 GHz conducted in February 2004 and August 2005 as part of a project to extend the ICRF to higher frequencies (Lanyi et al. 2007).

Altogether, this represents a total of 2697 maps at X band (8 GHz) from 577 ICRF sources and 2388 maps at S band (2 GHz) from 492 ICRF sources. Less sources have been imaged at S band because the southern-hemisphere sessions only observed at X band. There are up to 28 VLBI epochs available for the most intensively-observed source, whereas only one epoch is available for the least-observed sources. A sample of X-band VLBI images for three ICRF sources, as derived from the data of a RDV session conducted in December 2003, is shown in Fig. 1. From these images, one sees that only one of the three sources (0014+813) is relatively compact, while the two others (0003−066 and 0039+230) show extended structures. This fraction of compact sources is consistent with that found for the entire ICRF, as discussed in Sect. 3 below.

Based on these VLBI images, we derived the expected effects of intrinsic source structure on the VLBI delay astrometric quantities, following the algorithm of Charlot (1990). We then used the "structure index" indicator to define the astrometric source quality, as devised by Fey and Charlot (1997). Structure index values of 1 and 2 point to excellent and good astrometric suitability, respectively, while values of 3 and 4 point to poor suitability. A given source may have differing structure indices at X band and S band, depending on properties of the brightness distribution at each band. The structure index may also vary with time because of possible temporal evolution of the brightness distribution.

For each source, we obtained a series of structure index at each band according to the number of VLBI images available (see Charlot et al. 2006 for examples of such structure index series). Adopting a

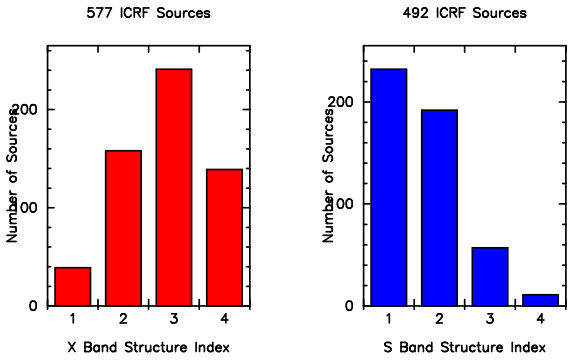

Figure 2: The structure index distribution at X band (8 GHz) and S band (2 GHz) for all ICRF sources that have a structure index available at these frequencies.

conservative approach, we chose the maximum value of the structure index as the source quality indicator when multi-epoch structure indices are available. In other words, if a source shows a structure index value of 3 or 4 at one or more epochs, it should be regarded as unsuitable for highly-accurate astrometry even though it has structure index values of 1 or 2 at some other epochs. This multi-epoch structure index value is the criterion used below for drawing statistics on source quality.

3. RESULTS

As noted above, we have now obtained structure indices for 577 sources at X band and 492 sources at S band (representing 80% and 69% of the current 717 sources of the ICRF, respectively). The X-band structure index distribution (Fig. 2) shows that 197 sources (or equivalently a portion of 34% of the sources) are astrometrically-suitable at this frequency according to our criterion (structure index value of either 1 or 2). At S band, 86% of the sources have a structure index value of either 1 or 2 (Fig. 2). This indicates that the contribution of the S-band structure to the dual-frequency (S/X) calibrated delay is usually smaller compared to the X-band structure contribution, as already noted in Fey and Charlot (1997). Comparing the X- and S-band structure indices individually for each source shows that, with three exceptions, all sources that have a S-band structure index of either 3 or 4 have also a X-band structure index of 3 or 4. Based on the S-band structure index indicator, we thus exclude an additional 3 sources, thereby leaving a total of 194 ICRF sources astrometrically-suitable at both frequencies.

In Fig. 3, the X-band structure index distribution is compared for each ICRF source category. As expected, the distribution is somewhat better for the defining sources than for the candidate and "other" sources. However, only about 40% of the ICRF defining sources have a structure index value of either 1 or 2. The fraction of suitable sources drops down to 32% for the candidate sources and 22% for the "other" sources, while it is 48% for the "new" sources. Overall, these results confirm that revision of source categories is mandatory for the next ICRF.

4. CONCLUSION

We have evaluated the astrometric suitability of 80% of the sources in the ICRF based on multi-epoch VLBI maps of their structures. From this analysis, a sample of 194 astrometrically-suitable ICRF sources that have compact or very compact structures according to our "structure index" indicator has been identified. It is anticipated that the remaining 20% of ICRF sources for which the astrometric suitability has not been assessed (mostly in the southern sky) will be imaged in the near future through further VLBI observing programs in the southern hemisphere. The astrometric suitability of the sources already imaged, which has been discussed in this paper, will also be refined as new VLBI sessions are processed and maps become available. This information will be essential for selecting the proper defining sources and generating the next ICRF by 2009.

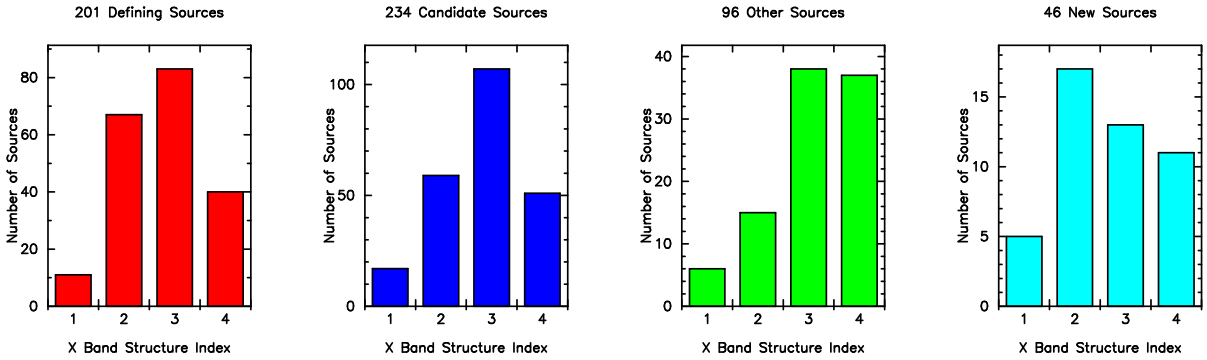

Figure 3: Distribution of the X-band (8 GHz) structure indices in each ICRF source category (defining, candidate, "other", "new"). The 577 ICRF sources with currently available structure indices are included in this figure.

5. REFERENCES

Charlot, P., 1990, "Radio-Source Structure in Astrometric and Geodetic Very Long Baseline Interferometry", AJ 99, pp. 1309–1326.

Charlot, P., Fey, A. L., Ojha, R., Boboltz, D. A., 2006, "Astrometric Suitability of ICRF Sources Based on Intrinsic VLBI Structure", in: International VLBI Service for Geodesy and Astrometry 2006 General Meeting Proceedings, Eds. D. Behrend and K. D. Baver, NASA/CP-2006-214140, pp. 321–325.

Fey, A. L., Clegg, A. W., Fomalont, E. B., 1996, "VLBA Observations of Radio Reference Frame Sources. I.", ApJS 105, pp. 299–330.

Fey, A. L., Charlot, P., 1997, "VLBA Observations of Radio Reference Frame Sources. II. Astrometric Suitability Based on Observed Structure", ApJS 111, pp. 95–142.

Fey, A. L., Charlot, P., 2000, "VLBA Observations of Radio Reference Frame Sources. III. Astrometric Suitability of an Additional 225 Sources", ApJS 128, pp. 17–83.

Fey, A. L., Ma, C., Arias, E. F., Charlot, P., Feissel-Vernier, M., Gontier, A.-M., Jacobs, C. S., Li, J., MacMillan, D. S., 2004, "The Second Extension of the International Celestial Reference Frame: ICRF-EXT.2", AJ 127, pp. 3587–3608.

Lanyi, G. E., Jacobs, C. S., Naudet, C. J., Zhang, L. D., Boboltz, D. A., Fey, A. L., Charlot, P., Fomalont, E. B., Geldzahler, B., Gordon, D., Ma, C., Romney, J. E., Sovers, O. J., 2007, "The Celestial Reference Frame at Higher Radio Frequencies: Astrometry from VLBA Observations at 24 and 43 GHz", AJ (in preparation)

Ma, C., Arias, E. F., Eubanks, T. M., Fey, A. L., Gontier, A.-M., Jacobs, C. S., Sovers, O. J., Archinal, B. A., Charlot, P., 1998, "The International Celestial Reference Frame as Realized by Very Long Baseline Interferometry", AJ 116, pp. 516–546.

MacMillan, D. S., 2006, "Radio Source Instability in the Analysis of VLBI Data", in: International VLBI Service for Geodesy and Astrometry 2006 General Meeting Proceedings, Eds. D. Behrend and K. D. Baver, NASA/CP-2006-214140, pp. 274–278.

Ojha, R., Fey, A. L., Johnston, K. J., Jauncey, D. L., Reynolds, J. E., Tzioumis, A. K., Quick, J. F. H., Nicolson, G. D., Ellingsen, S. P., Doodson, R. G., McCulloch, P. M., 2004, "VLBI Observations of Southern Hemisphere ICRF Sources. I.", AJ 127, pp. 3609–3621.

Ojha, R., Fey, A. L., Charlot, P., Jauncey, D. L., Johnston, K. J., Reynolds, J. E., Tzioumis, A. K., Quick, J. F. H., Nicolson, G. D., Ellingsen, S. P., McCulloch, P. M., Koyama, Y., 2005, "VLBI Observations of Southern Hemisphere ICRF Sources. II. Astrometric Suitability Based on Intrinsic Structure", AJ 130, pp. 2529–2540.

TIME SERIES ANALYSIS OF VLBI ASTROMETRIC SOURCE POSITIONS AT 24-GHZ

D.A. BOBOLTZ[1], A.L. FEY[1] & The K-Q VLBI Survey Collaboration
[1] U.S. Naval Observatory
3450 Massachusetts Ave., NW, Washington, DC, 20392-5420, USA
e-mail: dboboltz@usno.navy.mil, afey@usno.navy.mil

ABSTRACT. To date there have been 10 VLBI experiments observed over a period spanning 5 years and analyzed for the purpose of establishing a high-frequency (24 GHz) reference frame. The database now contains information on 274 sources and a total of 1052 images. From the data, we have produced a high-frequency astrometric catalog of 266 sources. Of these 266 sources, 88 of them have been observed in at least five epochs. We produced time series of source positions for each of the 88 sources and compare source position variations at 24 GHz with variations in the same sources at X band. Here we discuss the astrometric catalog, the stability of the sources at 24 GHz, and the possible implications for ICRF2.

1. INTRODUCTION

As part of a collaborative effort to extend the International Celestial Reference Frame (ICRF) to higher radio frequencies, we have observed a number of extragalactic sources at Q band (43 GHz) and K band (24 GHz) using the 10 stations of the Very Long Baseline Array (VLBA) operated by the National Radio Astronomy Observatory (NRAO). The long term goals of this program are: 1) to develop a high-frequency celestial reference frame (CRF) with a variety of applications including improved deep space navigation, 2) to provide the astronomical community with an extended catalog of calibrator sources for VLBI observations at 24 and 43 GHz, and 3) to study source structure and source stability at these higher frequencies in order to improve the astrometric accuracy of future reference frames.

Thus far, 10 epochs of observations have been taken over the course of 5 years from 2002–present. All 10 of these epochs included observations at 24 GHz. Additionally, in four of the 10 epochs, observations were also recorded at 43 GHz. The details of the observations, calibration, and data processing up to the production of an experiment database readable by the Calc/Solve software package will be discussed in a forthcoming paper (Lanyi et al. 2008). In these proceedings, we concentrate on the 10 K-band experiments only. In §2 we discuss the astrometric catalog produced from the K-band observations and compare source positions with several other catalogs. In §3 we describe the process of generating position time series for those sources observed in five or more epochs and the relevant source stability information available from the series.

2. ASTROMETRIC CATALOG OF SOURCE POSITIONS

To generate the astrometric catalog of source positions, we used the Calc/Solve software package maintained by the NASA Goddard Space Flight Center (GSFC). The 10 diurnal K-band experiments encompassed 82,354 measurements of bandwidth synthesis (group) delay and phase delay rate. Parameters estimated per session include twenty-minute piecewise linear continuous troposphere parameters; tropospheric gradients in the east-west and north-south directions, linear in time, estimated every six hours per 24-hr session; quadratic clock polynomials for the gross clock behavior; and sixty-minute piecewise linear continuous clock parameters. No ionosphere calibration was applied. ITRF2000 was used as a priori station positions and velocities. USNO Bulletin A was used for a priori Earth Orientation Parameters (EOP). Positions of the 266 sources having three or more measurements of group delay were the only global parameters and were linked to the ICRF by constraining the right ascension and declination zero points to those of the ICRF Defining sources (Ma et al. 1998). The weighted rms residuals of the resulting solution were 17.24 ps in group delay and 47.25 fs/s in phase delay rate.

The CRF resulting from this astrometric solution was compared to several existing X-band catalogs including USNO's latest solution, crf2007b (`http://rorf.usno.navy.mil/solutions/crf2007b/`), the

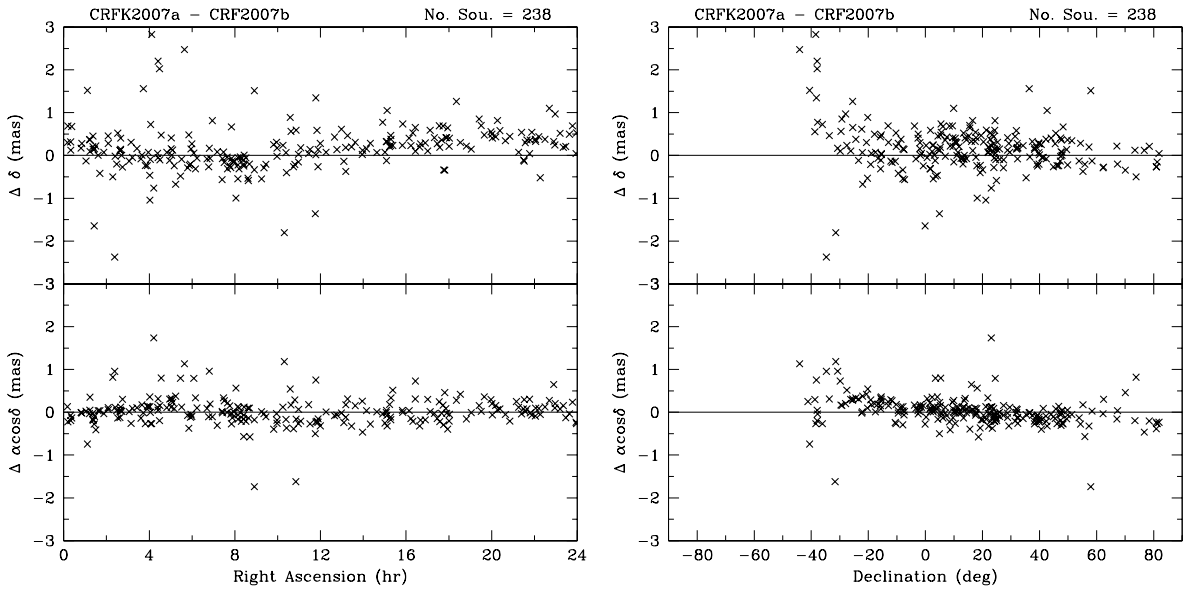

Figure 1: Source position differences ($\Delta\ \alpha\cos\delta$ and $\Delta\ \delta$) for the 237 sources in common between the crfk2007a (K-band) catalog and the crf2007b (X/S-band) catalog plotted as a function of right ascension (*left*) and declination (*right*).

ICRF catalog of defining sources (Ma et al. 1998), and ICRF Extensions 1 and 2 (Fey et al. 2004 and references therein). Shown in Figure 1 are the position differences in right ascension ($\Delta\ \alpha\cos\delta$) and declination ($\Delta\ \delta$) between crfk2007a and crf2007b plotted as a function of right ascension (*left*) and declination (*right*). There were a total of 238 overlapping sources between the two catalogs. The weighted mean position differences are 1 μas in $\Delta\ \alpha\cos\delta$ and 119 μas in $\Delta\ \delta$. The weighted root-mean-square (wrms) standard deviations of the position differences are 184 μas and 276 μas in $\Delta\ \alpha\cos\delta$ and $\Delta\ \delta$, respectively. From the plot, we also observe that any systematic effects between the two catalogs as a function of right ascension or declination appear to be small.

Listed in Table 1 are several additional catalog comparisons that were made. Each group of two rows shows the crfk2007a positions differenced with three variations of the ICRF catalog and, for comparison purposes, the USNO crf2007b catalog differenced with the same ICRF catalogs. The second column of the table shows the number of matching sources between the two catalogs being compared. Columns 3–6 list the weighted mean and wrms standard deviation of the position differences between the two catalogs being compared. These results indicate that relative to the ICRF, the K-band catalog is comparable to the X-band catalog. Although there are many fewer sources available in the K-band catalog, values for the wrms are at most a factor of 2.8 worse that those for the X-band catalog and are at best roughly equivalent.

Table 1: Comparison of Catalog Source Position Differences

	Num. of	$\Delta\ \alpha\cos\delta$		$\Delta\ \delta$	
	Matching	Wt. Mean	WRMS	Wt. Mean	WRMS
Catalogs	Sources	(μas)	(μas)	(μas)	(μas)
crfk2007a - ICRF Def.	77	−55	259	+80	353
crf2007b - ICRF Def.	212	−2	221	+8	255
crfk2007a - ICRF Ext. 1	192	−46	284	+80	337
crf2007b - ICRF Ext. 1	667	−21	180	−10	343
crfk2007a - ICRF Ext. 2	199	+4	199	+31	239
crf2007b - ICRF Ext. 2	717	+24	75	−33	84

3. TIME VARIATION OF K-BAND SOURCE POSITIONS

Time variation of the astrometric coordinates of CRF sources has been attributed to variability of their intrinsic structure (e.g. Fey, Eubanks & Kingham 1997). To investigate the stability of the high-frequency CRF source positions, we performed several astrometric solutions similar to that from which the astrometric catalog was derived. The difference here is that some fraction of the sources are treated as "arc" parameters (i.e. an estimate of the position was derived for each session in which the sources were observed). The estimation of source position stability was limited to 88 sources that were observed in five or more of the 10 VLBA epochs. Five epochs was considered a sufficient number of sessions (position estimates) per source to derive reliable statistics. Thus, an additional five astrometric solutions, with parameterization identical to the CRF solution described in §2, were produced. In each of these solutions, positions of approximately one fifth of the 88 sources were treated as "arc" parameters. The remaining sources in these five solutions were treated as global.

Shown in Figure 2 are the distributions of the wrms position variations in right ascension and declination from USNO solution crfk2007a position time series. For comparison, Figure 3 shows the distributions of the wrms position variations from the USNO X-band solution crf2007b position time series (`http://rorf.usno.navy.mil/solutions/crf2007b/`). Each distribution shows only the 67 sources that are common to both solutions. Shown in each figure are the mean and median wrms position variation for the 67 sources. Mean K-band position variations of ∼0.15 and ∼0.29 mas were found in right ascension and declination, respectively. For comparison, mean X-band position variations of ∼0.24 in right ascension and ∼0.33 mas in declination were determined for the same 67 sources. These results seem to indicate that the astrometric variations are smaller for sources at K-band versus X-band. The one caveat to this result is that the X-band variations include a much longer time history (back to 1979) and many more epochs of observations. A study, yet to be performed, will be to compute the X-band stability using 10 equivalent X-band experiments as was done for the catalog comparison described above.

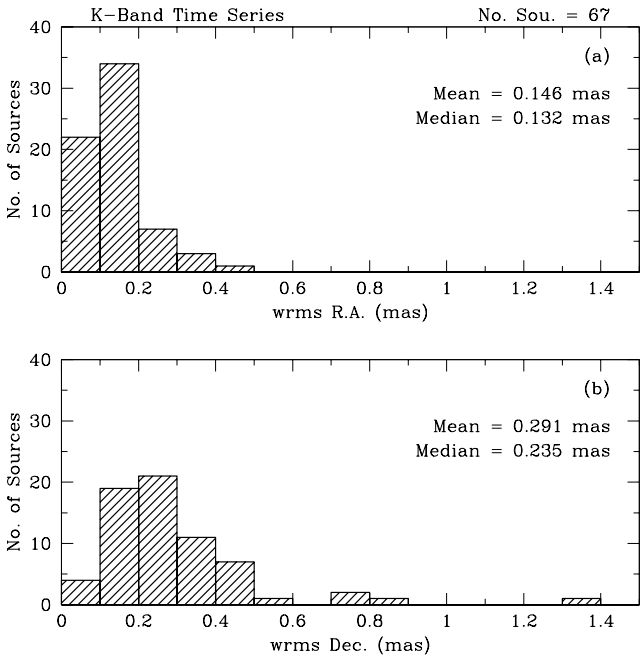

Figure 2: Distribution of the weighted rms position variation from USNO solution crfk2007a position time series for 67 K-band sources in a) Right Ascension and b) Declination.

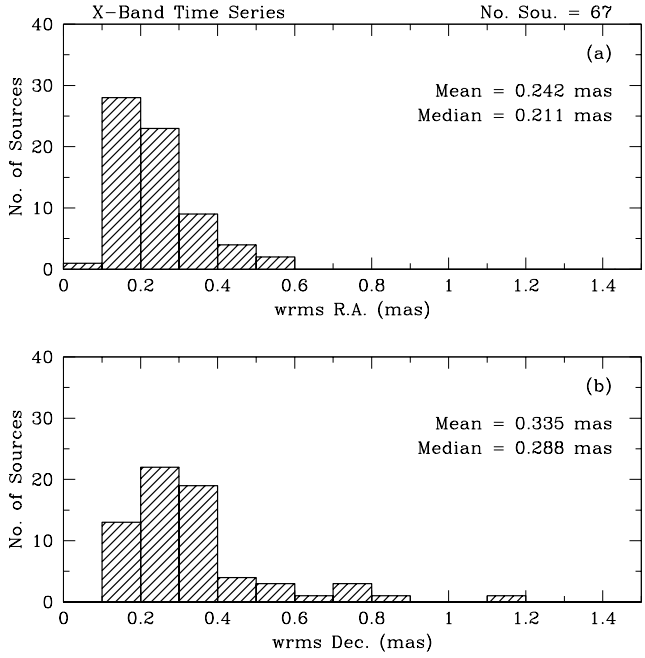

Figure 3: Distribution of the weighted rms position variation from USNO solution crf2007b position time series at X-band for the same 67 sources as shown in Figure 2. The two panels show the distribution in a) Right Ascension and b) Declination.

4. CONCLUSIONS

We have used the 10 high-frequency reference frame VLBA experiments recorded to date to produce an astrometric catalog of positions for 266 sources at 24 GHz. We find that this K-band catalog, while not yet at the precision of the best X-band catalogs, shows potential for future incorporation into the ICRF. In addition, we have produced time series of astrometric positions for 88 of the 266 catalog sources that were observed in five or more epochs. Preliminary results from these time series seem to indicate that the astrometric variations are smaller for sources at K-band versus X-band. This is again a promising sign for a future high-frequency celestial reference frame.

5. REFERENCES

Fey, A. L., Eubanks, M., & Kingham, K. A., 1997, "The Proper Motion of 4C39.25", AJ , 114, 2284

Fey, A. L., Ma, C., Arias, E. F., Charlot, P., Feissel-Vernier, M., Gontier, A. M., Jacobs, C. S., Li, J., & MacMillan, D.S., 2004, "The Second Extension of the International Celestial Reference Frame: ICRF-EXT.1", AJ , 127, 3587

Ma, C., Arias, E. F., Eubanks, T .M., Fey, A. L. Gontier, A. M., Jacobs, C. S., Sovers, O. J., Archinal, B. A. & Charlot, P., 1998, "The International Celestial Reference Frame as Realized by Very Long Baseline Interferometry", AJ , 116, 516

Lanyi, G. et al., 2008, "The Celestial Reference Frame at Higher Radio Frequencies: VLBA Astrometric Observations at 23 and 43 GHz", in preparation

PROPER MOTIONS OF REFERENCE RADIO SOURCES

O. TITOV
Geoscience Australia
PO Box 378 Canberra 2601 Australia
e-mail: oleg.titov@ga.gov.au

ABSTRACT. The motions of relativistic jets from the active extragalactic nuclei can reach hundred several microseconds per year and mimic proper motion of the distant radio sources observed by VLBI. Individual proper motion of these quasars is not correlated and exceed the small systematic effects induced by the rotation of the Solar system around the centre of the Galaxy. In this paper we search for the systematic effect and discuss the results.

1. INTRODUCTION

Multi-frequency VLBI can measure accurate positions of reference extragalactic radio sources. Several hundred such sources (mostly quasars and radio-galaxies) have positions known to an accuracy of better than 1 mas with respect to the Solar system barycentre (Ma et al, 1998). Apparent proper motions of these sources, presumably induced by the source structure changes, reach several hundred μas/year for selected radio sources (Ma et al. 1998, Fey et al. 2004, These variations of the radio source structure are supposed to have random orientations, therefore, the apparent proper motions should not be systematic. (Due to their large distances, transverse proper motions caused by the Solar system motion are negligible (Sovers et al, 1998).) However, systematic effects in the radio source positions can appear due to a variety of reasons, for instance, secular aberration drift, gravitational waves and the Hubble constant anisotropy, and in principle could be used to provide information about various cosmological processes.

2. SECULAR ABERRATION DRIFT, GRAVITATIONAL WAVES AND THE HUBBLE CONSTANT ANISOTROPY

On the Galactic scale, the Solar system barycenter rotates around the center of mass of the Galaxy with period about 200 million years. Centrifugal galactocentric acceleration of the Solar system barycentre results in the appearance of another effect of special relativity (secular aberration drift) that systematically changes positions of all celestial bodies (Gwinn et al., 1997, Sovers et al., 1998; Kovalevsky, 2003; Klioner, 2003; Kopeikin, Makarov, 2005). For the distance of the centre of the Galaxy of 10 kpc the magnitude of the galactocentric acceleration vector is about 5 μas/year and directed towards the center of the Galaxy. As a result, positions of all quasars should change in a form of additional systematic proper motion.

The effect of gravitational waves in the radio source proper motions has been described by Pyne et al. (1996) and (Gwinn et al., 1997). It can be detected as a degree 2 spherical harmonic (both 'magnetic' and 'electric' type) of the expansion of vector spherical functions (5/6 of the total effect comes to the l=2 spherical harmonic and 1/6 - to the l=3 spherical harmonic).

In a case of shear-free isotropic expansion of the Universe, the Hubble constant is uniform around the sky, so any transverse proper motion vanishes. However, if the Universe expansion is anisotropic, then the Hubble law $V = HR$ for the isotropic Universe should be replaced by

$$V = (e_{33}\sin^2\delta + \frac{1}{2}(e_{11}+e_{22})\cos^2\delta + \frac{1}{2}(e_{11}-e_{22})\cos 2\alpha\cos^2\delta)R = (H + \Delta H_3\sin^2\delta + \Delta H_{12}\cos 2\alpha\cos^2\delta)R \quad (1)$$

where e_{11}, e_{22}, e_{33} - diagonal elements of the expansion tensor. The Hubble constant here

$$H = \frac{1}{2}(e_{11} + e_{22}), \quad (2)$$

and two parameters that describe the Hubble constant anisotropy are given by

$$\Delta H_3 = e_{33} - \frac{1}{2}(e_{11} + e_{22}) \tag{3}$$

$$\Delta H_{12} = e_{11} - e_{22} \tag{4}$$

It is more essential that the transversal proper motions be given by

$$\mu_\alpha = -\frac{1}{2}(e_{11} - e_{22}) \sin 2\alpha \cos^2\delta = -\Delta H_{12} \sin 2\alpha \cos^2\delta \tag{5}$$

$$\mu_\delta = (e_{33} - \frac{1}{2}(e_{11} + e_{22})) \cos\delta \sin\delta - \frac{1}{2}(e_{11} - e_{22}) \cos 2\alpha \sin\delta \cos\delta = \frac{\Delta H_3}{2} \sin 2\delta - \frac{\Delta H_{12}}{2} \cos 2\alpha \sin 2\delta \tag{6}$$

It is obvious that if $e_{11} = e_{22} = e_{33}$ then $\Delta H_3 = \Delta H_{12} = 0$ and (1) reduces the conventional Hubble law and all proper motions (5)-(6) are to be zero.

3. RESULTS AND DISCUSSION

OCCAM software (Titov, Tesmer, Boehm, 2004) analysis VLBI data by the least squares collocation method (LSCM) (Titov, 2004). The LSCM minimizes a functional similar to the conventional least-squares method and, additionally, it takes into account intra-day correlations between observations. These correlations are calculated from external data, in the case of VLBI, from the data about stochastic behavior of hydrogen clocks and wet component of troposphere delays and gradients. All estimated parameters are split into three groups on their properties: stochastic, estimated for every epoch (hydrogen clock function and wet troposphere delays), daily or 'arc' parameters to be approximately constant within a 24-hour session, and so-called 'global' parameters whose are constant over the total period of observations. We treated the reference radio source positions and the secular aberration drift as global parameters (MacMillan, 2003).

The internal motion of relativistic jets in quasars produces significant changes in the observed radio source coordinates. Therefore, the positions of these astrometrically unstable quasars are treated as daily parameters to reduce the effect of instability on the estimates of other parameters. The first solution based on the ICRF radio source classification ("defining", "candidate" and "other" sources) (Ma et al, 1998). The second solution based on the radio source classification by Feissel-Vernier (2003) ("stable" and "unstable" sources). Though these two lists of radio sources are not independent, this approach allows accessing the sensitivity of results to variation of the list of reference radio sources. For the last two solutions all reference sources were split into the "no unstable close" (with redshift z$\leq$1) and " no unstable distant" (z$\geq$1) ones to produce independent estimates. The number of available redshifts in the existing database as large as 4.3 is limited by 352 "no unstable" radio sources therefore these last solutions based on 172 and 150 reference radio sources with a mean redshift z=0.57 and z=1.97, correspondingly.

Estimates of the secular aberration drift components are presented in Table 1. One can conclude that the overall average value (23 μas/year) provides a reasonable meaning for the indicated effect of secular aberration drift with the maximum 1σ standard error of 2.5 μas/year. The estimates of declination for all four solutions are in a good agreement. However, the estimates of right ascension for two first solutions and two last solutions are different, due to a decreased number of reference radio sources in last two solutions, especially it the southern hemisphere. We consider the coordinates from two last solutions as less reliable. From two first solutions the estimated aberration vector is directed towards the point with equatorial coordinates (α = 265 +/- 3, δ = 41 +/- 7). This effect causes apparent proper motions of all towards this 'focal point' with a maximum magnitude 23 μas/year (Fig 1).

The estimates of second order harmonic A(2,0), A(2,$\pm$1), A(2,$\pm$2) are less significant than for the secular aberration drift (Table 2 and 3). A deficit of radio sources in the southern hemisphere causes assymetry of their distribution around the sky, and, eventually, large correlation between some parameters. Also these parameter estimates are sensitive to the solution strategy, for instance, when NNR-constraints are introduced to the solutions. The 3σ standard error of 3-6 μas/year corresponds to uncertainty in the Hubble constant of 15-30 km/sec*Mpc. It exceeds the Hubble constant anomalies (10-12 km/s*Mpc) found by McClure and Dyer (2007) from the astrophysical data.

Nevertheless, for the 'distant' radio sources all these harmonic estimates (expect A(2,0)) are statistically significant, whereas, the same harmonics are negligible for the 'close' radio sources. It means that

the unknown factor generating in the second degree electric spherical harmonics (either gravitational waves, or the Hubble constant anisotropy) increases with distance to quasars.

More observations of distant radio sources in the southern hemisphere (under δ = -40) should be done in order to make more reliable conclusion. An addition, it is necessary to estimate the magnetic harmonics of the second degree within the procedure to verify an existence of the gravitational waves.

Solution	1	2	3	4
Reference radio sources	All except 102 'other'	All except 163 'unstable'	Close and not 'unstable'	Distant and not 'unstable'
Number of reference radio sources	1559	1441	172	150
Number of obs of reference radio sources	2.449,601	2.699,600	1.312,924	1.113,180
Secular aberration drift (μas/year)	25.3 +/- 2.2	21.9 +/- 2.0	23.2 +/- 2.4	21.7 +/- 2.5
Right Ascension	265 +/- 3	264 +/- 3	278 +/- 5	287 +/- 6
Declination	41 +/- 6	41 +/- 7	43 +/- 7	37 +/- 9

Table 1: Estimates of the vector harmonics l=1 for different sets of reference radio sources

Solution	1	3	4
Reference radio sources	All except 102 'other'	Close and not 'unstable'	Distant and not 'unstable'
Number of reference radio sources	1559	172	150
Number of obs of reference radio sources	2.449,601	1.312,924	1.113,180
A(2,0) (μas/year)	3.7 +/- 2.1	3.7 +/- 2.2	6.4 +/- 2.8
A(2,1) (μas/year)	7.4 +/- 0.9	1.6 +/- 1.0	8.2 +/- 1.5
A(2,-1) (μas/year)	-1.9 +/- 0.9	0.1 +/- 1.0	8.2 +/- 1.6
A(2,2) (μas/year)	-0.7 +/- 0.5	-1.4 +/- 0.6	4.4 +/- 0.9
A(2,-2) (μas/year)	-2.8 +/- 0.5	1.6 +/- 0.6	-1.2 +/- 0.9

Table 2: Estimates of the vector harmonics l=2 with NNR-constraints for different sets of reference radio sources

Solution	1	3	4
Reference radio sources	All except 102 'other'	Close and not 'unstable'	Distant and not 'unstable'
A(2,0) (μas/year)	7.3 +/- 4.3	2.7 +/- 5.2	11.2 +/- 5.2
A(2,1) (μas/year)	7.9 +/- 1.0	0.6 +/- 1.3	5.5 +/- 1.6
A(2,-1) (μas/year)	-1.2 +/- 0.9	-3.2 +/- 1.3	-6.9 +/- 1.6
A(2,2) (μas/year)	-2.2 +/- 0.6	-1.4 +/- 1.0	5.0 +/- 1.1
A(2,-2) (μas/year)	-8.0 +/- 1.3	1.5 +/- 1.9	4.1 +/- 2.1

Table 3: Estimates of the vector harmonics l=2 without NNR-constraints for different sets of reference radio sources

Acknowledgement. The paper is published with the permission of the CEO, Geoscience Australia.

4. REFERENCES

Ma, C. et al., 1998, "The international celestial reference frame as realised by very long baseline interferometry", AJ 116, pp. 516–546.

Fey, A. L., C. Ma, E.F. Arias, P. Charlot, M. Feissel-Vernier, A.-M. Gontier, C.S. Jacobs, J. Li, D.S. MacMillan, 2004, "The second extension of the ICRF - Ext.1 ", AJ 127, pp. 3587–3608.

Sovers, O. J., Fanselow J. L., Jacobs C. S., 1998, "Astrometry and geodesy with radio interferometry: experiments, models, results", Rev. Mod. Phys. 70, pp. 1393–1454.

Gwinn, C. R., Eubanks, T.M., Pyne, T., Birkinshaw, M., Matsakis, D. N., 1997, "Quasar proper motions and low-frequency gravitational waves", ApJ 485, pp. 87–91.

Kovalevsky, J., 2003, "Aberration in proper motions", A&A 404, pp. 743–747.

Klioner, S., 2003, "A practical relativistic model of microarcsecond astrometry in space", AJ 125, pp. 1580–1597.

Kopeikin, S. M. Makarov, V. V., 2005, "Astrometric effects of secular aberration", AJ 131, pp. 1471–1478.

Pyne. T., C. R. Gwinn, M. Birkinshaw, T. M. Eubanks, M. N. Demetrios, 1996, "Gravitational Radiation and Very Long Baseline Interferometry", ApJ 465, pp. 566–577.

Titov, O., Tesmer, V., Boehm, J., 2004, "OCCAM v.6.0 software for VLBI data analysis", In International VLBI Service for Geodesy and Astrometry 2004 General Meeting Proc (eds. Vandenberg N. V. and Baver, K. D.) NASA/CP-2004-212255, pp. 267–271.

Titov, O., 2004, "Construction of a celestial coordinate reference frame from VLBI data", Astron. Rep. 48, pp. 941–948.

MacMillan, D.S., 2003, "Quasar apparent proper motions observed by geodetic VLBI networks. In Future Directions in High Resolution Astronomy", The 10th Anniversary of the VLBA (eds. Romney, J. D. and Reid, M. J.) http:///www.arXiv:astrop-ph/0309826v1.

Feissel-Vernier, M., 2003, "Selecting stable extragalactic compact radio sources from the permanent astrogeodetic VLBI program", A&A 403, pp. 105–110.

McClure M. L., C. C. Dyer, 2007, "Anisotropy in the Hubble constant as observed in the HST Extragalactic Distance Scale Key Project Results", New Astronomy, 12, pp. 533–543.

INFLUENCE OF DIFFERENT STRATEGIES IN VLBI DATA ANALYSIS ON REALIZATIONS OF ICRF

S. BOLOTIN
Main Astronomical Observatory, National Academy of Sciences of Ukraine
Akademika Zabolotnoho Str. 27, 03680, Kiev, Ukraine
e-mail: bolotin@mao.kiev.ua

ABSTRACT. Positions of radio sources which are a realization of International Celestial Reference Frame (ICRF) can be estimated from VLBI observations. In this presentation we discuss different approaches in data analysis and the influence of applied strategy on the results. Application of these strategies are illustrated with a set of radio sources catalogs obtained from VLBI data analysis at the Main Astronomical Observatory (Kiev).

1. INTRODUCTION

In nowadays the International Celestial Reference Frame (ICRF) is realized by positions of extragalactic radio sources which are obtained from data analysis of geodetic and astrometric very long baseline (VLBI) observations. Efforts of many VLBI analysis centers are focused on producing new solutions of sources coordinates in the frame of international project ICRF-2, the second realization of the ICRF (e.g., C.Ma, this volume).

Estimated from VLBI observations coordinates of radio sources are depend on models of astronomical and geophysical effects which were applied in data analysis. Some mis-modeled or ill-modeled effects could increase random errors of source coordinates, another ones – systematic errors. One of well known examples of the last case is an influence of accounting of tropospheric gradients in data analysis on radio sources positions. In this paper we made an investigation of influence of various factors on the coordinates of radio sources.

2. COMPUTATION PROCEDURE

In order to investigate how the effects are distorting the resulting CRF we performed numerical tests. First of all, for selected set of VLBI observations, the data were analyzed and coordinates of radio sources (as well as stations positions and velocities, Earth orientation parameters (EOP), zenith delays and their horizontal gradients, etc.) were estimated. This solution of the CRF was used as the reference one. Then, studying the role of each of effect, the data analysis was performed without taking into account this effect (or option of a model) and resulting coordinates of radio sources were compared with the obtained from the reference solution. For both cases the set of VLBI sessions as well as data analysis procedures were the same.

A comparison of catalogs was performed in the following way: first, the parameters of a model of transformation between the reference and test catalogs were estimated with the least square method. Then, the model was applied to coordinates of the test catalog and weighted root means squares residuals for right ascension and declination were calculated.

We applied a model of transformation similar to that which was used in the IERS Annual Reports (e.g, 1993 IERS Annual Report), with added harmonic terms. The differences in right ascension, $\Delta\alpha$, and declination, $\Delta\delta$, are presented as:

$$\begin{aligned}\Delta\alpha &= A_1 \tan\delta\cos\alpha + A_2 \tan\delta\sin\alpha - A_3 + D_\alpha(\delta-\delta_0) + C_\alpha\sin(\alpha+\varphi_\alpha)\\ \Delta\delta &= -A_1\sin\alpha + A_2\cos\alpha + D_\delta(\delta-\delta_0) + B_\delta + C_\delta\sin(\alpha+\varphi_\delta),\end{aligned}$$

where A_1, A_2 and A_3 are small angles of global rotations about three axes; D_α and D_δ are slopes in right ascension and declination as functions of the declination; B_δ is a bias in the declination; C_α, φ_α and C_δ, φ_δ are amplitudes and phases of harmonic oscillations in right ascension and declination.

For data analysis all available VLBI observations which are good enough for simultaneous estimation of the Earth orientation parameters, Celestial and Terrestrial reference frames were processed. In total, 4,754,438 dual frequency delays acquired on 2,653 VLBI sessions from 1984 till mid of 2007 were processed.

The reference radio source catalog was obtained with the following assumptions. The VLBI data analysis was performed according to IERS Conventions (2003), with some exceptions: antenna thermal deformation model was not applied (due to lack of data for all stations) and the atmospheric pressure loading was modeled according to Petrov and Boy (2004) ephemeris.

Hydrostatic zenith delay was modeled according to Saastamoinen (1972). Ifadis mapping function (Ifadis, 1986) was used for both hydrostatic and wet components if station meteo parameters were good and NMFw2 (Niell, 1996) mapping function was used if the meteo parameters were suspicious.

Initial values of the CRF were taken from ICRF-Ext.1 catalog (IERS Annual Report, 1999). A priori values of stations positions and velocities were taken from ITRF2000 (Altamimi et al., 2002). The orientation of the CRF was linked by NNR constraint to ICRF-Ext.1; the origin, orientation and time evolution of the TRF were tied to ITRF2000 by NNT and NNR of positions and velocities constraints.

The following parameters were estimated in the solution: positions of sources, coordinates and velocities of stations as global parameters, the EOP on a session basis, clocks offsets, zenith delays and troposphere gradients as stochastic processes (random walk).

3. NUMERICAL TESTS, DISCUSSION

Several numerical tests were performed. We do not tested an influence of troposphere on coordinates of sources because it is well known effect and widely described in publications. The names of tests and their short descriptions are following. **Test-1**: The TRF estimation. In this test the coordinates and velocities of stations were not estimated and kept fixed to their priori values, ITRF-2000. **Test-2**: Polar motion estimation, the corrections of polar motion, p_x and p_y, were not estimated.

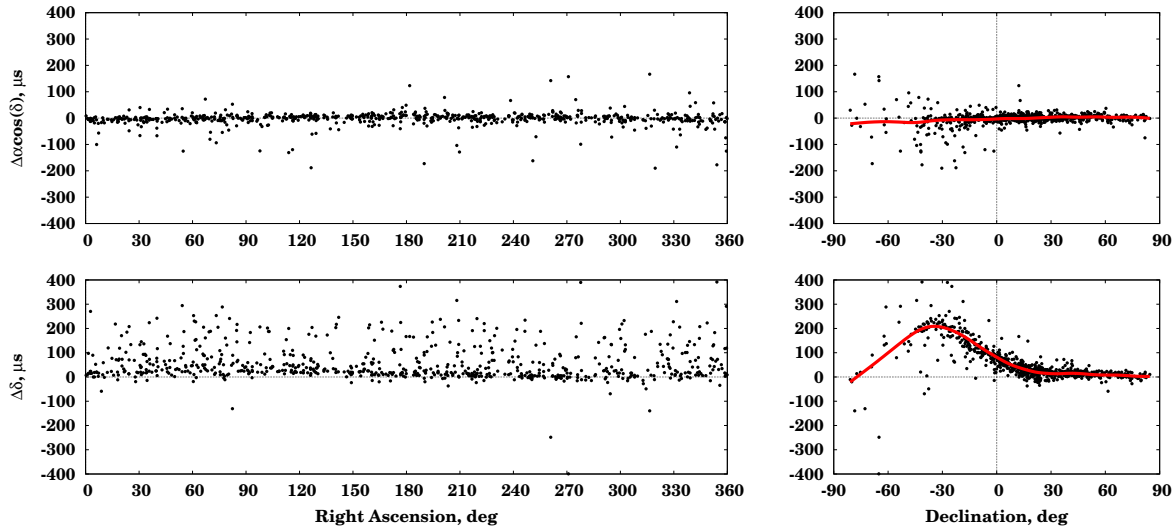

Figure 1: Differences of the catalogs for the **Test-2**, polar motion was held fixed, equal to a priori EOP(IERS)C04 solution.

Test-3: Estimation of subdiurnal Earth rotation parameters. The polar motion and $d(UT1-UTC)$ were parametrized and estimated on the frequency domains of $+1$, ± 2 and ± 3 cycles per day. **Test-4**: Subdiurnal variations in polar motion. The Ray et al. (1994) model of diurnal and semidiurnal p_x and p_y variations due to oceanic tides was turned off. **Test-5**: Subdiurnal variations in the rotation of the Earth, $d(UT1-UTC)$. The same as previous case, but the diurnal and semidiurnal variations of $d(UT1-UTC)$ was turned off. **Test-6**: Change of an ocean loading model. The ocean loading model CSR3.0 (Eanes, 1994) was applied instead of the GOT00.2 (Ray, 1999). **Test-7**: Nutation model, the old IAU-1980 Nutation theory was used instead of recommended by IERS Standards (2003) model IAU-2000.
Test-8: Effects in solid tides, degree 3 and latitude dependence of solid tides model was turned off.
Test-9: Influence of atmospheric loading, the model of atmospheric loading was not applied.

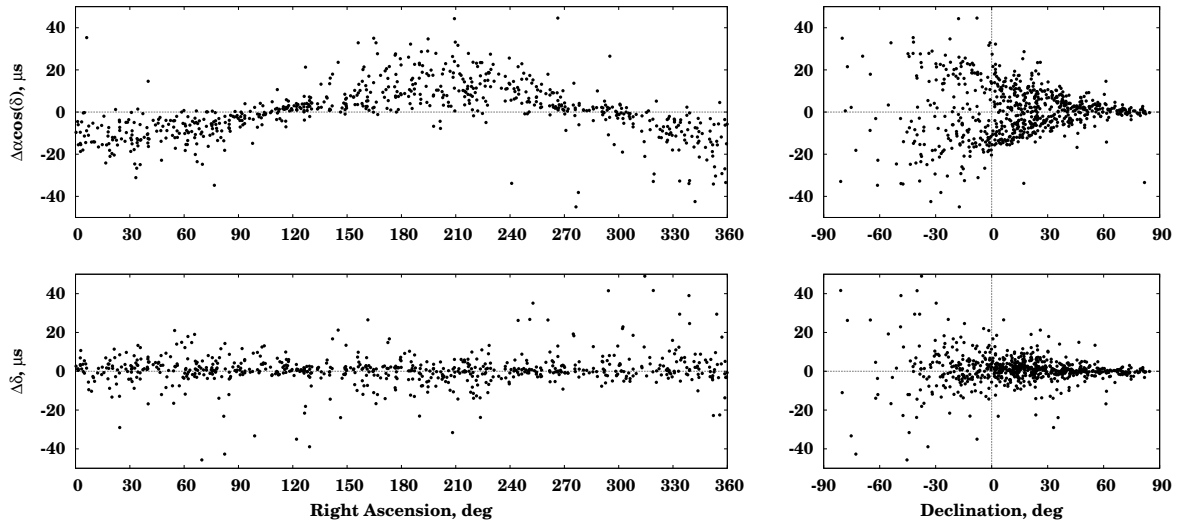

Figure 2: Differences of the catalogs for the **Test-7**, new nutation model IAU-2000 versus old theory IAU-1980.

Differences of sources coordinates between test catalog and the reference one are shown on the Figures 1 and 2 for the **Test-2** and **Test-7** cases. On the figures the standard deviations are not shown because they are greater than the differences in coordinates.

Name	A_1	A_2	A_3	D_α	D_δ	B_δ	C_α	φ_α	C_δ	φ_δ	ν_α	ν_δ
Test-1	13.6	10.2	24.1	71.5	112.4	−155.8	19.9	15.3	17.1	299.6	25.7	65.8
	9.5	9.8	7.9	13.2	7.3	6.6	9.8	24.0	11.7	34.8		
Test-2	−9.7	−0.6	4.4	11.2	−23.2	34.9	0.8	128.2	5.4	173.8	5.6	43.6
	3.1	3.2	2.6	4.3	2.4	2.3	2.7	238.8	3.6	38.6		
Test-3	−4.1	−4.3	−0.2	−1.2	−4.0	6.0	9.0	99.6	7.7	98.8	9.6	10.4
	1.5	1.5	1.2	2.0	1.2	1.1	1.3	9.6	1.8	12.4		
Test-4	3.1	13.5	0.1	−2.3	20.6	−23.2	12.0	193.4	19.2	256.8	12.3	19.3
	2.6	2.7	2.2	3.6	2.1	1.9	2.6	10.7	3.0	9.1		
Test-5	−20.4	−34.5	−2.8	13.0	0.6	−2.8	84.6	50.3	38.4	104.9	19.9	17.0
	3.0	3.1	2.5	4.2	2.4	2.2	3.0	1.9	3.7	5.1		
Test-6	0.3	−0.1	−0.1	−0.4	0.1	−0.1	1.2	241.5	0.5	9.0	0.6	0.7
	0.1	0.1	0.1	0.2	0.1	0.1	0.1	5.1	0.1	16.4		
Test-7	5.8	1.1	−1.4	−1.8	2.2	−1.6	14.3	252.6	5.2	349.2	3.0	3.5
	0.6	0.6	0.5	0.9	0.5	0.5	0.6	2.5	0.7	8.1		
Test-8	−10.5	−6.8	−0.7	−0.5	−3.4	3.7	7.2	66.8	17.1	155.6	2.6	7.6
	0.9	1.0	0.8	1.3	0.7	0.7	0.9	7.1	1.1	3.6		
Test-9	0.2	−0.0	−0.0	−0.1	0.1	−0.0	0.7	258.4	0.1	13.3	0.2	0.2
	0.0	0.0	0.0	0.1	0.0	0.0	0.0	2.8	0.0	25.7		

Table 1: Estimated parameters of transformation models and weighted post fit residuals of coordinates, ν_α and ν_δ. Units: A_1, A_2, A_3, B_δ, C_α, C_δ, ν_α and ν_δ are in μas; D_α and D_δ are in μas/rad; φ_α and φ_δ are in degrees. The standard deviations of the model parameters are shown on the second lines.

The results of estimations of transformation model parameters are summarized in the Table 1. In the table also displayed the post fit residuals in right ascension and declination of radio sources (i.e., after removing the systematic effects).

The first two cases, **Test-1** and **Test-2**, look very close to that which was obtained by Tesmer (2007). It is interesting to note that if geophysical effect which was checked here has periodic (or quasi periodic) oscillations on the frequency −1 cpd with respect to the crust of the Earth, then omitting the model of

this effect in data analysis would systematically distort the resulting Celestial reference frame. In this case, the systematic effect has significant harmonic terms in $\Delta\alpha$ and $\Delta\delta$.

4. CONCLUSIONS

In the conclusions we would like to emphasize that there is at least one geophysical effect which is not included in VLBI data analysis (due to lack of meteo parameters) and which has quasi periodic influence on stations coordinates, it is thermal deformation of radio telescope antennae. Omitting this effect (or incorrect modeling, which is worse) is systematically affecting the CRF on the level of 0.1–0.2 mas.

Acknowledgements. Our solutions are based on the VLBI observations provided by the International VLBI Service for Geodesy and Astrometry (IVS).

5. REFERENCES

Altamimi, Z., Sillard, P., & Boucher, C., 2002, "ITRF2000: A new release of the International Terrestrial Reference Frame for earth science applications", J. Geophys. Res. , 107(B10): 2114, doi: 10.1029/2001JB000561.

Eanes, R.J., 1994, "Diurnal and semidiurnal tides from TOPEX/POSEIDON altimetry", Eos Trans. AGU, 75(16):108

IERS Annual Report 1993, 1994, eds. M. Feissel, N. Essaïfi, Observatoire de Paris, Paris, France

IERS Annual report 1998, 1999, First extension of the ICRF, ICRF-Ext.1, Chapter VI, ed. D. Gambis, Observatoire de Paris, p. 87–114.

IERS Conventions (2003), IERS Technical Note 32, eds. D.D. McCarthy and G. Petit, Bundesamt für Kartographie und Geodäsie, Frankfurt am Main.

IVS: International VLBI Service data available electronically at http://ivscc.gsfc.nasa.gov

Ifadis, I.I., 1986, "The Atmospheric Delay of Radio Waves: Modeling the Elevation Dependance on a Global Scale", Technical Report No. 38L. – Chalmers U. of Technology, Göteburg, Sweden.

Ma, C., 2007, "Progress in the 2nd Realization of the ICRF", this volume.

Niell, A.E., 1996, "Global mapping functions for the atmosphere delay at radio wavelengths", J. Geophys. Res. , 101(B2), 3227–3246.

Petrov, L., Boy, J.-P., 2004, "Study of the atmospheric pressure loading signal in VLBI observations", J. Geophys. Res. , 109(B03405), doi:10.1029/2003JB002500.

Ray, R.D., Steinberg, D.J., Chao, B.F., and Cartwright, D.E., 1994, "Diurnal and Semidiurnal Variations in the Earth's Rotation Rate Induced by Oceanic Tides" Science, 264, pp. 830–832.

Ray, R.D., 1999, "A Global Ocean Tide Model From TOPEX/POSEIDON Altimetry: GOT99.2", NASA Technical Memorandum 209478.

Tesmer, V., 2007, "Effect of various analysis options on VLBI-determined CRF", Proc. of the 18th European VLBI for Geodesy and Astrometry Working Meeting, 12-13 April 2007, edited by J. Boehm, A. Pany, and H. Schuh, Geowissenschaftliche Mitteilungen, Heft Nr. 79, Schriftenreihe der Studienrichtung Vermessung und Geoinformation, Technische Universitaet Wien, ISSN 1811-8380.

EFFECT OF THE REFERENCE RADIO SOURCE SELECTION ON VLBI CRF REALIZATION

J.R. SOKOLOVA
Pulkovo Observatory
Pulkovskoe Ch., 65/1, St. Petersburg 196140, RUSSIA
e-mail: jrs@mars.hg.tuwien.ac.at

ABSTRACT. Up to now, four stability criteria based on different schemes have been used for the reference radio sources selection. Four lists of reference radio sources based on these schemes have been compiled. But significant inconsistencies between these lists were found. In this paper we tried to analyze an impact of these different selection schemes on the CRF solution as well as on radio source coordinate time-series.

1. INTRODUCTION

It is well known, that the selection of reference sources affects the precision and accuracy of the CRF derived from the VLBI observations. Therefore, it is important to select the most stable sources to be used as reference. So far four stability criteria based on different schemes have been derived for reference radio source selection and four list of stable sources were compiled applying these schemes.

1. The ICRF defining sources, published by Ma et.al. (1998) - 'ICRF'
2. Stable radio sources determined by Feissel-Vernier (2003)- 'FV'
3. Structure indices of radio sources set up by Charlot and Fey (1997) - 'ChF'
4. The list of Engelhardt and Thorandt (2006) - 'ET'

But significant inconsistencies between these lists of selected radio sources can be found (some examples of these inconsistencies are given in Table 1).

Source	ET	ICRF	ChF	FV
0003+380	-	+	-	+
0003-066	+	-	-	+
0300+470	+	-	+	+
0319+121	+	-	-	+
0306+102	+	+	-	+
0319+121	+	-	-	+
0420-014	+	-	-	-
0014+813	-	+	+	-
1611+343	+	-	-	+
2201+315	+	-	-	+
0237-233	-	-	-	+
2145+067	-	+	+	-

Table 1: Examples of the selection schemes inconsistencies. + Stable, - Unstable

2. TIME SERIES ANALYSIS

For our analysis we used the software package OCCAM 6.2 (LSQM) (Titov, et al., 2004). Radio source coordinate time series for 217 ICRF sources have been calculated and analyzed.

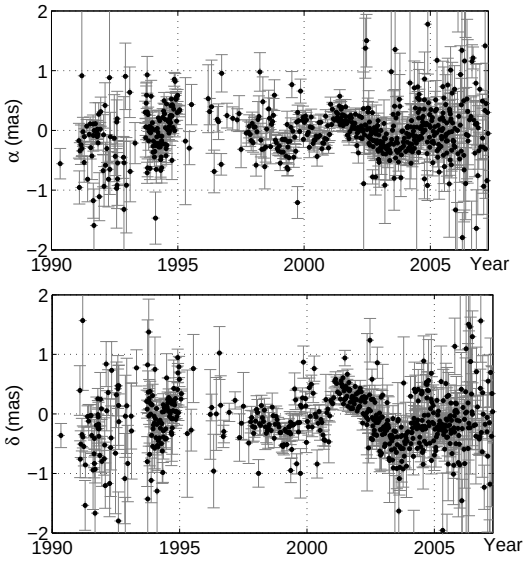

Source 2201+315

- ICRF "other" group
- Stable source by M. Feissel
- Stable (in first group of 121 radio sources) by G. Engelhardt and V. Thorandt
- Index 3 (X-band), and 1 (S-band) by Patrick Charlot

Fig. 1 Variation Radio Source positions by R.A and Dec.

One can see that the radio source positions demonstrate the synchronous change in both coordinates after 2001.0 (Fig 1). According to astrophysical data, the centroid of radio brightness had moved on 500 as from its original position by the end of 2003 and returned back by the end of 2004. The positional variations can be explained by jet motion in the south-west direction between 2001 and 2004. The direction is confirmed by the X-Band radio images from the USNO Radio Reference Frame Image Database (RRFID) (Fey and Charlot, 1997; Fey and Charlot, 2000)

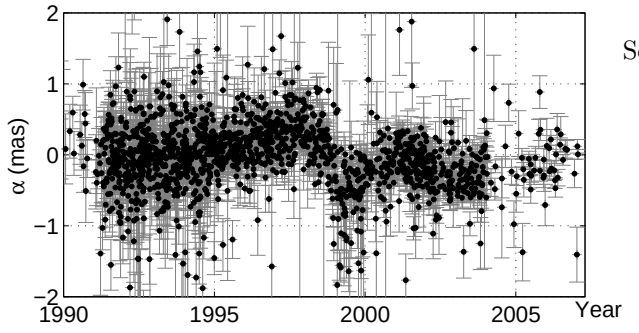

Source 2145+067

- ICRF "defining" group
- Unstable source by M. Feissel
- Unstable by G. Engelhardt and V. Thorandt
- Index 2 (X-band) by Patrick Charlot

Fig. 2 Variation Radio Source positions by R.A and Dec.

The set of radio images which is available at RRFID after 1994 shows a long jet in the south-east direction, moreover, structure of the jet is variable. Variations of radio source coordinates by R.A. can be expressed as linear trend and quasi periodical variations of 1.5 mas range (O. Titov, 2006)

3. IMPACT OF REFERENCE RADIO SOURCE SELECTION ON NUTATION PARAMETERS DURING GLOBAL SOLUTION

To calculate a global solution all sources have been splitted up into 3 groups:

1. Reference sources - for NNR constraints (group1)
2. Global sources - coordinate of these sources are treated as global parameters (group2)
3. Arc sources - coordinate of these sources are treated as local parameters (group 3)

According this division into groups two global solutions have been calculated:

- GG07JS01a - Number of reference sources = 212 ICRF "defining" sources, number of sources treated as arc parameters = 102 ICRF "other group"
- IGG07JS01b - Number of reference sources = 199 "stable" sources by M. Feissel, number of sources treated as arc parameters = 163 "unstable" sources by M. Feissel

To analyze the impact of applying different lists of reference sources on nutation offset estimations, two nutation time series have been calculated using these two CRF catalogues. After that we used a test, which can help us to get some independent estimates of the quality of these catalogues. The first estimate is the WRMS difference between the computed celestial pole offsets and the IAU2000A model supplemented with the Free Core Nutation (FCN) contribution. The second estimate is computed as weighted Allan deviation of the celestial pole (Malkin, 2007). The results of this test presented in table 2. show no significant improvement of the scatter of celestial pole offsets estimates.

Catalogue		FCN			ADEV	
	X	Y	Mean	X	Y	Mean
IGG07JS01a	99	105	102	103	106	105
IGG07JS02a	97	104	101	102	105	104

Table 2: Scatter of the celestial pole offset time series calculated with two catalogues. FCN column shows the scatter w.r.t. FCN model, the ADEV column shows Allan deviation. Unit as.

Thus we can consider that there is no impact of applying different lists of reference sources on the nutation offset estimations calculated from global solution when sources which were excluded from group 1 were added to group 2 or group 3. The effect of the applying different radio sources lists during daily solution will be much clearer due to fixing coordinates of all sources.

4. IMPACT OF REFERENCE RADIO SOURCE SELECTION ON NUTATION PARAMETERS DURING DAILY SOLUTION

To study the impact of source instability on nutation offset estimations, several nutation time series have been calculated during the daily solution (Kalman filter) in different modes. In this paper we present only a few of them:

1. NUT ALL - The coordinates of all sources have been fixed
2. NUT 2201+315 - The coordinates of all sources except 2201+315
3. NUT 2145+067 - The coordinates of all sources except 2145+067 have been fixed

Next step we calculated the differences between the NUT ALL and NUT 2201+315 (Fig. 3) and NUT 2145+067 (Fig. 6).

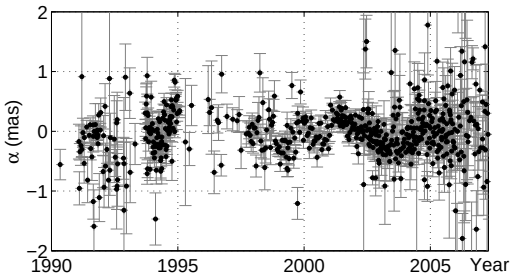

Fig. 3 Variation of Radio Source positions by R.A

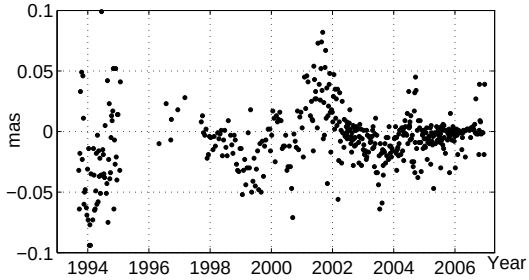

Fig. 4 Nutation Dpsi offset difference (NUT ALL - NUT 2201+315).

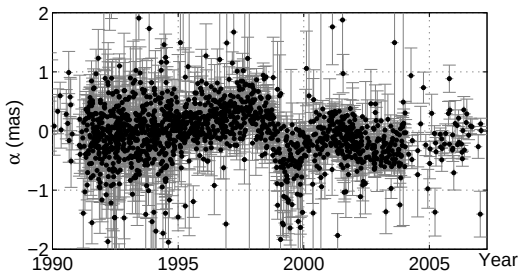

Fig. 5 Variation of Radio Source positions by R.A

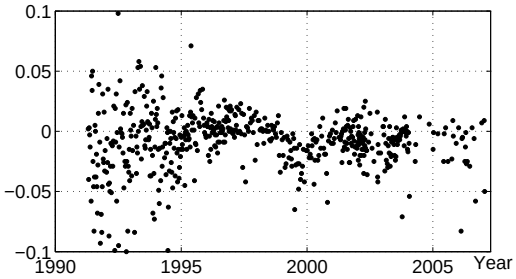

Fig. 6 Nutation Deps offset difference (NUT ALL - NUT 2145+067).

5. SUMMARY

Thus we can consider that:

1. All four selection schemes have significant inconsistencies. Thus, It is necessary to develop a combination of the statistical and astrophysical criteria with the analysis of nutation time series for the procedure of stable radio source selection. As a preliminary version of a list of 'stable' sources the mix of 'stable' lists by Charlot and by Feissel proposed by O. Titov can be used

2. Variations of radio source coordinates significantly affect on the determination of nutation time series during daily solution, in which coordinates of all sources are fixed.

6. REFERENCE

O. Titov, V. Tesmer, J. Boehm: OCCAM v.6.0 software for VLBI data analysis. In: Vandenberg, N., K. Baver (Eds.): IVS 2004 General Meeting Proceedings, NASA/CP-2004-212255, 267-271, 2004

A. Fey, Ma, C., Arias, E. F., et al. 2004, 'The Second Extension of the International Celestial Reference Frame: ICRF-Ext.2,' 2004, Astronomical Journal, 127, 3587

Ma, C., Arias, E. F., Eubanks, T. M., et al. 1998, AJ, 116, 516

Ma, C. 2001, in Proc. 15th Working Meeting on European VLBI for Geodesy and Astrometry, ed. D. Behrend and A. Rius, 187

Feissel-Vernier, M., 2003. Astronomy and Astrophysics Journal, 403, 105.

Charlot Patrick (2005), Radio source structures, web site reference: http://www.obs.u-bordeaux1.fr

G. Engelhardt and V. Thorandt 'First Steps to Investigate Long-Term Stability of Radio Sources in VLBI Analysis'. In: International VLBI Service for Geodesy and Astrometry 2006 General Meeting Proceedings, edited by D. Behrend and K. Baver, NASA/CP-2006-214140, 281-285, 2006., IVS 2006 General Meeting Proceedings

EXTRAGALACTIC OPTICAL-RADIO LINK RESEARCH AT USNO

N. ZACHARIAS[1], M.I. ZACHARIAS[1], D. BOBOLTZ[1], A. FEY[1], R. GAUME[1],
G.S. HENNESSY[1], K.J. JOHNSTON[1], R. OJHA[1]
[1] U.S. Naval Observatory
3450 Massachusetts Ave. N.W., Washington DC 20392
e-mail: nz, miz, db, alf, gaume, gsh, kjj, ro@usno.navy.mil

ABSTRACT. Over 500 counterparts of ICRF sources were observed during 24 deep CCD observing runs as part of the USNO CCD Astrograph Catalog (UCAC) project, providing a direct link to Tycho-2 stars. For some sources a positional accuracy of 10 mas is achieved. A sample of 12 extragalactic ICRF sources are being observed at the Naval Observatory Flagstaff Station (NOFS) 1.55-meter telescope over several years to monitor optical position stability. First high resolution imaging of selected sources are obtained at the Lick 3-meter AO system to correlate source structure with optical-radio centroid offsets. As part of the Space Interferometry Mission (SIM) preparatory science about 240 bright QSO's are monitored for photometric variability in B,V,R and I. The USNO Robotic Astrometric Telescope (URAT) will be able to combine deep CCD imaging of all ICRF2 target areas and millions of compact galaxies with a stellar, astrometric, all-sky survey of multiple epochs.

1. OPTICAL COUNTERPARTS OF ICRF SOURCES

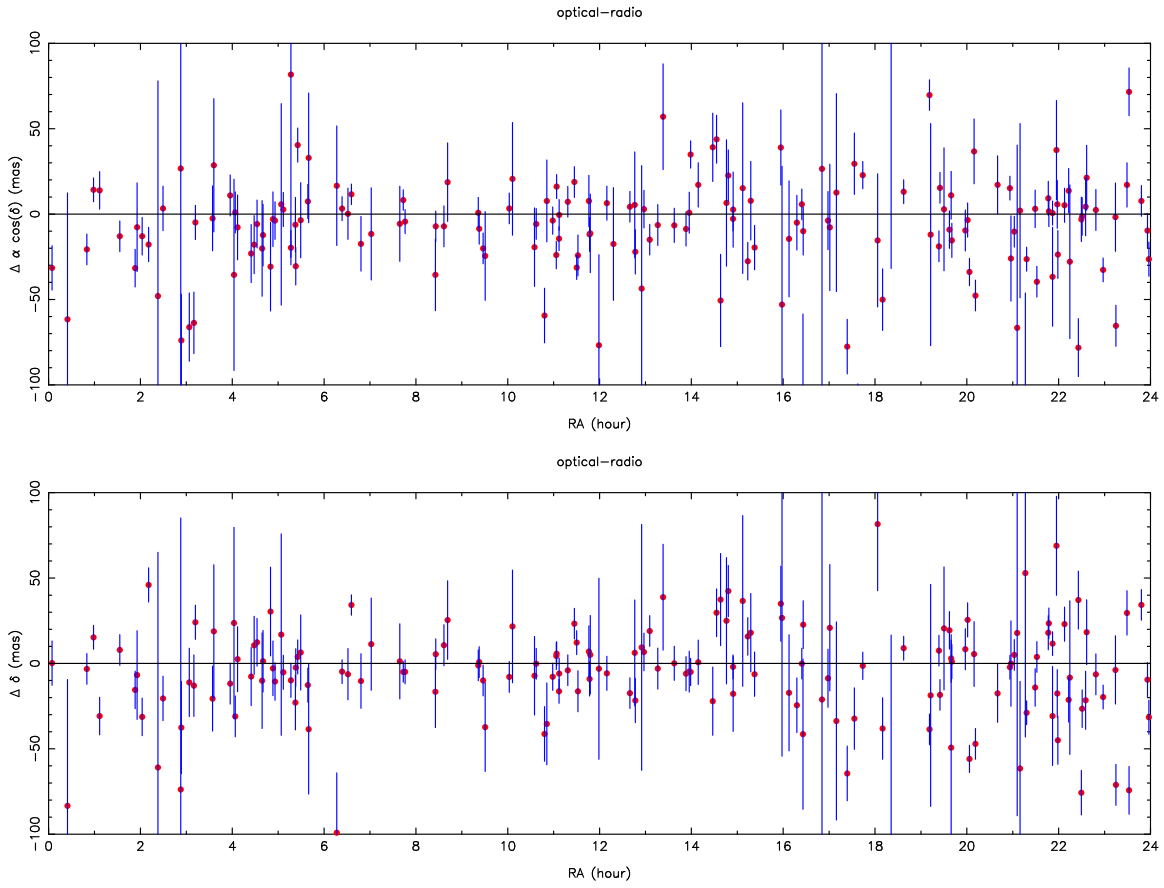

Figure 1: Observed optical-radio position offsets of 199 ICRF optical counterparts.

Between 1997 and 2004 the CTIO 0.9m, KPNO 0.9m and 2.1m telescopes were utilized in 24 observing runs to image over 500 optical counterparts of ICRF sources. Contemporaneous to these deep CCD imaging the USNO astrograph observed the same fields as part of the UCAC project (Zacharias et al. 2004) in order to provide a direct tie to the Tycho-2 and thus the Hipparcos reference frame. Reductions have been performed for 236 fields (mainly in the southern hemisphere) of which 199 gave optical counterpart position results (Figure 1), see also Zacharias & Zacharias (2005).

The total estimated positional error per coordinate for many sources is in the 10 to 20 mas range. However, a higher than expected fraction of sources show an optical-radio position offset larger than 3-sigma of the total error. Whether this is the result of underestimated systematic errors or caused by physics (optical source structure) is yet unknown.

2. OPTICAL ASTROMETRIC STABILITY ON MAS LEVEL

Between 2002 and Oct. 2007 484 CCD images were obtained with the Naval Observatory Flagstaff Station (NOFS) 1.55m Strand Reflector of a selection of 12 ICRF optical counterparts (see Table 1). The goal of this differential astrometry investigation is to assess the positional stability over time at optical wavelengths with single exposure standard errors of about 3 mas per coordinate and 14 to 77 observations per source. The targets were selected to cover a wide range in parameters (ICRF defining, contributing or other sources, quasar or BL-Lac object type, redshift, radio quality, radio structure index). For radio characterization see Fey & Charlot (1999).

source	I	t	mag	z	Q	SIX
0241+622	C	Q	12.2	0.04	18	2
0552+398	C	Q	18.0	2.37	96	2
0738+313	D	Q	16.1	0.63	61	4
0754+100	D	L	15.0	0.66	68	2
0839+187	D	Q	16.4	1.27	46	4
0851+202	C	L	15.4	0.31	83	2
0912+297	D	L	16.4	?	–	1
1656+053	C	Q	16.5	0.89	57	3
1830+285	D	Q	17.2	0.59	58	3
1937−101	C	Q	17.0	3.79	52	3
2059+034	D	Q	17.8	1.01	66	2
2201+315	O	Q	15.6	0.30	74	3

Table 1: Sources on the optical stability monitoring program at the NOFS 1.55m telescope. I = ICRF object type (D = defining, C = contributing, O = other), t = optical type (Q = QSO, L = BL-Lac), mag = approximate V magnitude, z = redshift, Q = radio quality, stability over time (0 = poor, 100 = excellent), and SIX = radio structure index (1 = very good, 4 = poor).

3. HIGH RESOLUTION OPTICAL IMAGING

In September 2007, following an unsuccessful attempt in 2006 (poor seeing), high-resolution (0.3 arcsec) images of 3 extragalactic, compact sources were obtained using the Lick 3-meter adaptive optics (AO) system. The source IRAS 0147+3554 clearly shows an asymmetric image profile due to structure of the underlying spiral galaxy. This is a program in collaboration with E. Gates, Lick Observatories.

USNO has also pursued observing opportunities using HST and the LuckyCam at ESO, however, no observing time was been granted yet. It will be very challenging to obtain sufficient observing time to even image once all optical counterparts of the current ICRF1 with high resolution at optical wavelengths, something which is being achieved regularly at radio frequencies.

4. BRIGHT QUASAR PHOTOMETRY

A total of 242 optically bright quasars, evenly distributed over all sky, are on a photometric monitoring program. The sources have been selected, regardless of radio flux, starting with the Veron catalog (Veron et al. 2000), as the optically brightest targets giving a good all-sky distribution and displaying symmetric, compact appearance on digitized Schmidt survey images. Most targets are in the 15 to 17 mag range with some as faint as 20th mag to fill gaps near the galactic plane. The optically very brightest quasars and BL-Lac objects were excluded due to asymmetric structure already visible on the arcsec level.

Quasars are being observed with the CTIO and NOFS 1.0-meter telescopes in B, V, R, and I bands. This program is part of the Space Interferometer Mission (SIM Planet-quest, see also Unwin et al. 2007) preparatory science within the "Astrophysics of Reference Frame Sources" SIM key science project (PI: K. Johnston). With the lack of high resolution optical images (see above) optical variability information can be used as the next best indicator for "stable" sources to select most appropriate candidates for a future SIM celestial reference frame, which needs about 50 pre-selected sources. Results from this program will also be used in the work leading to the construction of the future ICRF2 (Ma et al. 2007).

Photometric observations have been obtained for all sources, many with more than 1 epoch. Significant differences in observed magnitudes w.r.t. the Veron catalog are found. A paper is in presentation for AJ (Zacharias et al. 2008).

5. THE URAT PROJECT

The USNO Robotic Astrometric Telescope (URAT) project aims at an all-sky survey to extend the UCAC data to fainter limiting magnitudes and higher positional accuracies. URAT comes in 2 phases. The first will use the URAT focal plane at the existing USNO Astrograph "redlens", which also was used for the UCAC program. Phase 2 requires the construction of a new, dedicated, astrometric telescope of which the primary mirror has been manufactured while currently no funding is identified to complete that telescope. Table 2 gives an overview about the properties of the 2 phases of the URAT program.

parameter	URAT phase 1	URAT phase 2
telescope	redlens astrograph	new design
focal length	2.00 m	3.60 m
aperture	0.20 m	0.85 m
field of view	9.00 deg	4.50 deg
field diameter	324 mm	283 mm
pixel scale	0.905 ″/pix	0.515 ″/pix
sky cov./exposure	27 sq.deg	9.1 sq.deg
bandpass	670–760 nm	
brightness range	10–18 mag	13–21 mag
catalog accuracy	10 mas	5 mas
solve for	position, proper motion, parallax	
begin of survey	2009	not determined

Table 2: The above values for pixel scale and sky coverage assume the use of the "4-shooter" camera which is based on 4 CCD chips of 111 million pixel each (STA1600 chip). The catalog accuracy is for well exposed stars; at the limiting magnitude the errors will be about a factor of 3 larger.

Details of the optical design of URAT are given by Laux & Zacharias (2005), and Zacharias et al. (2006), while the project itself is described in Zacharias (2005, 2007). Latest progress with the detector development is presented in Zacharias et al. (2007). The 10k camera with a single CCD chip of the kind (95 mm by 95 mm, full-wafer device) saw first light in October 2007 and astrometric characterization of this back-illuminated detector is in progress at the USNO astrograph telescope. The "4-shooter" URAT focal plane assembly will be built in 2008.

The large sky coverage with a single exposure will allow multiple sky overlaps per year. With at least 2 years of operation on each site (northern and southern hemisphere) not only mean positions but also proper motions and parallaxes can be derived for all stars from the URAT observing program itself. The limiting magnitude will be deep enough to be able to access optical counterparts of ICRF sources directly.

The URAT program can provide highly accurate reference stars for the PanSTARRS and LSST projects.

6. CONCLUSIONS

The analysis of ICRF-2 sources at radio frequencies is in "good shape" (e.g. Ojha et al. 2005, Ma 2006) while the optical effort is lagging behind in characterization of optical counterparts (high resolution imaging, variability and geometric stability analysis), and positional accuracy. The Hipparcos Celestial Reference Frame is, 10 years after it became available, still the primary standard of the optical reference frame, with no significant deviations from the ICRF detected.

Current optical reference frame research is active in 3 areas: a) building on the Hipparcos and Tycho data and going to fainter stars for a densification of the existing optical reference frame (e.g. UCAC and URAT), b) maintaining the link between the currently bright optical reference frame (Hipparcos) and the radio-defined ICRF by observing the optically faint counterparts, and c) preparatory work for a future high accuracy optical reference frame (e.g. SIM and Gaia) which is likely to supersede the VLBI based radio reference frame. In all areas USNO is heavily involved.

7. REFERENCES

Fey, A. L., Charlot, P., 1999, "VLBA observations of radio reference frame sources. III. Astrometric suitability of an additional 225 sources", ApJSup 128, pp. 17–83

Laux, U., Zacharias, N., 2005, "URAT optical design options and astrometric performance", in Proc. "Astrometry in the Age of the Next Generation of Large Telescopes", Eds: Kenneth Seidelmann and Alice K.B. Monet ASP Conference Series 338, p.106–109

Ma, C., 2006, "Present Status Of The Celestial Reference System And Frame", IAU GA 2006 (Prague), JD 16, paper 2 in "Nomenclature, Precession and New Models in Fundamental Astronomy"

Ma, C. et al. 2007, "ICRF2 ...", these Proceedings

Ojha, R., Fey, A. L., Charlot, P., Jauncey, D. L., Johnston, K. J., Reynolds, J. E., Tzioumis, A. K., et al. 2005, "VLBI Observations of Southern Hemisphere ICRF Sources. II. Astrometric Suitability Based on Intrinsic Structure", AJ 130, pp. 2529–2540

Unwin, S. et al. 2007, "SIM science", PASP in press

Veron-Cetty, M.-P., Veron, P., 2003, "A catalogue of quasars and active nuclei: 11th edition", A&A 412, pp. 399–403

Zacharias, N., Urban, S. E., Zacharias M. I., Wycoff G. L., Hall D. M., Monet D. G., Rafferty T. J., 2004, "The UCAC2 release", AJ 127, pp. 3043–3059

Zacharias M. I., Zacharias N., 2005, "optical counterparts 2.1m", ASP Conf.Ser. 338, pp. 184–187, Eds. P. Kenneth Seidelmann & Alice K.B. Monet

Zacharias, N., 2005, "The URAT project", in Proc. "Astrometry in the Age of the Next Generation of Large Telescopes", Eds: Kenneth Seidelmann and Alice K.B. Monet ASP Conference Series 338, p. 98–103

Zacharias, N., Laux, U., Rakich, A., Epps, H., 2006, "URAT: astrometric requirements and design history", Proceed. SPIE 6267, p.22

Zacharias, N., Dorland, B., Bredthauer, R. et al. 2007, "Realization and application of a 111 million pixel backside-illuminated detector and camera", SPIE, 6690 paper 8

Zacharias, N. 2007, "Dense optical reference frames: UCAC and URAT", in Proceed. IAU Symp. 248 (Shanghai), in press

Zacharias, N., Ojha, R., Hennessy, G. et al. 2008, "Photometric monitoring of compact, optically bright quasars for SIM and other future celestial reference frames", in prep. for AJ

A GAIA ORIENTED ANALYSIS OF A LARGE SAMPLE OF QUASARS

A.H. ANDREI[1,2,3], M. ASSAFIN[2], C. BARACHE[3], S. BOUQUILLON[3], G. BOURDA[4], J.I.B. CAMARGO[2], J.-F. leCAMPION[4], P. CHARLOT[4], A.-M. GONTIER[3], S. LAMBERT[5], J.J. PEREIRA OSRIO[6], D.N. daSILVA NETO[2,7], J. SOUCHAY[3], R. VIEIRA MARTINS[1]

[1] Observatório Nacional/MCT
R. Gal. Jos Cristino 77, RJ, Brasil
e-mail: oat1@on.br
[2] Observatório do Valongo/UFRJ, Brasil
[3] SYRTE/Observatoire de Paris, France
[4] Observatoire de Bordeaux, France
[5] Observatoire Royal de Belgique
[6] Observatório Astronmico da Universidade do Porto, Portugal
[7] Universidade Estadual da Zona Oeste/RJ, Brasil

ABSTRACT. GAIA photometric capabilities should distinguish quasars to a high degree of certainty. With this, they should also be able to deliver a clean sample of quasars with a negligible trace of stellar contaminants. However, a purely photometric clean sample could miss a non negligible percentage of ICRF sources counterparts - and this interface is required to align with the ICRS and de-rotate the GCRF (GAIA Celestial Reference Frame), on grounds of continuity. To prepare a minimum clean sample forming the initial quasar catalogue for the GAIA mission, an all sky ensemble was formed containing 128,257 candidates. Among them there is at least one redshift determination for 98.75%, and at least one magnitude determination for 99.20%. The sources were collected from different optical and radio lists. We analyze the redshift, magnitude, and color distributions, their relationships, as well as their degree of completeness.

Complementary, the candidate sources enable to form an optical representation of the ICRS by its first principles, namely, kinematically non-rotating with respect to the ensemble of distant extragalactic objects, aligned to the mean equator and dynamical equinox of J2000, and realized by a list of adopted coordinates of extragalactic sources.

1. GAIA'S INITIAL QSO CATALOGUE AND CLEAN SAMPLE

The establishment of an initial quasar catalogue for the GAIA mission must fulfill criteria of quantity and sky distribution. The expected quantity of quasars to be detected by GAIA is of 400,000 objects or more, that is about four times the number of objects presently known. A much smaller number, between 6,000 to 10,000 (Mignard, 2001) is required for the definition of the fundamental frame. This sets the minimum requirements for the initial quasar catalogue clean sample, that is to zero level of contaminants. Since the all sky distribution (exempting the galactic disk) is also desirable, direct observations are out of question and the pre-existing quasar catalogues ought to be scrutinized. Figure 1 brings the schematics of the search strategy.

In practice, the major sources of known quasars are found in the following lists (i) Véron-Cetty & Véron (12th ed., 85,221 quasars with measured redshift); (ii) the SDSS DR5 release (74,869 quasars, selected from color criteria and confirmed through spectroscopic redshift); (iii) the 2dF 2QZ survey (22,655 quasars, selected from color criteria and confirmed through spectroscopic redshift); (iv) the ICRF and its extensions (717 radio-quasars and active galaxies); (v) the VLBA calibrator list (2005 version, 3,357 radio-flux stable quasars); (vi) the VLA calibrator list (2003 update, 1,860 radio-flux calibrators); (vii) the JVAS catalog (Jodrell Bank-VLA survey, 2,118 compact radio-sources); (viii) FIRST optical counterparts list (2,300 unresolved and 5,300 resolved stellar-like sources true matches with Cambridge APM scans of the POSS-I plates).

So, as the first step the common entries are sorted and a consolidated list is produced, including a

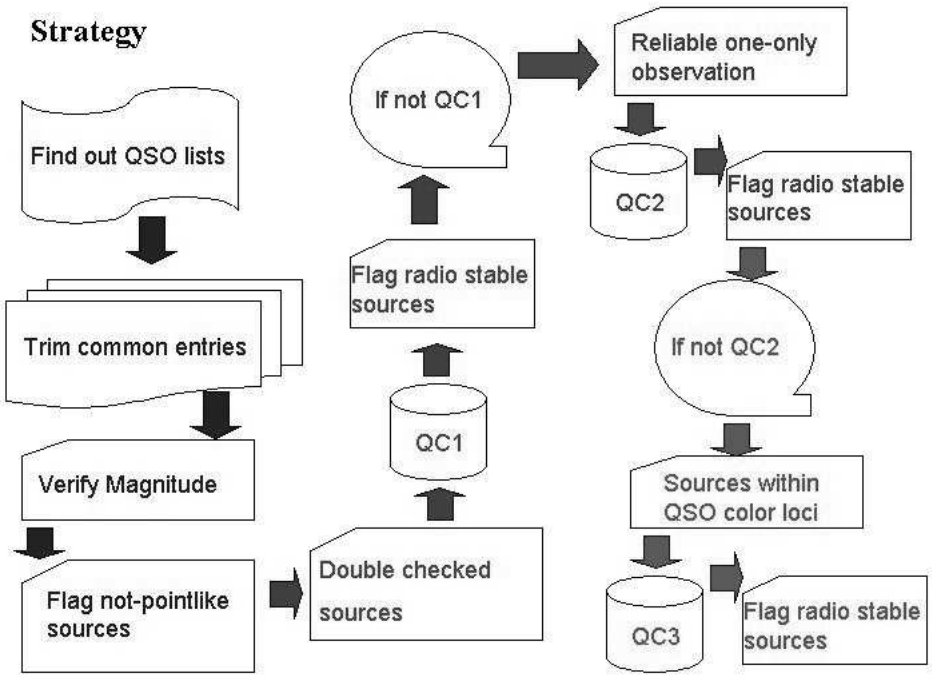

Figure 1: Schematics of the strategy of construction of the GAIA initial quasar catalogue and clean sample

reliability estimator and the radio astrometric accuracy. The consolidated list, plus details of redshift, multi-band magnitude and radio flux, is the aim of the VLQAC (Souchay et al., 2007) (see Table 1).

Since the consolidated list in none of its constituents derives from apparent magnitude limits in the G band, a check must then be performed to test each source G magnitude. The B1.0 and GSC2.3 catalogs present the whole sky complete up to magnitude V=20 (though reaching beyond in some zones). For most of the sky they contain the B, R, and I magnitudes, and so the G magnitude can be acceptably derived (Drimmel et al., 2005, have found that G $\approx$ R GSC) . With this the list is trimmed of its weaker sources (which will nevertheless be flagged as such and then kept), which would give rise to poor GAIA centroid determination.

Next, from available optical images, the objects PSF is compared to the stellar neighbors, in order to reject no point-like objects. Finally, the objects observational history is followed, to the effect of retaining a core of (at least) double-checked quasars. The objects passing through all checks form the clean sample. They are further flagged according to their history of stable radio emission.

However, the clean sample does not meet the even sky distribution desirable. In order to densify the initial quasar list the sources failing to enter the clean sample are included, and accordingly flagged to, based on two additional tests. The assured quality of the single observation reported. The placement in the QSO color loci. These additional criteria involve a one-by-one examination of sources resulting to a slower pace of each decision. Currently about one thousand of objects are being examined.

2. OPTICAL CELESTIAL REFERENCE FRAME

The construction of the OCRF (Optical Celestial Reference Frame) starts from the updated and presumably complete VLQAC (Very Large Quasar Catalog) list of QSOs, initial optical positions for those quasars are found in the USNO B1.0 and GSC23 catalogues, and from the SDSS Data Release 5. The initial positions are next placed onto UCAC2 based reference frames, following by an alignment to the ICRF, as represented by the optical counterpart of ICRF sources as well as of the most precise sources from the VLBA calibrator list and from the VLA calibrator list. Finally the OCRF axis are surveyed through spherical harmonics, contemplating right ascension, declination and magnitude terms.

The OCRF contains 105,000 quasars, well represented on all-sky basis, from -88.5 to $+89.5$ degree

Catalog Name	A	B	C	D	E	F	G	H	I	J	K
A (ICRF)	717	643	582	377	72	6	27	232	333	500	480
B (VLBA)	-	3,358	1,598	1,577	288	33	71	375	911	2,034	1,964
C (VLA)	-	-	1,702	1,272	203	10	52	308	576	1,133	1,090
D (JVAS)	-	-	-	2,110	253	6	53	238	547	1 306	1 267
E(SDSS)	-	-	-	-	74,885	2,053	553	1,316	11,736	69,705	62,764
F (2QZ)	-	-	-	-	-	22,974	0	479	619	19,508	17,277
G(FIRST)	-	-	-	-	-	-	972	141	528	874	798
H(H. & B.)	-	-	-	-	-	-	-	7,259	904	2,225	2,087
I(2MASS)	-	-	-	-	-	-	-	-	13,499	13,086	12,601
J(GSC23)	-	-	-	-	-	-	-	-	-	90,550	77,722
K(B1.0)	-	-	-	-	-	-	-	-	-	-	81,233

Table 1: Characteristics of the catalogs participating in the VLQAC.

of declination, and with 0.5deg as the average distance between adjacent elements. The global alignment to the ICRF is of 1.5mas, and the individual position accuracies are represented by 80mas + 0.1R (where R is the red magnitude). As a by product, significant equatorial corrections appear for all the used catalogues (but the SDSS DR5); an empirical magnitude correction can be discussed for the GSC23 intermediate and faint regimens; both the 2MASS and the preliminary northernmost UCAC2 positions show consistent astrometric precision; and the harmonic terms come out as always small.

The OCRF contains J2000 referred equatorial coordinates, and is completed by redshift and photometry information from the VLQAC. It is aimed to be an astrometric frame, and the basis for the GAIA mission initial quasars' list. It can be used as a test bench for quasars' space distribution and luminosity function tests. The OCRF is meant to be updated when of the release of new quasar identifications and newer versions of the used astrometric frames. In the later case it can itself be used to examine the interrelations between those frames.

Figure 2 brings the performance of the local astrometric correction by the UCAC2, in the left plot; the performance of the different director cosines rotations onto the VLBI frame, in the central plot; and the amplitude of the spherical harmonics, in the right plot.

3. REFERENCES

Andrei, A.H., Souchay, J., Zacharias, N., Smart, R.L., de Cameargo, J.I.B., da Silva Neto, D.N., Vieira Martins, R., Assafin, M., Barache, C., Bouquillon, S., Penna, J.L.; 2007; "An Optical Representation of the ICRS" ; Astronomy and Astropysics, in preparation.

Boyle, B.J., Croom, S.M., Shanks, T., Outram, P.J., Smith, R.J., Miller, L., Loaring, N.S.; 2001; "The 2dF QSO Redshift Survey", A New Era in Cosmology, ASP Conference Proceedings, Vol. 283. Edited by Nigel Metcalfe and Tom Shanks. ISBN: 1-58381-126-5. San Francisco: Astronomical Society of the Pacific, 2002., p.72.

Cutri R.M., Skrutskie M.F., Van Dyk S., Beichman C.A., Carpenter J.M., Chester T., Cambresy L., Evans T., Fowler J., Gizis J., Howard E., Huchra J., Jarrett T., Kopan E.L., Kirkpatrick J.D., Light R.M, Marsh K.A., McCallon H., Schneider S., Stiening R., Sykes M., Weinberg M., Wheaton W.A., Wheelock S., Zacarias N.; 2003; "The 2MASS All-Sky Catalog of Point Sources"; University of Massachusetts and Infrared Processing and Analysis Center (IPAC/California Institute of Technology)

Drimmel, R., Bucciarelli, B., Lattanzi, M. G., Spagna, A., Jordi, C., Robin, A. C., Reyl, C., Luri, X.; 2005 ; "What Gaia Will See: All-Sky Source Counts from the GSC2", Proceedings of the Gaia Symposium "The Three-Dimensional Universe with Gaia" (ESA SP-576). Held at the Observatoire de Paris-Meudon, 4-7 October 2004. Editors: C. Turon, K.S. O'Flaherty, M.A.C. Perryman.

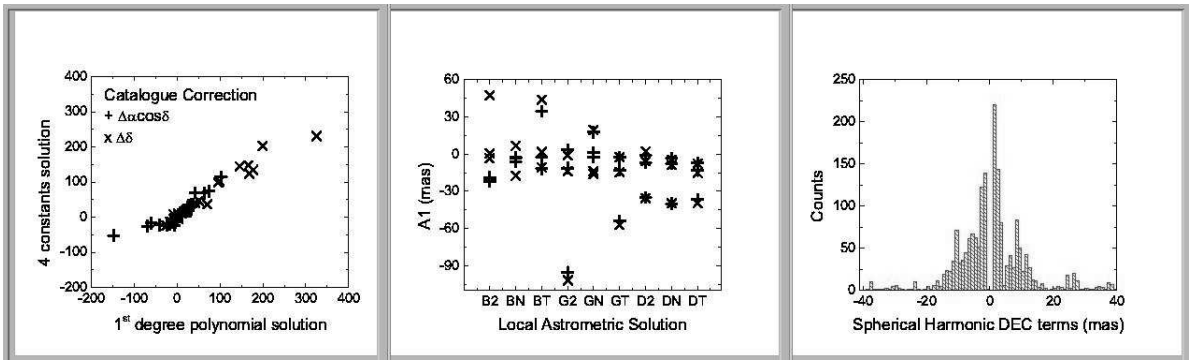

Figure 2: In the left plot, a comparison between the two representations used for the local astrometric correction towards the UCAC2 based frames. In the central plot, values obtained for the orientation angle A1 (rotation about the polar axis) from the different input (B-USNO B1.0, G- GSC23, D-SDSS DR5), different sets of coordinates (A, DEC, and both), and different local astrometric corrections ("+" $1s^{st}$ degree and "x" 4 constants). In the right plot, the amplitude of the significant spherical harmonics terms affecting the declination coordinates (the plot for RA is similar).

Kovalev, Y. Y.; Petrov, L.; Fomalont, E. B.; Gordon, D.; 2006; "The Fifth VLBA Calibrator Survey: VCS5", arXiv:astro-ph/0607524 and references there in

Ma, C., Arias, E. F., Eubanks, T. M., Fey, A. L., Gontier, A.-M., Jacobs, C. S., Sovers, O. J., Archinal, B. A., Charlot, P.; 1998; "The International Celestial Reference Frame as Realized by Very Long Baseline Interferometry", The Astronomical Journal, Volume 116, Issue 1, pp. 516-546.

McMahon, R.G., White, R.L., Helfand, D.J., Becker, R.H.; 2002; "Optical Counterparts for 70,000 Radio Sources: APM Identifications for the FIRST Radio Survey", The Astrophysical Journal Supplement Series, Volume 143, Issue 1, pp. 1-23.

Mignard, F.; 2001; "Observations of QSOs and Reference Frame with GAIA"; EAS Publications Series, Volume 2, Proceedings of "GAIA: A European Space Project", held 14-18 May, 2001 Les Houches, France. Edited by O. Bienaym and C. Turon. EDP Sciences, 2002, pp.327-339

Monet, D.G., Levine, S.E., Canzian, B., Ables, H.D., Bird, A.R., Dahn, C.C., Guetter, H.H., Harris, H.C., Henden, A.A., Leggett, S.K., and 19 coauthors; 2003; "The USNO-B Catalog", The Astronomical Journal, Volume 125, Issue 2, pp. 984-993.

National Radio Astronomy Observatory; 2006 "VLA Calibrator Manual", http://aips2.nrao.edu/vla/vlacalsearch.html.

Purger, N., Csabai, I., Budavri, T., Gyory, Z.; 2006; "Photometric Redshifts For The SDSS Data Release 5", The Virtual Observatory in Action: New Science, New Technology, and Next Generation Facilities, 26th meeting of the IAU, Special Session 3, 17-18, 21-22 August, 2006 in Prague, Czech Republic.

Souchay, J., Andrei, A.H., Barache, C., Bouquillon, S., Suchet, D., Baudin, M., Gontier, A.-M., Lambert, S., Le Poncin-Lafitte, C., Taris, F., Arias F.E.; 2007; "The construction of the Very Large Quasar Catalog (VLQAC)"; Astronomy and Astropysics, in preparation.

Véron-Cetty, M.-P., Véron, P. ; 2006 ; "A catalogue of quasars and active nuclei: 12th edition", Astronomy and Astrophysics, Volume 455, Issue 2, August IV 2006, pp.773-777.

Zacharias N., Urban S.E., Zacharias M.I., Wycoff G.L., Hall D.M., Germain M.E., Holdenried E.R., Winter L.; 2004; "The Second U.S. Naval Observatory CCD Astrograph Catalog (UCAC2)"; The Astronomical Journal, Volume 127, pp 3043-3059.

Wilkinson, P. N., Browne, I. W. A., Patnaik, A. R., Wrobel, J. M., Sorathia, B., 1998; "Interferometer phase calibration sources - III. The regions +20 <= $delta_B$1950 <= +35 deg and +75 <= $delta_B$1950 <= +90 deg" and references there in (the JVAS list can be accessed from ftp://ftp.aoc.nrao.edu/pub/sources.jvas)

A VLBI SURVEY OF WEAK EXTRAGALACTIC RADIO SOURCES FOR THE ALIGNMENT OF THE ICRF AND THE FUTURE GAIA FRAME

G. BOURDA[1], P. CHARLOT[1], R. PORCAS[2], S. GARRINGTON[3]

[1] Laboratoire d'Astrophysique de Bordeaux (LAB),
Observatoire Aquitain des Sciences de l'Univers (OASU),
Université Bordeaux 1, CNRS
BP89, 33270 Floirac, France
e-mail: Geraldine.Bourda@obs.u-bordeaux1.fr

[2] Max Planck Institute for Radio Astronomy
P.O. Box 20 24, 53010 Bonn, Germany

[3] Jodrell Bank Observatory, The University of Manchester
Macclesfield, Cheshire, SK11 9DL, UK.

ABSTRACT. The space astrometry mission GAIA will construct a dense optical QSO-based celestial reference frame. For consistency between the optical and radio positions, it will be important to align the GAIA frame and the International Celestial Reference Frame (ICRF) with the highest accuracy. Currently, it is found that only 10% of the ICRF sources are suitable to establish this link, either because they are not bright enough at optical wavelengths or because they have significant extended radio emission which precludes reaching the highest astrometric accuracy. In order to improve the situation, we have initiated a VLBI survey dedicated to finding additional high-quality radio sources for aligning the two frames. The sample consists of about 450 sources, typically 20 times weaker than the current ICRF sources, which have been selected by cross-correlating optical and radio catalogues. The paper presents the observing strategy and includes preliminary results of observation of 224 of these sources with the European VLBI Network in June 2007.

1. CONTEXT

The ICRF (International Celestial Reference Frame; Ma et al. 1998; Fey et al. 2004) is the fundamental celestial reference frame adopted by the International Astronomical Union (IAU) in August 1997. It is currently based on the VLBI (Very Long Baseline Interferometry) positions of 717 extragalactic radio sources, estimated from dual-frequency S/X (2.3 and 8.6 GHz) observations. The European space astrometry mission GAIA, to be launched by 2011, will survey about one billion stars in our Galaxy and 500 000 Quasi Stellar Objects (QSOs), brighter than magnitude 20 (Perryman et al. 2001). Unlike Hipparcos, GAIA will construct a dense optical celestial reference frame directly in the visible, based on the QSOs with the most accurate positions (i.e. those with optical apparent magnitude $V \leq 18$; Mignard 2003). In the future, the alignment of the ICRF and the GAIA frame will be crucial for ensuring consistency between measured radio and optical positions. This alignment, to be determined with the highest accuracy, requires hundreds of sources in common, with a uniform sky coverage and very accurate radio and optical positions. Obtaining such accurate positions implies that the link sources must have $V \leq 18$ and no extended VLBI structures.

In a previous study, we investigated the current status of this link based on the present list of ICRF sources (Bourda et al. 2008). We found that although about 30% of the ICRF sources have an optical counterpart with $V \leq 18$, only one third of these are compact enough on VLBI scales for the highest astrometric accuracy. Overall, only 10% of the current ICRF sources ($\simeq$70 sources) are thus available for the alignment with the GAIA frame. This highlights the need to identify additional suitable radio sources, which is the purpose of the project described here.

2. STRATEGY TO IDENTIFY NEW LINK RADIO SOURCES

Searching for additional radio sources suitable for aligning accurately the ICRF and the GAIA frame implies going to weaker radio sources having flux densities typically below 100 mJy. This can now be realized owing to recent increases in the VLBI network sensitivity (e.g. recording now possible at 1Gb/s) and by using a network comprising large antennas like the European VLBI Network (EVN).

A sample of about 450 radio sources, for which there are no published VLBI observations, was selected for this purpose by cross-identifying the NRAO VLA Sky Survey (NVSS; Condon et al. 1998), a deep radio survey (complete to the 2.5 mJy level) which covers the entire sky north of $-40°$, with the Véron & Véron (2006) optical catalogue. This sample is based on the following criteria: $V \leq 18$ (to ensure very accurate positions with GAIA), $\delta \geq -10°$ (for possible observing with northern VLBI arrays), and NVSS flux density ≥ 20 mJy (for possible VLBI detection).

The observing strategy to identify the most appropriate link sources from this sample includes three successive steps to detect, image and measure accurately the astrometric position of these sources: (i) to determine the VLBI detectability of these weak radio sources; (ii) to image and determine an accurate astrometric position for the sources detected in the first step; and (iii) to refine the astrometry for the most compact sources of the sample.

3. INITIAL VLBI RESULTS

The first observations for this project (experiment EC025A) were carried out in June 2007, with a network of four EVN telescopes (i.e. Effelsberg, Medicina, Noto, Onsala). Half of our sample (i.e. 224 target sources, most of which belong to the CLASS catalogue; Myers et al. 2003) was observed during this experiment to determine their VLBI detectability (step 1 described above). The rest of the sources were observed in October 2007.

Our results for EC025A indicate excellent detection rates of 99% at X band and 95% at S band, with 222 sources and 211 sources detected at X and S bands, respectively. The mean correlated flux densities have a median value of 32 mJy at X band and 55 mJy at S band (see Figure 1). In Figure 2, the comparison of the X-band flux density distribution for the EC025A, VCS (Beasley et al. 2002; Fomalont et al. 2003; Petrov et al. 2005, 2006; Kovalev et al. 2007) and ICRF sources shows that the sources of our sample are indeed much weaker. The average flux density of the sources detected in EC025A is 20 times and 7 times weaker than those of the ICRF and VCS sources, respectively.

The spectral index α of the 211 radio sources detected at both frequencies was also investigated. This parameter is defined by $S \propto \nu^{\alpha}$, where S is the source flux density and ν is the frequency. Its median value is -0.3 and most of the sources have $\alpha > -0.5$, hence indicating that they must have a dominating core component, which is very promising for the future stages of this project.

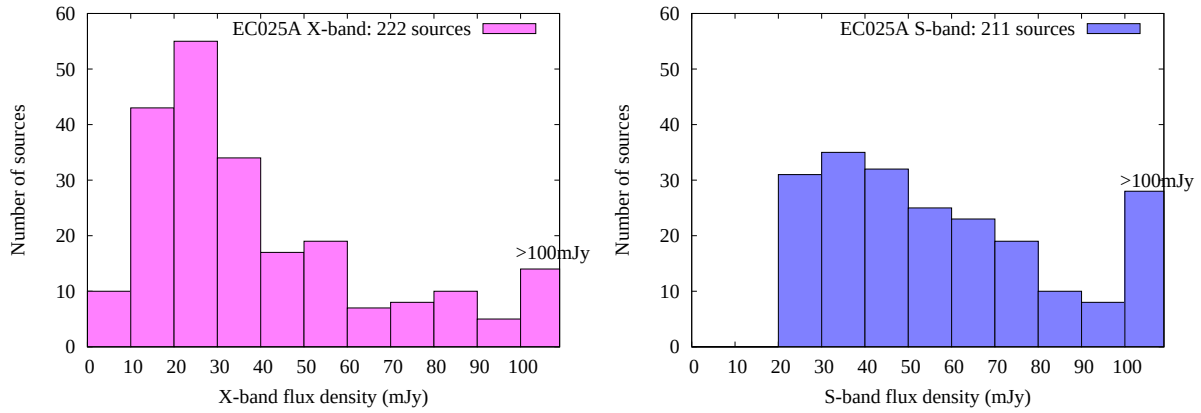

Figure 1: Mean correlated flux density distribution (units in mJy), at X band and S band, for the sources detected in our initial experiment (EC025A) conducted in June 2007.

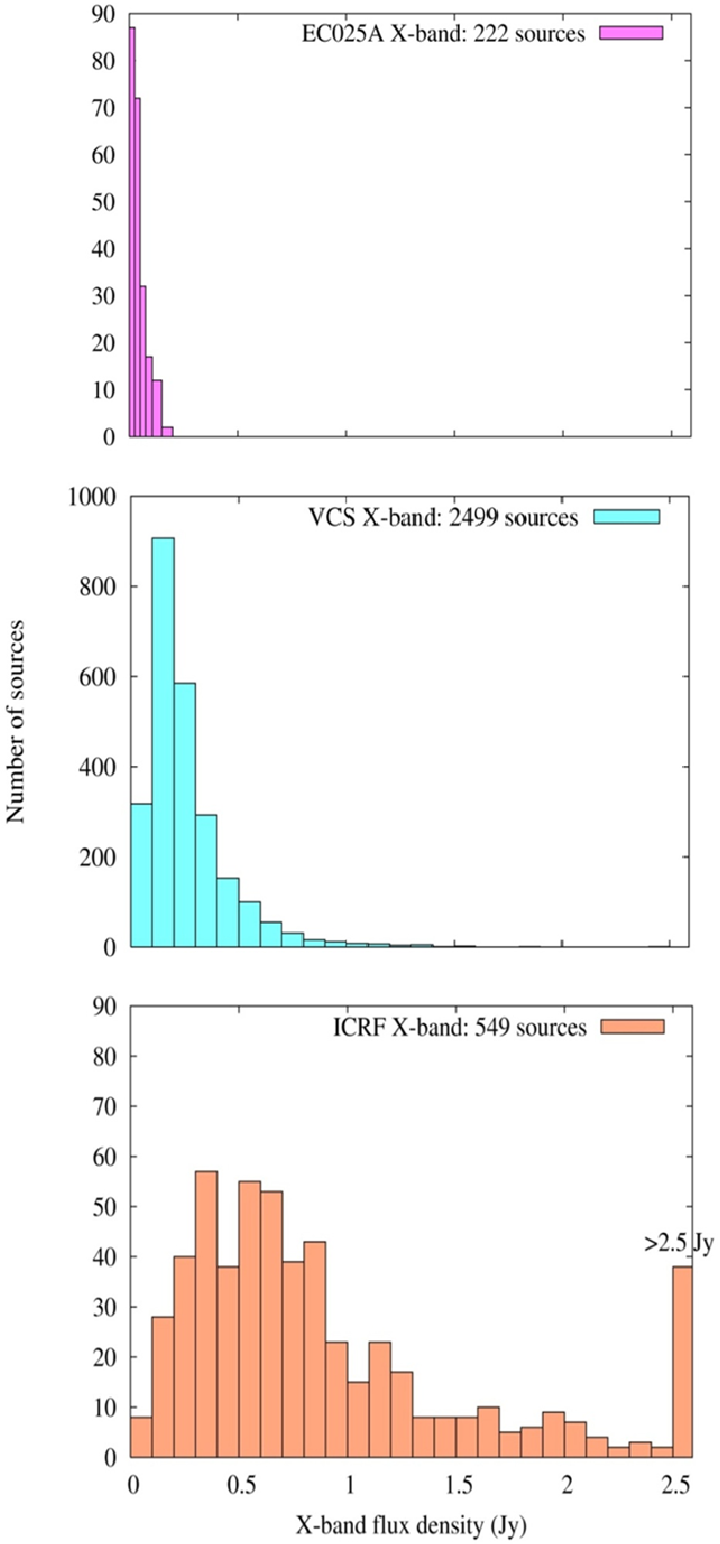

Figure 2: Comparison of the X-band flux density distribution (units in Jy) for the sources detected in EC025A and those from the VCS and ICRF catalogues.

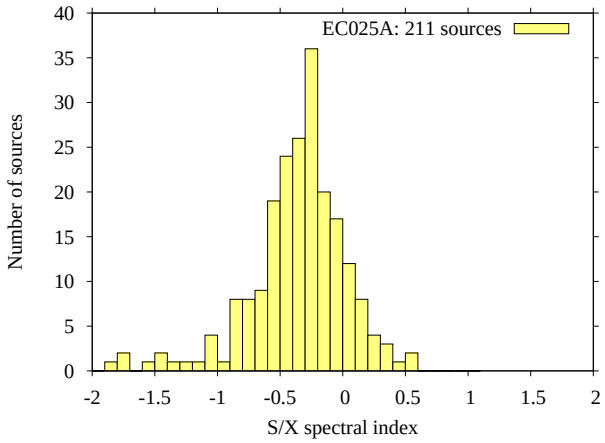

Figure 3: S/X spectral index distribution for the 211 weak extragalactic radio sources detected at both S and X bands during EC025A.

Acknowledgements. This work has benefited from research funding from the European Community's sixth Framework Programme under RadioNet R113CT 2003 5058187. The authors acknowledge the EVN, which is a joint facility of European, Chinese, South African and other radio astronomy institutes funded by their national research councils. They also thank Dave Graham for assistance with the correlation in Bonn, and John Gipson for advice when scheduling the observations. The first author would like to thank the CNES (Centre National d'Etudes Spatiales, France) for the post-doctoral position granted at LAB.

4. REFERENCES

Bourda, G., Charlot, P., & Le Campion, J.-F., 2008, "Astrometric suitability of optically-bright ICRF sources for the alignment of the ICRF with the future GAIA celestial reference frame", A&A , submitted.

Beasley, A.J., Gordon, D., Peck, A.B., Petrov, L., MacMillan, D.S., et al., 2002, "The VLBA Calibrator Survey-VCS1", Astrophy. J. Supp. Series 141, pp. 13–21.

Condon, J.J., Cotton, W.D., Greisen, E.W., Yin, Q.F., Perley, R., et al., 1998, "The NRAO VLA Sky Survey", AJ 115, pp. 1693–1716.

Fey, A.L., Ma, C., Arias, E.F., Charlot, P., Feissel-Vernier, M., et al., 2004, "The Second Extension of the International Celestial Reference Frame: ICRF-EXT.1", AJ 127, pp. 3587–3608.

Fomalont, E.B., Petrov, L., MacMillan, D.S., Gordon, D., & Ma, C., 2003, "The Second VLBA Calibrator Survey: VCS2", AJ 126, pp. 2562–2566.

Kovalev, Y., Petrov, L., Fomalont, E., & Gordon, D., 2007, "The Fifth VLBA Calibrator Survey: VCS5", AJ 133, pp. 1236–1242.

Ma, C., Arias, E.F., Eubanks, T.M., Fey, A.L., Gontier, A.-M., et al., 1998, "The International Celestial Reference Frame as Realized by Very Long Baseline Interferometry", AJ 116, pp. 516–546.

Mignard, F., 2003, "Realization of the inertial frame with GAIA", in: R. Gaume, D. McCarthy & J. Souchay (eds.), IAU 25 Joint Discussion 16: The International Celestial Reference System, Maintenance and Future Realizations, pp. 133–140.

Myers, S.T., Jackson, N.J., Browne, I.W.A., de Bruyn, A.G., Pearson, T.J., et al., 2003, "The Cosmic Lens All-Sky Survey - I. Source selection and observations", MNRAS 341, pp. 1–12.

Perryman, M.A.C., de Boer, K.S., Gilmore, G., Hog, E., Lattanzi, M.G., et al., 2001, "GAIA: Composition, formation and evolution of the Galaxy", A&A 369, pp. 339–363.

Petrov, L., Kovalev, Y., Fomalont, E., & Gordon, D., "The Third VLBA Calibrator Survey: VCS3", 2005, AJ 129, pp. 1163–1170.

Petrov, L., Kovalev, Y., Fomalont, E., & Gordon, D., "The Fourth VLBA Calibrator Survey: VCS4", 2006, AJ 131, pp. 1872–1879.

Véron-Cetty, M.-P., & Véron, P., 2006, "A catalogue of quasars and active nuclei: 12th edition", A&A 455, pp. 773–777.

ANALYSIS OF ASTROMETRIC POSITION TIME SERIES FOR ICRF-2

A.L. FEY & D.A. BOBOLTZ
U.S. Naval Observatory
3450 Massachusetts Avenue, NW
Washington, DC 20392-5420 USA
e-mail: afey@usno.navy.mil, dboboltz@usno.navy.mil

ABSTRACT. A second realization of the International Celestial Reference Frame, ICRF-2, is currently underway with a projected completion date concurrent with the 2009 IAU General Assembly. This work is being carried out by two working groups: the IERS/IVS Working Group will generate ICRF-2 from VLBI observations of extragalactic radio sources, consistent with the current realization of the ITRF and EOP data products and the IAU working group will oversee the generation of ICRF-2. Of primary importance to this work is the selection of a set of defining sources to be used to orient the ICRF-2 axes. These sources should be as positionally stable as can be determined with existing data and analysis. It is well known that compact extragalactic sources have variable and unpredictable emission structures on scales larger than the accuracy of their position estimates. Temporal variations of the intrinsic structure of these objects results in apparent motion when astrometric observations are made at several epochs. Generation and analysis of position time series is one method to address this issue. **Here we compare two methods for generation of position time series**.

1. PARAMETRIZATION OF TWO SOLUTIONS

Table 1: Parameters of Two Solutions

	usn000d	**usn001a**
Software	CALC/SOLVE	CALC/SOLVE
Data Used	1979-2007	1979-2007
Sessions	4170	4170
Observations	5238056	5238056
Solution Type	Baseline	Independent
No.of Solutions	8	4170
Reference Frame	NNR wrt ICRF	usno2007b
Atmosphere	20 min	20 min
Clocks	60 min	60 min
Gradients	6 hrs	6 hrs
Stations	Local	Fixed[a]
Sources	Global/$\frac{1}{8}$ Local	Local
EOP	Fixed[b]/UT1 Rates	Fixed[a]
Nutation	Offsets	No

[a] usno2007b
[b] Bulletin A

Two sets of global solutions using the CALC/SOLVE software were produced. Parametrization of the **usn000d** solution set followed that of the ICRF. The **usn001a** solution set consisted of 4170 "independent" solutions with fixed TRF and fixed EOP. Parametrization of the two solution sets is listed in Table 1. The only free parameters in the usn001a solution set were clocks, atmosphere including gradients and source positions.

2. ANALYSIS AND RESULTS

Table 2: Differences between Weighted Mean Positions and ICRF-Ext.2

	Matching	Weighted Mean±WRMS (μas)		Median (μas)	
Series	Sources	$\alpha\cos\delta$	δ	$\alpha\cos\delta$	δ
usn000d	679	15 ± 117	-29 ± 137	15	-20
usn001a	679	55 ± 193	-80 ± 244	69	-48

Table 3: Statistics of Time Series for Sources with $N_{epochs} \geq 10$

		Mean/Median of WRMS (μas)	
Series	No. Sources	$\alpha\cos\delta$	δ
usn000d	588	400/297	534/417
usn001a	588	672/417	880/664

Positions estimated in the two solutions were compared. The following preliminary conclusions can be drawn from these comparisons:

- Positions (weighted mean) derived from the usn000d time series agree more closely with ICRF-Ext.2 than those from usn001a (see Table 2)
- Positions from usn001a show more scatter than those from usn000d. The wrms scatter of positions is larger, on average, by about a factor of 1.7 (see Table 3)
- Although usn001a estimates position time series using a consistent TRF and EOP with no required NNR constraint on source positions, the resultant increased noise in the solution suggests that the parametrization of the usn000d solution is preferable
- The increased noise in the usn001a position time series is presumably due to the decrease in the number of free parameters in the solution and hence fewer un-modeled or mis-modeled parameters get absorbed elsewhere

STABLE RADIO SOURCES AND REFERENCE FRAME

A.-M. GONTIER, S.B. LAMBERT
SYRTE, Observatoire de Paris
61 av. de l'Observatoire F-75014 Paris
e-mail: anne-marie.gontier@obspm.fr, sebastien.lambert@obspm.fr

ABSTRACT. The analysis of geodetic VLBI sessions since the early days of VLBI allows one to get time series of radio source coordinates. The analysis of these time series in terms of time stability can help us in our quest for a subset of radio sources suitable for defining the axes of the next ICRF. What we do here is (i) to compute the time series, (ii) to select the most stable sources, and (iii) to assess that the reference frame as defined with these sources is more stable than the previously defined ICRF.

1. THE TIME SERIES AND THEIR SEMI-ANNUAL REPRESENTATIONS

We investigate time series of 521 sources having more than 10 observations between 1984.0 and 2007.5. Their characteristics are reported in Fig. 1. One sees the dependence of the noise and of the slope in declination, likely a consequence of the mis-corrected troposphere effect. It appears also that the time series are so noisy or sparse that only two statistical quantities can immediately be extracted (without refinement) with a good reliability (i) a (weighted) rms, and (ii) an irregular pattern, that can be obtained by filtering or by building (weighted) normal points at regular time intervals. For the latter item, we construct semi-annual normal points by taking the weighted mean of all data contained in a 1-yr interval around the epoch. Their associated uncertainty is simply the weighted rms of the same data.

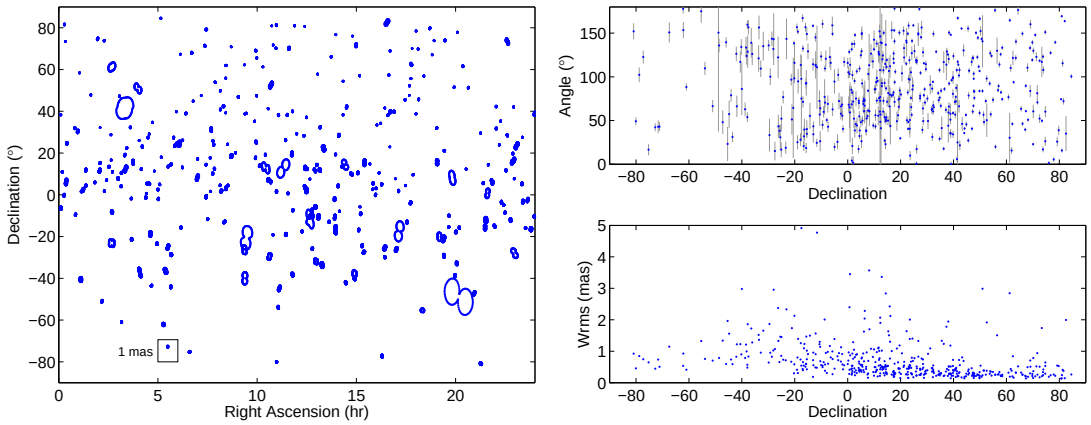

Figure 1: Left: Envelopes of variability (defined as the rms in a given direction) of the 521 radio sources investigated in this study. Top: Dependence of the angle of maximal variability with the declination. Bottom: Dependence of the rms on the declination.

2. STABLE SOURCES SELECTION SCHEME

We apply a simple selection scheme only playing with the rms and the slope. A source cannot actually be rejected only because of a high rms: if its position varies uniformly around the mean position, the net position of the source over a global analysis of a large number of sessions will be zero. However, an irregular pattern is a sign of danger: the source position can move away from the mean position during a long period of time and drive away the CRF axes during this period. Such a behavior is detectable by comparing the rms of the session time series against the rms of the normal points time series: indeed, in the latter case, the rms should remain high if an irregular pattern is present. If the period of time on which the irregular pattern shows up is sufficiently long compared to the complete time span of the global

analysis, the irregular pattern should appear as a slope. When the slope is not extreme (a phenomenon due either to a real, huge drift of the source or to an important lack of data) the relevant quantity to be estimated is the ratio of the slope by its uncertainty. A quite large slope associated with a large uncertainty does not mean that the slope is significant. Inversely, a slope having a small uncertainty means a violent underlying physical process moving the radio center away, and that the source have to be taken with great care (and even rejected!). In our investigation, the selection parameters have been tuned so that the number of elected sources reaches 200. Our subset contains 197 sources, of which 32% are in the 212 ICRF defining sources (Ma et al. 1998) and 68% in the 247 stable sources of Feissel-Vernier et al. (2006, referred to as MFV).

3. CHECKING THE STABILITY OF THE REFERENCE FRAME

The axis stability of the reference frame defined by the above-selected sources is assessed using the normal point time series. Four parameters of transformation between a semi-annual reference frame (defined by the semi-annual coordinates of the selected radio sources, if observed at the considered epoch) and a reference catalogue (here, the ICRF-Ext.2 of Fey et al. 2004) are computed. The relevant quantities to be examined are the relative variations of the four parameters from one to another epoch. The same computation is also done for two well-known subsets: the 212 ICRF defining sources and the 247 of MFV (Fig. 2). It appears that our selection of sources leads to significantly better stabilities for the angles A1 and A2 and for the tilt parameter dz compared to previously done selections (ICRF and MFV). For A3, MFV appears to be better than us. This study shows that the investigation of time series of radio source coordinates can give an interesting selection of sources suitable for defining a stable reference frame. It is obvious that this selection must supplemented by other selections done through other criteria (e.g., source compactness), particularly since our selection yields a poor number of sources in the southern hemisphere.

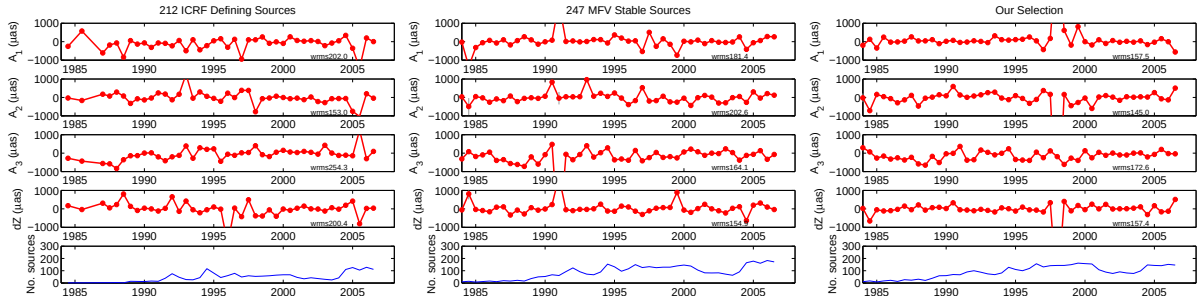

Figure 2: Transformation parameters between semi-annual reference frames with axes defined by the 212 ICRF defining sources, the MFV sources and our selection, respectively, as an illustration of the stability of the celestial reference frame.

4. REFERENCES

Feissel-Vernier, M., Ma, C., Gontier, A.-M., & Barache, C. 2006, Analysis issues in the maintenance of the ICRF axes, A&A 452, 1107

Fey, A.L., Ma, C., Arias, E.F., et al. 2004, The Second Extension of the International Celestial Reference Frame: ICRF-EXT.1, AJ 127, 3785

Ma., C., Arias, E.F., Eubanks, T.M., et al. 1998, The International Celestial Reference Frame as realized by very long baseline interferometry, A&A 116, 516

SOURCE POSITIONS TIME SERIES GENERATION AND ANALYSIS

S.L. KURDUBOV, E. SKURIKHINA
Institute of Applied Astronomy RAS
nab. Kutuzova, 10 St. Petersburg 191187 Russia
e-mail: ksl@ipa.nw.ru, sea@ipa.nw.ru

ABSTRACT. Time series for more than 600 sources were calculated with using QUASAR software from VLBI data processing. Source positions for every sources were obtained from single series analysis by two ways - with fixed coordinates of all another sources with and without EOP estimation.Time series analysis is performed with covariation analysis technique. The attempt was made to propose the parameter which can be used for selection of stable and unstable sources from analysis of source positions time series.

The main goal of this study is to propose the parameter which can be used for selection of stable and unstable sources from analysis of source positions time series. We suppose that white noise in source position time series mostly appears from the instrumental effects and thus the only variance is not good characteristic of source stability. We calculate the covariance function for time series and try to use second point of it as the characteristic parameter. Its value shows ho much the time series was correlated and does not matter that way it was correlated the random walk or piece-wise linear or some else.

Source positions time series iaa000b, iaa000c were calculated with using the software QUASAR created in IAA RAS in 2002 (Gubanov V. at all, 2002) and developed further in 2004-2006 (Gubanov V. at all, 2004, Gubanov V., 2004, Kurdubov S., 2007)). Most available VLBI observations (excluding DSN and VCS sessions) since August 1979 to May 2007 were used. Time series were generated from single session solution for every sources: one source for the session, coordinates of all another sources were fixed. Station positions were not estimated for both series. TRF was fixed by ITRF2005, CRF was fixed by ICRF-Ext.2(A. Fey¡ 2004). The next parameters were estimated in this solutions: position of one source, EOP (X_p,Y_p,UT1–UTC,X_c,Y_c)(only for iaa000b solution), WZD (linear trend and stochastic), troposphere gradient east and north, station clock offset (quadratic trend and stochastic).

We use the covariance function for analysis obtained time series. Because there are no conventional algorithm for obtaining covariance functions of non equidistant time series we use the follows two methods:

First method

For non equidistant time series:

$$\{x_i\}_{i=1}^{N},\ x_i = x(t_i),\ t_1 < t_2 < ... < t_N,\ i = 1, ..., N. \tag{1}$$

Estimation of the covariance function for equidistant time shifts:

$$\tau_k = \Delta\tau \cdot k,\ \Delta\tau = \frac{t_N - t_1}{M}, k = 0, ..., M-1,\ M < N.$$

was calculated by formula

$$q(\tau_k) = \frac{M-k}{M}\left(\sum_{i,j:\tau_k<|\gamma_{ij}|<\tau_{k+1}} x_i x_j\right)/m_k, k = 0, 1, ..., M-1.$$

here $\gamma_{ij} = t_i - t_j$, and m_k - number of γ_{ij} in the range from τ_k to τ_{k+1}. The $\Delta\tau$ was choosen 14 days.

Second method

Estimation of the covariance function q_k for not equidistant averaged time shifts τ_k:

$$q_k = \frac{\sum_{j=k+1}^{N-k} x_{k+j}x_j}{N},\ \ \tau_k = \frac{\sum_{j=k+1}^{N-k}(t_{k+j} - t_j)}{N-k},\ k = 0, 1, 2, ..., N-1. \tag{2}$$

By this ways we obtained covariance functions for all time series of all centers (these data will be available on the ftp server Next ICRF2 WG). The covariance functions for long time series were similar and in further computations we use the first one.

For the further analysis we use the values q_1 — the second point of covariance function. The first point q_0 is variance of the time series. But second point characterizes the variance of the correlated part in the time series.

We suppose that white noise in source position time series mostly appears from the instrumental effects and thus the only variance is not good characteristic of source stability. The second point of covariance function shows how much the time series are correlated and does not matter the origin of correlation the random walk or piece-wise linear or some else.

We calculate the coefficient $k = Max(q_1^{RA*cos(DE)}, q_1^{DE})$ for each time series and use it to apprise how much stable the sources is. In Table 1 are shown the most stable sources by this criteria ($k < 0.1$) and in Table 2 most unstable ($k > 0.5$). The 15 sources form Table 1 are presented in M. Feissel list of stable sources and 4 sources from Table 2 in unstable list.

Source	N_{sess}	k	Source	N_{sess}	k	Source	N_{sess}	k
1351-018	489	0.040	1255-316	121	0.078	1908-201	386	0.096
0111+021	109	0.048	1606+106	1854	0.082	0743+259	400	0.096
1128+385	955	0.049	1652+398	218	0.087	0642+449	937	0.096
2318+049	426	0.060	0556+238	385	0.089	0804+499	1115	0.096
0201+113	378	0.065	1417+385	173	0.091	0602+673	328	0.097
2209+236	139	0.068	1144+402	93	0.093	0749+540	630	0.098
0133+476	1027	0.076	0657+172	112	0.095			

Table 1: Most stable sources ($k < 0.1$)

Source	N_{sess}	k	Source	N_{sess}	k	Source	N_{sess}	k
0355+508	269	0.556	1354+195	78	0.688	1642+690	96	0.852
2128-123	558	0.573	1053+815	351	0.725	1253-055	140	1.212
1641+399	813	0.575	2007+777	224	0.777	0316+413	96	1.305
1226+023	709	0.581	1313-333	99	0.835			

Table 2: Most unstable sources ($k > 0.5$)

The main disadvantage of this method is that in can be applied only to the sources with at least hundred sessions.

REFERENCES

Gubanov, V., Surkis, I., Vereshagina, I., Rusinov, Yu. QUASAR Software. Parts I-IY // IAA Communications, 2002, P. 141-145.

Gubanov, V., Rusinov, Yu., Surkis, I., Kurdubov, S., Shabun, C.: Project: Global Analysis of 1979-2004 VLBI Data // Proc. IVS 2004 General Meeting (eds. N. Vandenberg and K. Baver), NASA, 2004, P. 315-319.

Fey, A. et al. The Second Extension of the International Celestial reference Frame: ICRF-Ext.2 // A.J., 127, 2004. P. 3587-3608.

Kurdubov, S., QUASAR software in IAA EOP service: Global Solution and Daily SINEX //EWGA Proceedings, 2007, ISSN 1811-8380, ed. J. Boem, A. Pany, H Schuh, p.79-81.

Kurdubov, S., Covariation analysis of the VLBI observations model stochastical parameters. IAA Works, No. 14, S.-Pb, 2006, 138-157. (in Russian)

Feissel-Vernier, M. (2003): Selecting stable extragalactic compact radio sources from the permanent astrogeodetic VLBI program, In: Astronomy and Astrophysics manuscript no. MS3523, March 10, 2003

PRECESSIONAL PARAMETERS OBTAINED FROM BIASED DATA OF HIPPARCOS-FK5 PROPER MOTIONS

M.J. MARTINEZ[1], F.J. MARCO[2], J.A. LOPEZ[2]
[1] Universidad Politcnica de Valencia, Dep. Matemtica Aplicada, E.T.S.I.I, Valencia, Spain
e-mail: mjmartin@mat.upv.es
[2] Uiversidad Jaume I, Dep. Matemticas
e-mail: marco@mat.uji.es, lopez@mat.uji.es

ABSTRACT. The Hipparcos catalogue provides a reference frame in optical wavelength for the new ICRS. The differences in the system of proper motions of Hipparcos and the previous materialization of the reference frame, the FK5, are expected to be caused only by the combined effects of the motion of the equinox of the FK5 as well as the Luni-solar and planetary precession, but several authors have signaled the existence of an inconsistency for the proper motion differences of the FK5-Hipparcos with the Δp values corresponding to the Luni-solar precession as determined from VLBI and LLR It is a fact that the widely employed parametric models do not remove the bias in the random variables. The introduction of a non parametric method, combined with the inner product in L^2 over S^2 shows the necessity of removing the bias. The precessional formulas should be rearranged to be used in this case. When applying this model, the obtained values for the precession corrections are very consistent with the ones currently adopted by the IAU.

1. INTRODUCTION

The study of the proper motion differences of the FK5-Hipparcos with the Δp value corresponding to the Luni-solar precession as determined from VLBI and LLR has revealed an inconsistency which has been explained, for example, by Walter & Herring (2005) due to errors of the FK5 proper motions caused by the galactic rotational effects and by slightly biased Hipparcos proper motions; Zhu (2000) suggested that one of the reasons for these discrepancies could be the internal biased proper motion system of the FK5. The question of the study of how to deal with the real data when bias exist has been developed in depth in Marco et al. (2004), where we propose a modification of the usual model to study the rotation between catalogues in order to remove the bias in proper motions following a GLAD model:

$$\begin{array}{c} \Delta\mu_\alpha \cos\delta = \Delta\dot{A} - \widetilde{w}_x \cos\alpha \sin\delta - \widetilde{w}_y \sin\alpha \sin\delta + \\ \widetilde{w}_z \cos\delta \\ \Delta\mu_\delta = \Delta\dot{D} + \widetilde{w}_x \sin\alpha - \widetilde{w}_y \cos\alpha \end{array} \quad (1)$$

This model is an auxiliary tool to deal with the data without trying to obtain any physical explanation

2. PRECESSION FROM HIPPARCOS AND FK5 PROPER MOTIONS

The angular rates of rotation spins w_x, w_y, and w_z allow us to obtain information about the Luni-solar precession according to the relationships (Fricke, 1977):

$$w_x = 0 \quad (2)$$
$$w_y = -\Delta p \sin\varepsilon \quad (3)$$
$$w_z = \Delta p \cos\varepsilon - (\Delta\lambda + \Delta e) \quad (4)$$

Δp is the Luni-solar precession, $\Delta\lambda$ is the planetary precession and Δe is the fictitious motion of the equinox Notice that w_x, w_y, and w_z represent the spins if we suppose that there is no bias in the data. We can not apply these formulas due to the fact that our model (1) contains two additional parameters to remove the bias, so the angles obtained are not exactly these ones. An homogeneous net of points over the whole sphere makes possible the use of statistic and numerical methods in order to contrast the

	$\widetilde{w}_x$	$\widetilde{w}_y$	$\widetilde{w}_z$	$\Delta\dot{A}$	$\Delta\dot{D}$
Statistical	0.3948	-0.5931	-2.1073	1.0029	0.2031
Numerical	0.4083	-0.5741	-1.9707	0.8769	0.2735

Table 1: Spin values for the FK5-Hipparcos proper motions comparison. Statistical stands for the direct application of (1) over 1277 common stars of Hipparcos and FK5; Numerical stands for the independent verification explained in Marco et al. (2004)

results: using KNP (a Kernel non parametric method, see Wand & Jones (1995) and $\Phi_y = -cos\alpha sin\delta$ and taking into account that $(KNP, Y_{21}) = w_y(\Phi, Y_{21})$ (see Marco et al. 2004), where (,) represents the usual inner product and $Y_{21} = 3sin\alpha sin\delta$ element of the functional basis of L^2 in S^2 functions (see for a further development of this method)

Using SH_2 (SH_2 denotes the development in spherical harmonics truncated at second order) and Φ_y and taking into account that $c_21(Y_21, Y_21) = w_y(\Phi_y, Y_21)$, (see Marco et al. (2004) where c_{21} represents the coefficient for the Y_{21} function in the development. So, we applied a KNP model and then we used formula (20) from Marco et al. (1996) over the points to numerically obtain the parameters (which are listed as 'numerical' in Table 1) At this stage, it is not possible to obtain the precessional parameters directly from these values and (3), (4) and (5). Instead, we need to obtain the 'inducted' values for these angles. As showed in Marco et al. (1996), the 'inducted' value w_z as deducted from the GLAD model is:

$$w_y = \Delta\dot{D} - \frac{\widetilde{w}_z sin(2\varepsilon)}{2} \tag{5}$$

As far as we have defined the residuals over the whole sphere it is possible to check the accuracy of the w_y value applying other independent methods. To this aim we use the KNP and the SH_2 methods to obtain a w_y value, from which we easily obtain Δp then, taking into account the evident relationship $w_z = \Delta\dot{A} + \widetilde{w}_z$ we obtain w_z and finally from (5), we compute Δe
The resulting values obtained using the statistical and the numerical methods are listed in Table 1.

3. CONCLUSIONS

The values for the correction of precession obtained from the GLAD model as inducted by a previous global KNP model are in very good agreement with the optimum values as obtained from VLBI and LLR, on the contrary of what happens when bias are not considered. The use of a model that not considers bias in this case is not adequate, and the conclusions derived from it are erroneous.

Acknowledgements. Part of this work was supported by a grant P1-1B2003-12 and P1-1B2006-11 from Fundacio Caixa Castello BANCAIXA and GV05/004 from the Generalitat Valenciana.

4. REFERENCES

Fricke, W. 1977. Basic Material for the Determination of Precession and of Galactic Rotation and a Rewiew of methods and Results. (Veröffentlichungen Astronomishes Rechen-Institut Heilderberg: G. Braun, Karlsruhe), No 28, 52
Marco F.J. et al 1996, IAU Symp 172, 487
Marco F.J. et al. 2004, A&A, 418,1159
Walter H.R., & Hering R. 2005. A&A, 431, 721
Wand M.P. & Jones M.C. 1995, "Kernel Smoothing", Chapman & Hall
Zhu Z. 2000. PASP, 112,1103

A STUDY OF VLBI2010 POTENTIAL FOR SOURCE STRUCTURE CORRECTIONS

W.T. PETRACHENKO[1], P. CHARLOT[2], A. COLLIOUD[2],T. HOBIGER[3], A.E.E. Niell[4]
[1] Geodetic Survey Division, NRCan
e-mail: Bill.Petrachenko@nrc-cnrc.gc.ca
[2] Observatoire de Bordeaux - CNRS/UMR 5804
e-mail:Patrick.Charlot@obs.u-bordeaux1.fr
e-mail:Arnaud.Collioud@obs.u-bordeaux1.fr
[3] Kashima Space Research Center, NICT
e-mail: hobiger@nict.go.jp
[4] MIT Haystack Observatory
e-mail: aniell@haystack.mit.edu

ABSTRACT. In October 2003, the International VLBI Service for Geodesy and Astrometry (IVS) installed Working Group 3 'VLBI2010' to examine current and future requirements for geodetic/astrometric VLBI including all components from antennas to analysis, and to create recommendations for a new generation of VLBI systems. Some important recommendations include: the use of larger networks; the use of smaller faster slewing antennas; the use of very high data rates; and, the use of multiple (e.g. 4) widely spaced bands to resolve RF phase ambiguities. When taken together, these recommendations result in a many-fold increase in the number of observations per session. UV coverage improves to the point where precise VLBI images of the ICRF sources can be constructed on a daily basis directly from the geodetic observations, therefore enabling source structure corrections to be calculated. Simulations are currently underway to evaluate the potential of this approach.

1. WHY ARE SOURCE STRUCTURE CORRECTIONS NEEDED?

The ideal radio source for reference frame definition has no structure or apparent variation in position. Real sources, on the other hand, typically have measurable structure, and to make matters worse, structure that often varies noticeably with time. Structure itself is manifest as a variation in interferometer delay, phase and amplitude with respect to baseline geometry. When these vary with time, this is usually manifest as apparent motion of the source.

2. THE IMPACT OF IVS'S VLBI2010

A strategy for mitigating the reference frame degradation due to source structure is to actively monitor that structure and correct for it. This has not been done routinely in the past because current operational geodetic/astrometric schedules do not include enough source observations to allow the creation of high quality images.

In 2003, the International VLBI Service for Astrometry and Geodesy (IVS) began a process of renewal. A working group was struck, called VLBI2010, to fully define by the year 2010, a next generation VLBI system with major goals of achieving 1 mm position accuracy and continuous observations.

The anticipated VLBI2010 operating modes resulting from rapid slewing antennas, higher data rates and broadband operation enable the possibility of a manifold increase in the number of observations per session. This opens up the practical possibility of routinely generating active source structure corrections from each operational geodetic/astrometric observing session.

3. GENERATING SOURCE STRUCTURE CORRECTIONS

Step1. The first step in generating structure corrections involves making images of the source. Based on the resulting maps, it is then possible to calculate, on a band-by-band basis, structure corrections for each input observation. The quality of the maps is dependent on two factors: UV coverage and signal-

to-noise ratio (SNR). UV coverage is a measure of the number of different geometries from which the source is observed. The new tactics being considered for VLBI2010, including larger global networks and faster slewing antennas, promise a quantum improvement in UV coverage. The high imaging potential of the VLBI2010 observing modes has been demonstrated through simulations. Although noise has not yet been included in the analysis, this extension of the simulations is expected in the near future.

Step2. This step involves aligning the map centres in different bands. VLBI observations are typically carried out in a number of different frequency bands, e.g. current geodetic VLBI operations use both S-band and X-band. In VLBI2010 observing modes, it is anticipated that four or more bands, spread over a frequency range of 2-15 GHz, will be used to both remove the effect of the ionosphere, and enable the use of the VLBI phase delays, which are about an order of magnitude more precise than currently used group delays. Since the generation of the maps requires the use of phase closure data, which, by its nature, has had all absolute position information removed, the images in the different bands need to be aligned after the the fact.

Fortunately, the output group and phase delays contain sufficient information to simultaneously resolve phase ambiguities and align the map centres. The ability to do this is dependent on both the frequency of the band and the number of observations of the source. Simulations indicate that in almost all cases, even for the lowest frequency band, it is possible to align the bands to better than about 20 uas (at the 1 sigma level).

Step3. The final step in applying source structure corrections is to identify a reference point in the map. Without corrections, this is naturally placed at the centroid of illumination. Unfortunately, the centroid is typically not fixed over time.

What would be better for geodesy/astrometry would be to associate some feature of the map with a positionally invariant physical feature of the source, typically the black hole at its core. The problem is that the majority of radio emission from the source is generated by dynamic jets emanating from the core, but not the core itself. Some success has been achieved by modeling the core-jet nature of the source as a point plus elliptic component [Fomalant].

Another tantalizing possibility presents itself with the multiband VLBI2010 data. The jet is usually viewed nearly end-on, and the image represents the point at with the jet becomes optically thick at that frequency. The higher the frequency, the closer the image is to the core. It may be possible to use the series of multi-frequency images enabled by the VLBI2010 operating modes to point towards (and perhaps infer) the position of the positionally invariant core of the quasar.

4. CONCLUSIONS

Although more simulation work needs to be done, this work has shown that anticipated VLBI2010 operating modes are likely to enable the implementation of effective source structure corrections making it possible to better associate VLBI observations with the positionally invariant point in each observed radio source. This is important for a number of reasons:

- It will improve the accuracy and stability of the ICRF.
- It will, in turn, improve the accuracy of EOP and the ITRF.
- It will help enable the "broadband delay" technique designed to resolve RF phase ambiguities and hence lead to about an order of magnitude improvement in the VLBI delay observable precision.
- It will result in the first routine production of inter-band image alignment, providing important new information about quasar jet structure and dynamics.
- It will provide an interesting astronomical data base of compact radio sources imaged on a daily basis.

5. REFERENCES

Fomalant, E. "VLBA Phase Referencing for Astrometric Use". In: International VLBI Service for geodesy and astrometry 2006 General Meeting Proceedings, pp 307-315.

CONNECTING THE DYNAMICAL FRAME TO THE ICRF BY USE OF NEAs OBSERVATIONS

E.I. YAGUDINA
IAA, RAS, St-Petersburg, Russia
10 Kutuzov quay, St-Petersburg, 191187, Russia
e-mail: eiya@ipa.nw.ru

ICRF (practical realization of ICRS) is now adopted as the fundamental celestial frame in astronomy. The Hipparcos catalogue is a primary realization of the ICRF at optical wavelengths. In spite of the fact that the ICRF is a quasi-inertial system there are a great number of problems associated with the use of the ICRF, the main of them being the connection of ICRF to dynamical systems. The parameters of this connection are known with insufficient accuracy and further work is necessary on the problem of mutual orientation of this systems at new level of accuracy using different new observations of different solar system objects.

In classical paper (Folkner et al.,1994) for relating DE200/LE200 to ICRF the combined array of VLBI measurements and LLR ones have been used. In the paper (Standish et al.,1995) the connection of dynamical system DE403/LE403 to ICRF was determined at level of mas accuracy by use VlBI observations relative to the sources from radio catalogue with spacecraft observations around the planets. The VLBI observations of spacecrafts relative to the planets at the distant star background are very precise but very rare and can be obtained for short time intervals. In the papers (Batrakov et al.,1999), (Batrakov and Chernetenko, 2001), (Chernetenko, 2007) these parameters relative to dynamical systems DE200/LE200, DE403/LE403 and DE405/LE405 were obtained on the basis of ground minor planet observations and observations of 48 minor planets by Hipparcos. In the present paper we suggest to use optical and radar NEAs observations for the purpose. We consider our results as preliminary ones and are going in nearest future to use the above objects for receiving the orientation parameters dynamical systems relative ICRF. For obtaining connection between FK5 catalogue and Hipparcos Mignard and Froschle (Mignard and Froschle, 1997) gave orientation angles between FK5 and Hipparcos at J2000.0. At present modern optical observations of planets and their satellites are transformed into ICRF by observers using transformation between the systems of their catalogues and ICRF (Hipparcos) system. The same approach was taken for NEAs observations in the present paper. In paper mentioned above (Batrakov and Chernetenko, 2001) the algorithms for determining orientation parameters are shown and angles of orientation connected with the old parameters, zero-points of star catalogues, are given. Using all the designations and formulae which are given in the papers of these authors, the connection between the angles of rotation and corrections to zero-points star catalogue can be written:

$$\epsilon_x = -\Delta\epsilon, \epsilon_y = \Delta L sin\epsilon, \epsilon_z = \Delta A - \Delta L cos\epsilon, \quad (1)$$

where ΔD is a characteristic of the declination star system permanent error, is not connected with the angles of turning. For velocities of changing these angles

$$\omega_x = -\Delta\dot{\epsilon}, \omega_x = \Delta\dot{L} sin\epsilon, \omega_z = \Delta\dot{A} - \Delta\dot{L} cos\epsilon. \quad (2)$$

Optical and radar observations of NEAs from the paper (Yagudina, 2002) were transformed to Hipparcos, that is, into ICRF. The interval of optical observations was about 90 years, the radar observations started in 1968. All the optical observations were taken from MPC catalogue (FK5 system), radar (doppler and delay)–from database "Small astrometric radar observations", JPL. The precision of optical observations is varied within the range from 1" to 0.5" and even smaller for observations after 1965, as for doppler–from 30.0 Hz to 0.1 Hz, delay– from 140 to 0.1μs. The number of optical observations is 16600, radar–345. The result (together with the results of other authors)are given in Table 1. It is in good agreement with the result of (Batrakov et all.,1999) but as compared with results from (Batrakov and Chenetenko, 2001) our values of the parameters and their errors are too big. In 2001 paper authors jointed to minor planets ground observations very precise observations of 48 minor planets observed by Hipparcos. As for NEAs observations in our paper the optical observations till 1950 year have very big error (from 1" to 0.5"). It

is possible to use this kind observations but it is necessary to eliminate the optical observations till 1950 year from our solution .

Orientation parameters mas,mas/y epoch	Folkner et al., 1994 VLBI, LLR J2000.0	Batrakov et al.,1999 12 minor planets 1991 07 02.0	Yagudina, 2002 30 NEA's 2001.8	Batrakov and Chernetenko,2001 12 m.pl.+Hip. 1991.25
ϵ_x	-2.0 ± 2.0	19.3 ± 17.3	19.1 ± 12.2	2.5 ± 1.3
ϵ_y	-12.0 ± 3.0	-18.8 ± 17.9	-23.0 ± 15.8	-12.7 ± 2.2
ϵ_z	-2.0 ± 3.0	41.8 ± 26.0	36.9 ± 10.9	1.4 ± 3.3
ω_x	–	1.3 ± 0.5	0.2 ± 0.1	0.4 ± 0.3
ω_y	–	-0.4 ± 0.6	0.4 ± 0.3	-0.7 ± 0.3
ω_z	–	1.6 ± 1.0	-0.2 ± 0.2	-0.9 ± 0.6

Table 1: Orientation parameters dynamical system DE200/LE200 with respect to ICRF

Orientation param. mas, mas/y	Chernetenko, 2007 15 minor pl.+48 m. pl. Hip.	This paper, 2007 30 NEA's+4 m.pl.
ϵ_x	-0.1 ± 0.9	-0.3 ± 2.1
ϵ_y	3.0 ± 1.1	4.8 ± 2.5
ϵ_z	-5.2 ± 1.6	-8.2 ± 2.9
ω_x	0.15 ± 0.08	0.2 ± 0.5
ω_y	0.66 ± 0.10	0.9 ± 0.6
ω_z	-0.40 ± 0.17	-0.5 ± 0.4

Table 2: Orientation parameters dynamical system DE403/LE403 with respect to ICRF

After excluding NEAs observations from 1900 to 1950 year the orientation parameters of DE403/LE403 with respect to ICRF were calculated and the result is represented by table 2. One can see that our results are worse than the results from the paper (Chernetenko, 2007). The reason is the high precision of Hipparcos observations of minor planets as compare with the ground optical observations of asteroids. Nevertheless, ground observations have an advantage of obtaining velocities of angles changes, that can not be obtained by Hipparcos observations.

REFERENCES

Folkner W. M et al., 1994, "Determination of the extragalactic-planetary frame tie from joint analysis of radio interferometric and lunar laser ranging measurements", A&A , 287, pp.279–289.

Standish, E. M. et al., 1995, "JPL planetary and lunar ephemerides, DE403/LE403. Interoffice Memorandum, 314.10.127, pp. 1-22.

Batrakov, Yu.V., et al., 1999,"Hipparcos catalogue orientation as obtained from observations of minor planets", A&A , 352, pp.703–711.

Batrakov, Yu. V., Chernetenko Yu.A., 2001,"The modern state of the problem determination of the mutual orientation star and dynamical systems by minor planet observations",in Finkelstein (eds) Trudy IAA RAS (in Russian), 6, 148–159.

Chernetenko Yu.A., 2007, "The usage of asteroids observations for determination some astronomical constants", in Finkelstein (eds) Abstracts The Second Russian conference KVNO-2007 (in Russian), pp.277–278.

Mignard F., Froschle M., 1997, "Comparison of the FK5 frame to Hipparcos", in Proceedings of the ESA Symposium "Hipparcos-Venice 97", ESA SP-402, p.57.

Yagudina, E.I., 2002, "The use of radar observations of Near-Earth asteroids and main belt minor planets for different astrometrical purposes", in Proceedings of Asteroids, Comets, Meteors (ACM 2002), Berlin, pp.385–388.

Session II

MODELS AND NUMERICAL STANDARDS IN FUNDAMENTAL ASTRONOMY

MODÈLES ET STANDARDS NUMÉRIQUES EN ASTRONOMIE FONDAMENTALE

CURRENT STATUS OF THE IAU WORKING GROUP FOR NUMERICAL STANDARDS OF FUNDAMENTAL ASTRONOMY

B. LUZUM[1], N. CAPITAINE[2], A. FIENGA[3], W. FOLKNER[4], T. FUKUSHIMA[5], J. HILTON[1], C. HOHENKERK[6], G. KRASINSKY[7], G. PETIT[8], E. PITJEVA[7], M. SOFFEL[9], P. WALLACE[10]
[1] U.S. Naval Observatory, USA
[2] Observatoire de Paris, France
[3] Observatoire de Besancon, France
[4] Jet Propulsion Laboratory, USA
[5] National Astronomical Observatory, Japan
[6] HM Nautical Almanac Office, UK
[7] Institute of Applied Astronomy RAS, Russia
[8] Bureau International des Poids et Mesures, France
[9] Dresden Technical University, Germany
[10] Rutherford Appleton Laboratory, UK

ABSTRACT. At the 2006 International Astronomical Union (IAU) General Assembly (GA), a proposal was adopted to form the Working Group (WG) for Numerical Standards of Fundamental Astronomy. The goal of the WG are to update "IAU Current Best Estimates" conforming with IAU Resolutions, the International Earth Rotation and Reference System Service (IERS) Conventions, and the Système International d'Unités (SI). Initial efforts have concentrated on determining which constants should be considered, the terminology regarding the description of the constants, and the dependence of the constant estimates on their associated models. The current status of WG activities and the anticipated future directions are presented.

1. INTRODUCTION

The IAU Working Group (WG) on Numerical Standards for Fundamental Astronomy has been tasked with updating the IAU Current Best Estimates (CBEs), conforming with the IAU Resolutions, IERS Conventions and Système International d'Unités whenever possible. As part of its effort to achieve this, the WG is working in close cooperation with IAU Commissions 4 and 52, the IERS, and the BIPM Consultative Committee for Units.

This is the third IAU WG to be tasked with producing CBEs and is adding to the legacy of the two previous WGs. The first Sub-group on Numerical Standards of the IAU WG on Astronomical Standards was headed by E.M. Standish and the WG report (Standish, 1995) established the rules which are still used today. For instance, this group decided on the two-tiered approach to the astronomical constants that we are currently using and also created the first CBEs for a list of IAU constants.

This work was continued by T. Fukushima and his IAU WG on Astronomical Standards (Fukushima, 2000; Fukushima, 2002). Many of the updates concerned work on constants in a general relativistic framework and improved estimates of the precession constant. This revised list of CBEs is the current IAU CBEs.

The excellent work of both these WGs has helped to establish the precedent and allows us to improve incrementally the values for which there are now better estimates.

2. CHANGES SINCE THE LAST CURRENT BEST ESTIMATES

In addition to the need to update the CBEs because of improved estimates, there have also been significant changes that impact the IAU CBEs. Since the IAU CBEs were adopted, the IERS Conventions 2003, a document widely used by the astronomical and geodetic communities, has been produced. This reference contains estimates of many of the constants included in the IAU CBEs.

One significant development was the adoption of a new precession model with IAU 2006 Resolution B1. This resolution accepted the conclusion of the IAU Division I Working Group on Precession and

the Ecliptic (Hilton *et al.*, 2006) and adopted the P03 precession theory of Capitaine *et al.* (2003). This resolution also replaced the terms lunisolar precession and planetary precession with precession of the equator and precession of the ecliptic. Another change is the redefinition of Barycentric Dynamical Time (TDB) that occurred with the adoption of IAU 2006 Resolution B3.

These resolutions fundamentally alter the status of the associated constants. For instance, the general precession found in the IAU CBEs is no longer the appropriate quantity to describe precession. It should be replaced with either the rate of precession of the equator in longitude (or of the Celestial Intermediate Pole), or a number of precession quantities or expressions. The resolutions also changed the status of the constant L_B to a defining constant.

3. CHANGES TO THE CURRENT BEST ESTIMATES

The current WG started where the previous IAU WG tasked with providing CBEs left off, by using the existing IAU CBEs as the starting draft. From this starting point, the WG has proceeded to update the CBEs based on internationally adopted values and recent research. Some examples are adopting values:

- from Committee on Data for Science and Technology (CODATA) 2006;
- suggested by the IAU Division I WG on Precession and the Ecliptic;
- based on recent research to modify most of the planetary masses and adding masses for Ceres, Pallas, Vesta, and Eris. These improvements are possible due to years of high-precision observations of spacecraft as they near planets and their satellites.

The interim CBEs chosen serve two significant purposes. First, they keep the IAU CBEs consistent, where possible, with international standards. They also keep the constants consistent with the most accurate estimates currently available, which is vital for enabling progress in research.

In summary, for the latest draft version, 6 additional constants have been added to that list, one constant has been superseded by another, and the numerical values for 10 additional constants have been replaced by more current values.

4. ADDITIONAL CONCERNS

In addition to updating the list of CBEs, the WG is beginning to address the larger issues surrounding the adoption of IAU CBEs. These include the mechanism to keep the CBEs current and the way in which these constants will be provided, the procedure to document the theoretical context of the constants, and whether the IAU should revise its current list of adopted constants to correspond with the new list of CBEs.

The mechanism for maintaining the IAU CBEs has been discussed and to date, three options have been considered. The current method is for the IAU to form a WG when it believes that the CBEs need to be updated. This method has worked in the past and there is no reason to believe that it would not work in the future. Another possibility would be to enlist the aid of the IERS Conventions Product Center to maintain the IAU CBEs. Since the IERS is an IAU service organization and it already has a mechanism in place to maintain CBEs, it is possible that the IERS Conventions could be used to maintain the IAU CBEs as well. The biggest problem with this method is that the user communities and the areas of research of the IERS and the IAU are slightly different and there is a possibility that these differences could be problematic. A third option is to create a permanent WG within IAU Commission 4 that would maintain the list of CBEs. One potential problem with this option is that in the past, the IAU has been reluctant to allow WGs to stand in perpetuity. More details will need to be obtained to determine the potential status of a WG either within an IAU Commission or Division.

When considering the way in which the CBEs will be provided, a few options have been suggested. The current method is to provide the CBEs with the maximum accuracy provided by the supporting scientific research. However, another option has been suggested to provide the CBEs with a decreased accuracy — essentially truncate the digits at the level where disagreement between estimates exists. This would allow for a longer shelf life for the constants. The obvious drawback to this method is that while these lower accuracy values may be sufficient for some users, they would not meet the needs of the users with the most stringent accuracy requirements. In order for this method to be viable, a list of the most

accurate constants would need to be easily accessible to the high-accuracy users. A third possibility would be to apply the decreased accuracy only to a potential list of constants to be submitted in the recommendations to the IAU for consideration as a new IAU System of Constants. This method has the advantage of keeping a list of constants with the highest possible accuracy (CBEs) while also creating a list of constants that will be more universally acceptable and have longer life (potentially new IAU System of Constants). The latter point is particularly apropos since the acceptance of any new System of Constants by the IAU General Assembly would be facilitated if the values to be adopted agreed (at least to the number of digits provided) with all reasonable research results and the longer life would be consistent with the long span between the adoption of new IAU Systems of Constants.

The numerical values for the CBEs are not numbers that exist in isolation; they are defined fully within the theoretical context in which they are estimated. The WG will need to account for this in the presentation of the CBEs by making the theoretical underpinnings apparent to the users of the CBEs. The level to which this is done and the method of achieving this are still under consideration.

Electronic information is likely to play an important role in achieving the proper level of documentation for the CBEs. The extent to which electronic information is used is also a topic that is still under consideration. Electronic media can either be used as a primary source for defining information or it can be used as a secondary source, providing supplemental information.

5. UPDATE OF IAU SYSTEM OF CONSTANTS

There are now significant differences between the CBEs and the current IAU system of constants. This is due to both increasing accuracy of estimates and to changes in astronomical theory. As a result of this, there appears to be a consensus to recommend to the 2009 IAU General Assembly that the IAU system of constants be updated. If this is to be accomplished, the WG will need to finalize the CBEs and be prepared to provide draft recommendations to the IAU by early 2009.

6. REFERENCES

Capitaine, N., Wallace, P. T., and Chapront, J., 2003, "Expressions for IAU 2000 precession quantities", A&A , 412, pp. 567–586, doi: 10.1051/0004-6361:20031539.

Fukushima, T., 2000, "Report on Astronomical Constants," "Proc. IAU Colloquium 180, Johnston, K. J., McCarthy, D. D., Luzum, B. J., Kaplan, G., pp. 417–427.

Fukushima, T., 2003, "Report on Astronomical Constants," Highlights of Astronomy, 13, International Astronomical Union, 2002, H. Rickman (ed.), pp. 107-112.

Hilton, J. L., Capitaine, N., Chapront, J., Ferrandiz, J. M., Fienga, A., Fukushima, T., Getino, J., Mathews, P., Simon, J.-L., Soffel, M., Vondrak, J., Wallace, P., William, J., 2006, "Report of the International Working Group on Precession and the Ecliptic," Celest. Mech. Dyn. Astr., 94, pp. 351–367.

Standish, E.M., 1995, "Report of the IAU WGAS Sub-group on Numerical Standards," Highlights of Astronomy, 12, International Astronomical Union, 1994, I. Appenzeller (ed.), pp. 180–184.

ON ASTRONOMICAL CONSTANTS

M.H. SOFFEL, S.A. KLIONER
Lohrmann Observatory,
Dresden Technical University, 01062 Dresden, Germany
e-mail: Michael.Soffel@tu-dresden.de

ABSTRACT. The set of astronomical constants conceptually fall into different categories; they are classified as natural constants, body constants or initial values. These categories are discussed in detail as is the problem of consistency and accuracy of such constants.

1. ASTRONOMICAL CONSTANTS FALL INTO DIFFERENT CATEGORIES

One of the central tasks of the IAU working group 'Numerical Standards in Fundamental Astronomy' (chair: Brian Luzum, USNO) is a selection of constants related with fundamental astronomy and to provide current best estimates of these constants together with their realistic errors. For that reason we thought it would be of general interest to discuss the relevance of these various constants that clearly fall into different categories that we classify as natural constants, body constants and initial values.

2. NATURAL CONSTANTS

Astronomical constants appear when the dynamics of an astronomical system is under discussion. From a fundamental point of view the dynamics of any physical system can be described by means of just a few fundamental physical interactions: gravity, electromagnetism, the weak or the strong force. These interactions are described by means of certain fields (the metric field g in the case of gravity; a vector potential A in the case of electromagnetism) that obey certain field equations: Einstein's equations in the case of General Relativity (GRT) or Maxwell's equations in the case of electromagnetism. These fundamental laws of nature contain certain natural constants describing certain properties of the interaction such as strength, propagation velocities etc. In GRT the Newtonian gravitational constant G plays a central role, in electromagnetism and Special Relativity (SRT) it is the vacuum speed of light c. In the microscopic world Planck's reduced constant $\hbar$ is of similar importance. As is well known the numerical values of three natural constants can be chosen arbitrarily (i.e., by law) thereby fixing the basic physical units. A well-known theoretical choice are geometrized units where $G = \hbar = c = 1$; the unit of time then is the Planck time $T_{\rm P} = (\hbar G/c^5)^{1/2} = 5.4 \times 10^{-44}\,$s, the unit of length is the Planck length $L_{\rm P} = cT_{\rm P} = 1.6 \times 10^{-35}\,$m and the unit of mass is $(\hbar c/G)^{1/2} = 2.2 \times 10^{-8}\,$kg. For practical purposes such units obviously are quite inconvenient.

Historically the basic physical units for time (the second), length (the meter) and mass (the kilogram) have been chosen by means of physical prototypes or properties of astronomical bodies. E.g., before 1956 the second was defined as the fraction of 1/86 400 of a mean solar day and then until 1967 as 1/31 556 925.8747 of the tropical year 1900. The meter in 1793 was defined as a fraction of 10^{-7} of the Earth's quadrant passing through Paris and in 1889 it was given by the international prototype of platinum-iridium rod kept at BIPM, Paris. Still the actual definition of the kilogram is through the platinum-iridium prototype of mass, also kept at BIPM. Such prototypes clearly have several disadvantages: precise copies have to be manufactured; they might change their properties due to interactions with the environment. There are indications that copies of the kilogram prototype became heavier in course of time; mass differences of up to $50\,\mu$g have been reported. Possibly the prototype has lost mass because of cleaning procedures.

For these reasons one tries to define the basic units through natural constants. This has been done for the second and the meter; soon this goal will also be realized for the kilogram, e.g., by counting the number of atoms of a macroscopic silicon-sphere (the Avogadro method; see e.g., Becker et al., 2001).

2.1. Defined and measurable natural constants

Today, the SI second is defined as: 'duration of 9 192 631 770 periods of the radiation corresponding to the transition between the two hyperfine levels of the ground state of the cesium-133 atom'. The SI meter is defined as 'length of the path traveled by light in vacuum during a time interval of 1/299 792 458 of a second. Note that these two definitions fix the vacuum speed of light once and forever; it has become a *defined* natural constant. In contrast to this the value for G is not defined; it is a *measurable natural constant*.

Clearly multiples of the SI second, SI meter or SI kilogram can be introduced for convenience without any problems. E.g., the Astronomical Unit might be defined by a fixed value in terms of the SI meter rather than by relation to a certain ephemeris (see, e.g., Klioner, 2007 for a discussion).

2.2. Problems related with natural units

The definition of a natural unit related with a defined natural constant is related with a corresponding fundamental law of nature (e.g., Special Relativity). In case a violation of that law will be detected in the future the definition might have to be abandoned because of serious problems. Consider, e.g., the definition of the meter and the isotropy of space. Using an old definition of the meter the famous experiment by Michelson and Morley from 1887 showed that the speed of light is independent of the propagation direction in space (isotropy of space). This fundamental experiment has been repeated over and over again. In recent time Stanwix et al. (2006) performed a Michelson-Morley experiment that uses two orthogonally orientated cryogenic sapphire resonator oscillators rotating in the laboratory. The result is that a possible upper limit for $\Delta c/c$ is of order 1.2×10^{-16} (see also Müller et al., 2007). Suppose that one day a violation of the isotropy of space will be found. In that case with the present definition of the meter the length of a meter stick would depend upon its orientation in space, really an unpleasant situation that would require a change in the definition of meter.

3. BODY CONSTANTS AND FRAMEWORK

The two astronomical constants G and c are related with GRT and Maxwell's theory of electromagnetism. In the latter case the properties of astronomically interesting light-rays follow from Maxwell's theory in the case of geometrical optics. On the other hand exact GRT is too complex to treat solar-system problems. Not even the constants describing certain aspects of astronomical bodies could be defined. These constants will be called 'body constants'; examples for such body constants are the mass of a body, its potential coefficients (mass multipole moments), its intrinsic angular momentum (spin) etc. Consider, e.g., the mass of an astronomical body which in Newton's theory of gravity is well defined and given as integral over the density. In Relativity because of the mass-energy equivalence ($E = mc^2$) all kinds of energy contribute to the inertial or gravitational mass even the gravitational field itself. Now, GRT is a non-linear theory and in principle one is not able to separate the gravitational field of a body A from that of another body B. For that reason one resorts to an approximation to GRT or a whole class of metric theories of gravity if one allows for a violation of Einstein's theory of gravity. Such an approximation will be called a 'framework'. For solar system applications usually one employs the (first) post-Newtonian framework (a weak field, slow motion approximation to GRT) or the parametrized post-Newtonian framework (PPN) with a suitable choice of coordinates (e.g., harmonic coordinates). This framework might contain additional constants such as the PPN-parameters β, γ, α_1 etc. whose numerical values are related with tests of GRT (deviations from $\beta = \gamma = 1$ and $\alpha_1 = 0$ indicate a violation of GRT at the post-Newtonian level). As is well known (e.g., Damour et al., 1991) body constants can be defined in the basic (post-Newtonian) framework. For $\beta = \gamma = 1$ and $\alpha_1 = 0$ the mass of a body E (Earth) can be defined in the local co-moving system (GCRS) with coordinates $(T, \mathbf{X})$ as (e.g., Damour et al., 1991)

$$M_E(T) = \int_E d^3\Sigma + \frac{1}{6c^2}\frac{d^2}{dT^2}\left(\int_E d^3X\mathbf{X}^2\Sigma\right) - \frac{4}{3c^2}\frac{d}{dT}\left(\int_E d^3X X^a\Sigma^a\right),$$

where Σ and Σ^a are the gravitational (energy-) mass density and mass current in the GCRS. Though this theoretical post-Newtonian expression for the mass of the Earth looks quite complicated it appears as parameter in the gravitational potential W_E outside the Earth in the simple, quasi-Newtonian form

$$W_E = \frac{GM_E}{R} + \dots .$$

Body constants can be considered as "constants" only within some accuracy limits. In general body constants will be time dependent. This time dependence together with their realistic errors has to be indicated explicitly, especially when our accuracy is close to that where the corresponding constant becomes time-dependent. For example, major sources for such a time dependence for mass variations in the solar system are dust accretion or energy loss and solar wind. For our Sun with luminosity $L = 4 \times 10^{33}$ erg/s the fractional mass variation is of order $\dot{M}/M \sim 10^{-13}$ per year.

4. INITIAL VALUES AND MODEL

Bodies with their body constants plus initial conditions appear in a dynamical model, e.g., for the motion of the gravitational N-body problem (ephemeris equations). Such a model might involve a variety of interactions (not only gravitational) and might contain additional constants describing certain features of them (e.g., a lag angle to describe the tidal friction in the Earth-Moon system). Examples are the basic equations for the DE, INPOP or EPM ephemerides and all the constants required in those equations. Note, that if we start with a certain model and add another interaction (e.g., we consider potential coefficients of higher order for a certain body of the model) we basically face *another model*. Initial values are intimately related with the underlying model. If the values of certain initial values are discussed the full underlying model has to be specified in some way or another. Note that in the relativistic framework this model includes not only physical ideas and assumptions, but also a series of pure conventions concerning the choice of coordinates.

In contrast to this one expects the body constants to have some well defined (time-dependent) values within a certain framework. Clearly given a certain data set different models will imply different values for them with certain errors. However, if realistic errors are given these values should be compatible with each other.

5. THE PROBLEM OF CONSISTENCY AND ACCURACY

To ensure consistency of several models realistic errors should be given. To this end correlations have to be studied, possibly different models or even different branches of science have to be consulted etc. This implies that chasing after the current best estimate of a constant is highly problematic as long as a realistic estimate of the error is not given. There are well known examples in the literature, e.g., related with a determination of $\dot{G}/G$, where five times the formal error is still an order of magnitude smaller than a realistic error (for $\dot{G}/G$ presently a realistic error is of order 6×10^{-13}/yr).

6. SUMMARY AND CONCLUSIONS

A new classification of astronomical constants into natural constants, body constants and initial values is suggested. The set of natural constants is divided into defined and measurable natural constants. They appear in fundamental laws of nature. Body constants can be defined in a certain framework such as the (first) post-Newtonian approximation to Einstein's theory of gravity. If the framework is fixed the body constants have a well-defined meaning and certain numerical values independent of the model used to interpret astronomical data. On the other hand initial values depend upon the subtleties of the concrete model. This implies that together with the numerical values all the details of the corresponding model should be indicated in some way or another. Finally, hunting for current best estimates is a necessary enterprize but meaningful only if realistic errors are given.

7. REFERENCES

Becker, P., Gläser, M., 2001, Physik in unserer Zeit 32, 254

Damour, T., Soffel, M., Xu, C., 1991, Phys.Rev. D43, 3273

Klioner, S.A., 2007, "Relativistic scaling of astronomical quantities and the system of astronomical units", A&A , in press

Müller, H., et al., 2007, Phys.Rev.Lett. **99**, 050401

Stanwix, P.L., et al., 2006, Phys.Rev. D74, 081101

RECENT PROGRESS IN CONCEPTS, NOMENCLATURE AND MODELS IN FUNDAMENTAL ASTRONOMY

N. CAPITAINE

Observatoire de Paris, SYRTE/UMR8630-CNRS,
61, avenue de l'Observatoire, 75014 – Paris, France
e-mail: n.capitaine@obspm.fr

ABSTRACT. The IAU 2006 resolutions B1, B2 and B3, adopted by the XXVIth IAU General Assembly (August 2006) and endorsed by the XXIVth IUGG General Assembly (July 2007), supplement the IAU 2000 Resolutions on reference systems. The aim of IAU 2006 Resolution B1 is to adopt a precession model as a replacement to the IAU 2000 precession in order to be consistent both with both dynamical theory and the IAU 2000 nutation. The aim of IAU 2006 Resolutions B2 and B3 is to address definition, terminology or orientation issues relative to reference systems and time scales that needed to be specified after the adoption of the IAU 2000 resolutions. This paper explains the changes resulting from the joint IAU 2000 and 2006 resolutions with respect to the previous position and reviews the progress in the concepts, nomenclature, models and conventions for fundamental astronomy. The paper also reports on practical aspects related to the Earth orientation parameters and describes the characteristics of the IAU high precision model for the celestial motion of the Earths pole.

1. THE IAU 2000/2006 RESOLUTIONS ON REFERENCE SYSTEMS

The IAU 1997 adoption of the International Celestial Reference System (ICRS) based on extragalactic radio-sources, and of the International Celestial Reference Frame (ICRF) (Ma et al. 1998) that realizes the ICRS, made it possible to refer to celestial reference systems at a sub-milliarcsecond accuracy. Then, several IAU resolutions on reference systems have been passed in 2000 and 2006 (and endorsed by the IUGG in 2003 and 2007, respectively), which have important consequences on the concepts, the nomenclature and the models for fundamental astronomy.

IAU 2000 Resolution B1.3 specifies that the systems of space-time coordinates for the solar system and the Earth within the framework of General Relativity are named the *Barycentric Celestial Reference System* (BCRS) and the *Geocentric Celestial Reference System* (GCRS), respectively and the time-coordinates, the *Barycentric Coordinate Time* (TCB) and the *Geocentric Coordinate Time* (TCG), respectively. It also provides a general framework for the metric tensor and coordinate transformations at the first post-Newtonian level(see Soffel et al. 2003) between the BCRS and the GCRS.

IAU 2000 Resolution B1.6 recommends the adoption of the IAU 2000 precession-nutation (version A corresponding to the model of Mathews et al. (2002), of 0.2 mas accuracy, and its shorter version B (McCarthy and Luzum 2002) with an accuracy of 1 mas).

IAU 2000 Resolution B1.7 specifies that the pole of the nominal rotation axis is the *Celestial Intermediate Pole* (CIP), defined as being the intermediate pole in the transformation between the International Terrestrial Reference System (ITRS) and GCRS, separating nutation from polar motion by a specific convention in the frequency domain.

IAU 2000 Resolution B1.8 recommends using the "non-rotating origins" (Guinot, 1979) as origins on the CIP equator in the celestial and the terrestrial reference systems. They were designated *Celestial and Terrestrial Ephemeris Origins*, but re-named *Celestial and Terrestrial Ephemeris Origins*, respectively by IAU 2006 Resolution B2; it also defines UT1 as linearly proportional to the *Earth Rotation Angle* (ERA) between those origins (Capitaine et al. 2000). It recommends that the ITRS to GCRS transformation be specified by the positions of the CIP in the GCRS and the ITRS, and the ERA. It finally recommends that the IERS continue to provide data and algorithms for the transformations referred to the equinox.

IAU 2000 Resolutions B1.6, B1.7 and B1.8 came into force on 1 January 2003. The models, procedures, data and software to implement these resolutions operationally had been made available by the IERS Conventions 2003 and the *Standards Of Fundamental Astronomy* (SOFA) activities (Wallace 1998). These

include the procedure based on non-rotating origins, but also the equinox based procedure, both being delivered with equal precisions.

As the precession part of the IAU 2000A model consists only in corrections to the precession rates of the IAU 1976 precession, which does not correspond to a dynamical theory, IAU 2000 Resolution B1.7 recommends the development of new expressions for precession consistent with dynamical theories and with IAU 2000A nutation. The 2003-2006 IAU Working Group on "Precession and the Ecliptic" (P&E WG) has looked at several solutions and recommended (Hilton et al. 2006) the adoption of the P03 precession theory (Capitaine et al. 2003), which was endorsed by IAU 2006 Resolution B1.

IAU 2006 Resolution B1 recommends the adoption (from 2009) of the P03 Precession as a replacement to the precession part of the IAU 2000A precession-nutation in order to be consistent with both dynamical theories and the IAU 2000 nutation. It also clarifies the definitions of the precession and of the ecliptic.

In parallel, the new terminology associated with the IAU 2000 resolutions, along with some additional definitions related to them, have been recommended by the 2003-2006 IAU Working Group on "Nomenclature for Fundamental Astronomy" (NFA WG) (Capitaine et al. 2007). This was endorsed by IAU 2006 Resolutions B2 and B3.

IAU 2006 Resolution B2, which is a supplement to the IAU 2000 Resolutions on reference systems, consists of two recommendations: 1) harmonizing "intermediate" to the pole and the origin (i.e. *Celestial and Terrestrial Intermediate Origins*, CIO and TIO instead of CEO and TEO, respectively) and defining the celestial and terrestrial "intermediate" systems; 2) fixing the default orientation of the BCRS and GCRS, which is, is unless otherwise stated, assumed to be oriented according to the ICRS axes.

IAU 2006 Resolution B3 recommends a re-definition of the Barycentric Dynamical Time (TDB) through a conventional linear relation between TDB and TCB.

2. PROGRESS IN THE CONCEPTS FOR FUNDAMENTAL ASTRONOMY

The space-time coordinates to be used in the framework of General Relativity

The IAU 2000/2006 Resolutions have provided clear procedures for theoretical and computational developments of the space-time coordinates to be used in the framework of General Relativity. The BCRS, which can be considered to be a global coordinate system for the solar System, has to be used (with TCB) for planetary ephemerides. In contrast, the GCRS should be considered as a local coordinate system for the Earth to be used (with TCG) for Earth rotation, precession-nutation of the equator, motion of Earth's satellite, etc. The spatial orientation of the GCRS is derived from that of the BCRS. Consequently, the GCRS is "kinematically non-rotating" so that Coriolis terms (that come mainly from geodesic precession) have to be considered when dealing with equations of motion in that system. For all practical applications, unless otherwise stated, the BCRS (and hence GCRS) is assumed to be oriented according to the ICRS axes. The expression of the transformation between the barycentric and geocentric coordinates (i.e. an extension of the Lorentz transformation) is defined at the first post-Newtonian level for space coordinates and at an extended level for the time coordinates.

The Terrestrial Time and Barycentric Dynamical Time

The IAU 2000/2006 Resolutions have clarified the definitions of TT and TDB. The new TT definition is a time scale differing from TCG by a constant rate, which is a defining constant. In a very similar way, the new TDB is a linear transformation of TCB, the coefficients of which are defining constants. The consequence is that TT (or TDB), which may be for some practical applications of more convenient use than TCG (or TCB), can be used with the same rigorous approach. This applies in particular to satellite orbit computations for TT and solar system ephemerides, or analysis of pulsars timings, for TDB.

The Celestial Intermediate Pole

The IAU 2000 definition of the CIP is such that (i) its GCRS motion includes all the terms with periods greater than 2 days in the GCRS (i.e. frequencies between -0.5 cycles per sidereal day (cpsd) and $+0.5$ cpsd); (ii) its ITRS motion, includes all the terms outside the retrograde diurnal band in the ITRS (i.e. frequencies less than -1.5 cpsd or greater than -0.5 cpsd). This corresponds to an extension of the IAU 1980 definition of the *Celestial Ephemeris pole* to the high frequency domain.

According to IAU 2000 resolutions, the GCRS position of the CIP replaces the classical precession and nutation quantities. It can be provided by expressions as function of time of the rectangular coordinates, X and Y of the GCRS direction of the CIP unit vector, which include precession and nutation and the frame bias between the pole of the GCRS and the CIP at J2000.0.

The Celestial and Terrestrial Intermediate Origins and Earth Rotation Angle

The IAU 2000/2006 Resolutions have provided a very straightforward definition of the Earth's diurnal rotation based on the angle (ERA) between the non-rotating origins, CIO and the TIO. The conventional linear transformation that defines UT1 from the ERA is (Capitaine et al. 2000):

$$\mathrm{ERA}(\mathrm{UT1}) = 2\pi[0.7790572732640 + 1.00273781191135448\ (\mathrm{JulianUT1date} - 2451545.0)] \qquad (1)$$

Note that the CIO is at present very close to GCRS longitude zero and almost stationary in longitude, while the equinox to which Greenwich sidereal time, GST, refers is moving at about 50 arcsec per year in GCRS longitude. Moreover, the CIO based procedure allows a clear separation between (i) the GCRS motion of the CIP (i.e. mainly precession-nutation) and (ii) the ERA, which is not model-dependent. In contrast, precession and nutation are mixed up with Earth's rotation into the expression of GST as function of UT1: GST(UT1, TT) = ERA − EO, where EO, represents the accumulated precession and nutation in right ascension and is therefore directly dependent on the precession-nutation models.

3. PROGRESS IN NOMENCLATURE FOR FUNDAMENTAL ASTRONOMY

The IAU NFA WG made a number of recommendations on terminology. It also produced the "IAU 2006 Glossary" providing definitions corresponding to the IAU 2000 resolutions as well as new definitions proposed by the WG, including those formally endorsed by the IAU in 2006 and the IUGG in 2007 (e.g. the ITRS). The IAU 2000/2006 Resolutions have provided the appropriate terminology for the pole, the Earth's angle of rotation, the longitude origins and the related reference systems.

Terminology choices related to the intermediate pole and origins

Terminology choices endorsed by the IAU 2006 Recommendations include harmonizing the name of the pole and the origin to "intermediate" and therefore using "Celestial Intermediate Origin" (CIO) and "Terrestrial Intermediate Origin" (TIO), respectively instead of CEO/TEO. The new nomenclature related to the newly defined pole and origins is using "intermediate" to describe the moving geocentric celestial reference system containing the CIP and the CIO (with its terrestrial counterpart containing the TIO); or giving the name "equation of the origins" (EO) to the distance between the CIO and the equinox along the intermediate equator, the sign of this quantity being such that it represents the CIO right ascension of the equinox, or equivalently, the difference between the Earth Rotation Angle and Greenwich sidereal time.

The "celestial intermediate reference system" (CIRS), based on the CIP and the CIO, replaces the classical celestial system based on the true equator and equinox of date. The CIRS can be derived from the GCRS with using the GCRS CIP coordinates X, Y and the quantity s positioning the CIO, which has been called the "CIO locator".

Terminology choices related to the procedural framework and equatorial coordinates

The new nomenclature associated with the procedural framework, is using"equinox based" and "CIO based" for referring to the classical and new paradigms, respectively; or choosing "equinox right ascension" (or "RA with respect to the equinox") and "intermediate right ascension" (or "CIO right ascension", or "RA with respect to the CIO"), for the azimuthal coordinate along the equator in the classical and new paradigms, respectively.

The IAU NFA WG recommendations include using the equatorial coordinates in an extended way, such that right ascension and declination be generic terms that can be referred to any equator (e.g. GCRS equator, CIRS equator, etc.) or to any origin on those equators (i.e. GCRS origin, CIO, equinox, etc.).

4. PROGRESS IN MODELS FOR FUNDAMENTAL ASTRONOMY

The IAU 2000/2006 Resolutions have adopted a high precision model for precession and nutation with two successive steps.

The first step was the adoption of the IAU 2000 precession-nutation model (MHB) of Mathews et al. (2002), which has been implemented in the IERS Conventions 2003. This model is composed of a nutation part and a precession part. In addition to the IAU 2000A model are frame bias values between the J2000 mean pole and equinox and the GCRS. The IAU 2000A nutation includes 1365 luni-solar and planetary terms, which are based on rigid Earth nutation transformed with the MHB transfer function based on basic Earth parameters (BEP) that have been fitted to VLBI data. That model is expected to have an accuracy of about 10 μas for most of its terms. In contrast, the so-called free core nutation

(FCN), which is due to geophysical effects and is largely unpredictable, is not part of the model. The precession part, which consists only in corrections to the precession rates of the IAU 1976 precession, was known to do not correspond to a dynamical theory.

The second step in the improvement of the IAU precession-nutation was the adoption (IAU 2006 Resolution B1) of the P03 Precession as a replacement to the precession part of the IAU 2000A precession-nutation in order to be consistent with both dynamical theory and the IAU 2000 nutation. The P03 model include improved expressions for both the precession of the ecliptic and the precession of the equator. The latter has taken into account the Earth's J_2 rate effect, mostly due to the post-glacial rebound. The P03 precession polynomial developments provide separately the developments for the basic quantities for the ecliptic and the equator that are directly solutions of the dynamical equations, and derived quantities, such as those for the GCRS coordinates of the CIP. These also include expressions for the P03 sidereal time that can been derived from the expression of the Earth Rotation Angle (itself independent of precession-nutation) and the expression for the equation of the origin, which is directly dependent on the precession-nutation.

The various ways of forming the precession-nutation matrix in the new IAU framework have been discussed in Capitaine & Wallace (2006) and the precession-nutation procedures consistent with IAU 2006 resolutions have been provided in Wallace & Capitaine (2006).

5. REFERENCES

Capitaine, N., Guinot, B., McCarthy, D.D., 2000, "Definition of the Celestial Ephemeris Origin and of UT1 in the International Celestial Reference Frame", A&A 355, 398–405.

Capitaine, N., Wallace, P.T., Chapront, J., 2003, "Expressions for IAU 2000 precession quantities", A&A 412, 567–586.

Capitaine N., Wallace P.T., 2006, "High precision methods for locating the celestial intermediate pole and origin", A&A 450, 855–872.

Capitaine, N., Andrei, A., Calbretta, M., et al. 2007, "Report of the Division I Working Group on 'Nomenclature for Fundamental Astronomy', *IAU Transactions*, Vol. 26A, Reports on Astronomy 2002-2005, O. Engvold (ed), Cambridge University Press, 59–62.

Guinot, B., 1979, "Basic Problems in the Kinematics of the Rotation of the Earth", in *Time and the Earth's Rotation*, D. D. McCarthy and J. D. Pilkington (eds), D. Reidel Publishing Company, 7.

Hilton, J., Capitaine, N., Chapront, J., et al., 2006, "Report of the International Astronomical Union Division I Working Group on Precession and the Ecliptic", Celest. Mech. Dyn. Astr. 94, 3, 351.

IAU 2000, *Transactions of the IAU* XXIVB; Manchester, Rickman. H. (ed), Astronomical Society of the Pacific, Provo, USA, 2001, 34–58.

IAU 2006, *Transactions of the IAU* XXVIB; van der Hucht, K.A. (ed).

IERS Conventions (2003), *IERS Technical Note 32*, D.D. McCarthy and G. Petit (eds), Frankfurt am Main: Verlag des desamts für Kartographie und Geodäsie, 2004.

IUGG 2007, IUGG Resolutions, http://www.iugg.org/resolutions/perugia07.pdf .

Ma, C., Arias, E. F., Eubanks et al., 1998, "The International Celestial Reference Frame as realized By Very Long Baseline Interferometry", A&A 116, 516.

Mathews, P.M., Herring, T.A., Buffet, B.A., 2002, "Modeling of nutation and precession: New nutation series for nonrigid Earth and insights into the Earth's interior", J. Geophys. Res. , 107(B4), doi: 10.1029/2001JB000390.

McCarthy, D.D. Luzum, B.J., 2003, "An abridged model of the precession-nutation of the celestial pole", Celest. Mech. Dyn. Astr. 85, 37–49.

Soffel, M., Klioner, S., Petit, G. et al., 2003, "The IAU 2000 Resolutions for Astrometry, Celestial Mechanics, and Metrology in the Relativistic Framework: Explanatory Supplement", AJ 126, 6, 2687.

Wallace P.T., 1998, *Highlights of Astronomy* Vol.11A, J.Andersen (ed.), Kluwer Academic Publishers, 11, 191.

Wallace P.T., Capitaine, N., 2006, "Precession-nutation procedures consistent with IAU 2006 resolutions", A&A 459, 3, 981.

RECENT MODELS OF THE PLANET MOTIONS AND FUNDAMENTAL CONSTANTS DETERMINED FROM POSITION OBSERVATIONS OF PLANETS AND SPACECRAFT

E.V. PITJEVA
Institute of Applied Astronomy RAS
Kutuzov Quay 10, 191187 St.-Petersburg, Russia
e-mail: evp@ipa.nw.ru

ABSTRACT. More recent planet ephemerides constructed at JPL, IAA RAS and IMCCE, their similarities, differences and solution parameters are considered. Data residuals for EPM2006 (IAA RAS ephemerides) are given. New values of planet and asteroid masses and Astronomical Unit are presented.

1. RECENT PLANET EPHEMERIDES

The most recent planet ephemerides having about the same accuracy and being adequate to modern observations have been constructed at JPL – DE414 (Standish, 2006), IAA RAS – EPM2006 (Pitjeva, 2007) and IMCCE – INPOP06 (Fienga *et al.*, 2007). All the basic versions of these ephemerides have been developed in the TDB coordinate system. Several test versions of these ephemerides for the TCB coordinate system (which are entirely equivalent to TDB ephemerides) were also constructed.

Common to all these ephemerides is the simultaneous numerical integration of the equations of motion of the nine major planets, the Sun, 300 or more biggest asteroids, the Moon, and the lunar physical libration performed in the Parameterized Post-Newtonian metric for General Relativity taking into account perturbations due to the solar oblateness and the massive ring of small asteroids. All the above ephemerides have been oriented to the International Celestial Reference Frame (ICRF) with the accuracy better than 1 mas by including into the total solution the 86 ICRF-base VLBI measurements of spacecraft near the planets (Magellan, Phobos MGS and Odyssey) made in 1989 – 2003.

The dynamical models of these ephemerides differ slightly by:

- the modeling of the lunar libration, but this difference doesn't influence significantly the planet epheme-rides (for the EPM ephemerides, the orbital and rotational motions of the Moon were modeled using Krasinsky's (2002) selenodynamical parameters improved from LLR observations);
- the modeling of the perturbations from asteroids (the dynamical model for INPOP06 includes perturbations from 300 asteroids, for EPM2006 from 301, and for DE414 from 342 ones, however, as was shown in the paper (Krasinsky *et al.*, 2002), including into integration the next 51 largest asteroids did not give a better solution due, perhaps, to uncertainty of their masses);
- the numerical integration also includes trans-Neptunian objects for the new EPM2007 ephemerides; for INPOP06 – Earth rotation necessary for the very long time integration in paleoclimate studies, and the additional term $\dot{\mu}_i^*$ of the solar system barycenter, although the impact of this term on displacement of the solar system barycenter is many orders less than the impact of trans-Neptunian objects;
- some procedures of correction (e.g. for the topography of the planet surfaces and the solar corona);
- sets of observations;
- sets of solution parameters.

Observations to which all ephemerides have been fitted are ranging to planets, the Martian landers and spacecraft, including the data of MGS and Odyssey for Mars and a number of spacecraft Jupiter data, differenced range, Doppler measurements, VLBI spacecraft observations and optical data of observations of the outer planets and their satellites. More than 400000 data presented in Tables 1,2 were used for the construction of the EPM2006 ephemerides. EPM2006, as distinct from other ephemerides, cover Russian ranging to Mercury, Venus, Mars (1961–1995) and more observations of satellites for all the outer planets which are more accurate than the observations of their parent planets and are practically free from phase

effect. At present, we are developing numerical theories of motion for main satellites of the outer planets and improving them to the observations.

Planet	Type of data	Time interval	N	$< O-C >$	σ
MERCURY	planet ranging (τ) [m]	1964–1997	746	0	575
VENUS	planet ranging (τ) [m]	1961–1995	1354	-2	584
	Magellan dr [mm/s]	1992–1994	195	0	0.007
	Magellan VLBI [mas]	1990–1994	18	1	2
MARS	planet ranging (τ) [m]	1965–1995	402	0	738
	Viking τ [m]	1976–1982	1258	0	8.8
	Viking $d\tau$ [mm/s]	1976–1978	14978	-0.02	0.89
	Pathfinder τ [m]	1997	90	0	2.8
	Pathfinder $d\tau$ [mm/s]	1997	7569	0	0.09
	MGS τ [m]	1998–2005	6429	-0.1	2.3
	Odyssey τ [m]	2002–2005	3441	-0.1	2.0
	spacecraft VLBI [mas]	1984–2003	44	0	0.8
JUPITER	spacecraft τ [m]	1973–1995	6	-538	2642
	spacecraft VLBI [mas]	1996–1997	24	-1	11

Table 1: Mean values and rms residuals for radiometric observations (MGS and Odyssey data are normal points representing more than 280000 original observations)

Planet	N	$< O-C >_\alpha$	σ_α	$< O-C >_\delta$	σ_δ
JUPITER	11562	3	103	-14	128
SATURN	12205	-1	192	-5	190
URANUS	10659	0	205	-5	251
NEPTUNE	9701	0	183	-1	240
PLUTO	4563	0	237	5	236

Table 2: Mean values and rms residuals for optical observations of planets and their satellites ($\alpha \cos\delta$ and δ in mas), 1913–2006

About 230 parameters have been determined while improving the planetary part of the EPM2006 ephemerides. The software for DE414 permits to determine 63 individual asteroid masses, although most masses are constrained using a priori values of the nominal masses. The solution for the planet part of DE414 includes 225 parameters and 34 parameters for the Moon. The number of the adjusted parameters for INPOP06 is 65.

The solution parameters of the planetary part of EPM2006 are:

- the orbital elements of all the planets and 14 satellites of the outer planets the observations of which have been used to improve the orbits of these planets;
- the value of the Astronomical Unit in kilometers;
- three orientation angles of the ephemerides relative to ICRF;
- 13 rotation parameters of Mars and the coordinates of three landers on the Martian surface;
- masses of Jupiter and the seven asteroids that perturb Mars most strongly, mean densities for three taxonomic classes of asteroids (C, S, M), the mass and the radius of the asteroid ring, the ratio masses of the Earth and the Moon;
- the solar quadrupole moment (J_2) and 15 parameters of the solar corona for different conjunctions with the Sun;
- eight coefficients of Mercury's topography and the corrections to the surface levels of Venus and Mars;
- five coefficients of the phase effect correction for the outer planets;

- constant bias for Viking-1, Viking-2, Pathfinder, MGS and Odyssey data and some other series of observations, that were interpreted as calibration errors of the instruments or as systematic errors of unknown origin;
- the relativistic parameters (β, γ, $\dot{G}/G$, $\ddot{G}/G$, the secular trend of the planet perihelia).

Some of these parameters, such as the masses of planets and asteroids and the value of the Astronomical Unit, are included into the list of numerical standards for fundamental astronomy. However, the general list of constants and initial values for underlying dynamical theories is too large, moreover the lists are different for different ephemerides and can change for any new solution. Thus, Bulletin WG "Numerical Standards of Fundamental Astronomy" (NSFA) should be supplied with pointers to the websites, where these exact dynamical models and constructed ephemerides are maintained, but not the values of all the ephemeris parameters.

Mean values and rms data residuals of the EPM2006 ephemerides are shown in Tables 1, 2. The detailed description of all the data used, plots of the observations residuals, and values of parameters obtained from the adjustment of the EPM ephemerides are given in the papers (Pitjeva, 2005a; Pitjeva, 2005b; Pitjeva, 2007). As for the accuracy and values of parameters, all the models are based on General Relativity, and certainly depend on many other factors, such as reduction techniques, dynamical models, the amount and quality of the observational data, the method used to fit the data, the amount of parameters included into the solution, and so on. Importantly, these differences are explained from a statistical point of view, and may serve for estimating real uncertainties of the solution parameters.

2. NEW VALUES OF MASSES AND THE ASTRONOMICAL UNIT

Masses of planets are the parameters of dynamical models of planet motions and, in principal, may be determined while fitting these models to the observational data. However, masses are determined more accurately from data of spacecraft orbiting and passing near planets or from observations of satellites of these planets than from position data of the parent planets. Actually, the planet masses of DE200 and DE405 were obtained by different people, different methods and with different errors, and they were chosen by E. M. Standish as the most reasonable at that time.

Some asteroids are double or have satellites and their masses are known now with reasonably good accuracy (five of such main biggest asteroids are included into integration). The masses of (433) Eros and (253) Mathilda have been derived by perturbations of the spacecraft during the NEAR flyby. Masses of the several most massive asteroids which affect Mars and the Earth more strongly have been estimated from the observations of Martian landers and the spacecraft orbiting Mars. In the classical method of determining the masses of asteroids, the perturbed body is another asteroid for which a close encounter with the perturbing body occurs. For some favorable cases if very close encounters are provided with useful data before and after the encounter an accurate determination of an asteroid mass may be obtained. For example, a new determination of (15) Eunomia has been recently obtained by A. Vitagliano and R.M. Stoss $(1.64 \pm 0.06) \cdot 10^{-11} M_\odot$ and confirmed by two independent groups (O. Kochetova and I. Baer, S. R. Chesley). As for masses of Ceres, Pallas and Vesta, many new significantly more accurate estimations have been obtained recently by different authors from close encounters with other asteroids and from their perturbations onto Mars.

In collaboration with Dr. Standish, we have chosen the best estimations of masses of planets and asteroids (Table 3) and offered them to the IAU WG NSFA (see http://maia.usno.navy.mil/NSFA/CBE.html). The ratio of the masses of the Earth and the Moon has been obtained by E. M. Standish while fitting the DE414 to all the data; the masses of Venus and Mars have been determined by Konopliv and colleagues from the data of spacecraft Magellan for Venus and MGS and Odyssey for Mars; the masses of Jupiter and Saturn have been obtained by Jacobson and the colleagues from the data of spacecraft near these planets and the Earth-based observations of the satellites of these planets; the mass of Pluto has been improved recently by Tholen and colleagues from astrometrical observations of Charon and the two small Pluto's satellites; the mass of Eris has been estimated by Brown and Schaller from observations the Eris's satellite Dysnomia. Values and their errors of the asteroid masses are road ones taken from looking at a number of recent sources.

The value of the Astronomical Unit in SI meters or after dividing by the the speed of light in SI seconds is one of basic parameters of DE and EPM ephemerides. The value τ_A=499.00478368061 [SI s] was obtained for ephemerides DE405 constructed by Standish (1998). However, at present this value is slightly obsolete. For WG NSFA we have proposed the mean value: τ_A = 499.004783826(10) [SI s],

Planet	Previous values	New values	Year	Authors
M_M/M_E	$1.23000345(5)\cdot10^{-2}$	$1.23000371(4)\cdot10^{-2}$	2006	Standish
$M_\odot/M_V$	$4.0852371(6)\cdot10^5$	$4.08523719(8)\cdot10^5$	1999	Konopliv et al.
$M_\odot/M_{Ma}$	$3.098708(9)\cdot10^6$	$3.09870359(2)\cdot10^6$	2006	Konopliv et al.
$M_\odot/M_J$	$1.0473486(8)\cdot10^3$	$1.047348625(17)\cdot10^3$	2003	Jacobson
$M_\odot/M_{Sa}$	$3.497898(18)\cdot10^3$	$3.4979018(1)\cdot10^3$	2006	Jacobson et al.
$M_\odot/M_P$	$1.3521(15)\cdot10^8$	$1.36578(32)\cdot10^8$	2007	Tholen et al.
$M_\odot/M_{Eris}$		$1.191(14)\cdot10^8$	2007	Brown et al.
$M_{Ceres}/M_\odot$	$4.39(4)\cdot10^{-10}$	$4.72(3)\cdot10^{-10}$	2007	Pitjeva,Standish
$M_{Pallas}/M_\odot$	$1.59(5)\cdot10^{-10}$	$1.03(2)\cdot10^{-10}$	2007	Pitjeva,Standish
$M_{Vesta}/M_\odot$	$1.69(11)\cdot10^{-10}$	$1.35(2)\cdot10^{-10}$	2007	Pitjeva,Standish

Table 3: New values of masses of planets and asteroids proposed to WG NSFA

taken from papers (Standish, 2005 and Pitjeva, 2005). However, all the values of τ_A were obtained while fitting DE and EPM ephemerides constructed for the TDB coordinate system. The conversion τ_A from TDB ephemerides to TCB ephemerides is ambiguous. There are two different versions of conversion to TCB ephemerides proposed by Brumberg and Simon, Fukushima, and Standish. Thus, I think that the constant $\tau_A = 499.004783826(10)$ [SI s] should be followed by the words "the TDB coordinate system".

3. REFERENCES

Brown, M.E. and Schaller, E.L., 2007, "The mass of dwarf planet Eris", Science, 316, p. 1585, doi: 10.1126/science.1139415.

Fienga, A., Manche, H., Laskar, J., Gastineau, M., 2007, "INPOP06: a new numerical planetary ephemeris", A&A , in print.

Jacobson, R.A., 2003, "JUP230 orbit solution".

Jacobson, R.A., Antreasian, P.G., Bordi, J.J., Criddle, K.E., Ionasescu, R., Jones, J.B., Mackenzie, R.A., Pelletier, F.J., Owen Jr., W.M., Roth, D.C. and Stauch, J.R., 2006, "The gravity field of the Saturnian system from satellite observations and spacecraft tracking data", AJ 132(6), pp. 2520-2526.

Konopliv, A.S., Banerdt, W.B., and Sjogren, W.L., 1999, "Venus Gravity: 180th Degree and Order Model", Icarus, 139, pp. 3–18.

Konopliv, A. S., Yoder, C. F., Standish, E. M., Yuan, D. N., Sjogren, W. L., 2006, "A global solution for the Mars static and seasonal gravity, Mars orientation, Phobos and Deimos masses, and Mars ephemeris", Icarus, 182, pp. 23-50.

Krasinsky G.A., 2002, "Selenodynamical parameters from of LLR observations of 1970-2001", Communication of IAA RAS, 148, pp. 1–27.

Krasinsky, G. A., Pitjeva, E. V., Vasilyev, M. V., and Yagudina E. I., 2002, "Hidden mass in the asteroid belt", Icarus, 158, pp. 98–105.

Pitjeva, E.V., 2005a, "High-precision ephemerides of planets – EPM and determinations of some astronomical constants", Solar System Research., 39(3), pp. 176–186.

Pitjeva, E.V., 2005b, "Precise determination of the motion of planets and some astronomical constants from modern observations", IAU Coll. N 196 / Transit of Venus: new views of the solar system and galaxy (ed. D.W. Kurtz), Cambridge: Cambridge University Press, pp. 230–241.

Pitjeva, E. V., 2007, "National high-precision ephemerides of planets and the Moon — EPM", Proceedings of IAA RAS, 17, pp. 42–59 (in Russian).

Standish, E. M., 1998, "JPL Planetary and Lunar Ephemerides, DE405/LE405", Interoffice Memorandum, 312.F-98-048, pp. 1–18.

Standish, E. M., 2005, "The astronomical unit now", IAU Coll. N 196 / Transit of Venus: new views of the solar system and galaxy (ed. Kurtz D.W.), Cambridge: Cambridge University Press, pp. 163–179.

Standish, E. M., 2006, "JPL Planetary, DE414", Interoffice Memorandum, 343R-06-002, pp. 1–8.

Tholen, D.J., Buie, M.W., and Grundy, W., 2007, "Masses of Nix and Hydra", to be submitted to AJ .

Vitagliano, A. and Stoss, R.M., 2006, "New mass determination of (15) Eunomia based on a very close encounter with (50278) 2000CZ12", A&A , 455(3) pp. L29–31.

INPOP06, A NEW NUMERICAL EPHEMERIS

A. FIENGA[1,2], H. MANCHE[1], J. LASKAR[1], M. GASTINEAU[1]
[1] IMCCE, Observatoire de Paris
77 avenue Denfert-Rochereau, 75014 Paris
[2] Observatoire de Besançon
41 bis av. de l'Observatoire, 25000 Besançon
e-mail: agnes@obs-besancon.fr

ABSTRACT. [1]

INPOP06 is the new numerical planetary ephemerides developed at the IMCCE-Observatoire de Paris. INPOP (Intégrateur Numérique Planétaire de l'Observatoire de Paris) is a numerical integration of the motion of the nine planets and the Moon fitted to the most accurate available planetary observations. It also integrates the motion of 300 perturbing main belt asteroids, the rotation of the Earth and the Moon libration. We used more than 55000 observations including the last tracking data of the Mars Global Surveyor (MGS) and Mars Odyssey (Odyssey) missions. The accuracy obtained with INPOP06 is comparable to the accuracy of last versions of the JPL DE ephemerides (DE414, Standish 2003, JPL IOM, 312N, 03; Konopliv et al. 2006, Icarus, 182, 23) and of the EPM ephemerides (EPM2004, Pitjeva 2005, Sol. Syst. Res., 39, 176).

The reader should refer to the full paper (Fienga et al., 2008) for a detailed description of this new planetary ephemeris. The account of the ongoing effort on the fit of the INPOP ephemeris to lunar laser ranging data is provided in the companion paper (Manche et al., 2008) of the present volume.

REFERENCES

Fienga, A., Manche, H., Laskar, J., Gastineau, M., 2008, "INPOP06. A new planetary ephemeris", A&A 477, pp. 315–327

Manche, H., Bouquillon, S., Fienga, A., Laskar, J., Francou, G., Gastineau, M., 2008, "Towards INPOP07, adjustment to LLR data", this Volume

[1] Presentation given by J. Laskar

TOWARDS INPOP07, ADJUSTMENTS TO LLR DATA

H. MANCHE[1], S. BOUQUILLON[2], A. FIENGA[1,3], J. LASKAR[1], G. FRANCOU[2], M. GASTINEAU[1]
[1] IMCCE, Observatoire de Paris
77 avenue Denfert-Rochereau, 75014 Paris
e-mail: manche@imcce.fr
[2] SYRTE, Observatoire de Paris
77 avenue Denfert-Rochereau, 75014 Paris
e-mail: Sebastien.Bouquillon@obspm.fr
[3] Observatoire de Besançon
41 bis av. de l'Observatoire, 25000 Besançon
e-mail: agnes@obs-besancon.fr

ABSTRACT. INPOP06 is the latest numerical planetary ephemeris developed at IMCCE (Paris-Observatory). In this version, the motion of planets has been fitted to observations (Fienga et al. 2008). In INPOP07, currently in development, the motion of the Moon will be moreover fitted to Lunar Laser Ranging observations (about 17000 data over 36 years, from 3 different sites). We present here our fitting process, the physical effects taken into account in the computation of the residuals and our latest results.

1. REDUCTION OF OBSERVATIONS

A LLR data is the measurement of the round-trip travel time for laser pulses between a station on the Earth and a lunar reflector. The expression of the outward journey (a similar computation can be made for the downward one) is:

$$\Delta T = \frac{\|\overrightarrow{BL_2} + \overrightarrow{LR_2} - (\overrightarrow{BE_1} + \overrightarrow{ES_1})\|}{c} + \Delta T_{GR} + \Delta T_{atm} \quad (1)$$

where

- c is the speed of the light
- $\overrightarrow{BL_2}$ is the solar system barycentric position of the center of mass of the Moon at time of reflection
- $\overrightarrow{LR_2}$ is the selenocentric position of the reflector at time of reflection
- $\overrightarrow{BE_1}$ is the solar system barycentric position of the center of mass of the Earth at time of emission
- $\overrightarrow{ES_1}$ is the geocentric position of the station at time of emission
- ΔT_{GR} is the time delay due to the light deviation due to the curvature of space
- ΔT_{atm} is a time delay due to the atmosphere

All these vectors are expressed in the ICRF.

The coordinates of $\overrightarrow{BL_2}$ and $\overrightarrow{BE_1}$ are directly provided by the INPOP ephemeris. From the fixed positions of the reflectors in the selenocentric reference frame, some small displacements are added, due to the solid tides raised by the Earth and the Sun, and due to the variation of the spin of the Moon. The transformation to the ICRF to obtain $\overrightarrow{LR_2}$ is then obtained using the libration angles that are integrated in INPOP at the same time as the orbits of the planets. Finally, $\overrightarrow{ES_1}$ is computed according to the IERS Conventions 2003 (McCarthy and Petit, 2004). From the position of the station in ITRF2000, some small displacements due to the following physical effects are taken into account:

- tectonic plate motion
- solid tides raised by the Sun and the Moon

- atmospheric loading
- ocean loading
- polar tide

The transformation to ICRF is then computed with the method explained in IERS Conventions 2003 (chapter 5), using the coordinates of the Celestial Intermediate Pole and the Earth Orientation Parameters given by the C04 series (UT1-UTC, polar motion, and corrections to the CIP coordinates). Finally, relativist corrections due to the transformation from a frame whose origin is the center of mass of the Earth to the ICRF whose origin is the solar system barycenter are applied. The same kind of corrections should be taken into account for the Moon, but have been neglected up to now.

The expression of ΔT_{GR} can be found in (Williams & al. 1996); only the terms due to the Sun and the Earth are taken here into account. To compute ΔT_{atm}, the (Marini & Murray 1973) model is used, it is described in the IERS Conventions 2003 (chapter 9).

Up to now, the transformation between TT and the time used in the ephemeris (T_{INPOP}) is taken from the expression of Fairhead & Bretagnon (1990). But this expression, computed from the planetary solution VSOP (fitted on DE200), is not entirely consistent with another ephemeris. In INPOP07, for better consistency, the difference $TT - T_{INPOP}$ will be integrated at the same time as the orbits of the planets, using the formalism of S. Klioner (2007) and in agreement with the IAU 2006 Resolution 3. Nevertheless, it should be noted that this change will have no significant effect on the residuals (Observation minus Computation).

2. ADJUSTMENTS AND FIRST RESULTS

The first version INPOP05 was built to retrieve the JPL's solution DE405, with the same dynamical model, initial conditions and parameters. In INPOP06, after some improvements of the dynamical model, the initial conditions and parameters were fitted to planetary observations (Fienga et al. 2008). But LLR data were not used in the fit of INPOP06, and in order to constrain the orbit of the Moon, its initial conditions (and time delays used in the computations of tide effects) were fitted on the Earth-Moon distance of DE405. As a result, over 30 years around J2000, the difference on the Earth-Moon distance between DE405 and INPOP06 is less than 8 mm.

In a first step, we use the model described in the previous section for the reduction of the LLR observations with INPOP06. The observations are the ones of Grasse (Observatoire de la Côte d'Azur, France), between 1987 and 2005. We only fit the coordinates of the 4 lunar reflectors in the selenocentric frame. The difference between observation and computation of the light times (O-C), divided by the speed of light and by 2 to get a one way distance are shown in figure 1; the standard deviation ($\sigma = 30$ cm) is important compared to the precision of the observations (a few cm).

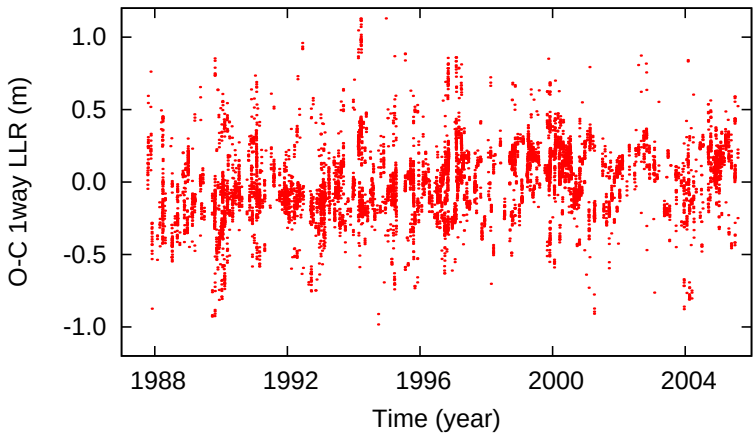

Figure 1: LLR residuals (m) for INPOP06 on Grasse's data from 1987 to 2005.

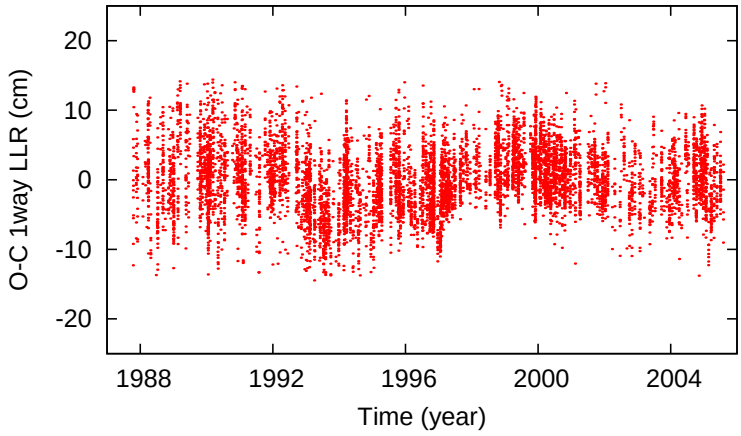

Figure 2: LLR residuals (cm) for INPOP07 on Grasse's data from 1987 to 2005.

With INPOP07 (work in progress), initial conditions and parameters are directly fitted to same LLR data (Grasse between 1987 and 2005). In this second step, the different fitted constants (used in the dynamical model and/or in the reduction process) are:

- inital conditions (at J2000) of the Earth-Moon vector
- initial conditions of the libration angles
- selenocentric positions of the reflectors
- geocentric position of the station (Grasse)
- time delays used in the computation of the tide effects
- Love numbers of the Moon
- lunar coefficients of the potential
- C/MR^2 of the Moon (third moment of inertia divided by the mass and the square of the mean equatorial radius)
- the value of an offset observed in the residuals between February 1997 and June 1998 (around 0.7ns)

That is a total of 53 parameters.

The residuals are shown in figure 2. The standard deviation is $\sigma = 4.64$ cm much better than the one obtained with the solution INPOP06. Note that 179 observations over 8441 have been rejected according to the 3σ criterion during the fitting process.

We use the parameter fitted to Grasse's LLR data to compute the residuals with Mac Donald's observations between 1969 and 2006.

Figure 3 shows the residuals for Mac Donald between 1969 and 1985. The standard deviation ($\sigma = 42$ cm) is consistent with the precision of the observations at that epoch.

Between 1988 and 2006, some problems appear for recent observations of Mac Donald's observatory (see figure 4). Before 1999, the standard deviation ($\sigma = 4.7$ cm) is quite the same as for Grasse's data on the same period. But suddenly, after 1999, one can notice a severe degradation in the residuals ($\sigma > 1$ m). According to Randall L. Ricklefs (Mac Donald's observatory), it seems that this problem could come from the detector, that is 30 years old and not as efficient as in the past. Nevertheless, we can take into account these recent observations by eliminating at each step some of them according to the 3σ criterion. On that period, with 30% of data rejected, a first estimation of the standard deviation is $\sigma = 7$ cm.

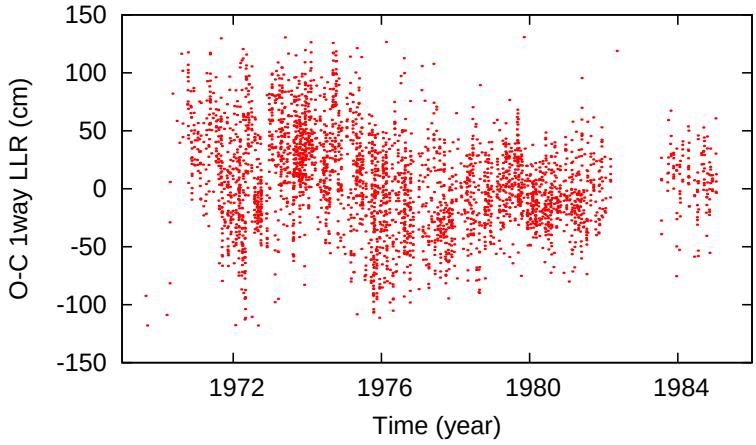

Figure 3: LLR residuals (cm) for INPOP07 on Mac Donald's data from 1969 to 1985.

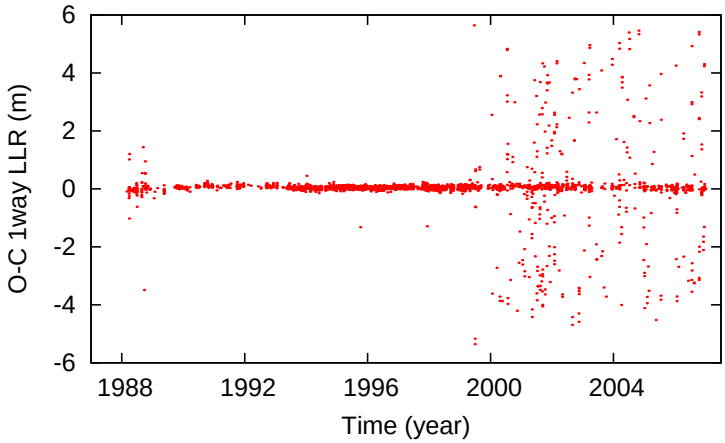

Figure 4: LLR residuals (m) for INPOP07 on Mac Donald's data from 1988 to 2006.

Finally, it should be stressed that the INPOP07 solution described here is still a preliminary version; the final solution will be fitted on all available LLR data, from the 3 sites, Mac Donald, Grasse and Haleakala, from 1969 to 2006.

3. REFERENCES

Fairhead L., Bretagnon P., 1990, "An analytical formula for the time transformation TDB-TT", A&A 229, pp. 240-247

Fienga, A., Manche, H., Laskar, J., Gastineau, M., 2008, "INPOP06. A new planetary ephemeris", A&A 477, 315-327

IAU 2006 Resolution 3, "Re-definition of Barycentric Dynamical Time, TDB", XXVIth International Astronomical Union General Assembly, 2006, Prague

Klioner, S., 2007, *personnal communication*

Marini, J. W., Murray, C. W., 1973, "Correction of laser range tracking data for atmospheric refraction at elevations above 10 degrees", NASA-TM-X-70555, Goddard Space Flight Center, Greenbelt, MD

McCarthy, D. D., Petit, G., 2004, "IERS Conventions (2003)", IERS technical Note n 32

Williams, J. G., Newhall, X. X., Dickey, J. O., 1996, "Relativity parameters determined from lunar laser ranging", Physical Review D, Volume 53, Issue 12, pp. 6730-6739

PROSPECTS FOR IMPROVING THE MASSES OF MINOR PLANETS

J.L. HILTON
U.S. Naval Observatory
3450 Massachusetts Ave., NW, Washington, DC 20392, USA
e-mail: jhilton@usno.navy.mil

ABSTRACT. Among the largest uncertainties in the fundamental constants of astronomy are the masses of the minor planets. They constitute the largest source of uncertainty in the ephemerides of the inner planets. Few asteroid masses are known with an uncertainty of better than about 50%. With a few exceptions, minor planet masses are determined by observing the perturbation of a massive minor planet on a smaller one during a close encounter. The recent explosion of discoveries of minor planets and the increased accuracy of modern astrometric catalogs means that it may be possible to discover more such encounters. A series of simple filters were developed to search for these encounters. For example, three encounters were found with Ceres, which are almost certainly strong enough to provide a mass estimate with a significantly smaller uncertainty than current estimates prior to Dawn's arrival there in 2015.

1. INTRODUCTION

The masses of the minor planets are one of the least known of the constants of fundamental astronomy. Few minor planets have masses with reliable uncertainties less than 1% the majority have masses based on assumptions of their size deduced from photometry and chemical makeup deduced from spectroscopy. At the same time, the perturbations of the minor planets constitute the largest unsolved problem in the refinement of the ephemerides of the inner planets (Standish & Fienga 2002).

As a part of the mission planning for the Dawn Mission[1] to (1) Ceres and (4) Vesta, a study was done (Hilton 2008) to determine if there were any encounters between now and Dawn's arrival at these two minor planets that could significantly improve upon the ∼1% uncertainty of the current best estimate for their masses provided by Konopliv et al. (2006). The results of this search is the main result of this paper.

2. THE TECHNIQUE

A series of simple filters were devised in Hilton (2008) to find those encounters that occur at a close enough distance and slow enough velocity to produce an observable change in the orbit of the perturbed minor planet. These filters are based on the expected change in the semi-major axis of the perturbed minor planet using the scattering equation

$$\tan\frac{1}{2}\theta = \frac{G(M+m)}{v^2 b} \tag{1}$$

where θ is the scattering angle, G is the gravitational constant, M and m are the masses of the massive and perturbed minor planets, respectively, v is the velocity of m relative to M, and b is the impact parameter[2]. For simplicity, Keplerian orbits are assumed. It is also assumed that $M \gg m$, so that the center of mass is essentially the center of mass of the massive minor planet and the mass of the perturbed minor planet can be ignored. These filters greatly constrain the search space for even the largest minor planet. Table 1 shows the parameter space in which a perturbed minor planet may be perturbed by Ceres or Vesta by enough to change the semi-major axis by 10^{-5} AU.

Although developed for the improvement of the masses of Ceres and Vesta, the techniques developed for finding these encounters are general and may be applied to the mass determination of any massive minor planet. All that is required for input are:

[1] http://dawn.jpl.nasa.gov/

[2] The minimum distance between m and M if there were no force between the two minor planets.

	Δa (AU)	Δe	$\Delta\omega$ ($\prime$)	i ($\prime$)
Ceres	0.014	0.012	21	41
Vesta	0.007	0.009	16	31

Table 1: Maximum differences in orbital elements that will allow a change of at least 10^{-5} AU to a perturbed minor planet.

- An initial order of magnitude estimate for the mass of the massive minor planet.
- A database of candidate perturbed minor planets with elements similar to those of the massive minor planet
- A time window over which observations of the perturbed minor planet will be available.

Fulfilling these requirements is a balancing act between several competing interests:

- The size of the perturbation by the massive minor planet is quite small, even for the largest minor planet. Thus, a long time span for observations is desired to maximize the observed effect of the perturbation.
- The perturbed minor planet is subject to perturbations by many other, relatively low mass minor planets. That is, it is subject to unmodelled forces. Thus, a short series of observations is desired to minimize the effects of the unmodelled forces.
- A larger perturbed minor planet is brighter and thus its position may be directly compared to state of the art astrometric catalogs such as the UCAC (Zacharias et al. 2004). This results in a more accurate orbit allowing a smaller perturbation to be detected. Thus, just as long as its mass is negligible in comparison to the massive minor planet, a larger perturbed minor planet is desirable.
- The size distribution of minor planets is a power law with a negative index (e.g. Bottke et al. 1005). Thus, the perturbed minor planet in an encounter with the massive minor planet is more likely to be small and dim instead of large and relatively bright.

Using the currently best possible time and space resolution for an optical astrometric observation, propagation of errors shows that to determine the mass of a large minor planet with an uncertainty of 5% using a single year of observations –six months prior to the encounter and six months afterward– requires a change in the semi-major axis of the perturbed minor planet $\sim 10^{-5}$ AU (Hilton 2008). The accuracy of the mass determination is directly proportional to the length of time over which the perturbed minor planet is observed both prior to and after the encounter and the change in the perturbed minor planet's semi-major axis. It is also directly proportional to the quadrature combination of the accuracy in the astrometric position and time of observation.

The effect of these filters is to constrain the volume of orbital element space that needs to be searched to find encounters likely to lead to a reliable, high accuracy minor planet mass determination. In the cases of Ceres and Vesta this space is further reduced by requiring that the encounter occur in the period between the discovery of the perturbed minor planet and Dawn's arrival at each of these two targets.

3. RESULTS FOR CERES AND VESTA

Unfortunately, for Vesta only a single encounter was found that could improve its mass. This encounter, with 2004 RO_{69}, does not occur until June 2011, only five months prior to Dawn's arrival at Vesta. Thus, there is simply not enough time to make the observations necessary to make a mass determination using this encounter. The best estimate of Vesta's mass will remain that of Konopliv et al. (2006) until a mass can be derived from Dawn's interaction with Vesta.

On the other hand, three excellent encounters were found for improving the mass of Ceres. These encounters are detailed in Table 2. Each encounter has its own unique advantages.

2004 BW_{137}. The encounter with 2004 BW_{137} is of interest because it is the earliest of the three. The current estimate of the uncertainty in the semi-major axis of 2004 BW_{137} from the AstDys web site (Knežević & Milani 2003) is 5×10^{-7} AU from 34 observations made between 2000 and 2005. If observations can be made of a similar accuracy to those prior to the encounter the potential uncertainty in the mass of Ceres derived from this encounter will be 0.2%. The next opposition of 2004 BW_{137} occurs during Nov. 2007. Thus, a preliminary Ceres mass from this encounter should be available in early 2008.

Perturbed Minor Planet	Date	a (AU)	v (m/s)	δa (AU)
2004 BW_{137}	2005.69	2.865	6	5×10^{-4}
4325 Guest	2008.58	2.749	18	1×10^{-4}
2000 EM_{61}	2013.14	2.802	-1	6×10^{-2}

Table 2: Encounters with Ceres prior to Dawn's arrival which have a potential for reducing the uncertainty in Ceres' mass.

4325 Guest. The encounter with 4325 Guest has two advantages. First, Guest was discovered in 1975 and has well over 700 observations. The current uncertainty in its semi-major axis as estimated by AstDys is 4×10^{-8} AU, an order of magnitude smaller than that of 2004 BW_{137}. Probably even more important is Guest is much brighter with a mean opposition V magnitude of approximately 15.7. This additional brightness means

- Guest may be observed for a longer period of time around its opposition.
- Guest may be observed by smaller telescopes than the other two test minor planets. Thus, there are more opportunities to observe it.
- Guest is bright enough that its position may be reduced using the accurate UCAC catalog.

Thus, Guest has the potential advantage of allowing more numerous and more accurate observations. As a result, it may yield a more accurate mass than 2004 BW_{137} even though the expected change in Guest's semi-major axis is only 1/5 that of 2004 BW_{137}.

2000 EM_{61}. The encounter of 2000 EM_{61} occurs in late January-early February 2013, just two years before Dawn's arrival at Ceres. However, the strength of the encounter is enormous with an estimated δa of 6×10^{-2} AU. The strength of the encounter arises from the extremely slow speed of 1 m s^{-1}. The most likely source of error in the size of the perturbation is thus an error in the encounter speed. Hilton (2008) shows that, assuming a Keplerian orbit, the value of δa depends on the encounter speed to the fifth power. Thus, if the encounter velocity was 2 m s^{-1} the value of δa would be only 1/32 of the estimated value. An error of this magnitude is unlikely. For example, the rate of change in the Keplerian orbit speed at 2.8 AU for an object in a heliocentric orbit is 0.02 mm s^{-1} km^{-1}. The AstDys estimate for the uncertainty in the semi-major axis of 2000 EM_{61} is 3×10^{-7} AU (45 km), so $\sigma_v \sim 0.001$ m s^{-1}. Similar error estimates may be made using the other orbital elements. Thus, the propagation errors would indicate that a highly accurate mass with an uncertainty well under 1% is likely to be obtained from observation of 2000 EM_{61} with Ceres.

4. CONCLUSIONS

The filters developed by Hilton (2008) are quite general and can be applied to searching for encounters with any massive minor planets. It is now possible to find encounters between a massive minor planet and a perturbed minor planet that are strong enough that an accurate mass may be determined with observation periods as short as a few years.

In particular, it appears the upcoming encounter of 2000 EM_{61} with Ceres will be so strong that a mass of Ceres with an accuracy of well under 1% can be determined in only a year of observation. Furthermore, the fact that such a strong encounter was found within such a short span of time indicates that it should be possible to find encounters with massive minor planets with mean diameters in the range of 150-200 km that will yield masses with $\sim 5-10\%$ uncertainties. Such minor planets individually have only about 1% the mass of Ceres, but they are much more numerous and significant perturbers of the inner planets. A search for such encounters will be the subject of further work.

5. REFERENCES

Bottke, W.F., Jr., Durda, D.D., Nesvorný, D., Jedicke, R., Morbidelli, A., Vokroulický, D. & Levison, H.F. 2005, "Linking the Collisional History of the Main Asteroid Belt to Its Dynamical Excitation and Depletion," Icarus, 179, 63–94

Hilton, J.L. 2008, "Prospects for Improving the Masses of (1) Ceres and (4) Vesta Prior to Dawns Arrival at These Minor Planets," in preparation

Knežević, Z. & Milani, A. 2003, "Proper Element Catalogs and Asteroid Families," A&A , 403, 1165–1173
Konopliv, A.S., Yoder, C.F., Standish, E.M., Yuan, D.-N., & Sjogren, W.L. 2006, "A Global Solution for the Mars Static and Seasonal Gravity, Mars Orientation, Phobos and Deimos Masses, and Mars Ephemeris," Icarus, 182, 23–50
Standish, E.M. & Fienga, A. 2002, "Accuracy Limit of Modern Ephemerides Imposed by the Uncertainties in Asteroid Masses," A&A , 384, 322–328
Zacharias, N., Urban, S.E., Zacharias, M.I., Wycoff, G.L., Hall, D.M., Monet, D.G. & Rafferty, T.J. 2004, "The Second U.S, Naval Observatory CCD Astrograph Catalog (UCAC2)," AJ , 127, 3043–3059

HARMONIC MODELS OF TIDE-GENERATING POTENTIAL OF THE TERRESTRIAL PLANETS

S.M. KUDRYAVTSEV
Sternberg Astronomical Institute of Moscow State University
13, Universitetsky Pr., Moscow, 119992, RUSSIA
e-mail: ksm@sai.msu.ru

ABSTRACT. High-accurate harmonic development of the tide-generating potential (TGP) of Mercury, Venus and Mars is made. For that the planets TGP values were first calculated on the base of DE/LE-406 numerical ephemerides over a long period of time and then processed by a new spectral analysis method. A feature of the method is the development is directly made to Poisson series where both amplitudes and arguments of the series' terms are high-degree polynomials of time. The new harmonic development of Mars TGP is made over the time period 1900-2100 and includes 767 second-order Poisson series' terms of minimum amplitude equal to 10^{-7} m^2/s^2. Similar series composing the Mercury and Venus TGP models are built over the time period 1000-3000 and include 1,061 and 693 terms, respectively. A modification of the standard HW95 format for representation of the terrestrial planets TGP is proposed. The number of terms in the planetary TGP models transformed to the modified HW95 format is 650 for Mercury, 422 for Venus, and 480 for Mars.

1. INTRODUCTION

Study of the tide generating potential (TGP) of the terrestrial planets is an actual task now. Several space missions scheduled to our neighbor planets, in particular to Mercury and Mars (e.g. Messenger by NASA, BepiColombo, NetLander by ESA and others) will perform in-situ measurements of the planetary nutation and tidal variations of the planets' gravity field. These effects are the result of the planet's body response to the perturbing TGP. Comparison of this response observed at different wave frequencies with the TGP harmonic model helps one to study the planet's internal structure.

There are several developments of the TGP for the terrestrial planets. The latest are the harmonic expansion of Mercury TGP made by Van Hoolst and Jacobs (2003) and expansion of Mars TGP done by Roosbeck (1999) and Van Hoolst et al. (2003). All these developments used VSOP87 analytical theory of the major planets motion (Bretagnon and Francou, 1988) as the source of planetary coordinates, and made a number of analytical transformation of VSOP87 harmonic series to obtain the planets TGP expansion. However, the accuracy of VSOP87 analytical theory is lower than that of the modern numerical ephemerides of the major planets. In particular, the current IERS Conventions (McCarthy and Petit, 2004) recommend the DE/LE-405 planetary/lunar numerical ephemerides (Standish, 1998) for precision studies.

In this paper we present a new harmonic development of the TGP for three terrestrial planets: Mercury, Venus and Mars. [A development of the Earth TGP is done in (Kudryavtsev, 2004).] The latest long-term planetary/lunar numerical ephemerides DE/LE-406 (they are the extension of DE/LE-405 over 6,000 years) are used as the source of the Sun, Moon and major planets coordinates. The expansion of the planetary TGP is made with use of a new modification of the spectral analysis method.

The expansion procedure and obtained results on harmonic development of the three terrestrial planets TGP are described in the following sections.

2. FORMULATION OF THE PLANETARY TGP

The TGP generated by external perturbing bodies (the Sun, major planets, etc.) at an arbitrary point P on the planet's surface is represented in our study as

$$V(t) = \sum_{n=1}^{\infty} \sum_{m=0}^{n} V_{nm}(t) = \sum_{n=1}^{\infty} \left(\frac{r}{R_{pl}} \right)^n \sum_{m=0}^{n} \bar{P}_{nm} (\sin \varphi') \left[C_{nm}(t) \cos m\theta(t) + S_{nm}(t) \sin m\theta(t) \right] \quad (1)$$

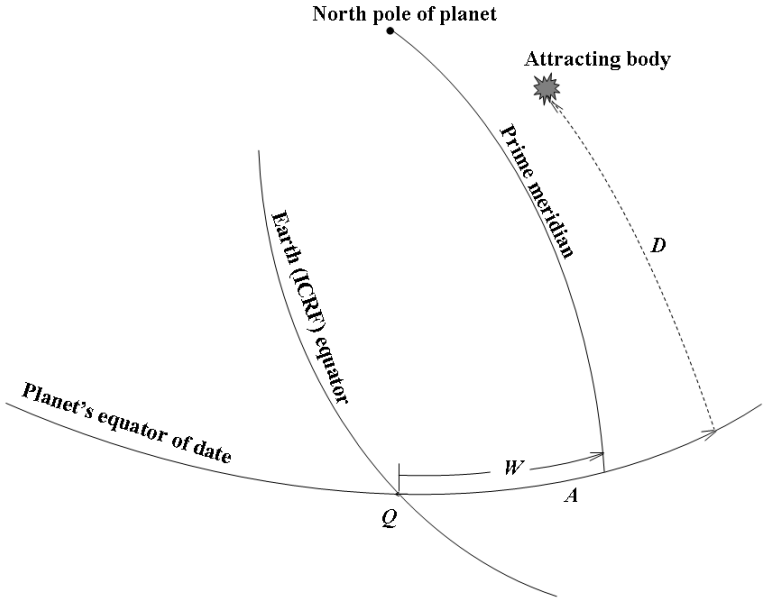

Figure 1: Spherical coordinates used when developing the terrestrial planets TGP

where $V(t)$ is the instantaneous value of the TGP at the point P at epoch t, and if $n = 1$

$$C_{10}(t) = \sqrt{\frac{15}{7}} \frac{\bar{J}_{2_{pl}}}{R_{pl}} \sum_j \mu_j \left(\frac{R_{pl}}{r_j(t)} \right)^4 \bar{P}_{30} \left(\sin D_j(t) \right), \tag{2}$$

$$C_{11}(t) = \sqrt{\frac{10}{7}} \frac{\bar{J}_{2_{pl}}}{R_{pl}} \sum_j \mu_j \left(\frac{R_{pl}}{r_j(t)} \right)^4 \bar{P}_{31} \left(\sin D_j(t) \right) \cos A_j(t), \tag{3}$$

$$S_{11}(t) = \sqrt{\frac{10}{7}} \frac{\bar{J}_{2_{pl}}}{R_{pl}} \sum_j \mu_j \left(\frac{R_{pl}}{r_j(t)} \right)^4 \bar{P}_{31} \left(\sin D_j(t) \right) \sin A_j(t) \tag{4}$$

if $n \geq 2$

$$C_{nm}(t) = \frac{1}{2n+1} \sum_j \frac{\mu_j}{R_{pl}} \left(\frac{R_{pl}}{r_j(t)} \right)^{n+1} \bar{P}_{nm} \left(\sin D_j(t) \right) \cos mA_j(t), \tag{5}$$

$$S_{nm}(t) = \frac{1}{2n+1} \sum_j \frac{\mu_j}{R_{pl}} \left(\frac{R_{pl}}{r_j(t)} \right)^{n+1} \bar{P}_{nm} \left(\sin D_j(t) \right) \sin mA_j(t); \tag{6}$$

r, φ' and λ are respectively the planetocentric distance, latitude and longitude of the point P; R_{pl}, $\bar{J}_{2_{pl}}$ are respectively the planet's mean equatorial radius and normalized dynamical form factor; μ_j, $r_j(t)$, $A_j(t)$, $D_j(t)$ are respectively the gravitational parameter, planetocentric distance and angular spherical coordinates of j^{th} perturbing body referred to the planet's equator of epoch t with an origin point Q - that being the node of the planet's equator of date on the standard Earth (ICRF) equator (Fig.1); $\bar{P}_{nm}$ are the normalized associated Legendre functions; the angle θ specifies the position of the local meridian of the point P relative to the origin point Q so that

$$\theta(t) = \lambda + W(t), \tag{7}$$

and $W(t)$ is the rotation angle of the planet's prime meridian reckoned from the node Q as defined by Seidelmann et al. (2000).

The coefficients $C_{nm}(t)$, $S_{nm}(t)$ contain all the necessary information about instantaneous positions of the perturbing bodies at every epoch t at which one calculates the TGP value $V(t)$.

Having harmonic expansions for $C_{nm}(t)$, $S_{nm}(t)$ done, one can further calculate time-dependent values of the TGP at an arbitrary point $P(r, \varphi', \lambda)$ on the planet's surface by using (1).

The tidal acceleration along the planet's radius (or 'the gravity tide') is defined as the radial derivative of the TGP

$$g(t) \equiv \frac{\partial V(t)}{\partial r} = \sum_{n=1}^{\infty} \frac{n}{r} \sum_{m=0}^{n} V_{nm}(t). \tag{8}$$

3. EXPANSION OF TGP FOR THE TERRESTRIAL PLANETS

We expand the coefficients $C_{nm}(t)$, $S_{nm}(t)$ of the planetary TGP model to finite second-order Poisson series of the following form:

$$C[S]_{nm}(t) = \sum_{k=1}^{N} \left[\left(A^c_{k0} + A^c_{k1} t + A^c_{k2} t^2 \right) \cos \omega_k(t) + \left(A^s_{k0} + A^s_{k1} t + A^s_{k2} t^2 \right) \sin \omega_k(t) \right] \tag{9}$$

where A^c_{k0}, A^c_{k1},$\cdots$, A^s_{k2} are constants and arguments $\omega_k(t)$ are forth-degree polynomials of time

$$\omega_k(t) = \nu_k t + \nu_{k2} t^2 + \nu_{k3} t^3 + \nu_{k4} t^4 \tag{10}$$

[$\nu_k, \nu_{k2}, \ldots$ are constants].

The expansion is made with use of a new modification of the spectral analysis method described in (Kudryavtsev, 2004). Prior to the expansion procedure we calculated numerical values of the coefficients $C_{nm}(t)$, $S_{nm}(t)$ according to (2)–(6) over a long interval of time. The latest long-term numerical ephemerides DE/LE-406 (Standish, 1998) are chosen as the source of the Sun, Moon and major planets coordinates. These ephemerides cover the time interval 3000BC–3000AD, and our expansion of the planetary TGP is centered at epoch J2000. So, in case of Mercury and Venus the time interval over which we sampled the planetary TGP values is chosen equal to 1000–3000, and the sampling step is one day. In case of Mars the time interval is 1900-2100, and the sampling step is 0.01 days only. It is necessary to set a small sampling step when calculating Mars TGP because of the fast motion of Martian moon Phobos (its orbital period is less than eight hours, and effect of Phobos attraction forms a large constituent in Mars TGP). A drawback of such a small sampling step is that the number of sampled TGP values (and as a consequence the computation time required by the spectral analysis method) dramatically increases, so we had to consider a smaller time interval for Mars than for the other two planets. MARTSAT analytical theory of Phobos and Deimos motion (Kudryavtsev et al., 1997) is chosen as the source of Martian moons coordinates. When calculating sample values for both Mercury and Venus TGP we took in account the attraction of the Sun, Moon, and all major planets (except Uranus and Neptune). For the case of Mars TGP the effect of both Phobos and Deimos attraction is additionally accounted. The radii and masses of the major planets, the Sun and Moon correspond to DE/LE-405/406 solution (Standish, 1998); the masses of Phobos and Deimos are taken from Konopliv et al. (2006).

The final expansion for the coefficients $C_{nm}(t)$, $S_{nm}(t)$ of Mars TGP includes 767 second-order Poisson series' terms of minimum amplitude equal to 10^{-7} m^2/s^2 (the maximum value for n is equal to 8 here), and expansion series for the coefficients of Mercury and Venus TGP include respectively 1,061 and 693 analogous terms (the maximum value for n is equal to 3 for the both planets TGP).

The values for the mean radius of every planet, R_{pl}, to be used in expression (1) along with the obtained series for coefficienties $C_{nm}(t)$, $S_{nm}(t)$ are as follows:

$R_{Mercury} = 2439.76$ km, $R_{Venus} = 6052.3$ km, $R_{Mars} = 3397.515$ km.

The expansion series for the coefficients $C_{nm}(t)$, $S_{nm}(t)$ are available on:

- for Mercury TGP: http://lnfm1.sai.msu.ru/neb/ksm/tgp_mercury/Mercury_TGP_coefficients.dat (the description of the data format: http://lnfm1.sai.msu.ru/neb/ksm/tgp_mercury/Readme.pdf);
- for Venus TGP: http://lnfm1.sai.msu.ru/neb/ksm/tgp_venus/Venus_TGP_coefficients.dat (the description of the data format: http://lnfm1.sai.msu.ru/neb/ksm/tgp_venus/Readme.pdf);
- for Mars TGP: http://lnfm1.sai.msu.ru/neb/ksm/tgp_mars/Mars_TGP_coefficients.dat (the description of the data format: http://lnfm1.sai.msu.ru/neb/ksm/tgp_mars/Readme.pdf).

We estimated the accuracy of calculation of the gravity tide at a mid-latitude 'station' (lander) on the planetary surface ($\varphi' = 50^\circ$, $\lambda = 0^\circ$) by means of the obtained TGP models. For every planet we found the maximum difference between the values of the gravity tide given by the relevant TGP harmonic development and 'exact' values of the tide obtained according to (1)–(8) with direct use of the perturbing bodies coordinates from DE/LE-406 numerical ephemerides and MARTSAT theory. The maximum difference between the two sets of values for the gravity tide on every planet is as follows:

- for Mercury: 0.8 nGal over the time interval 1000–3000;
- for Venus: 0.3 nGal over the time interval 1000–3000;
- for Mars: 1.1 nGal over the time interval 1900–2100.

4. REPRESENTATION OF THE PLANETARY TGP IN MODIFIED HW95 FORMAT

The coefficients $C_{nm}(t)$, $S_{nm}(t)$ are developed in a slowly precessing reference frame defined by the planet's mean equator of epoch with the node Q as the origin point (Fig.1). To represent the planetary TGP models in a planet-fixed (rotating) reference frame we employed and slightly modified the HW95 format suggested by Hartmann and Wenzel (1995) for the Earth TGP model. The planets TGP series transformed to the modified HW95 format (and description of the modified format) are available on:

- for Mercury: http://lnfm1.sai.msu.ru/neb/ksm/tgp_mercury/K07_Mercury.dat;
- for Venus: http://lnfm1.sai.msu.ru/neb/ksm/tgp_venus/K07_Venus.dat;
- for Mars: http://lnfm1.sai.msu.ru/neb/ksm/tgp_mars/K07_Mars.dat.

The number of terms in the planetary TGP harmonic models represented in the modified HW95 format is 650 for Mercury, 422 for Venus, and 480 for Mars.

Acknowledgements. The author is sincerely grateful to the Local Organizing Committee of the Journées 2007 for a grant. The work was supported in part by grant 05-02-16436 from the Russian Foundation for Basic Research.

5. REFERENCES

Bretagnon, P., Francou, G., 1988, "VSOP87: Planetary theories in rectangular and spherical variables", A&A , 202, pp. 309–315.

Hartmann, T., Wenzel, H.-G., 1995, "The HW95 tidal potential catalogue", Geophys. Res. Lett. , 22, pp. 3553–3556.

Konopliv, A.S., Yoder, C.F., Standish, E.M., Yuan, D.-N., Sjogren, W.L., 2006, "A global solution for the Mars static and seasonal gravity, Mars orientation, Phobos and Deimos masses, and Mars ephemeris", Icarus, 182, pp. 23–50.

Kudryavtsev, S.M., 2004, "Improved harmonic development of the Earth tide-generating potential", J. Geodesy , 77, pp. 829–838.

Kudryavtsev, S.M., Kolyka, Yu.F., Tikhonov, V.F., 1997, "New analytical theory of motion of Phobos and Deimos for navigation support of missions to Mars", ESA SP-403, pp. 377–382.

McCarthy, D.D., Petit, G. (eds.), 2004, "IERS Conventions (2003)", IERS Technical Note 32, Verlag des Bundesamts für Kartographie und Geodäsie, Frankfurt am Main.

Roosbeek, F., 1999, "Analytical developments of rigid Mars nutation and tide generating potential series", Celest. Mech. Dyn. Astr. , 75, pp. 287–300.

Standish, E.M., 1998, "JPL planetary and lunar ephemerides DE405/LE405", JPL IOM 312.F-98-048, Pasadena.

Van Hoolst, T., Jacobs, C., 2003, "Mercury's tides and interior structure", J. Geophys. Res. , 108(E11), pp. 5121–5136, doi:10.1029/2003JE002126.

Van Hoolst, T., Dehant, V., Roosbeck, F., Lognonné, P., 2003, "Tidally induced surface displacements, external potential variations, and gravity variations on Mars", Icarus, 161, pp. 281–296.

RECENT ADVANCES IN MODELING PRECESSION-NUTATION

V. DEHANT[1], S. LAMBERT[2], M. FOLGUEIRA[3], L. KOOT[1], N. RAMBAUX[1 4]
[1] Royal Observatory of Belgium
3 avenue Circulaire, B-1180 Brussels, Belgium
e-mail: v.dehant@oma.be; n.rambaux@oma.be; l.koot@oma.be
[2] SYRTE, Observatoire de Paris
61 avenue de l'Observatoire, F-75014 Paris, France
e-mail: sebastien.lambert@obspm.fr
[3] Universidad Complutense de Madrid
Sección Departamental de Astronomía y Geodesia, Facultad de Ciencias Matemáticas,
Universidad Complutense, ES-28040 Madrid, Spain
e-mail: martafl@mat.ucm.es
[4] Presently at JPL
Jet Propulsion Laboratory, Oak Grove Drive, Pasadena, CA 91109, USA
e-mail: ??@jpl.nasa.gov

ABSTRACT. Nutations are computed from modeling the gravitational forcing acting on the Earth from the Moon, the Sun and, to a minor extend, the other planets of the Solar system, and from modeling the interior of the Earth. One computes the Earth response to the gravitational forcing and then adds the geophysical effects from the surface liquid layers (atmosphere and ocean). The models for the interior of the Earth generally consider the existence of a liquid core, of a solid deformable inner core, and of a solid deformable inelastic mantle; the boundaries between the core and the inner core (ICB for Inner Core Boundary) and the core and the mantle (CMB for Core-Mantle Boundary) are flattened and can deform; the coupling mechanisms between the inner core, the outer core, and the mantle involve inertial coupling, gravitational coupling, pressure coupling, electromagnetic coupling, and viscous coupling. The last adopted model by the IAU and the IUGG, the so-called MHB2000 model from Mathews et al. (2002), considers all these coupling mechanisms except the viscous coupling, which is further considered in Guo et al. (2004). The rigid Earth nutations that are considered for this adopted model are those of Souchay et al. (1999).

In the present paper we concentrate on the steps performed within the group related to the Royal Observatory of Belgium, toward the next decimal of nutation theory and observation. In particular, we examine the improvements on observations, on atmospheric and oceanic contributions to nutation (for the free and forced nutations), and on the computation of dissipative and excitation mechanisms for nutation.

1. IMPROVEMENTS IN OBSERVATION

The improvement in VLBI observation is mainly coming from the consideration of criteria for radiosource stability and from a better ground station network choice. The influence of the ground station networks (R1 versus R4) has been studied by Lambert and Gontier (2007). The influence of radio source instability on VLBI results has been addressed at ROB in Lambert and Dehant (2007) and Lambert et al. (2007). In summary, we have considered various strategies constraining and estimating differently the radio source position following the stability index of the considered source (e.g., application of the No-Net-Rotation (NNR) either on the 212 ICRF defining sources or on the 247 most stable sources).

We have used these criteria for source stability at ROB. Lambert and Dehant (2007) and Lambert et al. (2007) address them in full detail. In summary, we have considered not only the sources from the ICRF (the so-called defining sources), but the stable sources, studying the structure index, the elevation cutoff considered, the number of observations of the same radio source (e.g., sources observed in more than 40 sessions), considering or not the no-net-rotation condition, and/or treating the sources with the addition of local/global parameters.

These different strategies applied to VLBI data have allowed us to determine a set of residuals with re-

spect to the MHB2000 model mentioned above. Because we wanted to study the effects not well modeled, we considered the MHB2000 model without the only atmospheric correction therein (the contribution from the atmosphere on the prograde annual nutation). The residuals represent thus the difference between VLBI observations with the different strategies and the MHB2000 model without atmospheric correction. In these residuals, we should then see the atmospheric contributions. Figure 1 shows these residuals for the main nutations. We have determined the FCN period from fitting on our new data with the different strategies for the choice of the radiosources and found that the period and quality factor are very stable. Our determination of the FCN period for instance lead to a value of 430.31 days (±0.02), very close the MHB2000 value of 430.20 days (±0.28).

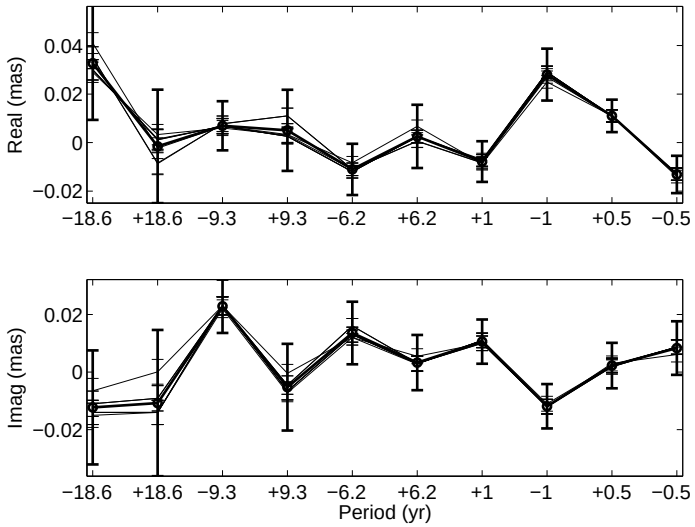

Figure 1: Residuals between VLBI observations with different strategies for the choice of the radiosources and MHB2000 without the annual atmospheric correction.

The different strategies applied to reduce the VLBI data are mainly influencing the 18.6 and 9.3 year nutations. This is to be expected as the strategies change mainly the long-term behaviour of the VLBI nutation time series.

Our aim is to better understand the interior of the Earth and therefore to obtain better results for the deep interior modeling from the new data series. More data are now handy with respect to the computation of MHB2000. We suspect that the increase of the time series with respect to the data set used for the MHB2000 construction would be seen in the evaluation of the inner core basic Earth parameters, i.e. the FICN period and quality factor. For these reasons we have decided to perform an experiment with the data and instead of analyzing the residuals with respect to MHB2000, we have analyzed the residuals with respect to MHB2000 when the inner core contributions are ignored. The new residuals represent then thus the difference between the VLBI observations with the different strategies and the modified MHB2000 model with atmospheric corrections at the prograde annual period but without inner core contributions. Figure 2 shows these residuals for the main nutations and for one of the strategies applied for the construction of Figure 1. The residuals are taken for a longer time span than MHB2000 as our data are going to 2007. The difference with MHB2000 is thus considered to be mainly the inner core contribution. This difference is mainly observed on the 18.6 year nutations (and mainly the retrograde 18.6 year nutation), and on the semi-annual nutation.

2. IMPROVEMENTS ON THE THEORY; BASIC GEOPHYSICAL PARAMETERS

As explained in Section 1, many nutation models are constructed from the convolution of rigid Earth nutation series with transfer function incorporating basic geophysical parameters that can either be approximate from our knowledge of the Earth interior or determined from the VLBI observation themselves. Improvements in the theory came recently from the determination of all sorts of coupling at the second order int this approach. In particular, Lambert and Mathews (2006) have considered all coupling mechanism between tides and nutations; Folgueira et al. (2007) have considered all couplings between the

Poisson terms of the tidal potential and the Earth response. These kinds of improvements are at the level of the microarcsecond. Further improvements will come from a better determination of the basic geophysical parameters involved in the transfer function of the Earth. These parameters, as defined in MHB2000, are the parameters entering in the Earth transfer function, and, in particular, in the FCN and FICN periods and quality factors. For an analytical approach such as the one developed in Mathews et al. (1991, see also Dehant et al. 1993), the values of the eigenfrequencies determined from the Liouville equations are approximated by:

$$\sigma^{\Re}_{FCN} = -\Omega\left(1 + \frac{A}{A_m}\left[\alpha_f - \kappa_f + K^{\Re}_{CMB} + \frac{A_s}{A_f}K^{\Re}_{ICB}\right]\right) \quad (1)$$

$$\sigma^{\Im}_{FCN} = -\Omega\frac{A}{A_m}\left(K^{\Im}_{CMB} + \frac{A_s}{A_f}K^{\Im}_{ICB}\right) \quad (2)$$

$$\sigma^{\Re}_{FICN} = -\Omega\left(1 - \left[\alpha_s\alpha_2 + \kappa_s - K^{\Re}_{ICB}\right]\right) \quad (3); \qquad \sigma^{\Im}_{FICN} = -\Omega K^{\Im}_{ICB} \quad (4)$$

where $\sigma^{\Re}_{FCN}$, $\sigma^{\Im}_{FCN}$, $\sigma^{\Re}_{FICN}$, and $\sigma^{\Im}_{FICN}$ are the real ($^{\Re}$) and imaginary ($^{\Im}$) parts of the FCN and FICN frequencies; Ω is the uniform Earth rotation frequency; A, A_m, A_f, and A_s are the principal moments of inertia of the whole Earth, the mantle, the outer core, and the inner core, respectively; α_f and α_s are the dynamical flattenings of the outer core and inner core; κ_f and κ_s are the compliances for the boundary deformations at the CMB and ICB respectively; $K^{\Re}_{CMB}$, $K^{\Im}_{CMB}$, $K^{\Re}_{ICB}$, and $K^{\Im}_{ICB}$ are the real ($^{\Re}$) and imaginary ($^{\Im}$) parts of the coupling constants at the CMB and ICB; and $\alpha_2 = A'e'/A_s\alpha_s(1+\alpha_g) - \alpha_g$ where α_g is a measure of the strength of the gravitational torque between a tilted inner core and the rest of the Earth (see Mathews et al., 1991), and A' and e' are the equatorial moment of inertia and dynamical ellipticity, respectively, of an homogeneous ellipsoid of the same dimensions as the inner core but having the same density ρ_f as the core fluid at the ICB.
As seen from Eq. (3), the determination of the real and imaginary parts of the FICN frequency $\sigma^{\Re}_{FICN}$ and $\sigma^{\Im}_{FICN}$ is perfectly equivalent to the determination of the real and imaginary parts of the ICB coupling constant, $K^{\Re}_{ICB}$ and $K^{\Im}_{ICB}$, provided that we consider that the inner core is in hydrostatic equilibrium and thus knowing the hydrostatic dynamical flattening α_s. Knowing the real and imaginary parts of the ICB coupling constant, $K^{\Re}_{ICB}$ and $K^{\Im}_{ICB}$, the imaginary part of the CMB coupling constant $K^{\Im}_{CMB}$ can be determined from $\sigma^{\Im}_{FCN}$ by using Eq. (4). Eq. (1) relates $\sigma^{\Re}_{FCN}$ to a combination of the real part of the CMB coupling constant $K^{\Im}_{CMB}$ and the core flattening α_f that can thus not be uniquely determined from $\sigma^{\Re}_{FCN}$. One way to solve the problem is to suppose a theoretical relation between the real and imaginary parts of the CMB coupling constant, $K^{\Re}_{CMB}$ and $K^{\Im}_{CMB}$. This is equivalent to a perfect understanding of the coupling mechanisms at the CMB, which is far to be the case. A first step in the direction of a solution has been performed by Mathews et al. (2002) who supposed that the coupling at the CMB was mainly due to the reaction to stretching by the nutation of the CMB magnetic field. The electromagnetic coupling was further examined together with viscous coupling by Guo et al. (2004). The topographic coupling has been estimated by Wu and Wahr (1997) with a numerical approach and by Folgueira and Dehant (2007) with an analytical approach. Using these kinds of assumption, it is possible to estimate the departure from hydrostatic equilibrium flattening at the CMB.

Figure 2 represents the determination of the real and imaginary parts or equivalently the period and quality factor of the FICN. The arrows indicate the values proposed in MHB2000. The contributions from the different forced nutations and for the possible changes arising from the different strategies for the VLBI data analysis as explained in the previous section are shown in different colors.

We have then computed the contribution to the forced nutations from the different possibilities for the FICN period and quality factor. We have observed that the contribution at the 18.6 retrograde nutation, one of the most sensitive nutation to the FICN parameters as shown in Section 2, as computed from MHB2000 is very close to our best determination, i.e. -0.16 mas (milliarcsecond) on the real part of 18.6 year retrograde nutation and 0.21 mas on the imaginary part.

3. TIME DOMAIN APPROACH FOR A BETTER DETERMINATION OF THE BASIC GEOPHYSICAL PARAMETERS

The geophysical parameters presented here above have been fitted from the amplitudes of the forced nutations, which have been, in turn, determined from the VLBI data (the delays). This procedure involves three steps: (1) a determination of the nutation in longitude and in obliquity as a function of time from

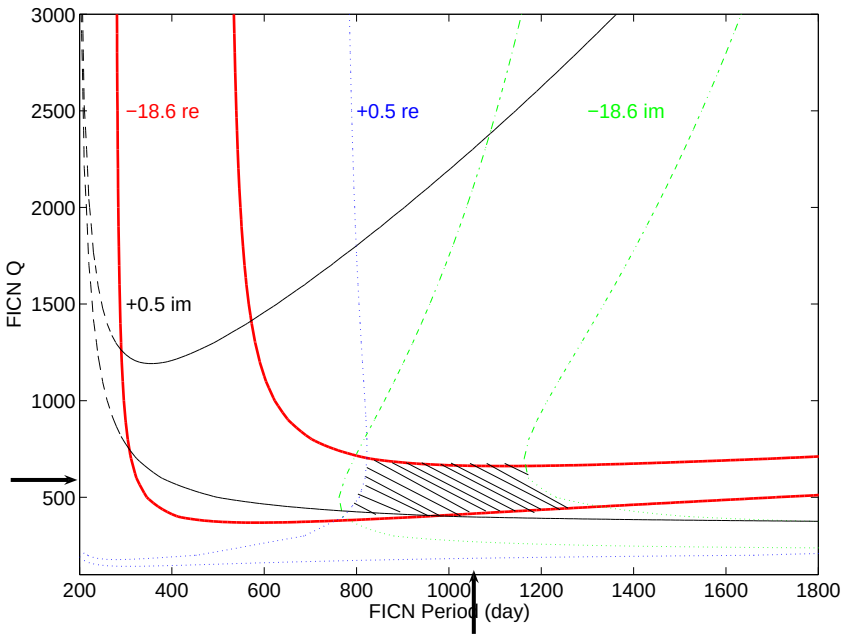

Figure 2: Period and quality factor of the FICN determined from the different forced nutations individually and for the possible uncertainties in the data arising from the different strategies for the VLBI analysis. The numbers on the curves indicate the nutation periods in years; "re" for their real part; "im" for their imaginary part. The hatched area indicates the intersection of the different possibilities for the parameters. The arrows indicate the values proposed in MHB2000.

the VLBI data, (2) a Fourier transform and an estimation of the in-phase and out-of-phase parts of the nutation amplitudes for the main forced nutations, and (3) an estimation of the basic Earth geophysical parameters. Laurence Koot has been working recently on a new approach, determining the basic Earth geophysical parameters directly from the nutation in longitude and in obliquity as a function of time. This new procedure avoids one step of the previous approach in three steps (called the frequency domain approach) as it fits the parameters directly on the nutation data in the time domain. This time domain approach allows accounting for the time variable error on the nutation data. This error on nutation is very much changing with time as the observations have become better and better. Another advantage of the new Koot procedure is that it allows to get probability distribution on the parameters (see Koot et al. 2007).

The frequency domain approach showed correlation between amplitudes of some of the nutations such as the 9.3 and 18.6 year nutations; the new approach developed by Koot et al (2007) is that it uses a Bayesian inversion method which allows dealing with the non-linear nutation model and to get probability distributions on the parameters. With the new Bayesian approach, most of the parameters have the same values as MHB2000 but with a smaller error. However, some parameters have a different estimated value: the global dynamical flattening and the imaginary parts of the coupling constants K_{CMB} and K_{ICB} leading to a different estimation for the quality factors of the FCN and FICN modes.

4. SURFACE FLUID LAYERS

The present-day limitation in the estimation of the geophysical parameters is the contamination from the ocean and atmosphere perturbing the nutation amplitudes. The surface fluid layers transfer their angular momentum to the solid Earth, therewith changing the Earth orientation and rotation. For nutation, the atmosphere and ocean angular momentum must be evaluated at a diurnal timescale in a terrestrial reference frame (corresponding to nutation in a celestial frame). This is not yet a very accurate determination and geophysical fluid corrections need further improvements: the tidal ocean, non-tidal ocean, and atmosphere angular momentum must be computed precisely in the retrograde diurnal

frequency band. The GGOS (Global Geodesy Observing System) project of the IAG aims at better understanding the mass transfers within the Earth with its fluid layers, which will therefore help to better achieve this objective in the future.

5. FREE CORE NUTATION

Last, but not least, the observed nutation series show a large contribution from the FCN free mode. This cannot be modeled yet as it would demand a very precise knowledge of the atmospheric excitation. The FCN free mode contribution to nutations needs to be estimated from epoch to epoch as done by Lambert for the IERS conventions.

6. PERSPECTIVES FOR NUTATIONS OF OTHER PLANETS

For a planet to have nutation, we must have an inclination from the symetry axis or mean rotation axis with respect to the ecliptic, we must have a rapidly rotating planet, and we must have a flattening (which is a consequence of the rapid rotation except for dynamic contribution). The Earth is not the only planet to have nutation: Mars has nutation as well. Mars has an inclination of about 25 degree and is rotating at about 24h40m. Mars nutations are mainly due to the Sun as the little moons of Mars, Phobos and Deimos have dimensions of the order of 20km. The main nutation of Mars is thus the semi-annual prograde nutation arising from the Sun as for the Earth nutation forced by the Sun. The amplitudes are roughly at the same level of magnitude for both planets (about 500 mas). Annual for Mars refers to one Martian year, i.e. about 687 terrestrial mean solar days. The semi-annual nutation corresponds to about 30 meters peak to peak at the surface of the Earth and 15 meters peak to peak at the Martian surface. Although the core is thought to be liquid from space geodesy observation (Konopliv et al. 2006), it is only determined from tidal contributions to the orbital motion of a spacecraft and is at the limit of the detection. Geochemical considerations tend to corroborate this statement as well: Mars would be in the phase of having a liquid core without inner core; this is possible if Mars contains a little bit more light elements than Earth in the core alloy. It is nevertheless very desirable to obtain another observation of the core state of Mars. Nutations would provide with this observation as they are enhanced by the FCN if the core is liquid. This enhancement is at the level of one percent for the semi-annual prograde nutation that is far from the FCN resonance (at around 256 days in the retrograde part of the spectrum). The ter-annual retrograde nutation at 229 days is close to the FCN; this is particularly true when the core is large. Indeed in Dehant et al. (2000a) a sequence of Mars interior models have been considered, constrained by the most probable moments of inertia as recently observed. These models have a core radius between 1268 km and 1668 km, corresponding to a 200 km uncertainty interval around the 1468 km radius of model A of Sohl and Spohn (1997). Dehant et al. (2000a and 2000b) have found an FCN period in the range [238, 288] days. The larger the core is, the lower the FCN period is. The value of the tidal Love number provided by space geodesy indicates a large core and therefore it is believed that the resonance on the retrograde ter-annual nutation will be high.

Observing nutation could be performed using the observation of one or a few landers at the surface of Mars as a function of time, for a long period (at least one Martian year). This opportunity will be provided by the future AURORA/ExoMars mission of ESA. The use of an X-band transponder on the surface of Mars will allow us to measure the Doppler effects on the radio signal from the rotation and orientation variations of Mars. The transponder is called LaRa for Lander Radioscience. The Principal Investigator of LaRa are V. Dehant and W. Folkner. The transponder is built by OMP (Orban Microwave Product), a Belgian industry. The mission is expected to be launched in 2013.

7. CONCLUSIONS

In summary, we may consider presently that the rigid Earth nutations are well determined. The FCN frequency is quite well determined from VLBI observations, even if we consider different strategies for computing nutation series, or even considering atmospheric contamination of the amplitudes. However, the same conclusion may not be drawn for the FICN. The 18.6 year retrograde nutation is the key nutation for getting the right FICN parameters (the 0.5 year prograde nutation also helps). The 18.6 year retrograde nutation is though not very well determined and its amplitude changes from one strategy of observation to the other. Different strategies for VLBI observations provide indeed different amplitudes of the 18.6 year retrograde nutation with respect to MHB2000 at the level of 60-70 mas. The FICN

frequency and quality factor are thus not yet very well constrained and VLBI observations still need improvement. The time domain approach looks very promising for a better determination of the basic Earth parameters.

Another important point for the future of nutation is the existence of a FCN free mode. This free mode contribution cannot be computed from atmospheric excitation as this last is not well known. It needs then to be observed and determined.

The atmosphere effects on nutations may be large and their determiantion from the angular momentum needs to be improved. The effects are important as nutations need to be corrected for, prior to the estimation of the Earth interior parameters.

The perspectives for the planet Mars provided by the future ExoMars mission and in particular the radioscience experiment LaRa are very promising for our understanding of the interior of Mars.

8. REFERENCES

Dehant, V., Defraigne, P., Van Hoolst, T., 2000a, "Computation of Mars' transfer function for nutation tides and surface loading", Phys. Earth Planet. Inter. 117, pp. 385–395.

Dehant, V., Van Hoolst, T., and Defraigne, P., 2000b, "Comparison between the nutations of the planet Mars and the nutations of the Earth", Survey Geophys. 21(1), pp. 89–110.

Folgueira, M., Dehant, V., 2007, "Estimation of the topographic torque at the core-mantle boundary on the nutation", this issue.

Folgueira, M., Dehant, V., Rambaux, N., Lambert, S.B., 2007, "Impact of tidal Poisson terms to non-rigid Earth rotation", Astron. Astrophys., 469(3), pp. 1197-1202, DOI: 10.1051/0004-6361:20066822.

Konopliv, A.S., Yoder, C.F., Standish, E.M., Yuan, D.N., Sjogren W.L., 2006, "A global solution for the Mars static and seasonal gravity, Mars orientation, Phobos and Deimos masses, and Mars ephemeris", Icarus 182(1), pp. 23–50, doi: 10.1016/j.icarus.2005.12.025.

Koot, L., de Viron, O., Dehant, V., 2007, "Estimation of Earth interior parameters from a Bayesian inversion of nutation time series", this issue.

Lambert, S.B., Mathews, P.M., 2006, "Second-order torque on the tidal redistribution and the Earth's rotation", A&A 453(1), pp. 363–369, doi: 10.1051/0004-6361:20054516.

Lambert, S.B., Dehant, V., 2007, "The Earth's core parameters as seen by the VLBI", A&A 469, pp. 777–781, doi: 10.1051/0004-6361:20077392.

Lambert, S.B., Gontier, A.M., 2007, "A Comparison of R1 and R4 IVS Networks", IVS 2006 General Meeting Proceedings, pp. 264–268.

Lambert, S., Dehant, V., Gontier, A.M., 2007, "Some issues in the Earth's interior exploration with VLBI", this issue.

Guo, J.Y., Mathews, P.M., Zhang, Z.X., Ning, J.S., 2004, "Impact of inner core rotation on outer core flow: the role of outer core viscosity", Geophys. J. Int. 159(8), pp. 372–389, doi: 10.1111/j.1365-246X.2004.02416.x.

Mathews, P.M., Buffett, B.A., Herring, T.A., Shapiro, I.I., 1991, "Forced nutations of the Earth: influence of inner core dynamics, 1. Theory", J. Geophys. Res. (Solid Earth) 96, pp. 8219-8242.

Mathews, P.M., Herring, T.A., Buffett, B.A., 2002, "Modeling of nutation and precession: New nutation series for nonrigid Earth and insights into the Earth's interior", J. Geophys. Res. (Solid Earth) 107(B4), CiteID: 2068, doi: 10.1029/2001JB000390.

Sohl, F., Spohn, T., 1997, "The interior structure of Mars: Implications from SNC meteorites", J. Geophys. Res. 102(E1), pp. 1613–1636, doi: 10.1029/96JE03419.

Souchay, J., Loysel, B., Kinoshita, H., Folgueira, M., 1999, "Corrections and new developments in rigid earth nutation theory. III. Final tables "REN-2000" including crossed-nutation and spin-orbit coupling effects", A&A 135, pp. 111–131.

Wu, X., Wahr, J.M., 1997, "Effects of non-hydrostatic core-mantle boundary topography and core dynamics on Earth rotation", Geophys. J. Int. 128(1), pp. 18–42.

IAU SYMPOSIUM No. 78 "NUTATION AND THE EARTH'S ROTATION" *(held in Kiev, May 1977)* AS A FIRST STEP IN THE CONSIDERATION OF THE NON-RIGID EARTH NUTATION THEORY

Ya.S. YATSKIV[1], A.A. KORSUN'[2],

Main Astronomical Observatory, National Academy of Sciences of Ukraine
27 Zabolotnoho St., Kiev, 03680 Ukraine
e-mail: [1]yatskiv@mao.kiev.ua, [2]akorsun@mao.kiev.ua

1. THE BEGINNING

The Journées 2007 will take a look into the future of the nutation theory. But what that future will look like depends to some extent on what the past was. So, the authors try to have a look back into the beginning of the discussions on the new theory of nutation which took place at the IAU Symposium No. 78 "Nutation and the Earth's rotation" held in Kiev thirty years ago.

The theory of nutation used before 1984 in the reduction of astronomical observations was based on the assumption that the Earth is a rigid body. For this model a single coefficient of nutation in obliquity called the constant of nutation was be adopted in the IAU System of Astronomical Constants. Others coefficients of nutational terms were related by the rigid-Earth theory to the constant of nutation.

The IAU (1964) System of Astronomical Constants (Fricke et al., 1966) was the first attempt to develop international standards that were appropriate to the reduction of high precision of astronomical measurements. For the computation of nutation Woolard's rigid-Earth theory along with the constants listed in his classical work (Woolard, 1953) was adopted. The constant of nutation used by Woolard was based on observational results, namely the Newcomb's value $N = 9.''210$.

The astronomers who set up that system of constants admitted that a revision would be necessary very soon. Due to great progress made in space research such revision took place in twelve years.

W. Fricke was a man of action for the creation of an improved system of astronomical constants once again. The work on this system was shared by three Working Groups formed by the IAU Commission 4 in 1970. "Each of the Working Groups (Precession, Planetary Ephemerides, Units and Time-scale) consisted of members of various Commissions. About 40 astronomers have actively contributed to the tasks. A Joint Report of the Working Groups containing six recommendations was edited by R. L. Duncombe, W. Fricke, P. K. Seidelmann and G. A. Wilkins and submitted to the IAU General Secretary. The Executive Committee decided that the recommendations should be discussed in a joint meeting of IAU Commission 4, 8 and 31 with the view to its being adopted in Grenoble. The Joint Meeting took place on August 26, and the recommendations were adopted." (Fricke, 1976).

In spite of the large discrepancies between the rigid-Earth theory of the nutation and observations the value of the constant of nutation used in previous system of constant (reduced to the epoch J2000) was retained in the IAU (1976) System of Astronomical Constants. Nevertheless, a special recommendation concerned with the nutation theory was adopted by the IAU.

This recommendation was not voted by the unanimity of the IAU members who participated in the Joint Meeting, and a very animated discussion started on two points:

(i) In any high accuracy computation of the nutation, it is indispensable to take into account the influence of the elasticity of the mantel and of the existence of a fluid core in the Earth; this meant

that it was absolutely necessary to elaborate a new theory for the nutation in order to replace Woolard's theory.

(ii) One must reexamine the question of the choice of the axis (reference pole) of which the equations of nutation must describe the motion.

One of the authors (Ya.Ya.) took part in this discussion and proposed to hold a special IAU Symposium precisely in Kiev to attack the problem. The background for this proposal was as follows.

At Kiev E. Fedorov and his pupils were actively busy with investigations of the theory of nutation and determinations of nutation coefficients from observations (Fedorov, 1963; Yatskiv, 2000). E. Fedorov made the first attempt to determine the principal nutation term coefficients in obliquity and in longitude separately. He thought it more reasonable to compare his observation results to the predictions of new theory of nutation taking into consideration the effect of an elastic mantle and a liquid core of the Earth. In addition Fedorov assumed that tabular nutation must describe the motion of the axis of angular momentum with respect to the body-fixed coordinate system which was determined from observations. This assumption was in contradiction with R. Atkinson's opinion and the IAU recommendation on the choice of the axis of figure for tabular nutation.

The proposal to hold a symposium on nutation became particularly to the point, and urgent, because of the creation of the FK5 and this was why the idea was actively supported by W. Fricke and Prof. E. Müller as the Assistant General Secretary of the IAU. Later on one of the authors (Ya.Ya.) remembered (Yatskiv, 1998):

"During the years 1973–1976, Professor Edith Müller was Assistant General Secretary of the IAU, and was responsible, in that capacity, of the organization of Symposia and Colloquia, as well as of the Regional Meeting of the IAU. As there is always, at the IAU, more proposals for meetings than possibilities to actually put them on their way, it is a need for the Assistant General Secretary to be of a particular punctuality, and strictly objective. As a rule, one presents proposals for organizing IAU symposia in due time, i.e. at least two years ahead of time. However, during the XVI-th General Assembly of the IAU (at Grenoble, France, 1976), Professor Walter Fricke and myself were forced, because of various circumstances, to ask Edith Müller to make an exception for our project, and to accept that the Symposium No. 78, "Nutation and the Earth's rotation" be held in Kiev, as early as in May 1977.

Edith Müller met us in her office, listened very carefully, and made clear to us that very little time was left to prepare the Symposium. She listened again to our argumentation: I gave her the insurance that the Local Organizing Committee would do its utmost for the success of the endeavour. Then she gave her agreement for the holding of this Symposium, and she convinced the Executive Committee."

2. REMEMBERING THE IAU SYMPOSIUM No. 78 "NUTATION AND THE EARTH's ROTATION"

The objectives of the Symposium were clearly stated, they concerned with two main topics:

(i) the *choice* of the axis to which the ephemeris of the forced nutation should refer;

(ii) the *requirements* for an improved series of nutation for computing the ephemeris.

The Scientific Organizing Committee (SOC) was formed as quick as possible. E. P. Fedorov and R. O. Vicente (Co-Chairmen) invited W. Fricke, J. Kovalevsky, P. Melchior, N. Pariisky, M. Rochester, C. Sugava, G. Wilkins and Ya. Yatskiv (who presided over the LOC) to be members of the SOC.

The Symposium was sponsored by the Commission 19 and co-sponsored by Commissions 4, 8 and 31. It was held in Kiev (former USSR) from 23 to 28 May 1977. (May is the most beautiful month in Kiev city).

There were 114 registered participants from 14 countries. Thirty-eight invited and contributed papers were presented at the Symposium, including observational results as well as their geophysical interpretation. The review papers by Wilkins, Fedorov, Yatskiv, Vicente and Melchior provided a sound overview of two main topics of the Symposium. The controversy on these topics, however was very large. This resulted in hot discussions at the Symposium which that preceded the adoption of the symposium resolutions concerned with the theoretical and observational studies of nutation. The report on these discussions was prepared by G. Wilkins (1977).

The Proceedings of the IAU Symposium No. 78 on Nutation and the Earth's rotation were edited by E. P. Fedorov, M. L. Smith and P. L. Bender (1977).

3. ON THE IAU SYMPOSIUM No. 78 RESOLUTIONS

Three resolutions were adopted, namely:

Resolution No. 1

IAU Symposium No. 78 *recommends* that the decision of the 16th General Assembly of the IAU that "the tabular nutation shall include the forced periodic terms listed by Woolard for the axis of figure..." shall be annulled and that nutation of the true pole of date with respect to the mean pole of date should be computed for the motion of the instantaneous axis of rotation of the mantle.

Resolution No. 2

IAU Symposium No. 78 *recommends* that the following set of coefficients be substituted for the corresponding coefficients in Woolard's series for the nutation in order to provide a more accurate representation of the forced nutation of the axis of rotation of the Earth due the luni-solar perturbing forces, and that this amended series be referred to as the "IAU (1977) nutation series".

Period	in $\Delta\varepsilon$	in $\Delta\psi \sin\varepsilon$
18.6 years	+ 9.″206	– 6.″843
9 years	– 0.091	+0.083
1 year	+0.006	+0.058
0.5 year	+0.569	–0.520
22 days	+0.022	–0.020
27 days	0.000	+0.028
13.7 days	+0.091	–0.083

Resolution No. 3

IAU Symposium No. 78 *requests* that the President of IAU Commission 4 set up a small working group of experts to prepare a fully documented proposal for the adoption of a new series for nutation at the IAU General Assembly in 1979, and recommends that the group shall take into account the desirability of basing this proposal on resolution No. 2 of this Symposium.

The former two resolutions were absolved from consideration very soon and the latter was realized by the Working Group on Nutation established by the President of the IAU Commission 4 V. K. Abalakin in 1977. This Working Group presented a report to the IAU General Assembly (Montreal, 1979). What happened afterwards is another story.

4. REFERENCES

Fedorov, E. P., 1963, "Nutation and Forced Motion of the Earth's Pole", The MacMillan Co, New York.

Fedorov, E. P., Smith, M. L., Bender, P. L. (eds): 1977,"Nutation and the Earth's Rotation", Dordrecht, Holland: Reidel Publ. Comp.

Fricke, W., Brouwer, D, Kovalevsky, J., Mikhailov, A. A., and Wilkins G. A., 1966, Trans. Int. Astron. Union, 12 B.

Fricke, W., 1976, Astronomical constants. The IAU (1976) System adopted in Grenoble. La Gazette d'Uranie. XVI-e Assemblee Generale, 1 September, 8, Grenoble.

Wilkins, G. A., 1977, "Report of general discussions at the IAU Symposium No. 78 on Nutation and the Earth's Rotation". In the book "Nutation and the Earth's rotation", (eds. E. P. Fedorov, M. L. Smith, P. L. Bender), Dordrecht, Holland: Reidel Publ. Comp.

Woolard, E. W., 1953, "Theory of the Rotation of the Earth Around its Center of Mass", Astron. Papers for Amer. Ephemeris XV, Pt, I. Washington, D.C.

Yatskiv, Ya., 1998, "From our first meeting, she confided in me", In the book "Remembering Edith Alice Müller" (eds. Appenzeller et al.), Dordrecht, Netherlands: Kluwer Acad. Publ.

Yatskiv, Ya., 2000, "Fedorov's attempt to solve the nutation", Journees-2000, Paris.

ESTIMATION OF EARTH INTERIOR PARAMETERS FROM A BAYESIAN INVERSION OF NUTATION TIME SERIES

L. KOOT[1], A. RIVOLDINI[1], O. DE VIRON[2], V. DEHANT[1]
[1] Royal Observatory of Belgium
Avenue circulaire 3, B-1180, Brussels, Belgium
e-mail: laurence.koot@oma.be, attilio.rivoldini@oma.be, v.dehant@oma.be
[2] Institut de Physique du Globe de Paris, associé au CNRS et à l'Université de Paris VII
Place Jussieu 4, 75252 Paris, France
e-mail: deviron@ipgp.jussieu.fr

ABSTRACT. The nutation response of the Earth to the external gravitational torque is affected by the Earth internal structure. Because the torque is known very accurately, the high precision nutation observations allow to constrain Earth interior parameters. A non-rigid Earth nutation model has been proposed by Mathews et al. (2002). This model is semi-analytical: the analytical equations of the model depend on parameters, related to the Earth interior, which are fitted to the observations. In this paper, we develop a new fit procedure relying on an estimation of the geophysical parameters directly from the nutation data in time series. This allows to use all the information of the time-domain data and to take into account the time dependent uncertainties on the data. We use the Bayesian inversion method, which is well-suited for the non-linear nutation model and easily accommodates the possibility of having uncertainties in the nutation model itself. Finally, the results are compared with those obtained by Mathews et al. (2002).

1. INTRODUCTION

The rotation of the Earth is affected by the gravitational torque exerted on its equatorial bulge by the Moon, the Sun and, to a lesser extent, the other planets. As a response to this torque, the rotation axis of the Earth changes its orientation and describes a large circle around the perpendicular to the ecliptic plane, called the "precession" motion, while small periodic variations of this motion -due to periodic changes in the relative positions of the celestial bodies- are called "nutations". The precession/nutations motion is observed very precisely with the Very Long Baseline Interferometry (VLBI) technique. The main interest of nutation for studying the Earth's interior relies on the fact that the gravitational torque, at the origin of nutation, is known very precisely from celestial mechanics. Since the nutation response of the Earth to this torque depends on its internal structure, the accurate VLBI observations of nutation allow to constrain parameters of the Earth interior model.

2. EARTH INTERIOR AND NUTATION MODELS

The Earth interior model used for nutation modeling by Mathews et al. (2002) is that of a three layered Earth (mantle, liquid outer core and solid inner core) spheroïdally stratified, meaning that the density, the potential and the elastic parameters are constant on the same spheroïdal surfaces. The Earth model is assumed to be deformable and the deformations are due, on the one hand, to the external tidal potential and, on the other hand, to the rotational potentials of the Earth and of the fluid and solid cores. The Earth deforms anelastically, leading to a small time delay between the forcing and the deformational response. The model also includes the effects of the external geophysical fluids: ocean tides and atmospheric seasonal cycles.

The dynamical equations describing the nutation of the Earth are the equations of the angular momentum budget for each part of the Earth. They relates the time variation of the angular momentum of each part to the total torque applied to it. Those torques are due to the external tidal potential and to the interactions between the different layers of the Earth model. Those interactions are from several origins: gravitational (attraction between the masses of the different regions), inertial (pressure on the elliptical boundaries), friction, topographic, and electromagnetic.

The angular momentum of each of the three regions inside the Earth is a function of the inertia tensor and its instantaneous rotation vector. The inertia tensor depends on the way the masses are distributed inside the Earth. It can be written as the sum of the inertia tensor of the unperturbed ellipsoidal steadily rotating reference Earth and small increments due to the deformations and to the ocean tides. The increments due to the deformations are expressed as a linear combination of the potentials at the origin of the deformations (namely the tide generating potential and the three centrifugal potentials). The complex constants of proportionality, describing how each potential increments the inertia tensor, are called the "compliances". Ocean tides also perturb the inertia tensor due to the redistribution of mass in the ocean itself, and to the deformations induced by the surface load. Relative motions in the ocean with respect to the Earth create additional angular momentum. Ocean tides effects on nutation are obtained from an ocean tide model derived from the satellite altimetry data TOPEX/Poseidon.

The geophysical parameters of the above described Earth model are (1) the dynamical ellipticities, defined as a ratio between the equatorial and radial principal moments of inertia, (2) the compliances, describing the deformations, and (3) coupling constants characterizing all the interactions between the regions except gravitational and inertial couplings which are taken into account explicitly. Some of those parameters which have a large influence on nutation can be estimated from the VLBI nutation data.

3. PARAMETERS ESTIMATION METHOD

The first main aspect of the inversion procedure we have developed is that we use the VLBI data time series. This is new with respect to the classical procedure, used by Mathews et al. (2002), which consists in the extraction of the amplitudes and phases of the 21 main terms in frequency. Using the data directly in the time domain has the advantage that (1) it allows us to use all the available data, not only the 21 main periodic terms and (2) it better takes into account the time variability of the error on the VLBI data, which is due to the improvements in the measurement technique and to the additional stable radiosources considered over time.

The second point of our procedure is that, rather than the linearized least-squared method used by Mathews et al. (2002), we use a Bayesian inversion method. This method offers the advantage that the highly non-linear nutation model has not be linearized. Within the Bayesian method, the parameters are considered to be random variables. The joint probability density function (pdf) is inferred from the data and from prior knowledge associated with the parameters. Moreover, the Bayesian framework allows to easily include modeling errors, which takes into account the imperfection in the modeling. Those imperfections come from the simplicity of the Earth interior modeling, the ocean tides effects computed from data, the atmospheric effects,...

4. RESULTS

The probability density functions (pdf) obtained for the Earth interior model parameters are presented on the Figures 1, 2, and 3 for the dynamical ellipticities, compliances and coupling constants respectively. The pdf's are summarized by their expectation value and 3-sigmas credible range. Those values are shown in Table 1 together with the ones obtained by Mathews et al. (2002) for comparison.

4.1. Dynamical ellipticities

The estimated values for the dynamical ellipticities confirm the well-known fact that the flattenings of the whole Earth and fluid core are more important than those predicted by hydrostatic equilibrium (see e.g. Gwinn et al. 1986). Our estimation is in agreement with that of Mathews et al. (2002) in the sense that there is a large overlap between the three-sigma domains. However, we think that, for the whole Earth dynamical ellipticity, the agreement of our result with that of Mathews et al. (2002) is quite fortuitous because, depending on the length of the data series, the estimated value is different. This can be explained by the fact that this parameter is estimated mainly on the trend of the data which represents the precession. This trend is highly correlated with the 18.6 years nutation term, which is poorly known as only 28 years of data are available.

4.2. Compliances

In this work, the complex compliances are estimated from the nutation data, whereas in Mathews et al. (2002), only the elastic contribution to the compliances were estimated from the data while the anelastic contributions were computed theoretically. Figure 2 shows the result for the compliance

Parameter	Definition	This paper	MHB
e	Earth dynamical ellipticity	0.0032845471 ± 4	0.0032845479 ± 13
e^f+Re(K^{CMB})	Core dynamical ellipticity + coupling at the CMB (real part)	0.0026701 ± 7	0.0026680 ± 21
Re(κ)	Compliance for the Earth (real part)	0.0010528 ± 63	0.0010466 ± 99
Im(κ)	Compliance for the Earth (imaginary part)	-0.0000108 ± 70	0.00000529
Re(γ)	Compliance for the fluid core (real part)	0.00198548 ± 90	—
Im(γ)	Compliance for the fluid core (imaginary part)	0.00000933 ± 99	—
Im(K^{CMB})	Coupling at the CMB (imaginary part)	-0.0000205 ± 7	-0.0000185 ± 15
Re(K^{ICB})	Coupling at the ICB (real part)	0.00104 ± 19	0.00111 ± 11
Im(K^{ICB})	Coupling at the ICB (imaginary part)	-0.00185 ± 16	-0.00078 ± 14

Table 1: Numerical values of the Earth interior parameters and comparison with the values of Mathews et al. (2002). The second column gives the values for the inversion performed in this paper. The errors are on the last written digits and correspond to 3 σ. Numerical values obtained by Mathews et al. (2002) are listed in column four.

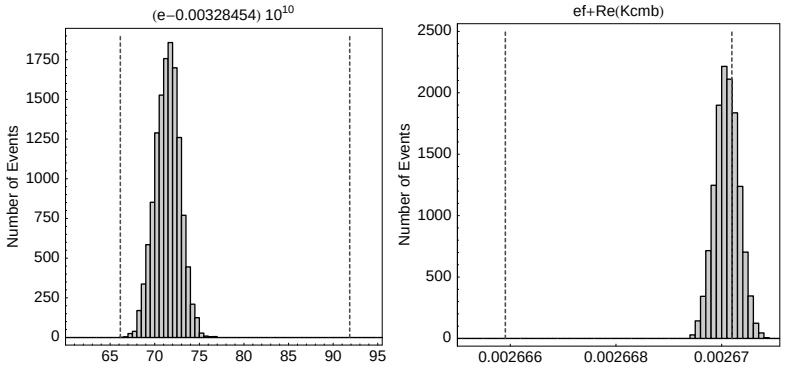

Figure 1: Marginal pdf's for the dynamical ellipticities of the whole Earth and fluid core, obtained from the Bayesian inversion of the nutation data. The dashed vertical lines represent the 3 σ-range of values obtained by Mathews et al. (2002).

describing the deformability of the whole Earth under the action of an external potential. The real part of this compliance is in agreement with Mathews et al. (2002) while the imaginary part is completely different. This difference can be explained by the fact that, the value of Mathews et al. (2002), because it has been computed theoretically from anelasticity models, represents purely the imaginary part of the compliance due to anelasticity. On the other side, our value being estimated from the nutation data, it is contaminated by the mismodeling of the ocean tides effects, which give also rise to imaginary contributions to the compliances. The fact that our estimated value is negative (which is not physically meaningful, as the deformational response of the Earth must lag behind the forcing) reflects the imperfection in the ocean tides modeling. Mathews et al. (2002) also deduced from their computations that the ocean tide contributions must be somewhat erroneous and decided to scale the current oceanic term by a 0.7 factor. This example shows the limitation of the estimation process: the mismodeling of certain effects can be absorbed by some parameters.

4.3. Coupling constants

The coupling constants characterize several types of interactions between the layers such as electromagnetic, viscous or topographic couplings. This makes their interpretation rather difficult because the individual effects can not easily be separated. The estimations we obtain for those parameters are not always in agreement with Mathews et al. (2002). For the imaginary part of the coupling constant at the ICB, our result is even very different, putting forward the fact that this parameter is probably the one that can be the less reliably estimated from nutation data. This is not really surprising as the parameters related to the inner core have a smaller effect on nutation than those of the outer core and mantle.

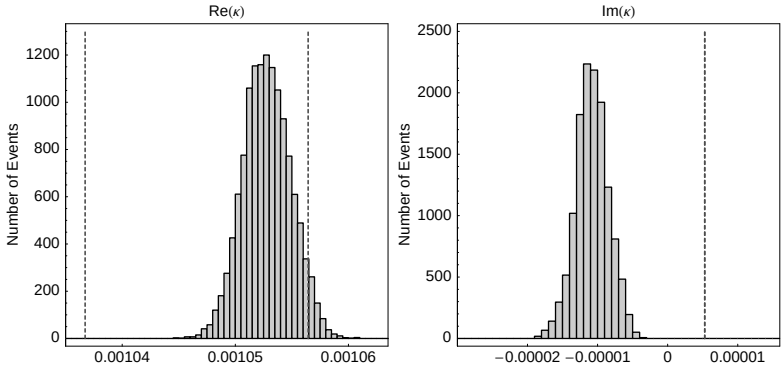

Figure 2: Marginal pdf's for the compliances, obtained from the Bayesian inversion of the nutation data. For Re(κ), the dashed vertical lines represent the 3 σ-range of values obtained by Mathews et al. (2002) for the purely elastic Earth plus the theoretically computed anelastic contribution. The dashed vertical line for Im(κ) represents the theoretical value computed by Mathews et al. (2002).

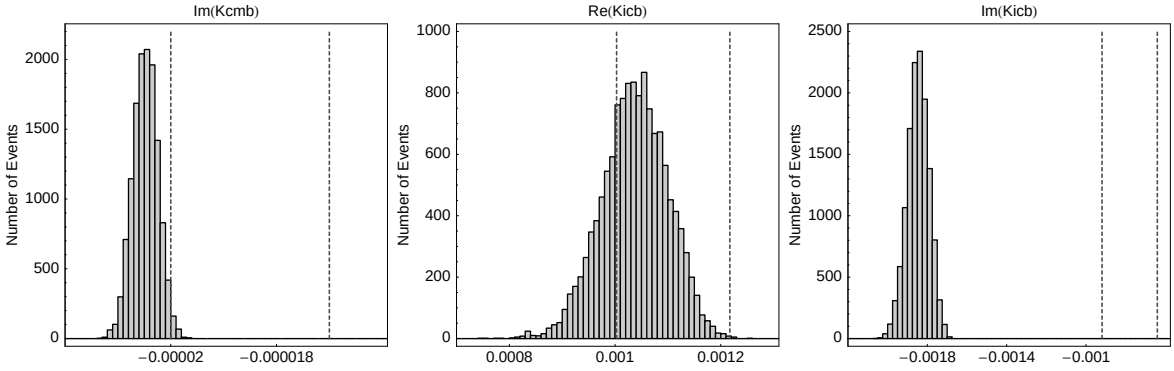

Figure 3: Marginal pdf's for the coupling constants, obtained from the Bayesian inversion of the nutation data. The dashed vertical lines represent the 3 σ-range of values obtained by Mathews et al. (2002).

5. CONCLUSIONS

The VLBI nutation data allow to estimate Earth interior parameters, such as the dynamical ellipticities of the Earth and fluid core, the compliances and the coupling constants. This estimation can be performed directly from the nutation data time series, there is no need of the extraction of amplitudes at some given frequencies, as it is done by Mathews et al. (2002). Some of our estimates are not in agreement with those of Mathews et al. (2002). This is due to the use of a different inversion strategy and the seven years of additional data. In particular, our estimation of the imaginary part of the coupling constant at the ICB is very different from that of Mathews et al. (2002) putting forward the fact that its interpretation in terms of physical couplings must be performed carefully.

6. REFERENCES

Gwinn, C. R., Herring, T. A., Shapiro, I. I., 1986, "Geodesy by radiointerferometry: studies of the forced nutations of the Earth, 2, Interpretation", J. Geophys. Res. , 91, 4755-4765.

Mathews, P. M., T. A. Herring, and B. A. Buffett, 2002, "Modeling of nutation and precession: New nutation series for nonrigid Earth and insights into the Earth's interior", J. Geophys. Res. (Solid Earth), 107, B4, 10.1029/2001JB000390.

VLBI OBSERVATIONS OF NUTATION, ITS GEOPHYSICAL EXCITATIONS AND DETERMINATION OF SOME EARTH MODEL PARAMETERS

J. VONDRÁK[1], C. RON[1]
[1] Astronomical Institute, Academy of Sciences of the Czech Republic
Boční II, 141 31 Prague 4, Czech Republic
e-mail: vondrak@ig.cas.cz, ron@ig.cas.cz

ABSTRACT. Very Long-baseline Interferometry (VLBI) has been used to observe nutation for more than 25 years, with ever increasing accuracy. The amplitudes and phases of individual nutation terms are sensitive to some parameters of the geophysical Earth model. Dominant are the resonant period P and quality factor Q of retrograde Free Core Nutation (FCN) that depend on the flattening of the outer fluid core. The period (in celestial frame) is approximately equal to 430 days. In principle, all nutation terms are affected by these resonance effects, but the most affected is the annual retrograde term that is closest to the resonance. Nutation is dominantly driven by external torques, and it contains, as a multiplicative factor, the dynamical ellipticity of the Earth. Relatively small (near-diurnal in terrestrial frame) geophysical excitations are amplified by the resonance, so they also have non-negligible influence on nutation. The aim of the present study is to take these effects into consideration and determine the period and quality factor of the Earth at the FCN frequency. An attempt to derive from them also the dynamical flattening of the whole Earth and its fluid core is made, taking into account other effects, such as electro-magnetic coupling between the core and the mantle.

1. INTRODUCTION - RESONANCES IN EARTH ORIENTATION

Due to the existence of a flattened fluid and rigid inner core, there are strong resonances in near-diurnal (in terrestrial frame) part of the spectrum, leading to a significant modification of nutation amplitudes, and also to a non-negligible influence of geophysical excitations in nutation. The resonances are characterized by Mathews-Herring-Buffet (Mathews et al. 2002, paper further referred to as MHB) transfer function, the strongest one being the retrograde Free Core Nutation (FCN):

$$T(\sigma) = \frac{e_R - \sigma}{e_R + 1} N_\circ \left[1 + (1+\sigma) \left(Q_\circ + \sum_{j=1}^{4} \frac{Q_j}{\sigma - s_j} \right) \right]. \qquad (1)$$

This transfer function, which is expressed in a complex form, gives a ratio between the non-rigid and rigid Earth model nutation amplitude for a given terrestrial frequency σ (expressed in cycles per sidereal day). $e_R = (C-A)/A = 0.0032845075$ is the ellipticity of the rigid Earth used to compute the 'rigid' solution. The other parameters are in general complex constants, among which s_j are the resonant frequencies (of Chandler wobble, retrograde FCN, prograde FCN and Inner Core Wobble, respectively). Recently, we demonstrated (Vondrák and Ron 2007) that the atmospheric and oceanic effects can excite free core nutation, and that their contributions of nutation are of the order of 100μas.

2. ESTIMATION OF PARAMETERS $N_\circ$ AND s_2

We use the basic equation (1), together with the observed values of some nutation amplitudes, to estimate some of the parameters on its right-hand side. Parameter $N_\circ$ is a common multiplier in Eq (1) that is closely connected with the dynamical ellipticity of the whole Earth, parameter s_2 is the complex resonant frequency due to the flattening of outer fluid core. We estimate these parameters from the observed amplitudes and phases of seven nutation terms, with periods 6798, 3399, 365.26, 182.62, 121.75 and 13.66 days. To this end, we use the VLBI-based celestial pole offsets (IVS 2005) with respect to the IAU 2000 nutation (Mathews et al. 2002) and 2006 precession (Capitaine et al. 2003) models. The

IAU2000 model of nutation contains an empirical correction in prograde annual nutation ('MHB Sun-synchronous correction'), supposedly due to atmospheric excitation, which we removed from the observed amplitude at this frequency. We kept all other parameters in MHB transfer function constant, and made the solution in successive approximations. The following series of VLBI celestial pole offsets were used:

- Geoscience Australia (AUS) solution in the interval 1984.0–2007.6;
- Goddard Space Flight Center (GSFC) solution in the interval 1979.6–2007.2;
- Paris Observatory (OPA) solution in the interval 1984.0–2007.1;
- U.S. Naval Observatory (USNO) solution in the interval 1979.6–2007.2;
- International VLBI Service (IVS) combined solution in the interval 1979.6–2006.9.

The parameters $N_\circ$ (real) and s_2 (complex) were determined in weighted least-squares estimation, and from the latter one the FCN period P and quality factor Q computed:

$$P = 0.99727/\left[\mathrm{Re}(s_2) + 1\right], \quad Q = -\mathrm{Re}(s_2)/2\mathrm{Im}(s_2) \tag{2}$$

The results are displayed in Tab. 1; first five rows show our estimation from different VLBI solutions, with no geophysical excitation applied. The last row displays the MHB values, for comparison. The table

Table 1: Results of estimating the parameters from VLBI observations

Solution	P	Q	$N_\circ$
AUS	-429.98 ± 22	19985 ± 837	1.00001100 ± 357
GSFC	-430.11 ± 18	19544 ± 633	1.00001046 ± 297
OPA	-430.27 ± 16	19839 ± 593	1.00000826 ± 260
USNO	-430.07 ± 18	19348 ± 646	1.00000818 ± 295
IVS	-430.22 ± 16	20741 ± 645	1.00000921 ± 256
MHB	-430.21	19998	1.00001224

shows a very good agreement of all estimated parameters; they are mutually consistent within the limits of their formal uncertainties, and they are also very close to MHB values.

3. GEOPHYSICAL EXCITATIONS, ESTIMATION OF SOME EARTH PARAMETERS

Next we calculate the influence of geophysical effects, namely the atmospheric and oceanic excitations, on nutation. We consider that the existing equatorial excitation series χ (in complex form) are all given in terrestrial reference frame, so they must be first transformed into χ' in celestial (non-rotating) frame, by using a simple formula $\chi' = -\chi \mathrm{e}^{\mathrm{i}\phi}$, where ϕ is the Greenwich sidereal time. Because we are interested only in long-periodic motions in celestial frame (i.e., precession-nutation) we smoothed out all excitations with periods shorter than 10 days, using the smoothing (Vondrák 1977) with $\varepsilon = 6$ day^{-6}. The following geophysical excitations were used, all in 6-hour intervals, to estimate the effects in nutation:

- Atmospheric Angular Momentum (AAM) functions (pressure and wind terms): NCEP/NCAR reanalysis in 1983.0–2007.0 (Salstein 2005); ERA40 in 1979.0–2001.0 (Dobslaw and Thomas 2007);
- Oceanic Angular Momentum (OAM) functions (matter and motion terms): ECCO model in 1993.0–2006.2 (Gross et al. 2005); Ponte model in 1993.0–2000.5 (Ponte and Ali 2002); OMCT model in 1979.0–2001.0 (Dobslaw and Thomas 2007).

These series were further used in the following combinations:

- NCEP AAM with inverted barometer (IB) correction (1983.0–2007.0),
- NCEP AAM without IB correction (1983.0–2007.0),
- NCEP AAM(IB) + ECCO OAM (1993.0–2006.2),
- NCEP AAM (IB) + Ponte OAM (1993.0–2000.5), and
- ERA40 AAM + OMCT OAM (1983.0–2001.0)

to integrate numerically the broad-band Liouville equations after Brzezinski (1994), here expressed in complex form:

$$\ddot{P} - \mathrm{i}(\sigma'_C + \sigma'_f)\dot{P} - \sigma'_C\sigma'_f = -\sigma_C \left\{\sigma'_f(\chi'_p + \chi'_w) + \sigma'_C(a_p\chi'_p + a_w\chi'_w) + \mathrm{i}\left[(1+a_p)\dot{\chi}'_p + (1+a_w)\dot{\chi}'_w\right]\right\}. \tag{3}$$

$P = \mathrm{d}X + \mathrm{i}\mathrm{d}Y$ is geophysically excited motion of Earth's spin axis in celestial frame, $\sigma'_C = 6.32000 + 0.00237\mathrm{i}$, $\sigma'_f = -0.0146011 + 0.0001533\mathrm{i}$ rad/day are the Chandler and FCN frequencies in celestial

frame, and $\sigma_C = \sigma'_C - \Omega$ is the Chandler frequency in terrestrial frame ($\Omega = 6.30038$ rad/day is the angular speed of Earth's rotation). χ'_p, χ'_w are excitations (matter and motion term) in celestial frame, and $a_p = 9.2 \times 10^{-2}$, $a_w = 5.5 \times 10^{-4}$ are dimensionless numerical constants. Numerical integration of Eq (3), using four-order Runge-Kutta method and 6-hour step, yields the geophysical contribution in time domain; an example of such integration is depicted in Fig. 1, where both pressure and wind term are considered. The comparison with VLBI observations (IVS solution) shows a very good agreement.

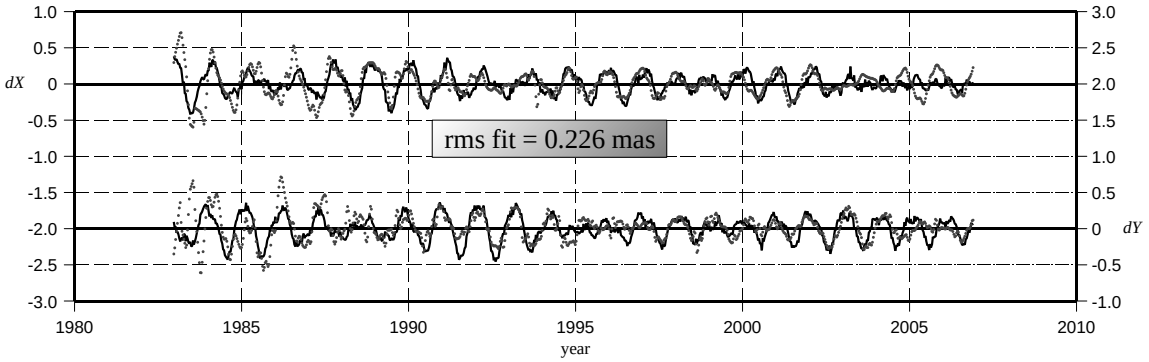

Figure 1: Nutation excited by NCEP AAM(IB), line, and VLBI observations, dots, in mas.

Next we made a spectral analysis of the results, which revealed that all four combinations of geophysical excitation mentioned above yield a similar pattern – there are significant peaks only at FCN, annual and semi-annual periods. Therefore, we made a least-squares estimation of sine/cosine terms in $\mathrm{d}X$, $\mathrm{d}Y$ for these periods, and then calculated the prograde/retrograde complex amplitudes A^+, A^- by using the relation $\mathrm{d}X + \mathrm{i}\mathrm{d}Y = -\mathrm{i}\sum_k (A_k^+ \mathrm{e}^{\mathrm{i}\omega_k} + A_k^- \mathrm{e}^{-\mathrm{i}\omega_k})$. The results are shown in Tab. 2, in comparison with MHB Sun-synchronous correction (last row). The next step was to remove the 'real' geophysical

Table 2: Atmospheric and oceanic contributions to nutation and their uncertainties σ [μas]

Excitation	annual				semi-annual				
	prograde		retrograde		prograde		retrograde		
AAM + OAM	Re	Im	Re	Im	Re	Im	Re	Im	σ
NCEP(IB)	−3.4	+109.7	−69.9	−18.7	−44.2	−55.7	−1.8	+0.9	±2.7
NCEP	+13.8	+91.5	−76.8	−52.1	−25.5	−52.5	−6.5	−1.0	±4.9
NCEP(IB)+ECCO	−0.6	+110.7	−32.2	−69.1	−46.5	−53.9	−6.2	−21.8	±4.6
NCEP(IB)+Ponte	+80.3	+107.4	+86.4	−135.6	−26.3	−62.1	+9.2	−9.6	±8.5
ERA40+OMCT	−64.9	+180.3	−64.3	+5.6	−17.9	−77.3	+0.3	+3.4	±6.8
MHB Sun-synchr.	−10.4	+108.2	–	–	–	–	–	–	–

excitations from the VLBI-observed nutations, instead of the MHB Sun-synchronous correction. To this end, we used the IVS combined solution and the excitations of Tab. 2 with the lowest uncertainties, i.e., NCEP(IB), NCEP and NCEP(IB)+ECCO. Then, the analysis similar to Section 2 was made to derive parameters P, Q, and $N_\circ$. The results are shown in Tab. 3, where they are compared with VLBI solution from which MHB Sun-synchronous correction was removed (i.e., identical with the row IVS of Tab. 1).

Table 3: Results of estimating the parameters from VLBI observations, with geophysical effects removed.

Solution	P	Q	$N_\circ$
NCEP(IB)	-431.00 ± 23	20530 ± 911	1.00001437 ± 368
NCEP	-431.18 ± 21	19892 ± 781	1.00001506 ± 335
NCEP(IB)+ECCO	-430.96 ± 19	17584 ± 636	1.00001708 ± 1700
MHB Sun-synchr.	-430.22 ± 16	20741 ± 645	1.00000921 ± 256

The parameters derived above can be, together with some other parameters, further utilized to estimate the dynamical flattening of the fluid core e_f and of the whole Earth H_d. Namely we use the

formula, following from MHB expressions (37) and (38):

$$e_f = \tilde{\beta} - \frac{A_m}{A}\left[\mathrm{Re}(s_2) + 1\right] - \mathrm{Re}(K^{CMB}) - \frac{A_s}{A_f}\mathrm{Re}(K^{ICB}), \tag{4}$$

giving the relation between the flattening and parameters $\tilde{\beta}$ (compliance), A, A_m, A_s, A_f (moments of inertia of the whole Earth, its mantle, solid and fluid core, respectively), K^{CMB} and K^{ICB} (electromagnetic couplings at core-mantle and inner core boundaries). When we use our value $\mathrm{Re}(s_2) = -0.00231406 \pm 103$, corresponding to NCEP(IB)+ECCO solution of Tab. 3, the numerical values from PREM Earth model (Mathews et al. 1991) $\tilde{\beta} = 6.160 \times 10^{-4}$, $A_m/A = 0.88621$, $A_s/A_f = 0.0064616$ and MHB paper $\mathrm{Re}(K^{CMB}) = 2.32 \times 10^{-5}$, $\mathrm{Re}(K^{ICB}) = 1.11 \times 10^{-3}$ (the latter two being known to only 10%), we arrive at $e_f = 0.0026364 \pm 23$, whose uncertainty is however fully limited by the imprecision of electro-magnetic couplings. The dynamical ellipticity of the whole Earth can be calculated from our $N_\circ$ and rigid Earth value $H_{dR} = e_R/(1 + e_R)$ by a simple relation $H_d = (C - A)/C = N_\circ H_{dR} = 0.0032738041 \pm 110$.

4. CONCLUSIONS

Unlike in the recent study by Lambert and Dehant (2007), all VLBI solutions studied yield similar values of estimated parameters $N_\circ, s_2$, consistent within their standard errors. Forced nutations due to the excitation by the atmosphere and oceans are significant at annual and semi-annual frequencies; they are similar for different oceanic models used, and the prograde annual term is in a good agreement with the value of the MHB empirical Sun-synchronous correction. The application of geophysical excitations yields a slightly longer period of retrograde FCN, and a larger value of a common multiplier $N_\circ$, than the MHB Sun-synchronous correction. Determination of the flattening of the core and of the whole Earth, based on these values, is possible, but the precision of the former is severely limited due to the not well known electro-magnetic couplings.

Acknowledgments. This study was supported by the grant LC506 awarded by the Ministry of Education, Youth and Sports of the Czech Republic.

5. REFERENCES

Brzezinski, A., 1994, "Polar motion excitation by variations of the effective angular momentum function: II. Extended model", Manuscripta Geodaetica, 19, pp. 157–171.

Capitaine, N., Wallace, P.T., Chapront, J., 2003, "Expressions for IAU 2000 precession quantities", A&A , 412, pp. 567–586.

Dobslaw, H., Thomas, M., 2007, "Simulation and observation of global ocean mass anomalies", J. Geophys. Res. , 112, doi: 10.1029/2006JC004035.

Gross et al., 2005, "Atmospheric and oceanic excitation of decadal-scale Earth orientation variations", J. Geophys. Res. , 110(B5), B09405.

IVS, 2005, "International VLBI Service products", `http://ivscc.gsfc.nasa.gov/`.

Lambert, S., Dehant, V., 2007, "The Earth's core parameters as seen by VLBI", A&A , 469, pp. 777–781.

Mathews. P.M., Buffet, B.A., Herring, T.A., Shapiro, I.I., 1991, "Forced nutations of the Earth: Influence of inner core dynamics 2. Numerical results and comparisons", J. Geophys. Res. , 96(B5), pp. 8243–8257.

Mathews, P.M., Herring, T.A., Buffet, B.A., 2002, "Modeling of nutation and precession: New nutation series for nonrigid Earth and insights into the Earth's interior", J. Geophys. Res. , 107(B4), doi: 10.1029/2001JB000390.

Ponte, R.M., Ali, A.H., 2002, "Rapid ocean signals in polar motion and length of day", Geophys. Res. Lett. 29, 10.1029/2002GL015312.

Salstein, D., 2005, "Computing atmospheric excitation functions for Earth rotation/polar motion", Cahiers du Centre Européen de Géodynamique et de Séismologie, 24, pp. 83–88.

Vondrák, J., 1977, "Problem of smoothing observational data II", Bull. Astron. Inst. Czechosl. 28, pp. 84–89

Vondrák, J., Ron., C., 2007, "Quasi-diurnal atmospheric and oceanic excitation of nutation", Acta Geodyn. Geomater. 4(148), pp. 121–128

ON OBSERVABILITY OF THE FREE CORE NUTATION

L. PETROV
NVI, Inc./NASA GSFC
Code 698, NASA GSFC, Greenbelt, MD 20771 USA
Leonid.Petrov@lpetrov.net

ABSTRACT. Neither astronomical technique, including VLBI, can measure nutation directly. Estimates of parameters of the nutation model are produced by solving the LSQ problem of adjusting millions parameters using estimates of group delay. The choice of the mathematical model for nutation used in the estimation process of analysis of group delays affects our ability to interpret the results. Ignoring these subtleties and using parameters of the nutation model either in the form of time series, or in the form of empirical expansion as "VLBI measurement of nutation", opens a room for misinterpretation and mistakes. Detailed analysis of the problem reveals that the separation of forced nutations, atmospheric nutations, ocean nutations, and the retrograde free core nutation requires invoking some hypotheses, and beyond a specific level becomes uncertain. This sets a limit of our ability to make an inference about the free core nutation.

1. INTRODUCTION

There are several basic misconceptions concerning the theory of nutation.

Misconception 1: *"VLBI measures nutation"*. In fact, VLBI measures . . . the thermal noise at receivers with a tiny admixture of the noise from an observed extragalactic source. VLBI is the technique for the evaluation of the spectrum of the cross-correlation function using records of thermal noise synchronized by independent clocks. Using cross-spectrum, group delays can be estimated. The theory of wave propagation describes the dependence of group delay on the motion of the emitter and receivers, the properties of propagation media, and the phase fluctuations inside the electronic equipment. This dependence can be reduced to a parametric model, and parameters of this model can be adjusted using all available estimates of group delays.

Thus, nutation parameters are not measured, but estimated together with more than a million other parameters. Unlike to direct measurements, these estimates are heavily depends on a subjective choice of parameterization. One cannot adjust only nutation parameters — in that case the fit would be very poor. For this reason, one should not interpret nutation parameters alone, they have sense only as a part of the overall mathematical model that describes the motion of the station network.

Misconception 2: *"There exists a theory of forced nutation with accuracy comparable to observations"*. An elaborate theory of the non-rigid Earth nutation was developed by Wahr (1980) in 1970-s. It explained 91% of the deviation of the real Earth nutations from the absolute rigid body nutations. Numerical values of nutation expansion in the framework of this theory were computed using some integral quantities that depends on profiles of density and elasticity parameters inside the Earth. These profiles were derived from analysis of seismological data. However, the disagreement of Wahr's theory with observations is currently at a 500-σ level.

> *If it disagrees with experiment it is wrong. In that simple statement is the key to science. It does not make any difference how beautiful your guess is. It does not make any difference how smart you are, who made the guess, or what his name is — if it disagrees with experiment it is wrong. That is all there is to it.*

Feymann (1965), page 156.

Thus, we are compelled to acknowledge that the theory of nutation is wrong. Numerous attempts to improve the theory were undertaken, but they all failed. In recognition of this failure, some authors resorted to fitting parameters of their theories to the adjustments of nutation angles from VLBI analysis — just the quantities that the theory is supposed to predict. Certainly, by fitting a set of ad hoc parameters, one can get a set of coefficients of nutation expansion that may have whatever small fit to nutation angle adjustments. But this mathematical trick does not make the theory correct, and this

set of coefficients cannot be called theoretical, but should be called empirical. Empirical expansions were presented in papers of Herring et al.(1986), Getino & Ferrandiz(2001), Shirai & Fukushima(2001), Mathews et al.(2002), Krasinsky & Vasilyev(2006)

The fact there is no precise theory of forced nutation, has important consequences. First, fitting parameters cannot be interpreted in terms consistent with the failed theory. Second, the residuals between the empirical theory and adjustments to nutation angles derived from VLBI analysis of group delay should not be interpreted as quantities with a specific physical meaning.

Misconception 3: *"An elaborate theory of nutation is needed for practical applications"*. Nutation has two major constituents: forced nutation with the precisely known excitation exerted by the Moon and the Sun and the constituents excited by the re-distribution of oceanic and atmospheric masses. The latter term is unpredictable in principle. The accuracy of determination of the nutation expansion from analysis of VLBI group delays has passed the level of atmospheric nutation contribution in 1990s. Therefore, even a precise theory of forced nutation would have been built, that theory would not be able to predict nutation with the accuracy comparable with observations. Similar to Chandler wobble, nutation parameters will have to be always determined from observations without any theory in mind.

2. DETERMINATION OF THE FREE CORE NUTATION

We consider here that N stations observe K celestial physical bodies. It is assumed that each station is associated with a reference point. In the case of VLBI antennas, this is the point of projection of the moving axis to the fixed axis. Observing stations receive electromagnetic radiation emitted by celestial bodies, and each sample of the received signal is associated with a time stamp from a local frequency standard synchronized with the GPS time. Analysis of voltage and time stamps of received radiation eventually allows us to derive the differences in the photon propagation time from observed bodies to reference points of observing stations. These distances depend on relative positions of stations with respect to observed bodies. The instantaneous coordinate vector of station i, in the inertial coordinate system at a given moment of time $\vec{r}_i^{\,\mathrm{C}}(t)$ is represented as the sum of a rotation and translation applied to a vector $\vec{r}_i^{\,\mathrm{T}}(t)$ in the terrestrial coordinate system as

$$\vec{r}_i^{\,\mathrm{C}}(t) = \widehat{\mathcal{M}}_a(t)\ \vec{r}_i^{\,\mathrm{T}} \ +\ \vec{q}_e(t) \times \vec{r}_i^{\,\mathrm{T}} \ +\ \vec{d}_i^{\,\mathrm{T}}(t) \ +\ \vec{T}(t) \tag{1}$$

where $\widehat{\mathcal{M}}_a(t)$ is the a priori rotation matrix, $\vec{q}_e(t)$ is the vector of small rotation, $\vec{T}(t)$ is the translational motion of the network of stations, and $\vec{d}_i(t)$ is a displacement vector of an individual station. Equations of photon propagation tie the instantaneous vector of site coordinates $\vec{r}_i(t)$ with vectors of observed physical bodies and their time derivatives. These relationships allow us to build a system of equations of conditions. Solving these equations, we can get estimates of expansion of the vector $\vec{q}_e(t)$ over some basis functions.

It has been demonstrated by Petrov(2007) that coefficients of expansions of the vector $\vec{q}_e(t)$ over the Fourier and B-spline bases can be found directly in a single LSQ solution that uses VLBI group delays estimates without resorting to intermediate time series. This means that we can estimate directly the spectrum of the Earth orientation variations from estimates of VLBI group delays. The portion of the spectrum of variations in q_1, q_2 considered as a complex process $q_1 + iq_2$ in the frequency range $[-1.5\Omega, -0.5\Omega]$, where Ω is the positive nominal frequency of the Earth rotation $7.292115146706979 \cdot 10^{-5}$ rad s^{-1}, is called nutation.

The nutation spectrum can be represented as a sum of two components: the forced nutation — a rail of with very sharp peaks with exactly known frequency, and the retrograde free core nutation (RFCN) — a band-limited continuous process with frequencies around the retrograde free core nutation frequency $-7.30901 \cdot 10^{-5}$ rad s^{-1}. Extensive discussion of nutation theory can be found in the monograph of Moritz(1987) and in the modern paper of Krasinsky(2006).

The problem of estimation of the free core nutation is reduced to the filtration of the observed spectrum of the Earth's rotation variations. The principle difficulty in separation of the RFCN from forced nutations is that their spectrum is overlapping, as figure 1 demonstrates.

We can separate the two constituents assuming 1) the RFCN is a band-limited process with known frequency band and unknown excitation; 2) the forced nutation is the purely harmonic process with known frequencies, known excitation, and a response function being *a smooth function* of frequency.

For practical implementation of this approach one should determine a) the band of the RFCN process and b) the empirical response function of forced nutations.

Figure 1: Spectrum of the free core nutations and forced nutations. Circles denote the power of the rigid Earth nutations, disks denote the power of the estimated nutation spectrum from VLBI group delays.

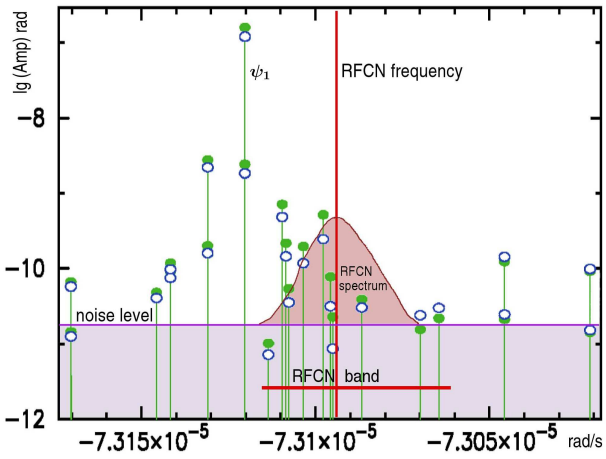

Empirical response function can be found with a data mining technique by comparing the spectrum of the Earth orientation with nutation constituents computed for the mechanical model of the absolutely rigid model. After a relatively short search, we find that complex amplitudes of forced nutations from VLBI data analysis A_e can be very well approximated to the theoretical amplitudes A_r for the mechanical model of the absolutely rigid Earth through this expression:

$$A_e(\omega) = [\alpha(\omega - \beta) + \frac{\gamma}{\omega - \delta}] \, (A_r(\omega) - A_n(\omega)) \tag{2}$$

where ω is the frequency, α, β, γ, and δ are complex parameters. A_n is the complex nutation amplitude caused by the non-tidal excitation, for instance, by the ocean and the atmosphere. It should be noted that functional dependence in the brackets of expression of 2, also called transfer function, can be derived analytically assuming 1) the triaxiality of the Earth's inertia ellipsoid is negligible; 2) the Earth consists of an elastic mantle and a liquid core; 3) the Earth's response is linear to the external torques. It should be stressed that although a simple theoretical considerations allow us to derive a parameterized expression similar to 2, the theory predicts *wrong* numerical coefficients, and therefore, it cannot be trusted.

Parameters α, β, γ, and δ can be determined from analysis of VLBI estimation results. We should be aware that 1) the estimates of coefficients α, β, γ, and δ heavily depend on a small set of constituents, including the constituent that corresponds to the ψ_1 tide, which is within the RFCN band; 2) estimation of the parameters of transfer function is a non-linear problem; 3) the oceanic and atmospheric contribution to the excitation has a significant uncertainty.

Using the estimates of the empirical transfer function, we can compute predicted forced nutations within the RFCN frequency band, and interpret the residual spectrum as the empirical RFCN spectrum. Predicted forced nutations have errors not only due to statistical uncertainties in the coefficients $\alpha, \beta, \gamma, \delta$, but also due to uncertainties in A_f and due to the errors of approximation in the expression 2. The fact that the spectrum of the RFCN and forced nutation is overlapping has important consequences: 1) the estimates of the RFCN spectrum have the statistical uncertainties due to the noise in VLBI group delay and the constraint uncertainties due to constituents separation, 2) estimates of the RFCN spectrum are not unique, but depend on assumptions made for parameterization of the empirical transfer functions; 3) estimates of the RFCN spectrum depend on the contribution of the ocean and the atmosphere on the main constituents of forced nutations.

Figure 2 shows an example of two estimates of the RFCN spectrum made under different assumptions for constituents separation. The estimation technique is described in details in Petrov(2007). It should be stressed that both spectra equally fit to VLBI group delays. The second spectrum shows a bi-modal pattern. We should resist to a temptation to rush inventing hypothesis for explaining this pattern.

In order to assess the sensitivity of the RFCN estimates to errors of oceanic and atmospheric contributions, I ran a Monte Carlo simulation. I ran 16 solutions and 1) added the Gaussian noise to estimates of nutations at K_1, S_1, P_1 due to uncertainty of ocean contribution with the standard deviation 150 prad; 2) added the Gaussian noise to estimates of nutations at ϕ_1, ψ_1 with the standard deviation 250 prad;

Figure 2: Estimates of the RFCN power spectrum from VLBI time delays from 1984 through 2007 and resonance constraints on forced nutation. A) Empirical transfer function from ψ_1, K_1, P_1, O_1, etc was extrapolated to the entire RFCN band; B) Forced nutations within the RFCN band were ignored and as a result they propagated to the estimates of the RFCN spectrum.

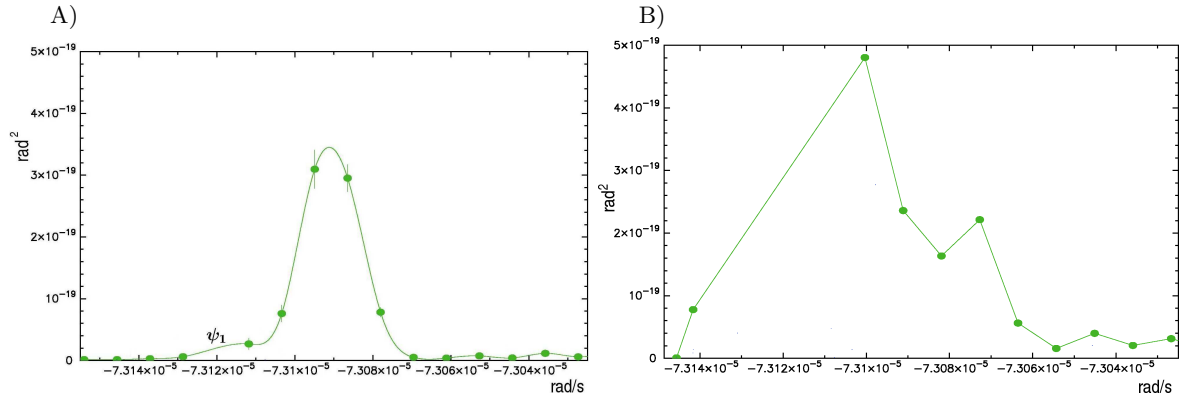

3) obtained new estimates of the empirical transfer function; 4) computed the new set of constraints on forced nutations. The added noise approximately corresponds to expected uncertainties of the oceanic and atmospheric contribution to nutation at these frequencies. Then I computed the rms of estimates of the RFCN spectra among these runs:

Uncertainty on the RFCN spectrum at different runs: 43 prad;
uncertainty on RFCN from noise in group delays: 19 prad.

We see that constraint uncertainty is dominating.

3. CONCLUSIONS

It was shown that the estimates of the RFCN spectrum depend on the mathematical model used for separation of the free and forced nutations. The estimates are not unique. Separation of nutations results in a constraint uncertainty. The constraint uncertainty sets the limit of accuracy of the RFCN spectrum estimates and dominates the error budget. Since the RFCN has a continuous spectrum within its band, more precise observations will not result in improving of the accuracy of the RFCN spectrum determination.

4. REFERENCES

Feynman R., "The Character of Natural Law", 1965, The MIT Press,

Getino J. & Ferrandiz J. M., 2001, "Forced nutations of a two-layer Earth model", MNRAS , 322, 785

Herring, T. A., Gwinn, C. R. & Shapiro, I. I., 1986, "Geodesy by radio interferometry: studies of the forced nutations of the earth. 1. Data analysis.", J. Geophys. Res., vol. 91, 4745

Krasinsky, G. A., 2006, "Numerical theory of rotation of the deformable Earth with the two-layer fluid core. Part 1: Mathematical model", Celes. Mech. Dyn. Astr. 96, 3–4, 169–217

Krasinsky, G. A., Vasilyev, M. V., 2006, "Numerical theory of rotation of the deformable Earth with the two-layer fluid core. Part 2: Fitting to VLBI data", Celes. Mech. Dyn. Astr. 96, 3–4, 219–237

Mathews P. M., Herring, T. A., & Buffett B. A., "Modeling of nutation and precession: new nutation series for nonrigid Earth an insights into the Earth's interior", 2002, J. Geophys. Res. 107, 10.1203/2001JB1000390

Moritz H., "Earth Rotation: Theory and Observation", 1987, Frederick Ungar, 617

Shirai, T., Fukushima, T., "Construction of a new forced nutation theory of the nonrigid Earth", 2001, AJ , 121, pp. 3270-3283.

Petrov L., "The empirical Earth rotation model from VLBI observations", A&A , vol. 467, p. 359, 2007.

Wahr, J. M., 1981, The forced nutations of an elliptical, rotating, elastic and oceanless Earth, Geophys. J. R. Ast. Soc., 64, 705

EARTH'S INTERIOR WITH VLBI... AND THE CELESTIAL REFERENCE FRAME?

S. LAMBERT[1], V. DEHANT[2], A.-M. GONTIER[1]
[1]SYRTE, Observatoire de Paris
61 av. de l'Observatoire F-75014 Paris
e-mail: sebastien.lambert@obspm.fr, anne-marie.gontier@obspm.fr
[2]Royal Observatory of Belgium
Avenue Circulaire 3, B-1180 Brussels
e-mail: v.dehant@oma.be

ABSTRACT. This paper proposes some insights into the sensitivity of nutation estimates and subsequent geophysical parameter determinations to the strategy adopted to handle the radio source coordinates during the astrogeodetic VLBI analysis. The calculations and results presented at the Journées 2007 have since then been reported in the paper Lambert et al. (2007). We invite the reader to consult this paper for further details and references and we chose to present here a summary of the most important ideas.

1. OBSERVATIONAL AND ANALYSIS STRATEGIES IN ASTROGEODETIC VLBI

Astrogeodetic VLBI aims to measure the relative orientation of the terrestrial and the celestial reference frames. It achieves this by observing radio sources from ground-based radio telescopes. In one observing session 6 to 12 antennas observe ∼80 sources. Repeating this every few days allows one to get orientation parameters (the well-known Earth orientation parameters, or EOP) and other relevant astrogeodetic quantities on a regular basis since 1984. Nevertheless, the VLBI instrument is changing at every session: the network array is different as well as the set of observed sources, making the realization of the terrestrial and celestial reference frames difficult and clearly introducing a source of error in the EOP themselves. Fig. 1 shows the observational history of some subsets of the 816 sources as observed in 2995 sessions analyzed at the Paris Observatory IVS Analysis Center. One clearly sees that the density of observing sources is significantly varying with time. The nutation offsets, basically the corrections to the IAU 2000A, that traduce a motion of the Earth's figure axis in space, show a pretty high noise level, although some patterns do show up (for instance the nearly diurnal free wobble associated with the free core nutation, and smaller annual and seasonal terms that can bring crucial information about the Earth's deformability). A consequence of the observing strategy is that a substantial part of the nutation offsets could be nothing but a propagated error due to a misleading analysis scheme and reflecting the radio source positional instabilities.

To evaluate this error, we propose to compare several analysis schemes that differ only in the way the radio source positions are handled (i.e., estimated as local or global parameters, and constrained). The International Celestial Reference Frame (ICRF, Ma et al. 1998), yields a catalogue of sources built on the basis of VLBI observations until 1995. It has been updated by Fey et al. (2004) and designated by ICRF-Ext.2. The simplest analysis scheme is to fix the radio source coordinates to their ICRF-Ext.2 values. However, doing so is implicitly considering that source positions have not changed since the release of the ICRF-Ext.2, which is wrong to some extent. A safer way is to estimate (either globally or locally) the radio source coordinates during the analysis, applying nevertheless a no-net rotation (NNR) constraint on some of them. The NNR is the mathematical translation of the fact that the source are globally and at any time non rotating with respect to the far universe. The ICRF yields 212 defining sources that are traditionally used for the NNR. However, Feissel-Vernier et al. (2006) (referred to as MFV in the following) yielded a set of 247 sources selected for their positional time stability. The same work selected 163 highly unstable sources, some of them being part of the 212 ICRF defining sources, that could obviously prevent the NNR from being verified along the complete observational time span. Table 1 reports on our analysis scheme that mix the ICRF and MFV subsets for the NNR and that put the unstable either as global or local parameters.

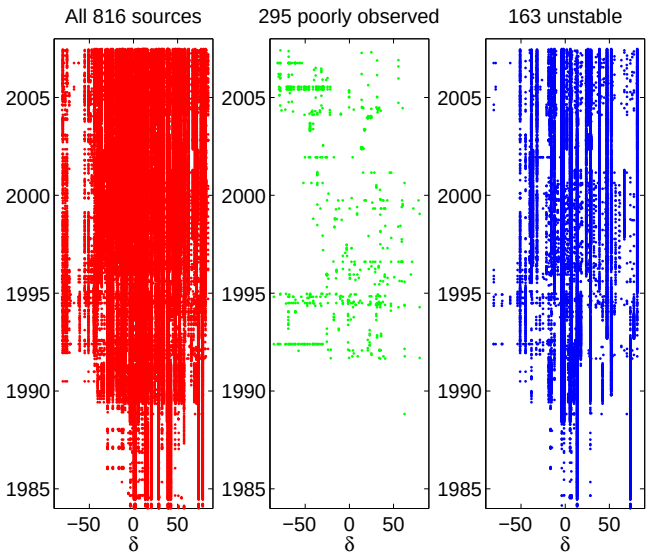

Figure 1: Observational history of (left) all the 816 sources, (middle) only the 295 sources having less than 20 observations in less than 2 sessions, and (right) the 163 unstable sources of Feissel-Vernier et al. (2006).

Table 1: Characteristics of the VLBI solutions used in this work. MFV: 247 stable sources of Feissel-Vernier et al. (2006); ICRF: 212 ICRF defining sources of Ma et al. (1998).

	No. sources			NNR	Postfit rms	rms δX	rms δY
	fixed	global	local		ps	μas	μas
A	816	0	0	-	24.0	165	167
B	0	816	0	ICRF	23.6	166	173
C	0	816	0	MFV	23.6	161	169
D	0	521	295	ICRF	23.6	162	170
E	0	521	295	MFV	23.6	161	169
F	0	653	163	ICRF	23.2	167	168
G	0	653	163	MFV	23.2	166	168

Our interest is to compare the various nutation offset time series obtained from the solutions designated A to G in Table 1. The comparison in terms of rms and noise is detailed in Lambert et al. (2007). Let us here write down some ideas about the comparison in terms of nutation amplitudes and Earth's interior parameters. We therefore propose to look at how the amplitude of the prominent nutation terms varies from one the another solution in A–G. In the nutation offsets taken as a complex time domain quantity $\delta X(t) + i\delta Y(t)$, we fit a number of terms of the form $(A^{\mathrm{Re}} + \mathrm{i}A^{\mathrm{Im}})\mathrm{e}^{\mathrm{i}\Theta}$ where Θ is a linear combination of the Delaunay's frequencies and phases. We choose to fit the prograde and retrograde 18.6-yr, 9.3-yr, 6.2-yr, annual, semi-annual, tri-annual, monthly and semi-monthly terms, along with a retrograde term of period 430.21 days (accounting for the nearly diurnal free wobble) and a linear trend. These terms are then corrected to remove the contribution of non-linear terms (see Lambert & Mathews 2006). Resulting amplitudes for A–G are reported in Fig. 2. It appears that the largest offsets to MHB are on the prograde annual and on the retrograde 18.6-yr nutations. The thick, red line represents an average of the solutions, the associated red error bars represent the cumulated error due to (i) the least-squares fit (estimated as the square root of the sum of the squared formal errors) and (ii) to the unperfect realization of the celestial frame. This latter contribution is obtained as the difference between the maximum and minimum amplitudes for each frequency. As already mentioned earlier, the influence of the celestial frame for annual and smaller periods is smaller than for longer periods.

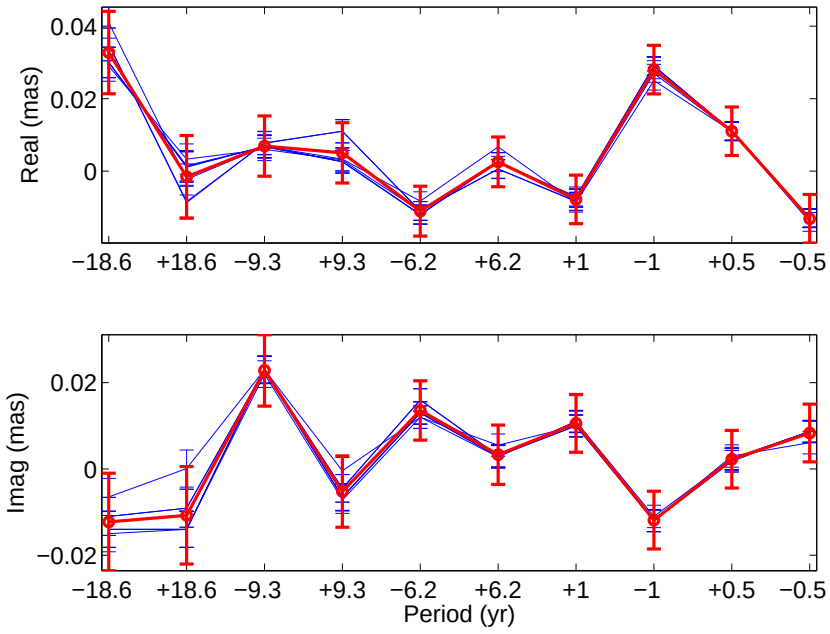

Figure 2: Amplitude of the VLBI residuals for prominent nutation periods against MHB from solutions A to G. The red, thick line is the averaged amplitude.

2. DOWN INTO THE EARTH'S INTERIOR

Nutation amplitudes give the response of the non rigid Earth to an excitative external potential. Though, for a rigid Earth, the admittance is simply the Earth's flattening, for a more complex stratified anelastic Earth with liquid core and solid inner core, the admittance is much more complex (see Mathews et al. 2002 for instance and reference therein). This admittance include strong resonances associated with the main ellipsoidal layers (mantle, core and inner core) and known as the Chandler wobble, the retrograde free core nutation (RFCN) and the free inner core nutation (FICN), respectively. The former one acts only in the long-periodic band in the Earth-fixed frame of reference and is therefore irrelevant here. However, the resonant frequencies of the latters, adjusted on VLBI data, are of −430.21 days and 1024.36 days, respectively, following Mathews et al. Let us look at the sensitivity of these parameters to the celestial frame instability already propagated into nutation amplitudes.

The method of retrieving the RFCN and FICN resonant frequencies is detailed in Lambert et al. (2007) and elsewhere in the literature. The obtained values of the resonant RFCN and FICN periods P and quality factors Q are reported in Fig. 4 wherein the uncertainties represent the formal error of the least-

squares fit. The influence of the analysis strategy can be seen by comparing P and Q from one to the other solution. One can see that the RFCN period goes from −430.30 to −430.32 days, an interval smaller than the least-squares standard error which amounts to 0.08 day. The quality factor is stable within less than 200. The FICN period stays between 1042 and 1113 days (with a formal error around 120 days). Its quality factor is between 885 and 974 with error bars of 200.

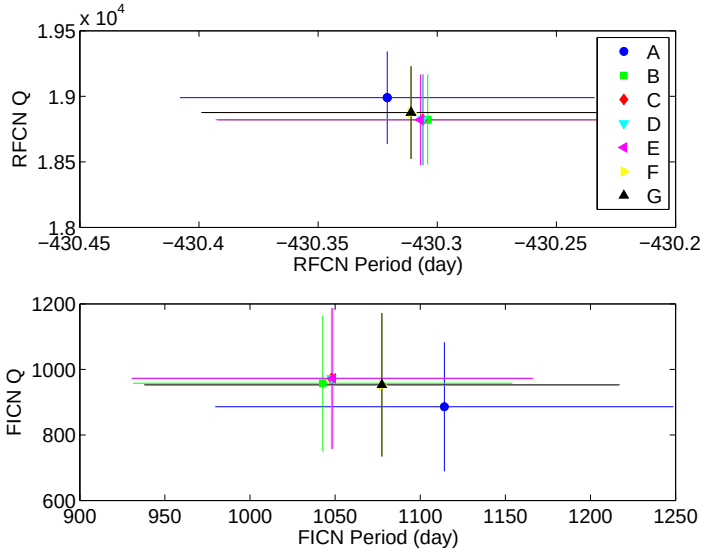

Figure 3: Resonant period and quality factor of the RFCN and of the FICN estimated from various VLBI solutions A to G.

Our work points out the order of magnitude of the error coming from the positional instability of the radio sources and the handling of the celestial frame in VLBI-derived nutation analyses for use in geophysics. This error can produce an additional error in the estimates of nutation spectral components of 15 μas for the 18.6-yr term, and that decreases for shorter periods. In terms of resonant frequencies of the outer and inner cores, this means an uncertainty of a few tenth of day on the RFCN period and of 200 on Q, and an uncertainty of less than 100 days on the FICN period and of 100 on Q. Although not within the scope of this paper, finding the best strategy for taking account of radio source instabilities in geodetic VLBI analysis remains a challenging question for the near future. Solutions A to G were processed with analysis strategies that are currently in use through the VLBI community. It is therefore expected that some operational solutions proposed within the VLBI community will be more reliable for geophysical investigations since they bring Earth orientation parameters with a best internal accuracy.

3. REFERENCES

Feissel-Vernier, M., Ma, C., Gontier, A.-M., & Barache, C. 2006, Analysis issues in the maintenance of the ICRF axes, A&A 452, 1107

Fey, A.L., Ma, C., Arias, E.F., et al. 2004, The Second Extension of the International Celestial Reference Frame: ICRF-EXT.1, AJ 127, 3785

Lambert, S.B., & Mathews, P.M. 2006, Second-order torque on the tidal redistribution and the Earth's rotation, A&A 453, 363

Lambert, S.B., Dehant, V., & Gontier, A.-M. 2007, Celestial frame instability in VLBI analysis and impact on geophysics, A&A accepted for publication

Ma., C., Arias, E.F., Eubanks, T.M., et al. 1998, The International Celestial Reference Frame as realized by very long baseline interferometry, A&A 116, 516

Mathews, P.M., Herring, T.A., & Buffett, B.A. 2002, Modeling of nutation and precession: New nutation series for nonrigid Earth and insights into the Earth's interior, JGR 107(B4), doi:10.1029/2001JB000390

CONCISE ALGORITHMS FOR PRECESSION-NUTATION

P. T. WALLACE[1], N. CAPITAINE[2],
[1] STFC / Rutherford Appleton Laboratory
Harwell Science and Innovation Campus, Didcot, Oxfordshire OX11 0QX, UK
e-mail: p.t.wallace@rl.ac.uk
[2] Observatoire de Paris, SYRTE/UMR8630-CNRS,
61, avenue de l'Observatoire, 75014 – Paris, France
e-mail: n.capitaine@obspm.fr

ABSTRACT. The precession-nutation models based on the IAU 2000A nutation series involve several thousand amplitude coefficients, many under 1 μas in size, and the sines and cosines of about 1350 angles. For the many applications that do not require the utmost accuracy this represents an unnecessary or even excessive computational overhead. The IAU 2000B model offers one alternative, an order of magnitude smaller than IAU 2000A and delivering classical nutation components of 1 mas accuracy in the current era. In a recent paper (Capitaine & Wallace 2007), the main results of which are provided here, we looked at other options, based on series for the CIP coordinates and the CIO locator and with the GCRS to CIRS rotation matrix as the end product. Truncation of the series provides most of the savings, but certain other measures can be taken also. Three example formulations are presented that achieve 1 mas, 16 mas and 0.4 arcsec accuracy throughout 1995-2050 with computational costs 1, 2 and 3 orders of magnitude less than the full models. A few examples of possible applications are presented.

1. INTRODUCTION

The IAU 2000A model for precession-nutation includes terms at about 1350 frequencies, and coefficients as small as 0.1 μas. Although for many applications the size of the model is not an important consideration, this is not always the case. Use of the full models is natural when the application demands it and/or computing resources are ample. But often a lower accuracy will suffice, and then the full models are an unnecessary overhead. Sometimes computing resources are so limited that the full models are unaffordable: unless some interpolation or look-up scheme is devised, a simplified model must be used. The IAU recognized this need, adopting in addition to the full-accuracy model an equinox based lightweight alternative of 1 mas accuracy, namely 2000B (McCarthy & Luzum 2003). The recent paper by Capitaine & Wallace (2007, CW07) addresses the more general problem of how to construct a concise and efficient CIO based model that achieves any given level of accuracy, and the present paper presents some of the results of that work.

2. METHODS

The transformation from celestial (GCRS) to terrestrial (ITRS) coordinates can be written out as:

$$\mathbf{v}_{\rm ITRS} \;=\; \mathbf{R}_{\rm PM} \cdot \mathbf{R}_3(\theta) \cdot \mathbf{R}_{\rm NPB} \cdot \mathbf{v}_{\rm GCRS} \qquad (1)$$

where the vectors $\mathbf{v}_{\rm GCRS}$ and $\mathbf{v}_{\rm ITRS}$ are the same direction with respect to the two reference systems, the matrix $\mathbf{R}_{\rm NPB}$ represents the combined effects of frame bias and precession-nutation and defines the directions of the celestial intermediate pole and origin (CIP and CIO), $\mathbf{R}_3(\theta)$ is Earth rotation angle and the matrix $\mathbf{R}_{\rm PM}$ is polar motion. The objective is to devise formulations for $\mathbf{R}_{\rm NPB}$ that achieve different compromises between accuracy and computing costs over a specified time interval.

There are several ways of forming $\mathbf{R}_{\rm NPB}$ (see Capitaine & Wallace 2006), and abbreviated forms of any of these could be developed. But the method based on direct series for (i) the CIP coordinates X, Y and (ii) the quantity $s + XY/2$ that locates the CIO is particularly attractive. Separate treatment of bias, precession and nutation is avoided, each of the three series makes the same contribution to final accuracy (e.g. no $\sin\epsilon$ factors to consider), and other aspects can be optimized individually. Furthermore, simple truncation of the series is likely to deliver a nearly optimal result, without resorting to least-squares

fitting or harmonic analysis. The method includes a number of opportunities for trading off accuracy against computing costs and these have been developed in CW07. In summary:

- Truncating the X, Y series is where the biggest savings lie. Each term in X or Y consists of a sine and cosine component at a given frequency. The "purist" approach is to regard each term as a vector and to truncate based on modulus – so that coefficients are either dropped or retained in pairs. But because almost all terms have phases such that either the sine or cosine coefficient dominates, truncating by individual coefficient, i.e. usually retaining only one of the pair, avoids wasteful and ineffectual tiny values in the final series. The relationship between number of retained coefficients and the 1995-2050 CIP accuracy is shown in Figure 1.

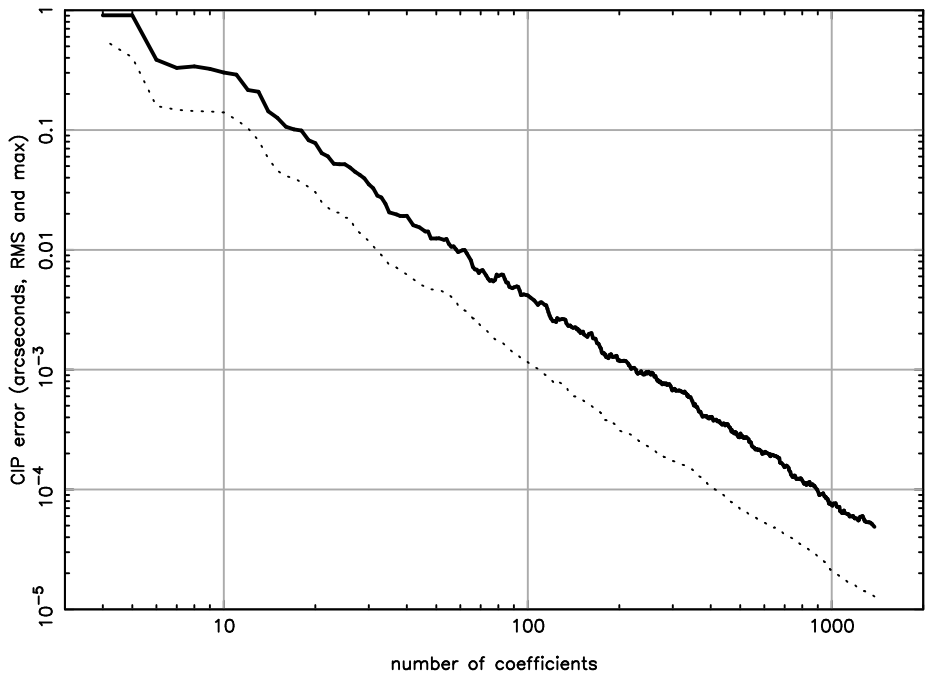

Figure 1: The variation of CIP accuracy with differing cut-offs applied to the individual coefficients of the X, Y series. The horizontal axis is the number of retained coefficients, each of which is either a sine or cosine term at a particular frequency and power of (t) and contributes to either X or Y. The vertical axis is the error in the position of the CIP, compared with that predicted by the full series. The heavy line shows the maximum error during the interval 1995-2050; the dotted line is the RMS error in the same interval.

- The $s + XY/2$ series is much shorter than those for X and Y but there are still opportunities for worthwhile savings. Only a handful of terms is needed to achieve 1 mas, and for the most concise models s can be neglected altogether. Note that the X and Y used to remove the $XY/2$ term do not have to be very accurate, so that whatever approximate values have already been calculated will be more than adequate.

- There are obvious opportunities for approximating the $\mathbf{R}_{\rm NPB}$ matrix elements, exploiting the facts that the CIP z-coordinate is nearly unity and the angle s is small. During 1995-2050, accuracies of a few μas can be achieved without resorting to trigonometric functions or square roots, and even a matrix that contains only the values 0, 1, X and Y achieves 0.1 arcsecond accuracy.

- The series for X, Y and $s + XY/2$ are functions of the fundamental arguments, a set of 14 angles. They comprise the five Delaunay variables l, l', F, D and Ω, eight planetary longitudes, and the general precession. Each is a polynomial in time: the expressions for the Delaunay variables use five coefficients (i.e up to t^4) , all the others just two. Potential savings, from omitting unused arguments and truncating the series for the Delaunay variables, are always modest, but worthwhile for the more approximate $\mathbf{R}_{\rm NPB}$ formulations.

- The full X, Y series contain terms with periods from 3.5 days to almost 100 millennia. In a restricted time span, for example 1995-2050, the terms of longer period produce nearly fixed offsets in X and Y. Using 1000 years as the cut-off eliminates 33 terms and gives offsets of $-634.2\,\mu$as in X and $+1421.45\,\mu$as in Y. These can be combined with the CIP bias and used for all the concise formulations.

3. EXAMPLE CONCISE FORMULATIONS

Table 1 summarizes the performance of three models obtained with the techniques just described, using the SOFA implementation of the full IAU 2000A model as the reference. Figures for IAU 2000B are also included, for comparison.

model	*coeffs*	*freqs*	*RMS*	*worst*	*speed*
reference	4006	1309	-	-	1
IAU 2000B	354	77	0.28	0.99	7.6
CPN_b	229	90	0.28	0.99	15.3
CPN_c	45	18	5.4	16.2	138
CPN_d	6	2	160	380	890
		mas	mas		

Table 1: Three concise models (designated CPN_b, CPN_c and CPN_d) compared.

Concise model CPN_b aims to equal the performance of IAU 2000B. The peak errors during 1995-2050 are shown in Figure 2. It was obtained by truncating the X and Y series at $50\,\mu$as and the $s + XY/2$ series at $60\,\mu$as, using slightly simplified expressions for the matrix elements but retaining full-accuracy fundamental-argument expressions. It requires fewer coefficients than IAU 2000B and is twice as fast. Its accuracy is such that the unmodeled free core nutation is itself an important limitation.

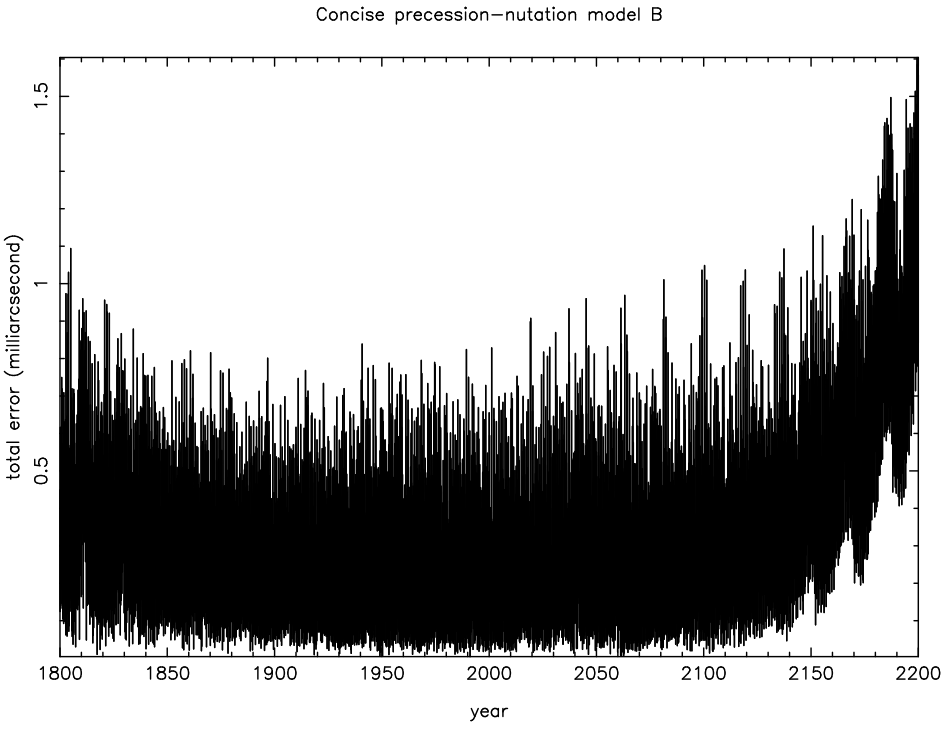

Figure 2: The 400-year performance of the example concise formulation CPB_b. The model achieves better than 1 mas (worst case) during the interval 1995-2050.

Concise model CPN_c achieves 16 mas performance between 1995 and 2050, which is better than the

old IAU 1976/1980 model that is still in wide use for low-accuracy applications, and considerably shorter. The X and Y cutoffs are 2.5 mas, leaving only 42 coefficients, plus another three to obtain the CIO locator s. Using 2-coefficient fundamental-argument expressions also offers savings, and a speed well over 100 times faster than the full IAU 2000A model is achieved.

Concise model CPN_d could be a good choice for applications where polar motion will normally be neglected, such as pointing small telescopes. It is almost 1000 times faster than the full IAU 2000A, and despite needing only six coefficients achieves 0.4 arcsec (worst case) during the 1995-2050 test interval.

4. EXAMPLE APPLICATIONS

Only a minority of practical applications require the full accuracies delivered by current models. Examples of applications where somewhat reduced accuracy is acceptable and where improved speed is potentially beneficial include:

- Satellite orbit predictions: see Vallado & Seago (2006).
- Pulsar timing analysis: the recent TEMPO2 analysis software (Edwards et al. 2006) uses IAU 2000B.
- The pointing of telescopes and antennas: accuracy needs are set by the limitations of refraction predictions and the mechanical imperfections of the telescope and mount.
- Occultation predictions.
- The IERS could consider adopting a concise model as an alternative basis for the publication of celestial pole offsets dX, dY. At present, users are put to the expense of computing the full model, only to add corrections to the results. Were the IERS to add to its tabulations dX, dY values with respect to a shorter model (say CPN_b), this would produce an identical final CIP X, Y at a fraction of the computing costs.

5. REFERENCES

Capitaine, N., Wallace, P.T., 2006, "High precision methods for locating the celestial intermediate pole and origin" A&A 450, 855

Capitaine, N., Wallace, P.T., 2007, "Concise CIO based precession-nutation formulations" A&A (in press, DOI: 10.1051/0004-6361:20078811, CW07)

McCarthy, D.D., Luzum, B.J., 2003, "An abridged model of the precession-nutation of the celestial pole" Celest. Mech. Dyn. Astr. 85, 37

Edwards, R.T., Hobbs, G.B., Manchester, R.N., 2006, "TEMPO2, a new pulsar-timing package – I. An overview" MNRAS 369, 655

Vallado, D.A., Seago, J.H., 2006, "Implementation issues surrounding the new IAU reference systems for astrodynamics" 16th AIAA/AAS Astrodynamics Specialist Conference, Tampa, FL, Jan. 22-26, 2006, AAS 06-134

BETTER PROPER MOTIONS ACCURACY FOR STARS WITH HIPPARCOS SATELLITE AND GROUND-BASED OBSERVATIONS

G. DAMLJANOVIĆ
Astronomical Observatory
Volgina 7, 11160 Belgrade, Serbia
e-mail: gdamljanovic@aob.bg.ac.yu

ABSTRACT. About 15 years elapsed since the HIPPARCOS ESA satellite mission observations (the epoch of Hipparcos Catalogue is 1991.25). The errors of the Hipparcos stars proper motions were close to 1 mas/year, and nowadays the error of apparent places of these stars is more than 15 mas. It exceeds the error of Hipparcos stars positions (about 1 mas) by one order of magnitude. Some parts of the sky (presented via Hipparcos stars data) are with bigger errors than mentioned ones, the shortness of the Hipparcos observations yields bigger proper motions errors of double or multiple stars than the single ones, etc. There are numerous astrometric ground – based observations of some stars referred to Hipparcos Catalogue. Here, the data of latitude variations of 26 instruments are used to improve the Hipparcos proper motions in declination μ_δ of observed stars. The method and results are presented here.

1. INTRODUCTION

After less than four years of the Hipparcos satellite observations and a few years of analysis, at the end of 1997, the optical counterpart of the ICRF appeared. It was the HIPPARCOS Catalogue (ESA, 1997) with astrometric data for 118218 stars: the magnitudes of stars are until 12 (mostly between 7 and 9), the standard error of positions is about 1 mas (at the epoch of the catalogue 1991.25), the standard error of the proper motions $\mu_\alpha \cos\delta$ and μ_δ is near 1 mas/yr, etc. Some time after that, a few new catalogues were finished with better accuracy of proper motions: ACT, FK6, GC+HIP, TYC2+HIP, TYCHO-2, ARIHIP, EOC-2 (Vondrák, 2004), EOC-3, etc. The period of Hipparcos satellite observations is not enough to get a good accuracy of proper motions for some stars as double or multiple ones. Some regions of Hipparcos Catalogue are with bigger errors of proper motions than other ones. Also, the calculated apparent positions of Hipparcos stars are about 15 mas now (15 years after 1991.25) with the errors of proper motions of about 1 mas/yr; 15 mas is near the ground – based error of observed positions and one order bigger than the error of Hipparcos positions. The astro-geodesy observations need better accuracy of calculated apparent positions of Hipparcos stars, and during last decade some investigations started to improve proper motions of these stars by using their ground-based observations.

Here, the latitude variations of 10 PZT (photographic zenith tube), 14 ZT (visual zenith – telescope), 1 FZT (floating zenith – telescope) and 1 VZT (visual zenith tube), made in accordance with the Earth rotation programmes and covering the interval 1899.7 – 1992.0, with the OA00 (Vondrák, 2002) solution of the EOP were used to improve the accuracy of Hipparcos μ_δ. The method of this investigation is different than the one used for EOC-2. The determined corrections of Hipparcos μ_δ are with accuracy similar to one of ARIHIP, EOC-2 and EOC-3 proper motions data.

2. DATA AND CALCULATIONS

The data of seven ZT ILS stations (Carloforte, Cincinnati, Gaithersburg, Kitab, Mizusawa, Tschardjui and Ukiah) covering the interval 1899.7 – 1979.0, 10 PZT instruments (3 at Washington, 2 at Mizusawa and Richmond, 1 at Ondřejov, Punta Indio and Mount Stromlo), and the other 8 stations (Belgrade ZT, Blagoveschtschensk ZT, Irkutsk ZT, Poltava ZT, Pulkovo 2 ZT, Varsovie ZT, Mizusawa FZT, Tuorla-Turku VZT) were used. It is $\mu_\delta = (\delta_1 - \delta_2)/(t_1 - t_2)$ with the error $\epsilon_{\mu_\delta} = (\epsilon_1^2 + \epsilon_2^2)^{1/2}/|t_2 - t_1|$, where δ_1 and δ_2 are two positions of the star for the epochs t_1 and t_2, respectively. Both positions are in the same system. The standard errors of δ_1 and δ_2 are ϵ_1 and ϵ_2, respectively. It is evident that ϵ_{μ_δ} is proportional to $1/t$. Then, it is possible to get better accuracy ϵ_{μ_δ} than the Hipparcos one if there is long observational interval t and lot of observations of any observed star (or star pair) per year, even

Hipparcos accuracy of star positions is much better than ground – based one. Each ZT or FZT star pair was observed from a few until few hundred times per year, and the accuracy of one ZT star pair observation is near $0.2''$ (it is similar situation in the case of PZT and VZT star observations). Also, the time intervals of some stars (or star pairs) observations are few decades long. During calculations, both data (ground – based and Hipparcos ones) were used for any star; the latitude data with Hipparcos ones give better results than only latitude ones. In the case of the ILS stations (with nearly the same latitude $+39.^o1$), during calculations of any star pair, the data (latitude variations φ_i) of all 7 ILS ZT stations were used. Similar situation is for stars observations of PZT stations Punta Indio – Mount Stromlo and Washington – Mizusawa. Each mentioned code (CA, etc.) is in line with the monograph (Vondrák et al., 1998). Some effects were removed from received data (Vondrák et al., 1998).

The main effect presented into the star pair latitude changes φ_p is the polar motion part. That effect was calculated (by using the Kostinski formula $\Delta\varphi_i = x_i \cos\lambda_W + y_i \sin\lambda_W$) and removed from φ_p values. The polar motion coordinates x and y are from mentioned EOP solution OA00. The longitude λ_W is west of the zero meridian. The systematic variations (local, instrumental, etc.) for each instrument were calculated and removed from φ_p values, also. For each star pair, the average values of φ_p values (without the polar motion and systematic variations) give the points r'_n (about one point per year, n ones for observed interval). Without the polar motion and systematic variations, the values φ_p are mostly with catalogue errors. It is $\Delta\varphi_p + (d\varphi_p/dt)t \approx (\Delta\delta_S + \Delta\delta_N)/2 + t(\Delta\mu_{\delta_S} + \Delta\mu_{\delta_N})/2$ (Vondrák et al. 1998), where: $\Delta\delta_S$ and $\Delta\delta_N$ are corrections of declinations (for S and N star, respectively), $\Delta\mu_{\delta_S}$ and $\Delta\mu_{\delta_N}$ are corrections of μ_δ (for S and N star, respectively), t is the time. To calculate the corrections of star pairs (of common ZT/Hipparcos stars) μ_δ, the Least Squares Method and the linear model were used (Damljanović, 2005) $r'_n = a + b(t_n - 1991.25)$, where r'_n is the star pair residue, t_n (in years) is the epoch instant of r'_n, a is in line with $(\Delta\delta_S + \Delta\delta_N)/2$, b is in line with $(\Delta\mu_{\delta_S} + \Delta\mu_{\delta_N})/2$. The values a and b, for each ZT star pair, are in line with the epoch of Hipparcos Catalogue (1991.25). The points r'_n and the Hipparcos one are with suitable weights (Damljanović et al., 2006). The ZT and FZT data give the corrections (of Hipparcos μ_δ values) but to star pairs because the ZT and FZT observations were made for star pairs in line with Horrebow – Talcott method. The author found the original way to solve this problem and to separate them (Damljanović and Pejović, 2006). In the case of PZT and VZT observations, we are using the similar procedure (Damljanović, 2005; Damljanović and Vondrák, 2005), but instead of latitude of observed star pair (of ZT) it is the latitude of single star observation (of PZT). The calculated value of a is in line with $\Delta\delta$, and the value of b is in line with $\Delta\mu_\delta$. The main results are in mentioned papers (Damljanović and Pejović, 2006; Damljanović et al., 2006).

Acknowledgements. This work is a part of projects No 146004 "Dynamics of celestial bodies, systems and populations" and No 146022 "History and Epistemology of Natural Sciences" (Ministry of Science of R. Serbia). I wish to thank Dr.Vondrák for the data and support during preparing PhD thesis "Improvement of accuracy of proper motions of Hipparcos Catalogue stars using optical latitude observations".

3. REFERENCES

Damljanović, G., 2005, "Photographic zenith tube observations to improve Hipparcos proper motion in declination of some stars", Serb. Astron. J., 170, pp. 127-132.

Damljanović, G., Vondrák, J., 2005, "Improved proper motions in declination of some Hipparcos stars derived from observations of latitude", Proc. of the Journées 2004 Systèmes de Référence Spatio-Temporels, Fundamental Astronomy: New concepts and models for high accuracy observations, N.Capitaine (ed.), Observatoire de Paris, pp. 230-231.

Damljanović, G., Pejović, N., Jovanović, B., 2006, "Improvement of Hipparcos proper motions in declination", Serb. Astron. J., 172, pp. 41-51.

Damljanović, G., Pejović, N., 2006, "Corrections of proper motions in declination by using ILS data", Serb. Astron. J., 173, pp. 95-99.

ESA, 1997, The Hipparcos and Tycho Catalogues, ESA SP – 1200.

Vondrák, J., 2002, Private communication.

Vondrák, J., Pešek, I., Ron, C., Čepek, A., 1998, "Earth orientation parameters 1899.7 – 1992.0 in the ICRS based on the HIPPARCOS reference frame", Astron. Inst. of the Academy of Sciences of the Czech R., Publ. No. 87.

Vondrák, J., 2004, "Astrometric star catalogues as combination of Hipparcos/Tycho Catalogues with ground – based observations", Serb. Astron. J., 168, pp. 1-7.

GEOPOTENTIAL OF A TRIAXIAL EARTH WITH A RIGID INNER CORE IN ANDOYER CANONICAL VARIABLES

A. ESCAPA[1], J. GETINO[2], J.M. FERRÁNDIZ[1]
[1] Dpto. Matemática Aplicada. Escuela Politécnica Superior.
Universidad de Alicante. E-03080 Alicante. Spain
E-mail: Alberto.Escapa@ua.es
[2] Grupo de Mecánica Celeste. Facultad de Ciencias
Universidad de Valladolid. E-47005 Valladolid. Spain

ABSTRACT. We derive analytical expressions for the geopotential of a three-layer Earth model composed by a triaxial rigid mantle, a triaxial fluid outer core and a triaxial rigid inner core, extending previous works performed on the basis of an axial-symmetric three-layer Earth model (Greiner-Mai *et al.* 2000, 2001). In order to consider these expressions within the framework of the Hamiltonian theory of the rotation of the non-rigid Earth, we work out the problem in terms of a set of canonical variables arising from associating an Andoyer-like variables to each layer of the Earth, in the same way as it is described in Escapa *et al.*(2001). With the help of Wigner theorem (Kinoshita *et al.* 1974), we obtain the development of the geopotential of this Earth model in a mantle attached reference frame. Finally, we analyze the dependence of each geopotential coefficient of the second degree on the triaxiality and figure axis of the rigid inner core.

1. CANONICAL CONSTRUCTION OF THE GEOPOTENTIAL VARIATION

Let us consider a three-layer Earth model composed of a rigid mantle, an homogeneous fluid core and a rigid inner core, sharing a common barycenter O. Let us attach to the mantle and the inner core two reference frames $T_m = \{O; \vec{e}_{1m}, \vec{e}_{2m}, \vec{e}_{3m}\}$ and $T_s = \{O; \vec{e}_{1s}, \vec{e}_{2s}, \vec{e}_{3s}\}$ whose vectorial basis are constituted by the principal axis of the mantle and of the inner core, respectively. Under the prescribed conditions, the relative motion of the inner core with respect to the mantle is given by a rigid rotation of the reference frame T_s with respect to the reference frame T_m around O. As a consequence of this internal motion the density distribution inside the Earth viewed from T_m changes with time, it induces a time variation in the gravitational field originated by the Earth, that is to say, in the geopotential. By considering the decomposition sketched in the figure (Escapa *et al.* 2001) we infer that the temporal variation of the geopotential is exclusively due to the auxiliary body (subscript ab) and can be written as

$$\Delta U = U_{ab}(r, \delta', \alpha') - U_{ab}(r, \delta, \alpha), \tag{1}$$

where r, δ, α are the distance, latitude and longitude of the external point with respect to the frame T_m and their primmed counterparts are referred to the frame T_s. This expression should be referred to a single reference frame, which usually coincides with the reference frame of the mantle T_m. Since the frame T_s can be brought to the frame T_m by means of a rotation and considering the usual expansion of the geopotential in terms of the spherical harmonics (e.g. Kinoshita *et al.* 1974), the problem that we have faced is equivalent to determine how are transformed the spherical harmonics by a rotation. The solution of this problem is given by Wigner theorem (e.g. Kinoshita *et al.* 1974) that states that under a counterclockwise rotation around the x or z axes, which brings the frame T_m into de frame T_s (primed variables), the spherical harmonics in both frames are linearly related, being the coefficients of the linear combination functions of the parameters that characterize the rotation between the frames T_m and T_s.

One possible choice to describe these parameters is to employ the Andoyer-type canonical variables described in Escapa *et al.* (2001) for modelling analytically the rotation of a three-layer Earth model. This set is composed by eighteen variables: λ, μ, ν, Λ, N, M for the total Earth, λ_f, μ_f, ν_f, Λ_f, N_f, M_f for the fluid and λ_s, μ_s, ν_s, Λ_s, N_s, M_s for the inner core. The meaning of these variables (Escapa *et al.* 2001), and the auxiliary angles I, σ, I_f, σ_f, I_s and σ_s, are related with the angular momentum of the Earth, the fluid and the inner core and their projections in different reference frames. In particular,

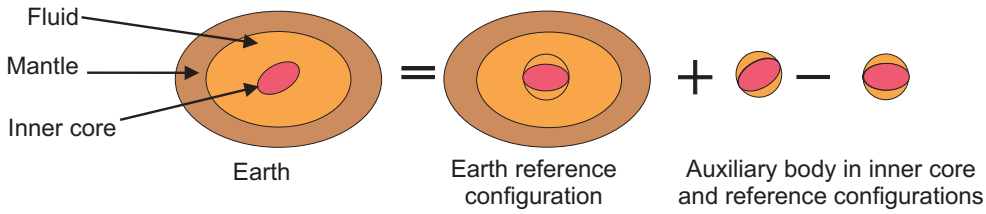

it can be shown that the rotation which brings the T_m frame into the T_s frame is given by a rotation matrix $\mathbf{R}(\lambda_s,\, I_s,\, \mu_s,\, \sigma_s,\, \nu_s)$.

2. DISCUSSION OF THE SECOND DEGREE TERMS

Accordingly to the above described procedure, we can obtain for the second degree terms of the geopotential the following expression

$$\Delta U^{(2)} = \frac{G}{r^3} A_{ab} \sum_{m=0}^{2} \left\{ \left[e_{ab} a_{2m}(t) + d_{ab} \tilde{a}_{2m}(t) \right] C_{2m}\left(\delta, \alpha\right) + \left[e_{ab} b_{2m}(t) + d_{ab} \tilde{b}_{2m}(t) \right] S_{2m}\left(\delta, \alpha\right) \right\}$$

where we have introduced the ellipticity $e_{ab} = (C_{ab} - A_{ab})/A_{ab}$ and triaxiality $d_{ab} = (B_{ab} - A_{ab})/A_{ab}$ parameters and $C_{2m}\left(\delta, \alpha\right)$, $S_{2m}\left(\delta, \alpha\right)$ represent the real surface spherical harmonics of second degree and order m. This formula, which is a cumbersome function of the variables $\lambda_s, I_s, \mu_s, \sigma_s, \nu_s$ through the coefficients $a_{2m}(t)$, $\tilde{a}_{2m}(t)$, $b_{2m}(t)$ and $\tilde{b}_{2m}(t)$, can be simplified by assuming that in the rotational motion of the inner core the reference frames T_m and T_s are almost coincident. In addition, we will consider that the vectors $\vec{e}_{\vec{L}_s}$ and $\vec{e}_{3s}$ also remain close. These conditions are commonly assumed in Earth rotation studies of three-layer models. In terms of the canonical variables these geometrical relationships are expressed by the fact that the angles I_s, σ_s and $\nu_s + \mu_s + \lambda_s$ are small.

Therefore, we can keep only first order terms in these angles in the geopotential variations, obtaining the non-vanishing expressions

$$\begin{aligned} a_{21}(t) &= \sigma_s \sin\nu_s + I_s \sin\left(\nu_s + \mu_s\right), b_{21}(t) = -\left[\sigma_s \cos\nu_s + I_s \cos\left(\nu_s + \mu_s\right)\right], \\ \tilde{b}_{21}(t) &= \sigma_s \cos\nu_s + I_s \cos\left(\nu_s + \mu_s\right), \tilde{b}_{22}(t) = -\left(\nu_s + \mu_s + \lambda_s\right)/2. \end{aligned} \quad (2)$$

From a geometrical point of view, the right hand sides of the equations (2) are related with the x and y components of the vector $\vec{e}_{3s}$ in the frame T_m, and with the angle between the vectors $\vec{e}_{1m}$ and $\vec{e}_{1s}$. Let us underline that we have obtained two extra terms to the geopotential variation, $\tilde{b}_{21}(t)$ and $\tilde{b}_{22}(t)$, which are caused by the triaxiality. Moreover, the temporal variation associated to the harmonic $S_{22}\left(\delta, \alpha\right)$ is exclusively due to the triaxiality and vanishes, in our order of approximation, in the axial-symmetric case. In view of the slight triaxiality of the inner core, as well as its small moment of inertia when compared with that of the Earth, these terms are expected to be small. Anyway, they could play a role for other planets or natural satellites that have a more massive inner core. On the other hand, it would be interesting to provide the analytical expressions that determine the temporal evolution of the canonical parameters $\lambda_s(t), I_s(t), \mu_s(t), \sigma_s(t), \nu_s(t)$, and therefore of $a_{2m}(t)$, $\tilde{a}_{2m}(t)$, $b_{2m}(t)$ and $\tilde{b}_{2m}(t)$, within the framework of the current Earth rotation models. This work is in progress and will be presented in a forthcoming communication.

Acknowledgements. This work has been partially supported by Spanish projects I+D+I, AYA2004-07970 and AYA2007-67546 and *Junta de Castilla y León* project VA070A07.

3. REFERENCES

Escapa, A., J. Getino and J. M. Ferrándiz, J. Geophys. Res. (Solid Earth), 106, 11387–11397, 2001.
Greiner-Mai, H., Jochmann, H. and Barthelmes, F., Phys. Earth Planet. Inter., 117, 81-93, 2000.
Greiner-Mai, H. and Barthelmes, F., Geophys. J. Int. , 144, 27-36, 2001.
Kinoshita, H., Hori, G. and Nakai, H., Ann. Tokyo Astron. Obs., Second Ser., 14, 14-35, 1974.

ESTIMATION OF THE TOPOGRAPHIC TORQUE AT THE CORE-MANTLE BOUNDARY ON NUTATION

M. FOLGUEIRA[1,2], V. DEHANT[3]
[1] Universidad Complutense de Madrid
Instituto de Astronomía y Geodesia, Facultad de Ciencias Matemáticas,
Universidad Complutense, ES-28040 Madrid, Spain
[2] SYRTE, Observatoire de Paris
61 avenue de l'Observatoire, F-75014 Paris, France
e-mail: martafl@mat.ucm.es
[1] Royal Observatory of Belgium
3 avenue Circulaire, B-1180 Brussels, Belgium
e-mail: v.dehant@oma.be

ABSTRACT. We study analytically the effect of the existence of CMB (core-mantle boundary) topography on the Earth's nutation. To that aim, we have considered an Earth model with a rigid mantle, a homogeneous and incompressible fluid core, and a slightly non-hydrostatic core-mantle boundary.

1. MOTIVATION AND RESEARCH DESIGN OF THE STUDY

This work is the first in a series of steps carrying out the progress of the European Descartes Sub-project entitled: *"Computation of the topographic coupling at the core-mantle boundary and its effect on the nutation"*. The principal milestones of the workplan and their specific objectives are as follows:

[1] Methodology and strategies to obtain the expressions for the topographic coupling:

- To establish the differential equations and boundary conditions describing the problem,
- To study the best analytical method for obtaining the solutions,
- To perform an analytical development of the coefficients describing the dynamic pressure, as function of parameters of the boundary topography,
- To determine the topographic torque.

[2] Comparison with the results from Wu and Wahr (1997) using a numerical technique.

[3] Application of the results to other celestial bodies of the solar system.

2. DIFFERENTIAL EQUATIONS AND PRELIMINARY RESULTS

In order to describe the diurnal wobbles or nutations of the Earth, we consider the Liouville equations for the angular momentum conservation. We have simplified the problem considering a rigid mantle and a homogeneous and incompressible fluid core. With the objective of computing the topographic torque, we have considered a slightly non-hydrostatic core-mantle boundary, from which we have computed the topographic torque. To that aim, we need to establish the equations and the boundary conditions.

- Linearized Navier-Stokes equation:

$$\frac{\partial \vec{V}}{\partial t} = -\frac{1}{\rho_f}\nabla P + \vec{b} - \vec{\omega}\times(\vec{\omega}\times\vec{r}) - 2\vec{\omega}\times\vec{V} - \frac{\partial\vec{\omega}}{\partial t}\times\vec{r} \quad (1)$$

where $\times$ indicates a cross-product, $\vec{V}$ is the velocity of the fluid relative to the reference frame, P is the Eulerian pressure and ρ_f is the fluid density. The body force $\vec{b} = \bigtriangledown\Phi_0 + \nabla\phi_1 + \nabla\phi_e$ (sum of the self unperturbed gravitational attraction $\nabla\Phi_0$, the mass redistribution gravitational attraction $\nabla\phi_1$, and the lunisolar gravitational attraction $\nabla\phi_e$ per unit mass).

- Boundary condition at the core-mantle boundary (CMB): $\vec{n}\cdot\vec{V}=0$ ($\vec{n}$ is the normal to the surface); it is expressed as a function of the boundary topography; the non-hydrostatic boundary surface is expressed using: $r=r_0\left[1+\sum_{n=1}\sum_{m=-n}^{n}\varepsilon_n^m Y_n^m(\vartheta,\lambda)\right]$ (r_0 is the surface mean radius)

- Condition of incompressibility: $\nabla\cdot\vec{V}=0$.

Wu and Wahr (1997) obtained the solutions of the differential equations (1), after extensive developments, using a numerical technique of integration. Our purpose here is to work out such integration by means of an analytical method in order to do a comparison between the two approaches. To this aim, we have decomposed the velocity as: $\vec{V}=\vec{u}+\vec{v}=\Omega\,L\,\vec{q}+\vec{v}$, where L is the maximum radius of the core, $\vec{v}$ is the Poincaré fluid velocity in the case of nutation and $\vec{q}$ is a non-dimensional velocity which equation and conditions can be expressed as:

$$\begin{cases} i\,\sigma_m\,\vec{q}+\,2\,\vec{\hat{z}}\times\vec{q}+\,\nabla\Phi\;=\;0 \\ \\ \nabla\cdot\vec{q}\;=\;0 \\ \\ \vec{n}\cdot\vec{q}+\,\Omega^{-1}\,L^{-1}\vec{n}\cdot\vec{v}\;=\;0 \end{cases} \tag{2}$$

where $\Phi=\frac{\phi}{\Omega^2\,L^2}$ and $\phi=\frac{p}{\rho_f}+\chi$, Φ being called the non-dimensional dynamic pressure and χ is an unspecified function. The time dependence of the variables is considered as $e^{i\sigma t}$. When introduced in non-dimensional equations as above, the frequency to be used is σ_m instead of σ, where $\sigma=\Omega\sigma_m$. After some algebra of the first equation of (2), one can obtain the following expression for $\vec{q}$ as a function of $\nabla\Phi$:

$$\vec{q}\;\;=\;\;\frac{-i\,\sigma_m}{4-\sigma_m^2}\left[\nabla\Phi\;-\;\frac{2}{i\,\sigma_m}\,\vec{\hat{z}}\times\nabla\Phi\;-\;\frac{4}{\sigma_m^2}\,(\vec{\hat{z}}\cdot\nabla\Phi)\,\vec{\hat{z}}\right]\quad\text{where:}\quad\Phi\;=\;\sum_{l=1}a_l^k\,P_{lk}(\frac{\sigma_m}{2})\,Y_l^k(\vartheta,\lambda) \tag{3}$$

where $\vec{\hat{z}}$ is the unit vector in the z-direction, $P_{lk}(\frac{\sigma_m}{2})$ and $Y_l^k(\vartheta,\lambda)$ are, respectively, the Legendre polynomials and the associated Legendre functions of the first kind.

Using the boundary condition for $\vec{q}$ (third equation of (2)) and the expression of $\vec{q}$ in function of Φ (Eq. (3)), after a lot of developments, one obtains the analytical expressions for the coefficients a_l^k at the first order in the small quantities such as ϵ_n^m. The preliminary results are shown in Table 1, where we have kept only the coefficients significantly higher than $0.1\epsilon_n^m$.

Coefficients	Term in m_f^+	Term in m_f^-
a_1^0	$0.4\,\epsilon_3^1$	
a_1^1	$0.3\,\epsilon_3^2$	
a_2^0	$-0.7\,\epsilon_2^1$	
a_2^{-1}	$-1.0\,\epsilon_2^0$	
a_2^2		$-0.2\,\epsilon_2^1$
a_3^0	$-3.5\,\epsilon_3^1$	
a_3^1	$0.2\,\epsilon_3^2$	$-0.6\,\epsilon_3^0$
a_3^2	$0.1\,\epsilon_3^3$	$-0.3\,\epsilon_3^1$
a_3^3		$0.04\,\epsilon_3^2$
a_4^0	$-0.3\,\epsilon_2^2$	$0.4\,\epsilon_2^0$
a_4^{-1}	$9.6\,\epsilon_2^0$	

Table 1. Analytical expressions for a_l^k in function of the parameters ϵ_n^m.

3. REFERENCE

Wu, X., Wahr, J.M., 1997, "Effects of non-hydrostatic core-mantle boundary topography and core dynamics on Earth rotation", Geophys. J. Int. 128(1), pp. 18–42.

CONSIDERATIONS ABOUT SOME PROBLEMS ON FUNCTIONAL PARAMETRICAL MODELS IMPLEMENTATION FROM A DISCRETE SET OF DATA

F.J. MARCO[1], J.A. LOPEZ[1], M.J. MARTINEZ[2]
[1] Universidad Jaume I, Dep. Matematicas, Castellon, Spain
e-mail: marco@mat.uji.es, lopez@mat.uji.es
[2] Universidad Politecnica de Valencia, Dep. Matematica Aplicada E.T.S.I.I, Valencia, Spain
e-mail: mjmartin@mat.upv.es

ABSTRACT. The least squares method is widely used in Fundamental Astronomy in the determination of some parameters that are usually coefficients of functional developments based on certain regularity hypothesis about the developed function. This hypothesis of regularity in the working domain, together with the spatial distribution of the discrete data and their statistical properties should be carefully treated if we want to obtain reliable results. The use of a kernel based method is shown as a robust procedure and allows to generalize, in numerical terms, the usual least-squares statistical treatment.

1. PROBLEMS INVOLVING PARAMETRICAL ADJUSTMENT FOR BIASED DATA

Given α_i, δ_i, Z_i be a set of n discrete values on the celestial sphere. A parametrical adjustment is given by the search of such c_k that $Z_i = \sum_k c_k \Phi_k(\alpha_i, \delta_i)$ for functions Φ_k. Some aspects of the problem are: The points α_i, δ_i, are homogeneously distributed on the celestial sphere (other case can be similarly considered using an estimation of the density function from the discrete data), Z_i are the random variable values of Z. Z is also the function, searched as an adjustment, this will require some hypothesis (usually, the supposition of a integrable square on the sphere) The discrete distribution of Z_i values is determined by its mean and variance. The residual $R = Z - \sum_k c_k \Phi_k$ is also understood as random variable as well as a function. With two random variables Z_i and Y_j over the same set α_i, δ_i, the search of the $Z_i = \sum_k c_k \Phi_k(\alpha_i, \delta_i)$, $Y_i = \sum_k d_k \Psi_k(\alpha_i, \delta_i)$ developments can be done with the same considerations that before. Another possibility is to suppose $c_k = d_k$ for a given reordenation of the Φ_k, Ψ_k basis. This case does not exclude the individual studies, but the basis functions will be different in each case. We shall use pairs $\Delta\alpha cos\delta$, $\Delta\delta$ or $\Delta\mu_\alpha cos\delta$, $\Delta\mu_\delta$ where Δ represents the differences in α, δ or in the proper motions $\mu_\alpha cos\delta$, μ_δ for two different catalogues. Provided the usual regularity hypothesis, there are spherical harmonics developments for each of the individual variables-functions. Analogously, it is possible to suppose a priori that the variables are related in pairs by means of infinitesimal rotations or spins, respectively. We use the same notation for the random variables and the function. The existence of infinitesimal rotations (or spins) should be compatible with the analytical and statistical properties for each variable-function considered. We are going now to deal with the functional and the statistical adjustment. They both are related to the most general least squares method: Given a function Z, which is defined in the unity sphere and has integrable square, then it may be developed in spherical harmonics. In practice, the series should be truncated up to an order m through the minimization problem $\left\| Z - \sum_{k=0}^{m} c_k \Phi_k \right\|_2^2 = \frac{1}{4\pi} \int_{S^2} \left[Z - \sum_{k=0}^{m} c_k \Phi_k \right]^2 d\sigma$, where the inner product is the usual in $L^2(S^2)$, and $c_k = (Z, Y_k)_2 / (Y_k, Y_k)_2$ is $c_k = (Z, Y_k)_2$ in case of normalized basis. To notice the analogies with the statistical treatment, let us take the development in order zero whose coefficient is $c_0 = \int_{S^2} Z d\sigma$ which coincides with the mathematical expectation of Z (as a random variable). The harmonics spherical adjustment requires as a necessary condition the computation of the mean of the random variable that minimizes its variance, because c_0 minimizes $\frac{1}{4\pi} \int_{S^2} [Z - c_0]^2 d\sigma = Var(Z)$. In other words: the least squares method is the one that purposes, among all the unbiased estimators, the one with least variance (Gauss-Markov Theorem). If we identify Z and $\sum_{k=0}^{n} c_k Y_k$ with their random variables, it is clear that $E[Z] = E\left[\sum_{k=0}^{n} c_k Y_k \right] = c_0$, in consequence, the adjustment function preserves

the mathematical expectation and minimizes the variance (among the estimators resulting from the truncation up to m-order). The natural generalization leads to the use of kernel non-parametrical models to obtain the regression of a random variable. In addition, it is also possible to consider a spatial distribution not necessary homogeneous, because the density functions are estimated by kernels. We are going to consider two problems involving parametrical adjustment for biased data. Problem 1: Let us take a lineal geometrical (GL) adjustment given by: $\Delta\alpha\cos\delta = \varepsilon_x\Phi_x + \varepsilon_y\Phi_y + \varepsilon_z\Phi_z$, $\Delta\delta = \varepsilon_x\Psi_x + \varepsilon_y\Psi_y$ then, $E[\Phi_x] = E[\Phi_y] = 0$, $E[\Phi_z] \neq 0$, $E[\Psi_x] = E[\Psi_y] = 0$ and $E[\Delta\alpha\cos\delta] = \varepsilon_z E[\Phi_z]$, $E[\Delta\delta] = 0$. To compute ε aiming to the second members to be estimators of least variance for the first, having into account that $r = \Delta\alpha\cos\delta - \sum\varepsilon_x\Phi_x$ (or $r = (\Delta\alpha\cos\delta)^2 + (\Delta\delta)^2$), the variance is $Var(r) = E\left[r^2\right] - (E[r])^2 = E\left[(\Delta\alpha\cos\delta - \sum\varepsilon_x\Phi_x)^2\right] - (E[\Delta\alpha\cos\delta] - \varepsilon_z E[\Phi_z])^2$ which has an extra term. The normal equations can not be the same, due to the existence of bias. The easiest way to solve this is the introduction of an auxiliary term in Right Ascension.
Problem 2: if the $\Delta\delta$ sample has bias, then the usual GL can not be used (if the sample is homogeneously distributed, then the computed values for the $E[\Psi]$ will be null). So, in practice, it is necessary to include an artificial term for this bias in order to generalize the GL model. The artificial terms included are null if there is no bias. Conclusion: if a random variable has bias, the adjustment should have this fact into account and it is absurd to consider an unbiased model with biased data. Several authors have not taken this fact into account and they have used unbiased models to adjust biased samples. The conclusions that they have reached are necessary wrong. Specially dealing with the rotations Hipparcos-FK5, the corrections of the parameters for the Luni-solar precession and the (fictitious) motion of the Equinox.

2. AUXILIARY USE OF THE NON PARAMETRICAL ADJUSTMENT FOR THE COMPUTATION OF THE PARAMETERS

We shall consider a one-dimensional distribution X. Its generalization in the sphere may be seen in (Marco et al., 2004, A&A 418) Let $x_1, ..., x_n$ be points, and $K(x)$ a function that is no negative in $[-1, 1]$, null in the rest and with integral the unity. Let $h_x > 0$, we define $f_h(x) = \frac{1}{nh_x}\sum_{i=1}^{n} K\left(\frac{x-x_i}{h_x}\right)$ as an estimation of the density of the random variable X. (About the criteria to choose h_x, see for example Simonoff, 1996, "Smoothing Methods in Statistics", Springer Verlag). Consider a bidimensional distribution $(x_1, y_1), ..., (x_n, y_n)$. A regression function, may be defined as $m(x) = E[Y|X = x] = \int_D y\frac{f(x,y)}{f(x)}dy$. If we approximate the joint and marginal densities by means of K, then we obtain: $m(x) = \frac{1}{nh_x}\sum_{i=1}^{n} y_i K\left(\frac{x-x_i}{h_x}\right)$.
Let us consider the minimization of $\frac{1}{nh_x}\int_D (y-m)^2 f_h(x)dx$ where $m = m(x)$ is the expectation of Y conditioned to $X = x$. The optimum m provides the previous expression; also, when obtaining m, the variance minimized is that of Y. So, it is natural the application of a non parametrical adjustment with the same properties than the parametrical (no bias for the definition of m, minimal variance due to the employed method). There is an extra advantage: we have a function defined over the whole domain (the celestial sphere) which preserves the statistical of the discrete data without making hypothesis about the geometrical properties of the function to be adjusted. If, for example, we denote as Ξ the (continuous) non parametrical adjustment for the $\Delta\mu_\alpha cos\delta$ data and we suppose that the function to adjust can be developed in spherical harmonics, then the coefficient of the normalized harmonics Y_i, is computed as the inner product (Ξ, Y_i) which should be discretised. Other important case is the computation of the rotations or the spins. We denote as Π the non parametrical adjustment for $\Delta\mu_\delta$, their bias is computed as $(\Pi, 1)$ and this value is independent of any model. This procedure has been used in the non parametrical adjustment for $\Delta\mu_\alpha cos\delta$ and $\Delta\mu_\delta$, and we have searched spins plus bias adjustment, through the conjunct minimization of $(\Delta\mu_\alpha cos\delta - Model)^2 + (\Delta\mu_\delta - Model)^2$. The obtained values for the bias coincide with the initial sample and the inducted values inducted for the spins unbiased by the bias and the biased spins coincide with the values obtained through products with spherical harmonics We conclude the existence of a total compatibility with the amplified geometrical model when there is bias. This is the case of the Luni-Solar precession and the fictitious Equinox motion. The consideration of bias in the model explains the discrepancies in the values of precession and Equinox motion much better than the models that do not consider bias.

Acknowledgements. Part of this work was supported by a grant P1-1B2006-11 from Fundacio Caixa Castello BANCAIXA.

NON-RIGID EARTH ROTATION SERIES

V.V. PASHKEVICH
Central (Pulkovo) Astronomical Observatory of Russian Academy of Science
Pulkovskoe Shosse 65/1,196140, St. Petersburg, Russia
e-mail: pashvladvit@yandex.ru

SUMMARY

The last years a lot of attempts to derive a high-precision theory of the non-rigid Earth rotation was carried out. For these purposes the different transfer functions are used. Usually these transfer functions are applied to the series representing the nutation in longitude and in obliquity of the rigid Earth rotation with respect to the ecliptic of date. The aim of this investigation is a construction of the new high-precision non-rigid Earth rotation series (SN9000), dynamically adequate to the DE404/LE404 ephemeris over 2000 years, which are expressed as a function of Euler angles ψ, θ and ϕ with respect to the fixed ecliptic plane and equinox J2000.0. *The early stages of the previous investigation:* 1. The high-precision numerical solution of the rigid Earth rotation have been constructed (V.V.Pashkevich, G.I.Eroshkin and A.Brzezinski, 2004), (V.V.Pashkevich and G.I.Eroshkin, Proceedings of Journees 2004). The initial conditions have been calculated from SMART97 (P.Bretagnon, G.Francou, P.Rocher, J.L.Simon,1998). The discrepancies between the numerical solution and the semi-analytical solution SMART97 were obtained in Euler angles over 2000 years with one-day spacing. 2. Investigation of the discrepancies is carried out by the least squares and by the spectral analysis algorithms (V.V.Pashkevich and G.I.Eroshkin, Proceedings of Journees 2005). The high-precision rigid Earth rotation series S9000 are determined (V.V.Pashkevich and G.I.Eroshkin, 2005). *The next stage of this investigation:* 3. The new high-precision non-rigid Earth rotation series (SN9000), which are expressed as a function of Euler angles, are constructed by using the method (P.Bretagnon, P.M.Mathews, J.-L.Simon: 1999) and the transfer function MHB2002 (Mathews, P. M., Herring, T. A., and Buffett B. A., 2002).

CONCLUSIONS

1. The exact expressions for the algorithm of Bretagnon et al. (1999) are obtained. 2. The new semi-analytical solution of the non-rigid Earth rotation SMN (SMART97 + MHB2002) is derived. 3. The high-precision non-rigid Earth rotation series SN9000, which are expressed as functions of Euler angles and are dynamically adequate to the ephemeris DE404/LE404 over 2000 years, are constructed. The geophysical models of SMN and SN9000 solutions includes the same effects that model MHB2002. The discrepancies between S9000 and SN9000 minus discrepancies between SMART97 and SMN for the Newtonian case (Dynamical case) and for the relativistic one (Kinematical case) depicted in Figure 1. *The comments to Figure 1:* Kinematical solution of the rigid Earth rotation= Dynamical solution of the rigid Earth rotation + Geodetics corrections; Dynamical solution of the non-rigid Earth rotation= Dynamical solution of the rigid Earth rotation + Transfer function; Kinematical solution of the non-rigid Earth rotation (SMN) = Dynamical solution of the non-rigid Earth rotation (SMN) + Geodetics corrections; Kinematical solution of the non-rigid Earth rotation (SN9000)= Kinematical solution of the rigid Earth rotation (S9000) + Transfer function.

Acknowledgements. The author highly appreciates for very useful discussions with Prof. A. Brzeziński. The investigation was carried out at the Central (Pulkovo) Astronomical Observatory of the Russian Academy of Sciences and at the Space Research Centre of Polish Academy of Science, under a financial support of the Cooperation between Russian and Polish Academies of Sciences, Theme No 31.

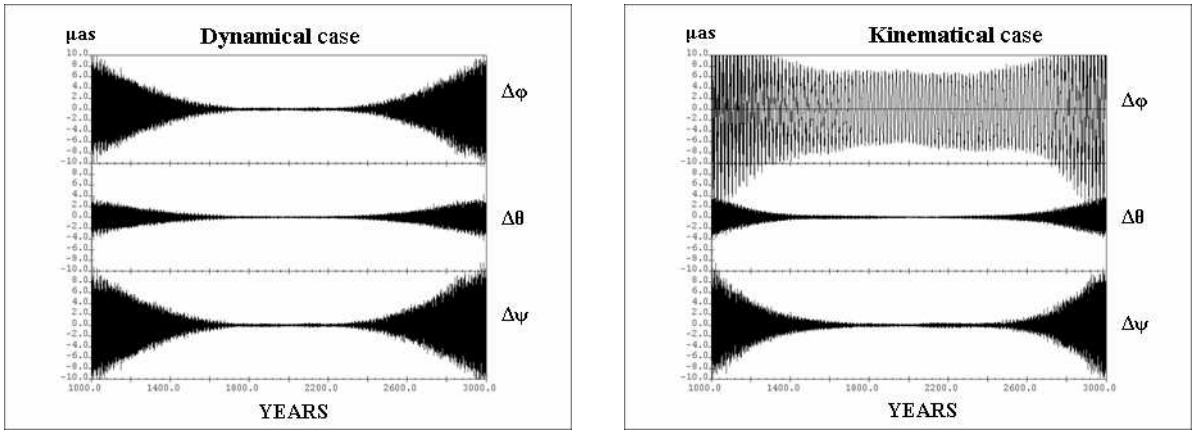

Figure 1: The discrepancies between S9000 and SN9000 minus discrepancies between SMART97 and SMN.

REFERENCES

Bretagnon, P., Francou, G., Rocher P., Simon J.L., 1998, "SMART97: A new solution for the rotation of the rigid Earth", Astron. Astrophys. , 329, pp. 329–338.

Bretagnon, P., Mathews, P.M.,Simon, J.-L., 1999, "Non Rigid Earth Rotation", in Proc. of Journees 1999: Motion of Celestial Bodies, Astrometry and Astronomical Reference Frames Les Journees 1999 & IX. Lohrmann - Kolloquium, (Dresden, 13-15 September 1999), pP. 73–76.

Mathews, P. M., Herring, T. A., and Buffett B. A., 2002, "Modeling of nutation and precession: New nutation series for nonrigid Earth and insights into the Earth's Interior", J. Geophys. Res., 107, B4, 10.1029/2001JB000390.

Pashkevich, V.V., Eroshkin, G.I. and Brzezinski, A., 2004, "Numerical analysis of the rigid Earth rotation with the quadruple precision", Artificial Satellites, Vol. 39, No. 4, Warszawa, pp. 291–304.

Pashkevich, V.V. and Eroshkin, G.I., 2004, "Spectral analysis of the numerical theory of the rigid Earth rotation", in Proc. of Journees 2004: Fundamental Astronomy: New concepts and models for high accuracy observations (Observatoire de Paris, 20-22 September 2004.), pp. 82–87.

Pashkevich, V.V. and Eroshkin, G.I., 2005, "Choice of the optimal spectral analysis scheme for the investigation of the Earth rotation problem", in Proc. of Journees 2005: Earth dynamics and reference systems: five years after the adoption of the IAU 2000 Resolutions (Space Research Centre of Polish Academy of Sciences, Warsaw, Poland, 19-21 September 2005), pp. 105–109.

Pashkevich, V.V. and Eroshkin, G.I., 2005, "Application of the spectral analysis for the mathematical modelling of the rigid Earth rotation", Artificial Satellites, Vol. 40, No. 4, Warszawa, pp. 251–260.

ANALYTICAL THEORY FOR THE MOTION OF AN ASTEROID IN THE GRAVITATIONAL FIELD OF A MIGRATING PLANET

I.V. TUPIKOVA
Lohrmann Observatory, TU Dresden Germany
01062 Germany, Dresden, Mommsenstr 13
e-mail: irina.tupikova@googlemail.com

ABSTRACT. A new perturbation method for the determination of proper elements of an asteroid in the gravitational field of a migrating planet is developed.

1. MIGRATION OF THE BIG PLANETS AND PERTURBATION THEORY

Planetary migration which, as is now widely accepted, had happened in the late stages of planetary formation (Fernadez & Ip 1984; Malhotra,1993), has forced the orbital resonances to sweep through a large region of the Solar system. Extremely time-consuming numerical simulations applied to a specifically formulated N-body problem (thousands of planetosimals with non-zero masses interact with the planets but not with each other) had strengthened the idea that some extraordinary orbital properties of Kuiper belt objects (including Pluto) are just a natural consequence of the migration of the big planets. On the other side, to follow the dynamical evolution of a concrete asteroid, it is sufficient to model the orbital migration of a perturbing planet with a time variation of its semi-major axis already gained from numerical simulations as was proposed in (Malhotra,1995):

$$a_b(t) = a_b^c - \Delta a_b \exp(-t/\tau)\,.$$

Here, a_b^c is the semi-major axis of the migrating planet at the current epoch, Δa_b is the migration interval over the total migration time τ. Being very simple, the implification of this formulae in classical perturbation techniques is really a challenge. First, the effect of migration introduces a non-standard time-dependence in the equations of the massless bodies; second, this effect is very small and acts over very long time spans which requires new standards for the orders of approximations and degrees of small parameters involved in the algorithm. It is also clear, that out of the two standard ways - successful integrations or canonical transformations - one should choose the second one in order not to suppress the migration effects by the artificial secular and mixed terms appearing in the first approach.

We have developed a special modification of the standard Lie-series based averaging procedure allowing to construct an analytical solution to the problem with an arbitrary migration law $a_b(t)$ in the absence of resonances, extendable to all successive approximations and to all degrees of eccentricities e, e_b and inclinations i, i_b.

To keep all the advantages of the Lie-series method, the scheme requires a canonical set of variables, for example, Delaunay elements (the final results have been transformed to non-singular elements) to keep the canonical form of the equations of motion. The chain of transformations induced by generating functions $W^{(k)}$ designed to eliminate successfully the angular variables transforms the initial system with Hamiltonian R into the systems with a new Hamiltonians $R^{(k)}$ with final averaged Hamiltonian depending only upon the action variables.

2. ELIMINATION OF MEAN ANOMALIES IN THE CASE OF A MIGRATING PLANET

In case of one perturbing planet migrating according to a prescribed low, the Hamiltonian R depends explicitly upon t only via the elements of the perturbing body L_b and $l_b = \int \bar{n}_b\, dt + l_b^0$ and expanding $W^{(1)}$ and $R^{(1)}$ in series of both the "natural" small parameter $\mu_b = \mathcal{M}_b/\mathcal{M}_{\rm Sun}$ and the small parameter induced by the slow migration rate $\varepsilon_b = \dot{a}_b/(a_b\,\bar{n}b)$, the solution can be found in a successive way through

$$\left(-\bar{n}\frac{\partial}{\partial l} - \bar{n}_b\frac{\partial}{\partial l_b} -\right) W_{j,0}^{(1)} + r_j = R_j^{(1)}, \quad \left(-\bar{n}\frac{\partial}{\partial l} - \bar{n}_b\frac{\partial}{\partial l_b}\right) W_{j,k+1}^{(1)} - \dot{a}_b\frac{\partial}{\partial a_b} W_{j,k}^{(1)} = 0,$$

allowing to find all the components of $W_{j,k}^{(1)}$ after having chosen the parts of the averaged Hamiltonian $R_j^{(1)}$. The first component $W_{j,0}$ corresponds to the standard solution of the Hamilton-Jacobi equation without migration.

3. ELIMINATION OF LONGITUDES OF PERIHELION AND NODE IN THE CASE OF A MIGRATING PLANET

After elimination of mean anomalies from the equations of asteroid motion, as new secular part of the lowest order Hamiltonian, supporting the elimination of long-periodic terms, we may only choose

$$R_0^{(1)} = -K + \mu_b \left(A\, e^2 + B\, s^2\right)$$

with coefficients A and B depending upon the semi-major axes, and K being conjugate to t. Even in the case without migration, one is confronted with some series problems. First, the rest of the Hamiltonian has μ_b as coefficient; this implies that this small parameter cannot support the further transformations and as new ones we are forced to consider the eccentricities and inclinations of the bodies involved. Every term of the form $e^{k1}\, s^{k2}\, e_b^{k3}\, s_b^{k4}$ should now be considered as a term of order $k = k1+k2+k3+k4$ in a small parameter ε representing e, e_b, s, s_b. This crucial point distinguishing the perturbation theory methods in the gravitational N-body problem from those of satellite problems has really been underestimated in celestial mechanics. Second, the Poisson bracket (a core operation of the algorithm) involves the derivatives w.r.t. e and $s = \sin i/2$, and that means, that with every approximation some (but not all) terms will loose the degree in small parameter. As a consequence, to get a solution correct up to a certain degree in ε , a different number of approximations are needed for different terms. Third, the part of the new Hamiltonian of second order results not only from secular terms, but also from some periodical terms which have to be considered separately. These second-order terms present in the case without migration a simplified case of Lagrange's secular solution which is principally limited to terms of second order, not only in the secular part of the perturbing function, but also in the Lagrange equations. Looking for an algorithm extendable to any desired degree and keeping in mind, that the Lagrange secular solution doesn't exist in case of migrating planets, we have developed an explicit algorithm based completely on the Lie-transform method. The solution has been realized with two simple transformations subsequently eliminating the longitudes of node and perihelia. For the first transformation, one may consider as secular part $R_0^{(1)} = \mu_b\, B\, s^2$, and then choose the according generating function as being dependent only upon h to hence remove the longitude of node from the problem. The elimination of the longitude of perihelion will be then realized with the choice $R_0^{(1)} = \mu_b\, A\, e^2$ (Tupikova, 2007). Due to the presence of D'Alembert characteristics, both of these two transformations converge formally, but some terms keep the same order of magnitude for a number of approximations (while not reducing their order) and then increase their order with step 2. To be sure that the solution has been obtained rigorously up to a given order, we have to divide all the terms in the development of the perturbing function into special "order groups" and then trace the magnitude of every term during the successive approximations. The migration effects have been treated in the way discussed above.

4. PRECISION OF THE ALGORITHM

To check the precision of the algorithm, we have chosen some "bad" terms in the Kaula-type expansion of R that converge extremely slowly and eliminated all the periodical perturbations up to 8th order. As a result, we have computed analytically the "proper" elements of an asteroid for 10^9 years from the values of the "osculating" elements gained from the numerical integration of the differential equations considering only these "bad terms". In spite of all the theoretical difficulties involved, in the absence of resonances the proper elements keep remarkably constant values.

5. REFERENCES

Fernandez, J.A., Ip, W.H., 1984, Icarus, 58, pp.109-120.
Malhotra, R.,1993, Nature, 365, 819-821.
Malhotra, R.,1995, AJ , 110, pp.420-429.
Tupikova, I.,2007, in Anal. Meth. of Cel. Mech. July 8-12, Saint-Petersburg, Russia (to be publ.)

THE USE OF LLR OBSERVATIONS (1969-2006) FOR THE DETERMINATION OF THE CELESTIAL COORDINATES OF THE POLE

W. ZERHOUNI, N. CAPITAINE, G. FRANCOU
Observatoire de Paris
Syrte, 61 Avenue de l'Observatoire 75014 Paris
e-mail: wassila.zerhouni@obspm.fr, nicole.capitaine@obspm.fr, gerard.francou@obspm.fr

ABSTRACT. Analysis of Lunar Laser ranging observations allows to determine a number of parameters related to the dynamics of the Earth-Moon system. It also contributes to the determination of the Earth Orientation Parameters (EOP) such as precession-nutation, polar motion and UT1. Here, we focus on the determination of the precession-nutation corrections DX, DY to the conventional model for the coordinates of the CIP (Celestial Intermediate Pole) in the GCRS (Geocentric Celestial Reference System), which are used in this study, instead of the classical parameters determined in previous works.

1. INTRODUCTION

The Lunar Laser Ranging technique consists in determining the round-trip travel time of light pulses between a transmitter on the Earth and reflectors on the surface of the Moon. The actual observational data consists of 'normal points' built on the number of detected photons in the interval of the observations.
This technique has many applications in various domains including astronomy, lunar science, geodynamics, and gravitational physics. In the field of geodynamics, it defines intrinsically a dynamical system. It allows in particular the positioning of the dynamical mean ecliptic of J2000.0 with respect to the CIP (Celestial Intermediate Pole) and to the GCRS (Geocentric Celestial Reference System) using this transformation (for more details, see for example the IERS conventions or Capitaine et al. 2003) :

$$[CRS] = Q.R.W[TRS]$$

Q : is the matrix transformation for the motion of the CIP in the celestial system (X,Y),

$$Q = \begin{pmatrix} 1 - aX^2 & -aXY & X \\ -aXY & 1 - aY^2 & Y \\ -X & -Y & 1 - a(X^2 + Y^2) \end{pmatrix} .R_3(s)$$

R : is the matrix transformation for the Earth rotation,

$$R = R_3(-ERA)$$

W : is the matrix transformation for the polar motion in the ITRS (International Terrestrial Reference System),

$$W = R_3(-s')R_2(x_p)R_1(y_p).$$

2. CALCULATION AND RESULTS

In a first step, we have calculated the LLR residuals for (i) McDonald station during the period of 1969 to 2006 and (ii) CERGA station during the period of 1984 to 2005, using the P03 precession of Capitaine et al. (2003) as the model for precession and the MHB 2000 of Mathews et al. 2002 for the nutation. The residuals from MacDonald are represented on Fig 1. We note that the residuals have been improved from 1m in 1972 to 0.2 m in 2001. Then, in the bottom of this figure, we can note a degradation of the residuals since the end of 2001, due probably to instrumental errors.

In a second step, we made a new analysis with fitting the X, Y parameters (Celestial Pole coordinates). The preliminary results of the fitting and the formal errors are represented on Fig 2.

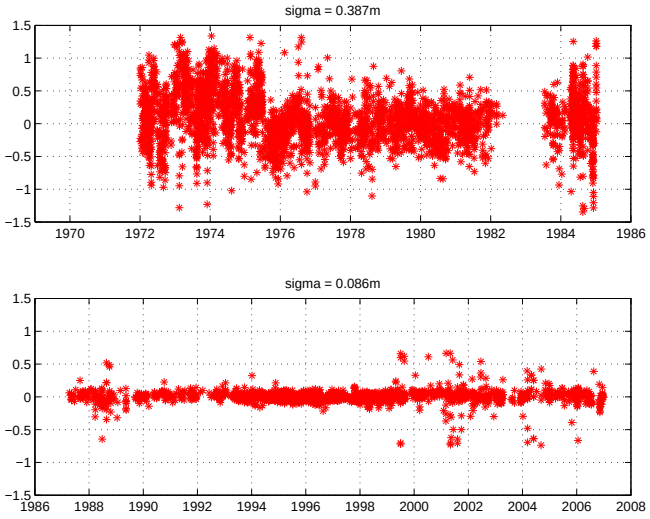

Figure 1: Residuals (in meters) from MacDonald LLR observations

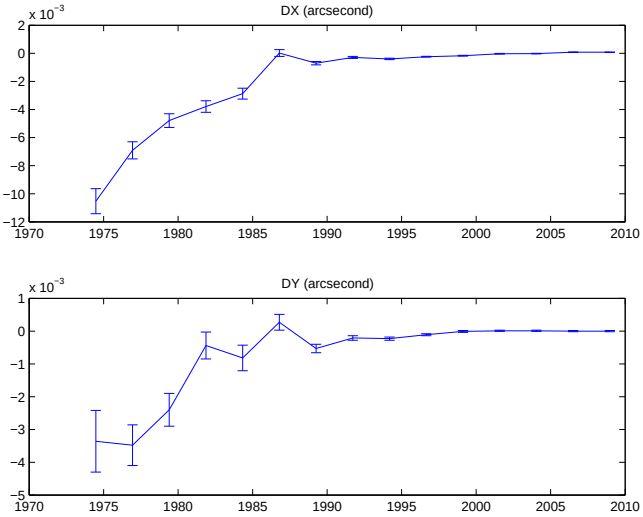

Figure 2: Corrections DX, DY to the conventional model at J2000.0

Each point represents the correction to DX, DY from the beginning of the observations until the date of the observation at that point. We note the improvement of the fitting since 1990 because the period of observation become longer and the observations more precise.
In this preliminary study, we have derived the celestial coordinates of the CIP (Celestial Intermediate Pole) at J2000.0 from LLR observations spanning the period 1969-2006. In a further study, we will use such determinations at appropriate intervals for deriving corrections to the precession-nutation model.

3. REFERENCES

Capitaine, N. et al., 2003, "Expressions for IAU 2000 precession quantities", A&A, 412, pp. 567-586.
Chapront, J. et al., 2002, "A new determination of lunar orbital parameters, precession constant and tidal acceleration from LLR measurements", A&A, 387, pp. 700-709.
Mathews, P. et al., 2002, "Modeling of nutation and precession: New nutation series for nonrigid Earth and insights into the Earth's interior", Geophys.Res, 107(B4), doi: 10.1029/2001JB00390.
McCarthy, D., IERS Technical Note 21: IERS Conventions (1996).

Session III

RELATIVITY IN FUNDAMENTAL ASTRONOMY

RELATIVITÉ EN ASTRONOMIE FONDAMENTALE

RELATIVITY IN FUNDAMENTAL ASTRONOMY: SOLVED AND UNSOLVED PROBLEMS

S.A. KLIONER
Lohrmann Observatory,
Dresden Technical University, 01062 Dresden, Germany
e-mail: Sergei.Klioner@tu-dresden.de

ABSTRACT. Nowadays it is no longer necessary to justify the importance of consistent relativistic modelling in the field of fundamental astronomy. Although in the last 20 years the theoretical foundations of relativistic modelling have been elaborated with a lot of care, there are a number of issues, mostly of practical character, that still require both theoretical discussions and practical implementations. These 'gray' areas of the modelling include modelling of rotational motion of celestial bodies, correct inclusion of multipole structure of the bodies in the translational equations of motion, interplay between numerical accuracy and analytical "order of magnitude" of various relativistic terms, relativistic scaling of astronomical quantities and units of measurements. An overview of the relativistic issues in the field of fundamental astronomy is given here from this critical point of view.

1. INTRODUCTION

The field of applied relativity has emerged about 40 years ago, when the growing accuracy of observations and the new observational techniques (like, radar ranging) have made it necessary to take relativistic effects into account on a routine basis. Since that time, applied relativity has evolved into one of the basic ingredients of fundamental astronomy, the discipline that includes celestial mechanics, astrometry, time scales and time dissemination etc. On the one hand, that development required significant theoretical efforts. Triggered also by the needs of applications at an engineering level, special theoretical techniques have been developed to construct the so-called local reference system (like GCRS) and to derived the equations of translational and rotational motion of a system of N bodies having arbitrary composition and shape. On the other hand, astronomers and engineers had to re-think and to re-formulate their problems in a language compatible with general relativity. The need to change the way of thinking from Newtonian "common sense" to relativistic is probably the source of many of the difficulties that non-experts have with relativity. In the same time the relativity itself is quite simple and elegant at least in the post-Newtonian approximation.

It seems to be natural and advantageous to review the status of applied relativity from time to time, and clearly formulate problems which we can consider as well understood and "solved" and also those problems which we have to classify open ones. Previous attempts to formulate unsolved problems in the field of celestial mechanics (including relativistic celestial mechanics) were undertaken by Brumberg & Kovalevsky (1986) and Seidelmann (1986). This short review is by no means intended to serve as a full update of those publications, but represents just a step in that direction.

2. THE IAU 2000 FRAMEWORK

The IAU 2000 framework for relativistic modelling (Soffel et al., 2003) represents a self-consistent theoretical scheme enabling one to model any kind of astronomical observations in the post-Newtonian approximation of general relativity. The framework has three main theoretical ingredients:

1. The theory of local reference systems (e.g. Geocentric Celestial Reference System, GCRS).
2. The post-Newtonian theory of multipole expansions of gravitational field.
3. Careful investigation of the orders of magnitude of various effects that has allowed to make the post-Newtonian reduction formulas for time scales as simple as possible.

The local reference systems have two fundamental properties:

A. The gravitational field of external bodies (e.g. for GCRS all solar system bodies expect the Earth) is represented only in the form of a relativistic tidal potential which is at least of second order in the local spatial coordinates and coincides with the usual Newtonian tidal potential in the Newtonian limit.

B. The internal gravitational field of the subsystem (e.g. the Earth for the GCRS) coincides with the gravitational field of a corresponding isolated source provided that the tidal influence of the external matter is neglected.

These two properties guarantee that the coordinate description of the local physical processes in the vicinity of the considered body (e.g. in the vicinity of the Earth in the case of GCRS) is as close as possible to the physical character of those processes. This means, for example, that if some relativistic effect is present in the coordinates (e.g., of a satellite of that body) the effect cannot be eliminated by selecting some other ("more suitable") coordinates and therefore has physical character.

It should be noted that although only one local reference system – GCRS – is defined by the IAU 2000 framework explicitly, the framework foresees GCRS-like local reference systems for each solar system body for which the local physics (e.g. the structure of the gravitational field and the theory of rotational motion) should be precisely formulated. For example, modelling of LLR data requires a local Celenocentric Celestial Reference System. Recent projects aimed at precise modelling of the rotational motions of Mercury and Mars will have to use the corresponding reference system for Mercury and Mars, respectively. All these local systems are defined by the same formulas as those given in the IAU 2000 framework for the GCRS, but with index E interpreted as referring to the corresponding body.

Moreover, a local reference system defined by the same IAU 2000 formulas, but constructed for a massless observer (with index E referring to a fictitious "body" of mass zero), is suitable to describe physical phenomena in the vicinity of that observer and, in particular, to define measurable quantities (observables) produced by that observer. The relation between this point of view and several standard ways to describe observables in general relativity is described by Klioner (2004).

Let us also mention that the IAU 2000 framework by no means restricts the freedom to use any other reference systems for the analysis and modelling of various phenomena. In some toy models possessing some special symmetries it may be advantageous to reflect those symmetries directly in the choice of the coordinates. This could help to formulate the problem and its solution in a simpler way. If those other reference systems are defined correctly, one can always find a coordinate transformation between the IAU 2000 reference systems and those other reference systems. The IAU 2000 framework suggests a standard choice of the reference systems. That standard choice can be used by those who do not want to care about the relativistic formulation by themselves. On the other hand, the IAU 2000 framework is also a particular set of reference systems in which all results and parameters obtained by different groups can be compared and combined, even if those groups use different relativistic formulation in their work.

3. THE IAU 2000 FRAMEWORK AND PPN FORMALISM

The IAU 2000 framework has been formulated within Einstein's general relativity. On the other hand, it is clear that modern high-accuracy astronomical observations open one of the most important ways to test the validity of general relativity. Most of the best current estimates of many relativistic effects come from high-accuracy astrometry (Will, 2006). A popular way to quantitatively test general relativity in the post-Newtonian approximation is to estimate from observations numerical parameters in the models formulated in the so-called Parametrized Post-Newtonian (PPN) formalism (e.g., Will, 2003). The PPN formalism is a phenomenological scheme covering a broad class of possible theories of gravity in the weak-field slow-motion (post-Newtonian) approximation. Many metric theories of gravity were investigated by the authors of the PPN formalism and a generic form of the post-Newtonian metric tensor of a system of N bodies was derived. That PPN metric tensor is a generalization of the BCRS metric tensor given in the IAU 2000 framework and contains a number of numerical parameters. At least two such numerical parameters are well known in the astronomical community: β and γ. These parameters have been often determined from observations.

Two attempts to generalize the general-relativistic theory of local reference systems onto the PPN formalism were undertaken until now: Klioner & Soffel (2000) and Kopeikin & Vlasov (2004). Although the two investigations are based on similar ideas and partially agree with each other, some important

details were treated differently. Future investigations should clarify which approach is more adequate for practical modelling of observations.

4. WELL-UNDERSTOOD PROBLEMS

Before proceeding to unsolved problems, it seems to be appropriate to give a list of problem which can be considered as solved ones.

- *Post-Newtonian* relativistic reference systems. This includes the theory of both global and local reference systems in the framework of general relativity, relativistic time scales, time synchronization and dissemination.
- *Post-Newtonian* equations of motion for test particles and massive bodies having only masses and no further structure of the gravitational field (the so-called Einstein-Infeld-Hoffmann (EIH) equations).
- Multipole structure of the *post-Newtonian* gravitational field. The Blachet-Damour multipole moments are used also in the IAU 2000 framework and represent a physically adequate and convenient way to deal with gravitational fields of arbitrary structure in general relativity.
- *Post-Newtonian* equations of motion of bodies with multipole structure.
- *Post-Newtonian* equations of rotational motion.
- *Post-Newtonian* theory of light propagation.
- Some properties of the *post-post-Newtonian* effects, but by no means so detailed understanding as for the post-Newtonian approximation.

Although all these topics are very well investigated from the theoretical point of view, it does not mean that no difficulties in practical use of these results can occur. A number of known difficulties are discussed in Section 6 below.

5. UNSOLVED AND POORLY KNOWN ISSUES

Let us now give a list of problems are still unsolved.

- Embedding of the post-Newtonian BCRS in the cosmological background. This question could be important for the interpretation of high-accuracy observations (Gaia, VLBI, etc.). Although some efforts in this direction have been started, the problem is far from being solved.
- Post-post-Newtonian relativistic reference systems (especially, the post-post-Newtonian definition of local reference systems like the GCRS)
- Multipole structure of the post-post-Newtonian gravitational field. The Blanchet-Damour moments are defined only in the post-Newtonian approximation. No similar results in the post-post-Newtonian approximation are known.
- The post-post-Newtonian equations of motion for N-body system. The post-post-Newtonian equations of motion (and even higher-order ones) are only known for a system of 2 bodies.

On the other hand, it is clear that the last 3 topic are currently not very interesting from the practical point of view, the only application being binary and double pulsars. The situation can, however, change very quickly if such observational techniques as laser ranging between spacecrafts become operational. Such projects like Lisa and Astron may need the post-post-Newtonian equations of motion to predict the motion of drag-free spacecraft with required accuracy.

6. ISSUES REPRESENTING PRACTICAL DIFFICULTIES

The problems listed in Section 4 above can be considered as solved from the theoretical point of view. However some of them still represent a lot of difficulties for non-experts. Some other problems being well understood theoretically still wait for practical implementation in numerical calculations. Let us give some examples:

- Although the general form of the *post-Newtonian* equations of motion of bodies with multipole structure is well known, these equations have never been applied explicitly in their full complexity in a numerical code. Important applications here are modelling of the figure-figure interaction in the Earth-Moon system for LLR, the influence of the structure of the Earth's gravity on the motion of spacecrafts during the fly-by maneuvers, etc. An improvement of practical models is necessary here.

- Numerical calculations with the *post-Newtonian* equations of rotational motion are rather tricky. Although the equations themselves have been formulated about 15 years ago, the first numerical results have appeared only recently (Klioner, Soffel, & Le Poncin-Lafitte, 2007).

- Relativistic time scales as a part of the IAU 2000 framework are traditionally difficult to understand for "Newtonian-thinking people". These time scales are (1) TCB and TCG as coordinate times of BCRS and GCRS, respectively, as well as (2) TDB and TT as scaled versions of them (Soffel et al., 2003; IAU, 2006). Although the concept of a coordinate time is crystal clear for people trained in relativity, coordinate time scales may sometimes be very confusing for people using "Newtonian common sense". In the literature one can sometimes meet wrong statements about astronomical time scales. For example, the following statements are **wrong**: (a) TCB is the time in the barycenter of the solar system, (b) TCG is the time at the geocenter, (c) TT is the time on the rotating geoid, (d) an ideal clock put in these three locations would keep TCB, TCG and TT, respectively. A discussion of these and other issues concerning time scales can be found in (Brumberg, Kopeikin, 1990; Klioner, 2008).

- One more **wrong** statement about time scales is that for TDB no location could be found where an ideal clock would keep it. and that this implies some non-SI "TDB seconds". This statement is probably one of the main reasons to introduce "TDB units" in various documents describing astronomical reduction algorithms. Arguments why the scaling from TCB to TDB does not imply any change of units have been put forward by Klioner (2008). Additional discussions and educational efforts are necessary here to achieve a consensus.

Another group of difficulties is related to the fact that the mathematical techniques commonly in use in relativity and in fundamental astronomy are sometimes very different. One example of different mathematical languages in these two fields is the expression for the torque in the rotational equations of motion. The relativistic torque cannot be written in terms of Legendre polynomials and their derivatives as it is the case with the Newtonian torque. Special mathematical machinery of symmetric trace-free (STF) tensors should be used for the relativistic torque. The corresponding mathematical expression takes totally different form compared to the Legendre polynomials and this makes them difficult to understand for the astronomical community (see Klioner, Soffel & Le Poncin-Lafitte (2008) for further details).

Another example is related to analytical and numerical orders of magnitude. In typical calculations in relativity the terms are taken into account or dropped based on their analytical order of smallness with respect to c^{-1} (or in some cases with respect to the Newtonian gravitational constant G). For example, the post-Newtonian approximation consists in taking into account all terms in the equations of motion of the order of c^{-2} and neglecting all higher-order terms. On the other hand, for practical calculations we should be more interested in numerical magnitudes of various terms rather than in their analytical orders of smallness.

As an example of this controversy let us consider the post-post-Newtonian expression for the Shapiro delay (gravitational time retardation) in the gravitational field of one spherically symmetric body with mass M in the framework of an extended version of the PPN formalism. A light ray (a photon) is propagating from position $\mathbf{x}_0$ where it is situated at moment t_0 to another position $\mathbf{x}_1$. The goal is to find moment t_1 at which the light ray reaches $\mathbf{x}_1$. Denoting $m = \frac{GM}{c^2}$, $R = |\mathbf{x_1} - \mathbf{x}_0|$, $x_0 = |\mathbf{x}_0|$, and

$x_1 = |\mathbf{x}_1|$ one has (Klioner, Zschocke, 2007)

$$\begin{aligned} c\,(t_1 - t_0) \;\; = \;\; & R \;+\; (1+\gamma)\, m \,\log \frac{x + x_0 + R}{x + x_0 - R} \\ & + \frac{1}{8}\,\epsilon\,\frac{m^2}{R}\,\left(\frac{x_0^2 - x^2 - R^2}{x^2} \;+\; \frac{x^2 - x_0^2 - R^2}{x_0^2}\right) \\ & + \frac{1}{4}\,(8(1+\gamma) - 4\beta + 3\epsilon)\; m^2\,\frac{R}{|\mathbf{x}\times\mathbf{x}_0|}\,\arctan\,\frac{x^2 - x_0^2 + R^2}{2|\mathbf{x}\times\mathbf{x}_0|} \\ & - \frac{1}{4}\,(8(1+\gamma) - 4\beta + 3\epsilon)\; m^2\,\frac{R}{|\mathbf{x}\times\mathbf{x}_0|}\,\arctan\,\frac{x^2 - x_0^2 - R^2}{2|\mathbf{x}\times\mathbf{x}_0|} \\ & + \frac{1}{2}\,(1+\gamma)^2\, m^2\,\frac{R}{|\mathbf{x}\times\mathbf{x}_0|^2}\,(x - x_0 - R)\,(x - x_0 + R) + \mathcal{O}(c^{-6}), \end{aligned} \tag{1}$$

where β, γ and ϵ are three numerical parameters of the extended PPN formalism. All these three parameters are equal to unity in general relativity and may have different numerical values in other theories of gravity. The post-post-Newtonian terms can attain about 10 meters for experiments in the solar system and should be taken into account for high-accuracy data. We see that this expression is quite complicated compared to the usual post-Newtonian one given by the first line of (1). However, if one estimates the numerical magnitudes of the post-post-Newtonian terms in (1) it turns out that only the last term is numerically relevant. The last term can be written together with the main post-Newtonian term in a compact way

$$c\,(t_1 - t_0) = R \;+\; (1+\gamma)\; m \;\log \frac{x + x_0 + R + (1+\gamma)\, m}{x + x_0 - R + (1+\gamma)\, m}\,. \tag{2}$$

All other post-post-Newtonian terms together can be estimated as

$$c\,\delta\, t_1 \le \frac{m^2}{d}\;\left(\frac{3}{4} + \frac{15}{4}\,\pi\right)\,. \tag{3}$$

where d is the impact parameter of the light ray with respect to the gravitating body. Since $d \ge L$, L being the radius of the body, one concludes that for any solar system experiments Eq. (3) gives at most 4 cm for a Sun-grazing ray. These terms can therefore be neglected for all present and planned experiments. Eq. (2) coincides with Eq. (8-54) of Moyer (2000) who derived this equations in a different and inconsistent way.

7. CONCLUSION

Applied relativity is a multidisciplinary research field. Progress here requires dedicated efforts both from the side of theoretical work and from the side of practical implementation of relativistic concepts and ideas into every-day astronomical practice. It is clearly a challenge to combine knowledge in theoretical general relativity and in practical observational techniques and modelling of complex astronomical phenomena (e.g. Earth rotation). For this reasons, one often fuzzily divides scientists into "experts in relativity" and "people doing practical calculations". For the former kind of people it is quite difficult to understand what the second kind of people really need for their work. Vice verse, for "practical people" it is not always easy to understand what the "theorists" suggest. Clearly, educational efforts on both sides are indispensable for further progress in the field of applied relativity.

8. REFERENCES

Brumberg, V.A., Kopejkin, S.A. 1990, "Relativistic time scales in the solar system", Cel.Mech.dyn.Astron., 48, 23

Brumberg, V.A., Kovalevsky, J., 1986, "Unsolved Problems of Celestial Mechanics" Cel.Mech. 39, 133

IAU, 2006, "Re-definition of Barycentric Dynamical Time, TDB", Resolution adopted by the XXVIth General Assembly

Klioner, S.A., 2004, "Physically adequate proper reference system of a test observer and relativistic description of the GAIA attitude", Phys.Rev. D 69, 124001

Klioner, S.A., 2008, "Relativistic scaling of astronomical quantities and the system of astronomical units", A&A , forthcoming
Klioner, S.A., Soffel, M., 2000, "Relativistic celestial mechanics with PPN parameters", Phys.Rev.D 62, 024019
Klioner, S.A., Soffel, M., Le Poncin-Lafitte, Ch., 2008, "Towards the relativistic theory of precession and nutation", this volume
Klioner, S.A., Zschocke, S., 2008, "Parametrized post-post-Newtonian analytical solution for light propagation", available from Gaia Livelink archive as GAIA-CA-TN-LO-SK-002-1, to be published in Classical and Quantum Gravity
Kopeikin, S., Vlasov, I., 2004, "Parametrized post-Newtonian theory of reference frames, multipolar expansions and equations of motion in the N-body problem", Physics Reports, 400, 209
Moyer, T.D., 2000, "Formulation for Observed and Computed Values of Deep Space Network Data Types for Navigation", Jet Propulsion Laboratory, California Institute of Technology
Seidelmann, P.K., 1986, "Unsolved Problems of Celestial Mechanics – The Solar System" Cel.Mech. 39, 141
Soffel, M. et al., 2003, "The IAU 2000 resolutions for astrometry, celestial mechanics and metrology in the relativistic framework: explanatory supplement", AJ , 126, 2687–2706
Will, C.M., 1993, Theory and experiment in gravitational physics (Cambridge: Cambridge University Press)
Will, C.M., 2006, "The Confrontation between General Relativity and Experiment", Living Review Relativity 9, 3, http://www.livingreviews.org/lrr

LOCAL TESTS OF GR AND REFERENCE FRAMES LINKING WITH GAIA ASTROMETRY OF ASTEROIDS

D. HESTROFFER[1], S. MOURET[1], J. BERTHIER[1], F. MIGNARD[2], P. TANGA[2]
[1] IMCCE, Observatoire de Paris, CNRS,
77 Av. Denfert-Rochereau, 75014 PARIS, France
e-mail: Hestroffer@imcce.fr
[2] Cassiopée, Observatoire de la Côte d'Azur, CNRS
06000 Nice, France

ABSTRACT. The Gaia satellite, an ESA cornerstone mission to be launched at the end of the year 2011, will observe a large number of celestial bodies including also small bodies of the solar system (mainly near-Earth objects and main-belt asteroids). The scanning telescope will observe all objects brighter than magnitude $V \leq 20$ providing, over the 5 years mission, high precision photometry and astrometry with an unprecedented accuracy ranging roughly from ≈ 0.3 to 3 milli-arcsecond on the CCD level, and depending on the target's magnitude. In addition, several hundreds of QSOs directly observed by Gaia will provide the kinematically non-rotating reference frame in the visible light, resulting in the construction of a 'Gaia-ICRF'. The positions of the asteroids hence enable to relate the dynamical reference frame as defined by the equations of motions to the kinematic one, and to further check the non-rotating consistency between both frames definition. Here we show the results of a variance analysis obtained from a realistic simulation of observations for such link. The simulation takes into account the time sequences and geometry of the observations that are particular to Gaia observations of solar system objects, as well as the instrument sensitivity and photon noise. Additionally, we show the achievable precision for the determination of a possible time variation of the gravitational constant $\dot{G}/G$. Taking into account the non-completeness of the actually known population of NEOs, we also give updated values for the nominal precision of the joint determination of the solar quadrupole J_2 and PPN parameter β. Comparison to the results obtained from other techniques is also given.

1. AN OVERVIEW

The Gaia mission is a cornerstone mission of the ESA Horizon 2000+ program. This next generation space astrometry mission will overcome the already important results achieved by the Hipparcos satellite's observations, or enabled by the Hipparcos/Tycho astrometric catalogues. Gaia will be launched at the end of 2011 and will have a 5 years lifetime. Although its main objective is to observe stars (3D Census of our Milky-Way), Gaia will also detect and observe a large number of 'secondary' sources: the distant quasars, and the closer solar system objects (SSOs). The bulk of solar systems objects will be made of the asteroids in the main belt (MBAs) and some additional but a good proportion of near-Earth objects (NEOs). Gaia is a survey satellite, not a pointing telescope, and is not specifically designed to observations of solar system objects; but its scanning law and limiting magnitude ($V \leq 20$) will allow good observations over 5 years of $\approx 300,000$ asteroids, a much larger sample than allowed by e.g. Hipparcos. One additional limitation is that the object should not be larger in size than ≈ 250 mas (Ceres and the Galilean satellites for instance will not get through the detection process). Also they will not be optimally observed if they move too fast: The CCD reading —in TDI mode— together with the particular windowing for telemetry-download are not adapted to the apparent motion of fast moving NEOs.

Nevertheless, there are many direct and indirect valuable scientific outputs from Gaia observations of

SSOs (e.g. Mignard et al., 2008): moderate imaging, radial velocity for calibration purpose, to accurate photometry and global astrometry. Here we will focus on what can be derived from the high accuracy astrometry of asteroids (varying between 0.3 and 3 mas, depending on the object magnitude) in terms of orbits improvement and small perturbative effects associated to these orbit 'measures'. These concern the positioning of the equinox and ecliptic in the optical-ICRS, and test of a possible net rotation between the two supposedly non-rotating frames (through a rotation $\mathbf{\Omega}$ and rotation rate $\mathbf{d\Omega/dt}$). It also concerns determination of asteroids mass (Mouret et al. 2007), test of GR from the perihelion precession (PPN β and solar J_2), and variation of the constant of gravity G. The fundamental relation that is fitted here, is a difference between observed and computed location on a great circle $\Delta\lambda = \lambda_o - \lambda_c = A.\mathbf{dC}$ linearized as mean of a small variation $\mathbf{dC}$ (correction to orbital elements, orbit perturbation from the model, different frame for the observed and computed value).

The general results of the variance analysis for the estimation of $\mathbf{dC}$ are given in Table 1. For further details and references the reader is referred to Hestroffer et al. (2008).

β	J_2	$\dot{G}/G$	$\mathbf{\Omega}$	$\mathbf{d\Omega/dt}$
–	–	year^{-1}	μas	μas/year
			$x-y-z$	$x-y-z$
5×10^{-4}	1×10^{-8}	2×10^{-12}	$5-5-14$	$1-1-5$

Table 1: Standard deviation for the various fitted parameters. The correlation between the solar quadrupole J_2 and the PPN parameter β can be as low as 0.11.

2. REFERENCES

Hestroffer D., Mouret S., Berthier J., Mignard F., and Tanga P., 2008. Reference frame linking and tests of GR with Gaia astrometry of asteroids. In: A Giant Step from Milli- to Micro-arcsecond Astrometry. Proceedings IAU Symposium No. 248, October 2008, Shanghai, China.

Mignard F., Cellino A., Muinonen K., Tanga P., Delbò M., DellOro A., Granvik M., Hestroffer D., Mouret S., Thuillot W., and Virtanen J., 2008. The Gaia Mission: Expected Applications to Asteroid Science. To appear in ASSL (E. Tedesco, ed.).

Mouret S., Hestroffer D., and Mignard F., 2007. Asteroid masses and improvement with Gaia. A&A 472, pp. 1017–1027, doi: 10.1051/0004-6361:20077479

GEODETIC RELATIVISTIC ROTATION OF THE SOLAR SYSTEM BODIES

G.I. EROSHKIN, V.V. PASHKEVICH
Central (Pulkovo) Astronomical Observatory of Russian Academy of Science
Pulkovskoe Shosse 65/1,196140, St. Petersburg, Russia
e-mailS: eroshkin@gao.spb.ru, pashvladvit@yandex.ru

ABSTRACT. The problem of the geodetic (relativistic) rotation of the major planets, the Moon, and the Sun is studied by using DE404/LE404 ephemeris. For each body the files of the ecliptical components of the vectors of the angular velocity of the geodetic rotation are determined over the time span from AD1000 to AD3000 with one day spacing. The most essential terms of the geodetic rotation are found by means of the least squares method and spectral analysis methods.

1. INTRODUCTION

In every relativistic ephemeris of the Sun, major planets, and the Moon the gravitational interaction is modeled by considering these bodies as non-rotating point masses. However, their geodetic (relativistic) rotation can be determined, as it will be shown here. In accordance with Landau and Lifshitz (1975), a geodetic rotation arises when a body, having non-zero moments of inertia, is orbiting in the Riemannian space of general relativity. It is the most essential relativistic component of the rotational motion of the Earth. A similar statement may be valid for other major bodies of the solar system. An ephemeris of the major bodies of the solar system, based on the relativistic equations of the orbital motion, contains data necessary for the calculation of the secular and periodic components of the vector of the angular velocity of the geodetic rotation of these bodies. It is well known that the vector of the angular velocity of the geodetic rotation of a body i is defined by the following expression

$$\bar{\sigma}_i = \frac{1}{c^2} \sum_{j \neq i} \frac{G m_j}{\left|\bar{R}_i - \bar{R}_j\right|^3} \left(\bar{R}_i - \bar{R}_j\right) \times \left(\frac{3}{2}\dot{\bar{R}}_i - 2\dot{\bar{R}}_j\right) .$$

Here c is the velocity of light; G is the gravitational constant; m_j is the mass of a body$j$; $\bar{R}_i,\ \dot{\bar{R}}_i, \bar{R}_j,\ \dot{\bar{R}}_j$ are the vectors of the barycentric position and velocity of bodies i and j. The symbol $\times$ means a vector product; the subscripts i and j correspond to the Sun, the major planets, and the Moon. Since the mass of the Sun is dominant in the solar system then the main part of $\bar{\sigma}_i$ for the major planets and the Moon is a result of the orbital motion of these bodies. It means that vector $\bar{\sigma}_i$ is almost orthogonal to the plane of the heliocentric orbit. For all planets (except Pluto) and the Moon the vectors $\bar{\sigma}_i$ are practically directed to the north pole of the ecliptic. The geodetic rotation of the Sun depends on the orbital motion of the major planets and the Moon. Only the component σ^Z, orthogonal to the plane of the fixed ecliptic J2000 is studied, because the geodetic rotation in the ecliptic plane is the most interesting phenomenon. For each body the file of the values of the ecliptical component σ^Z is formed over the time span from AD1000 to AD3000 with one day spacing. The secular and periodic components of the geodetic rotation vector are determined by means of the procedure which involves the least-squares method and spectral analysis methods. The result is presented in the form

$\sigma^Z = \sum_{k=0}^{6} \mathrm{T}^k \sum_{m=1} (A_{km} \sin\alpha_m + B_{km} \cos\alpha_m), \quad \alpha_m = \sum_{l=1}^{10} n_l \lambda_l$. The mean heliocentric longitudes of the planets $\lambda_1, \ldots, \lambda_9$ and the mean geocentric longitude of the Moon λ_{10} with respect to the fixed equinox J2000, adjusted to DE404/LE404 ephemeris, are taken from Brumberg and Bretagnon (2002). T means the Dynamical Barycentric Time (TDB) measured in thousand Julian years (tjy). The coefficients A_{km}, B_{km} are to be determined and n_l are some integer numbers. This procedure was earlier used by Pashkevich and Eroshkin (2005) for the construction of the high-precision semi-analytical series describing the rotation of the rigid Earth.

2. ANGULAR VELOCITY OF THE GEODETIC ROTATION

It is quite natural to begin with the determination of the components of the geodetic rotation of the Earth because its high-precision semi-analytical representation is elaborated by Brumberg and Bretagnon (2002). The values of the component σ^Z, orthogonal to the plane of the fixed ecliptic J2000, are calculated by means of DE404/LE404 ephemeris. As it was done in the paper of Bretagnon and co-authors (1998), the equatorial coordinate system of DE404/LE404 ephemeris is put to the fixed ecliptic and dynamical equinox J2000 in the result of two rotations: a rotation in the equator plane at the angle $-0".05294$ to the point of the dynamical equinox J2000 and the rotation at the angle $23°26'21".40928$ to the plane of the fixed ecliptic J2000.0. The behavior of the component σ^Z is depicted in Figure 1a.

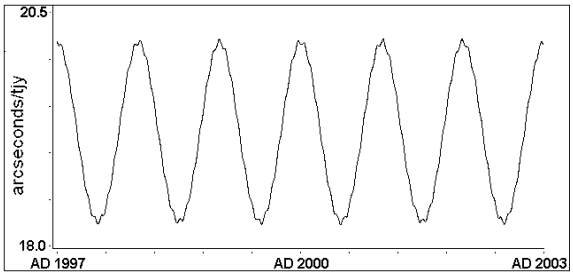

Figure 1a: σ^Z for the Earth (fragment)

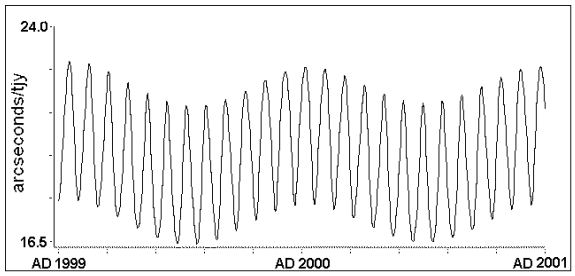

Figure 1b: σ^Z for the Moon (fragment)

In the result of processing 730500 data this component for the Earth is determined:

$$\sigma^Z = \{19".1988821 \ - \ 0".00017685\mathrm{T} + ... + 10^{-6}\dot{\lambda}_3\,[-34".285\cos\lambda_3 + 149".227\sin\lambda_3 + \\ +\mathrm{T}\,(-7".539\cos\lambda_3 - 5".682\sin\lambda_3) + \mathrm{T}^2\,(0".261\cos\lambda_3 - 0".291\sin\lambda_3) + ...] + \ ...\}\,/\mathrm{tjy}.$$

Here λ_3 is the mean longitude of the Earth, $\lambda_3 = 1.75347029148 + 6283.0758511455\,\mathrm{T}$. All symbols $\dot{\lambda}_i$ mean the time derivatives of the mean longitudes λ_i. From the paper of Brumberg and Bretagnon (2002) one can use the developments representing the geodetic rotation of the Earth in Euler angles for constructing the same component:

$$\sigma^Z_{BB} = \{19."19883018 - 0."00026965T + 10^{-6}\dot{\lambda}_3\,[(-34."28\cos\lambda_3 + 149."22\sin\lambda_3) + \\ +T\,(-7."54\cos\lambda_3 - 5."69\sin\lambda_3) + \ T^2\,(0."30\cos\lambda_3 - 0."29\sin\lambda_3)]\,\}\,/\mathrm{tjy}.$$

This result is essentially based upon the semi-analytical theory of the rigid Earth rotation SMART97 and the semi-analytical theory of the orbital motion of the major planets VSOP87 by Bretagnon and Francou (1988), while the results of the present paper are based upon DE404/LE404 numerical ephemeris. The remarkable difference in the coefficients of the secular term is explained by the different theories of the orbital motions. This statement is confirmed by the following. In the paper of Eroshkin and co-authors (2004) the high-precision numerical theory of the rigid Earth rotation, consistent to DE404/LE404 numerical ephemeris, was constructed. The results of the comparison of this theory with SMART97 theory are presented in the tables of the mentioned paper. By subtracting the coefficients of the dynamical solution from those of the kinematical solution the comparison of the geodetic rotation components, adequate to DE404/LE404 numerical ephemeris and SMART97 theory, is performed. In particular the difference in the secular term of the component $\sigma^Z$is calculated: $\Delta\sigma^Z = T0."00008611/\mathrm{tjy}$. This term is nearly equal to the difference between the secular terms in σ^Z and in σ^Z_{BB}. Taking into account also completely different methods of the determination of the coefficients of σ^Z and σ^Z_{BB}, one can state that they are in a good accordance. Thus the method of the determination of the geodetic rotation velocity vector is very accurate and effective. This method is applied to the other bodies of the solar system. The geodetic rotation of the Moon is determined not only by the Sun but also by the Earth. Figure 1b demonstrates it visually. Since Mercury is the nearest planet to the Sun then it is clear that its geodetic rotation has to be the most significant in the solar system. Some asymmetry in Figure 2a is explained by the relatively large eccentricity of the orbit of Mercury as compared to the other planet orbits (except Pluto's orbit). The sharp peaks of the curve correspond to Mercury's transits via perihelia. The behavior of the Pluto's component σ^Z depicted in Figure 2b is similar to that of Mercury, presented in Figure 2a. It is explained by the fact that the values of the eccentricities of the orbits of Pluto and Mercury are close to each other. There is no semi-analytical theory of the heliocentric motion of Pluto, nevertheless the mean heliocentric longitude of Pluto, with respect to the fixed equinox J2000.0, λ_9 is determined by the least squares method: $\lambda_9 = 0.2480488137 + 25.2270056856\mathrm{T}$.

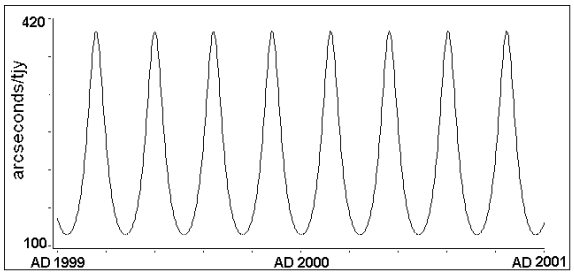

Figure 2a: σ^Z for Mercury (fragment)

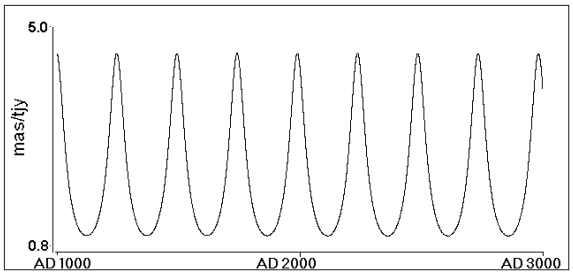

Figure 2b: σ^Z for Pluto

The geodetic rotation of the Sun arises when the Sun is orbiting relatively the barycentre of the solar system in the gravitational field of the major planets and the Moon. The vector of the geodetic rotation of the Sun is determined by the orbital motion of the planets. The axis of the angular velocity of the geodetic rotation is almost perpendicular to the plane of the ecliptic. Since the masses of the planets are essentially less than the mass of the Sun then the geodetic rotation of the Sun is very small. It is interesting to note that the periodic part of the vector $\bar{\sigma}$ for the Sun is determined not only by the motion of Jupiter, the heaviest planet, but also by that of Mercury, the nearest planet to the Sun, which has the largest mean motion.

Object	Secular part	Periodic part	Eccentricity of the orbit
Mercury	214".905T	$1086".273 \cdot 10^{-6} \sin\lambda_1 - 4882".196 \cdot 10^{-6} \cos\lambda_1$	0.206
Venus	43".124T	$-56".907 \cdot 10^{-6} \sin\lambda_2 - 64".182 \cdot 10^{-6} \cos\lambda_2$	0.007
the Earth	19".199T	$-34".285 \cdot 10^{-6} \sin\lambda_3 - 149".227 \cdot 10^{-6} \cos\lambda_3$	0.017
the Moon	19".495T	$-34".285 \cdot 10^{-6} \sin\lambda_3 - 149".227 \cdot 10^{-6} \cos\lambda_3$ $30".212 \cdot 10^{-6} \sin D$	
Mars	6".756T	$516".062 \cdot 10^{-6} \sin\lambda_4 \quad 229".326 \cdot 10^{-6} \cos\lambda_4$	0.093
Jupiter	0".312T	$82".830 \cdot 10^{-6} \sin\lambda_5 - 21".289 \cdot 10^{-6} \cos\lambda_5$	0.048
Saturn	0".069T	$-2".710 \cdot 10^{-6} \sin\lambda_6 - 53".014 \cdot 10^{-6} \cos\lambda_6$	0.056
Uranus	0".012T	$-22".280 \cdot 10^{-6} \sin\lambda_7 - 3".492 \cdot 10^{-6} \cos\lambda_7$	0.046
Neptune	0".004T	$1".847 \cdot 10^{-6} \sin\lambda_8 - 1".773 \cdot 10^{-6} \cos\lambda_8$	0.009
Pluto	0".002T	$57".447 \cdot 10^{-6} \sin\lambda_9 \quad 0".665 \cdot 10^{-6} \cos\lambda_9$	0.249
the Sun	0".001T	$6".226 \cdot 10^{-6} \sin\lambda_1 - 27".982 \cdot 10^{-6} \cos\lambda_1$ $55".823 \cdot 10^{-6} \sin\lambda_5 - 14".358 \cdot 10^{-6} \cos\lambda_5$	

Table 1: The main secular and periodic terms of the geodetic rotation

The angles of the geodetic rotation of the solar system bodies in the plane of the ecliptic are determined in the result of the analytical integration of the expression for the component σ^Z. The most essential secular and periodic terms are presented in Table 1. It is easy to see that the value of the secular part of the angle of the geodetic rotation of each planet depends on its distance from the Sun. The value of the periodic part depends on the distance from the Sun. It depends essentially on the eccentricity of the orbit. Mars and Pluto are examples of such dependence. The geodetic rotation of a planet varies when it moves in the eccentric orbit.

3. CONCLUSIONS

For the Sun and the superior planets (except Mars) the geodetic rotation is insignificant. Nevertheless in the case of the Sun it is rather interesting from the theoretical point of view. For the terrestrial planets and the Moon the geodetic rotation is considerable and has to be taken into account for the construction of the high-precision theories of the rotational motion. The geodetic rotation has to be taken into account if the influence of the dynamical figure of a body on its orbital-rotational motion is studied in the post-Newtonian approximation. In addition, the lunar laser range processing has to use the relativistic theory of the rotation of the Moon, as well as that of the Earth.

Acknowledgements. The investigation was carried out at the Central (Pulkovo) Astronomical Observatory of Russian Academy of Science and the Space Research Centre of Polish Academy of Science, under a financial support within the program of cooperation between Polish and Russian Academies of Sciences (Theme No.31).

4. REFERENCES

Bretagnon, P., Francou, G., 1988, "Planetary theories in rectangular and spherical variables", Astron. Astrophys., Vol. 202, pp. 309–315.

Bretagnon, P., Francou, G., Rocher P., Simon J.L., 1998, "SMART97: a new solution for the rotation of the rigid Earth", Astron. Astrophys., Vol. 329, pp. 329–338.

Brumberg, V.A., Bretagnon, P., 2000, "Kinematical Relativistic Corrections for Earths Rotation Parameters", Proc. of IAU Colloquium 180, eds. K. Johnston, D. McCarthy, B. Luzum, and G. Kaplan, U.S. Naval Observatory, pp. 293–302.

Eroshkin, G.I., Pashkevich, V.V., Brzezinski, A., 2004, "Numerical analysis of the rigid Earth rotation with the quadruple precision", Artificial Satellites, Vol. 39, No. 4, pp. 291–304.

Landau, L.D. and Lifshitz, E.M., 1975, "The Classical Theory of Fields", Oxford: Pergamon Press.

Pashkevich, V. V., Eroshkin, G. I., 2005, "Application of the spectral analysis for the mathematical modelling of the rigid Earth rotation", Artificial Satellites, Vol. 40, No. 4, pp. 251–259.

TOWARDS THE RELATIVISTIC THEORY OF PRECESSION AND NUTATION

S.A. KLIONER, M.H. SOFFEL, Ch. LE PONCIN-LAFITTE
Lohrmann Observatory,
Dresden Technical University, 01062 Dresden, Germany

ABSTRACT. A numerical theory of Earth rotation has been constructed using the post-Newtonian model of rigidly rotating multipole moments. The theory is constructed by numerical integration and treats all spectrum of relativistic issues in a consistent way: (1) relativistic times scales, (2) relativistic scaling of astronomical constants, (3) relativistic torques and (4) geodetic precession as an additional torque in the equations of rotational motion with respect to the kinematically non-rotating GCRS. In the quasi-Newtonian limit our theory reproduces SMART97 within the accuracy of the latter.

1. RELATIVITY AND EARTH ROTATION

Earth rotation is the only astronomical phenomenon which is observed with very high accuracy, but modelled in a Newtonian way. Although a number attempts to estimate and calculate the relativistic effects in Earth rotation have been undertaken (e.g., Bizouard et al., 1992; Brumberg & Simon, 2007 and reference therein) no consistent theory has appeared until now. As a result the calculations of different authors substantially differ from each other. Even the way geodetic precession/nutation is usually taken into account is just a first-order approximation and is not fully consistent with relativity (see below). On the other hand, the relativistic effects in Earth rotation are relatively large. For example, the geodetic precession ($1.9''$ per century) is about 3×10^{-4} of general precession. The geodetic nutation (up to 200 μas) is 200 times larger than the goal accuracy of modern theories of Earth rotation. One more reason to carefully investigate relativistic effects in Earth rotation is the fact that the geodynamical observations give important tests of general relativity (e.g., the best estimate of the PPN γ using large range of angular distances from the Sun comes from geodetic VLBI data) and it is dangerous to risk that these tests are biased bacause of relativistically flawed theory of Earth rotation.

The main goal of the project, the first results of which are presented below, is to develop a theory of Earth rotation fully compatible with the post-Newtonian approximation of general relativity. A new consistent and improved precession/nutation theory has first to be developed for the model of rigidly rotating multipoles described in Klioner et al. (2001). Here we consequently use the post-Newtonian definitions of the potential coefficients, tensor of inertia, dynamical equations in the GCRS and relativistic time scales. Besides, for the first time we apply a rigorous treatment of the geodetic precession and nutation.

2. RELATIVISTIC EQUATIONS OF EARTH ROTATION

The model which is used in this investigation was discussed and published by Klioner et al. (2001). Not going into physical details of the model let us summarize the model (T is TCG here):

$$\frac{d}{dT}\left(C^{ab}\,\omega^b\right) = \sum_{l=1}^{\infty}\frac{1}{l!}\,\varepsilon_{abc}\,M_{bL}\,G_{cL} + \varepsilon_{abc}\,\Omega^b_{\rm iner}\,C^{cd}\,\omega^d, \tag{1}$$

$$C^{ab} = P^{ac}\,P^{bd}\,\overline{C}^{cd}, \quad \overline{C}^{cd} = \text{const} \tag{2}$$

$$M_{a_1a_2\ldots a_l} = P^{a_1b_1}\,P^{a_2b_2}\ldots P^{a_lb_l}\,\overline{M}_{b_1b_2\ldots b_l}, \quad \overline{M}_{b_1b_2\ldots b_l} = \text{const}, \quad l \geq 2, \tag{3}$$

where the angular velocity of the Earth is assumed to be related to the orthogonal matrix $P^{ab}(T)$ as

$$\omega^a = \frac{1}{2}\,\varepsilon_{abs}\,P^{db}(T)\,\frac{d}{dT}\,P^{dc}(T), \tag{4}$$

and $\Omega^a_{\rm iner}(T)$ is the angular velocity of geodetic precession and nutation (e.g., Klioner et al. 2001). Here $\overline{C}^{cd}$ is the constant tensor of inertia of the Earth and $\overline{M}_{b_1 b_2 \ldots b_l}$ is the constant multipole moments of gravitational field field of the Earth. The model given above assumes that both the tensor of inertia and the multipole moments rotate rigidly (that is, it is assumed that all the time-dependence of them is given by one and the same orthogonal matrix $P^{db}(T)$). The relativistic torque is described by a set of tidal multiple moments G_L that is given explicitly by Eqs. (19)–(23) of Klioner et al. (2001).

As discussed by Klioner et al. (2001) there is a number of assumptions in the model (1)–(4). These assumptions, being formal ones, lead to a system of differential equations (1) very similar to those of Newtonian rigid body as described, for example, by Bretagnon et al. (1997,1998). These assumptions will be relaxed at a later stage of the work which will be devoted to the effects of non-rigidity of the Earth.

3. RELATIVISTIC DEFINITIONS OF THE ANGLES

One of the tricky points is the relativistic definition of the angles describing the Earth orientation. Exactly as Bretagnon et al. (1997,1998) we first define the rotated BCRS coordinates (x, y, z) by two constant rotations of the BCRS as realized by the JPL's DE403:

$$\begin{pmatrix} x \\ y \\ z \end{pmatrix} = R_x(23^\circ 26' 21.40928'')\, R_z(-0.05294'') \begin{pmatrix} x \\ y \\ z \end{pmatrix}_{\rm DE403} \tag{5}$$

Then the IAU 2000 transformations between BCRS and GCRS are applied to the coordinates (t, x, y, z), t being TCB, to get the corresponding spatially rotated GCRS coordinates (T, X, Y, Z). The spatial coordinates (X, Y, Z) are then rotated to get the spatial coordinates of the terrestrial reference system (ξ, η, ζ):

$$\begin{pmatrix} \xi \\ \eta \\ \zeta \end{pmatrix} = R_z(\phi)\, R_x(\omega)\, R_z(\psi) \begin{pmatrix} X \\ Y \\ Z \end{pmatrix} \tag{6}$$

Angles ϕ, ψ and ω are then used to parametrize the orthogonal matrix P^{ab} and therefore, to define the orientation of the Earth orientation in the GCRS. The meaning of the terrestrial system (ξ, η, ζ) here is the same as in Bretagnon et al. (1997): this is the reference system in which we define the harmonic expansion of the gravitational field with standard values of the coefficients C_{lm} and S_{lm}.

4. OVERVIEW OF THE NUMERICAL CODE

A numerical integration code has been written in Fortran 95. The software is carefully coded to avoid numerical instabilities and excessive round-off errors. Two numerical integrators with dense output – ODEX and Adams-Bashforth-Moulton multistep integrator – are built into the code. These two integrators can be used to control each other. The integrations are automatically performed in two directions – forth and back – that allows one to directly estimate the accuracy of integration. The code is able to use any type of arithmetic available with a given current hardware and compiler. For a number of operations, which have been identified as precision-critical, one has the possibility to use either the library FMLIB (Smith, 2001) for arbitrary-precision arithmetic or an ad hoc code using two double-precision numbers to implement quadrupole-precision arithmetic. The Fortran code for operations with STF tensors have been automatically generated by a specially designed computer-algebraic program in *Mathematica*. Our current baseline is to use ODEX with 80 bit arithmetic. The estimated errors of numerical integrations after 150 years of integration are below 0.001 μas. The performance of the code in this set-up is about 7 seconds for one year of integration on a typical personal computer.

Several relativistic issues have been incorporated into the code: (1) the full post-Newtonian torque using the STF tensor machinery, (2) rigorous treatment of geodetic precession/nutation as an additional torque in the equations of motion, (3) rigorous treatment of time scales (any of four time scales - TT, TDB, TCB or TCG - can be used as the independent variable of the equations of motion (although TT is certainly preferable from the physical point of view), (4) correct relativistic scaling of constants and parameters (e.g., the mass parameter GM of the Earth compatible with TT is not compatible with TDB). In order to test our code and the STF-tensor formulation of the torque we have coded also the

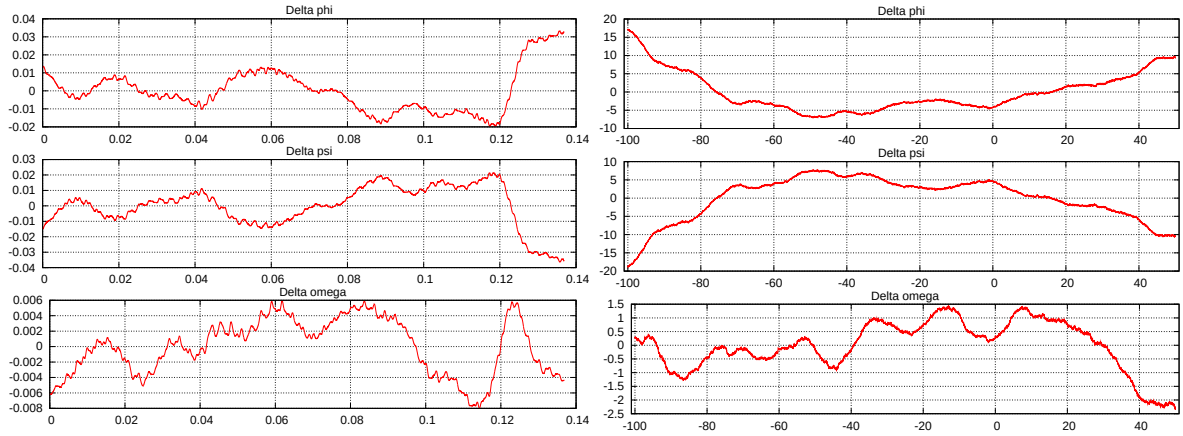

Figure 1: The differences in μas between the three angles ϕ, ψ and ω resulted from our numerical integrations and the full series of SMART97 for 50 days (left pane) and 150 years (right pane). The horizontal axes give time from J2000 in years. The curves on these plot closely repeat those on Figs. 3 and 4 of Bretagnon et al. (1998).

classical Newtonian torque with Legendre polynomials as described by Bretagnon et al. (1997, 1998) and integrated our equations for 150 years with these two torque algorithms. Maximal deviations between these two integrations was 0.0004 μas for ϕ, 0.0001 μas for ψ, and 0.0002 μas for ω. This demonstrates both the equivalence of the two formulations and the correctness of our code.

5. REPRODUCTION OF SMART97

As the first step, we have repeated the Newtonian dynamical solution of SMART97 using the Newtonian torque, the JPL ephemeris DE403 and the same initial values as in Bretagnon et al. (1997, 1998). Jean-Louis Simon (2007) has provided us with the unpublished full version of SMART97 (involving about 70000 Poisson terms for each of the three angles). We have calculated the differences between that full SMART97 series and our numerical integration. Detrended differences are shown on Fig. 1. A comparison of these differences and those given on Figs. 3–4 of Bretagnon et al. (1998) shows that we have succeeded to repeat SMART97 within the full accuracy of the latter.

6. THE EFFECT OF THE POST-NEWTONIAN TORQUE

In order to investigate the influence of the post-Newtonian torque in Eq. (1) as compared to the usual Newtonian torque, we have integrated the equations with the post-Newtonian and Newtonian torques and compared the results. The same initial conditions that we used to reconstruct the SMART97 solution were used for both integrations. Our results show that the post-Newtonian torque influences both precession and nutation. The effects in nutation are very small: the main effect is a correction to the main 18.6 year nutation term with the amplitude of 0.6 μas for ϕ and ψ and 0.4 μas for ω. This is very close to the estimates given by Bizouard et al. (1992). Besides that, secular or long-periodic terms appear in ϕ and ψ. A fit for the 150 years of integrations gives

$$\Delta\phi = 0.46 + 1492.85\,t - 8008.63\,t^2 + \ldots \quad (7)$$

$$\Delta\psi = -0.49 - 1560.82\,t - 5.53\,t^2 + \ldots \quad (8)$$

$$\Delta\omega = -0.22 - 0.31\,t - 6.22\,t^2 + \ldots\ . \quad (9)$$

Here the angles are given in μas and t in thousand years from J2000. It is clear that on the interval of only 150 years it is not possible to distinguish between long-periodic and secular terms. Longer integrations for the full range of JPL's DE404 showed that, as one can expect, the effect is a mixture of long-periodic and polynomial terms. The linear drift of $\Delta\psi$ given above is, however, close to that appearing for 6000 years of integration. Details will be published elsewhere.

7. GEODETIC PRECESSION/NUTATION AS AN ADDITIONAL TORQUE

In the framework of our model (1)–(4) geodetic precession and nutation are taken into account in a natural way by including the additional torque proportional to $\Omega^a_{\rm iner}$ in the equations of rotational motion. This additional torque reflects the fact that the GCRS of the IAU is defined to be kinematically non-rotating (see, Soffel et al. 2003). This way to account for geodetic precession is more consistent than the way used previously by a number of authors: (1) solving the Newtonian equations of rotation as if these were the equations in the dynamically non-rotating version of the GCRS and (2) adding the precomputed geodetic precession/nutation. The second step is fully correct since the geodetic precession/nutation is by definition the rotation between the kinematically and dynamically non-rotating versions of the GCRS and it can be precomputed since it is fully independent of the Earth rotation. The inconsistency of the first step comes from the fact that in the computation of the Newtonian torque the coordinates of the solar system bodies are taken from an ephemeris constructed in the BCRS. However, the dynamically non-rotating version of the GCRS *rotates* relative to the BCRS with the angular velocity $\Omega^a_{\rm iner}(T)$. It means that the BCRS coordinates of solar system bodies should be first rotated into "dynamically non-rotating coordinates" and only after that rotation those coordinates can be used to compute the Newtonian torque. Loosely speaking one can say that in order to have better consistency the arguments of the Newtonian solution (e.g., the dynamical solution of SMART97) should be corrected for geodetic precession/nutation. It is, however, clear that it is much more consistent and much simpler to consider the geodetic effects as an additional torque as we do in this work. Comparison of the results of numerical integrations with the geodetic torque and the kinematical solution of SMART97 shows the differences that are in well agreement with the scheme depicted above and amount to up to 200 μas after 100 years of integration.

8. FURTHER STEPS

The preliminary results of our project have to be improved in several directions. First, the model of rigidly rotating multipoles has to be completed. We have to (1) clarify the meaning of the initial conditions for the angles and their derivatives in the relativistic context (this implies a clear distinction between quantities defined in kinematically and dynamically non-rotating coordinates), (2) find meaningful values of the moments of inertia $\mathcal{A}$, $\mathcal{B}$ and $\mathcal{C}$ in the relativistic context. After that the non-rigidity of the Earth should be treated.

Acknowledgements. We are grateful to J.-L. Simon who has provided us with the full version of SMART97 theory and also answered our numerous questions concerning SMART97 and its constants.

9. REFERENCES

Bizouard C., Schastok, J., Soffel M.H., Souchay J., (1992) "Étude de la rotation de la Terre dans le cadre de la relativité général: premiere approche", In: *Journées 1992*, N. Capitaine (ed.), Observatoire de Paris, 76–84

Brumberg, V.A., Simon, J.-L., 2007, "Relativistic Extension of the SMART Earth's rotation theory and the ITRS-GCRS relationship", Notes scientifique et techniques de l'insitut de méchanique céleste, S088

Bretagnon, P., Francou, G., Rocher, P., Simon, J.L., 1997, "Theory of the rotation of the rigid Earth", A&A , 319, 305–317

Bretagnon, P., Francou, G., Rocher, P., Simon, J.L., 1998, "SMART97: a new solution for the rotation of the rigid Earth", A&A , 329, 329–338

Klioner, S.A., Soffel, M., Xu. C., Wu, X., 2001, "Earth's rotation in the framework of general relativity: rigid multipole moments", In: Influence of geophysics, time and space reference frames on Earth rotation studies (Proc. Journées' 2001), N. Capitaine (ed.), Paris Observatory, Paris, 232–238

Simon, J.L., 2007, private communication

Smith, D., 2001, "FMLIB", `http://myweb.lmu.edu/dmsmith/FMLIB.html`

Soffel, M. et al., 2003, "The IAU 2000 resolutions for astrometry, celestial mechanics and metrology in the relativistic framework: explanatory supplement", AJ , 126, 2687–2706

Session IV

PREDICTION, COMBINATION AND GEOPHYSICAL INTERPRETATION OF EARTH ORIENTATION PARAMETERS

PRÉDICTION, COMBINAISON ET INTERPRÉTATION GÉOPHYSIQUE DES PARAMÈTRES D'ORIENTATION DE LA TERRE

ACTIVITIES OF THE IERS WORKING GROUP ON PREDICTION

W. WOODEN
USNO Naval Observatory
3450 Massachusetts Avenue, N. W.
Washington, D. C. 20392, USA
e-mail: william.wooden@usno.navy.mil

ABSTRACT. The International Earth Rotation and Reference Systems Service (IERS) established a Working Group on Prediction (WGP) to investigate what IERS prediction products are useful to the user community in addition to making a detailed examination of the fundamental properties of the different input data sets and algorithms. The major goals and objectives of the WGP are to determine the desired Earth orientation prediction products, the importance of observational accuracy, which types of input data provide an optimal prediction, the strengths and weaknesses of various prediction algorithms, and the interactions between series and algorithms that are beneficial or harmful. To focus the research efforts of the WGP, the user community was polled to ascertain what prediction products are needed and at what level of accuracy. The current status of WGP activities and the anticipated future directions are presented.

1. INTRODUCTION

Earth orientation parameters (EOP), which provide the time-varying alignment of the Earth's terrestrial reference frame with respect to the celestial reference frame, are critical to modern navigation and space applications. EOP predictions are a necessity for real-time space applications such as Global Navigation Satellite Systems. The current IERS EOP prediction products, which were implemented more than 15 years ago, are generated by the IERS Rapid Service/Prediction Center (RS/PC) to provide data to real-time users and others needing highest quality EOP information sooner than that available in the final series published by the IERS Earth Orientation Center.

The Working Group on Prediction (WGP) was established to determine what can be done to improve the IERS prediction of Earth orientation. Specifically, the WGP was tasked to determine what prediction products are needed by the user community and to examine the fundamental properties of the different input data sets and algorithms (see IERS website http://www.iers.org/MainDisp.csl?pid=167-1100082). There are two areas of investigation: the input data (geodetic and geophysical information) and the algorithms used to process the data. The WGP establishment grew out of RS/PC concerns about the continued relevance of current products, new accuracy requirements, the impact of new data sets, and viable new prediction methodologies and the desire to build on the interest generated by the EOP Prediction Comparison Campaign of the Technology University of Vienna [IERS (2005), Kalarus *et al.* (2007)], and the efforts of the IERS Combination Pilot Project [IERS (2004)]. Another expectation of the RS/PC was a definitive assessment of the current state-of-the-art in EOP prediction.

2. GOALS AND OBJECTIVES

The goals and objectives of the WGP are the following:

1. Determine the desired EOP products - What is needed by the user community?
2. Determine the importance of the input data - What new data sets are available? Are data sets interchangeable? Are some inherently better?
3. Determine which types of input data create an optimal prediction - What is the noise of the series? What smoothing is best? What geophysical phenomena are being measured?
4. Determine the strengths and weaknesses of the prediction algorithms - Which algorithms perform best under what circumstances? How can problems be mitigated?

5. Determine the interactions between series and algorithms that are beneficial or harmful - What qualities of certain data sets make them well suited or poorly suited for certain algorithms?

3. CURRENT EOP PREDICTION ACCURACY

The RS/PC produces IERS Bulletin A and its associated standard and the daily rapid EOP data files. Bulletin A reports the latest determinations for polar motion (x,y), universal time (UT1-UTC), and the celestial pole offsets ($\delta\psi$, $\delta\epsilon$ and dx, dy) at daily intervals based on a combination of contributed rapid and preliminary analysis results using data from Very Long Baseline Interferometry (VLBI), Satellite Laser Ranging (SLR), and Global Positioning System (GPS) satellites. Predictions for variations a year into the future are also provided. Meteorological predictions of variations in Atmospheric Angular Momentum (AAM) are used to aid in the prediction of near-term UT1-UTC changes. The emphasis of the RS/PC is on near-term prediction (weeks) rather than long-term prediction (years) of EOP. Long-term stability and consistency with the other IERS products is achieved by aligning Bulletin A with the IERS final (Bulletin B) series, which is produced by the IERS Earth Orientation Center (EOC) at the Paris Observatory. Table 1 gives the prediction accuracies of the x- and y-components of polar motion and universal time from 2005 through the middle of 2007. Bulletin A values are compared with the final C04 results of the EOC. Additional information on the current IERS EOP prediction products is given by Stamatakos *et al.* (2007), Wooden *et al.* (2004), and the IERS Annual Reports [Dick and Richter,(2007)].

	2005				**2006**				**2007**		
Days in Future	PM-X (mas)	PM-Y (mas)	UT1-UTC (ms)	Days in Future	PM-X (mas)	PM-Y (mas)	UT1-UTC (ms)	Days in Future	PM-X (mas)	PM-Y (mas)	UT1-UTC (ms)
1	0.44	0.37	0.127	1	0.42	0.36	0.147	1	0.45	0.38	0.141
5	2.44	1.70	0.380	5	2.33	1.51	0.518	5	2.18	1.31	0.439
10	4.13	2.77	0.935	10	4.44	2.55	1.06	10	3.96	1.91	1.07
20	6.82	4.56	3.30	20	8.25	4.72	3.11	20	7.39	2.62	4.00
40	11.9	8.32	5.98	40	16.3	9.14	6.88	40	14.0	4.88	9.38
90	25.2	18.9	7.61	90	33.5	18.7	22.1	90	16.9	12.7	12.1

Table 1. Bulletin A prediction accuracies for polar motion (x-, y-components) and universal time (UT1-UTC).

4. EOP USER SURVEY

Given the variety of high-precision applications which need EOP predictions, the first task of the WGP was to determine whether the current products are adequate or whether modifications and/or improvements are necessary to meet more stringent requirements. Therefore, an easy-to-complete EOP user survey was developed by the WGP and posted on the IERS RS/PC website in order to address WGP goal #1. The IERS invited participation from those on the IERS mailing lists, those who receive RS/PC products, and any others thought to have an interest in EOP predictions. The first data call was issued in December 2006 and a second call went out in January 2007. The intent was to solicit information from current and potential users of EOP predictions to address the following questions and focus the WGP research effort:

1. Are the current IERS EOP prediction products, which were implemented more than 15 years ago, meeting the needs of the EOP user community.
2. Given the multitude of modern high accuracy applications, what characteristics of EOP predictions (type, accuracy, data spacing, data span, form, etc.) are required.

The survey form was designed to enable the WGP to determine who the major users of EOP information were. Specifically, were there different groups of users that had unique requirements or did all users have the same basic requirements? The survey began by asking some general information about the individual completing the survey. The intent was that if the individual had some specific recommendations that needed additional discussion, it would be easy to follow-up. Secondly, does the individual have a use for,

or anticipate a future use of IERS predictions? If the answer is positive, what information is needed to satisfy his/her requirements? We can then determine whether additional research is necessary to achieve the accuracies or timeliness needed. In addition we were interested in any specific improvements that might be recommended. Finally, the individual was asked to characterize the applications that utilize our predictions, *e.g.*, academic, engineering, operational, scientific, or other. The survey consisted of 10 questions that involved mostly checking boxes for a limited number of options. It was intended to be easy to complete and still provide enough characteristics to help the WGP determine where to focus its effort. The following figures summarize the results from the 71 surveys completed prior to 1 March 2007. Figure 1 shows the required accuracies for polar motion and universal time categorized by user application (indicated by different colors). The vertical axis represents the percentage of users in a given category and the horizontal axis shows the accuracy bins. Figure 2 shows the characteristics (prediction length, data spacing, update frequency, and formulation) of the predictions categorized by user application. Again, the vertical axis is the percentage of users categorized by application and the horizontal axis shows the options available for a given characteristic.

Figure 1. Required polar motion (in arc seconds) and universal time (in seconds) accuracies as a function of user application.

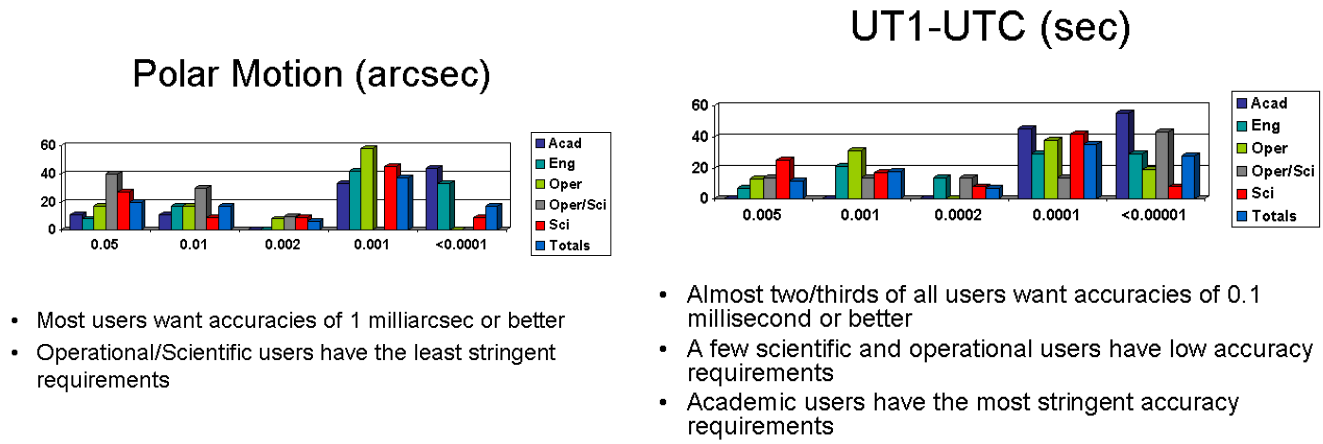

- Most users want accuracies of 1 milliarcsec or better
- Operational/Scientific users have the least stringent requirements

- Almost two/thirds of all users want accuracies of 0.1 millisecond or better
- A few scientific and operational users have low accuracy requirements
- Academic users have the most stringent accuracy requirements

The survey confirmed that there is a large group of operational users that need daily predictions, tabular data, one-day spacing, and predictions up to 30 days. Each category of user has different needs. Although some users would like to improve long term predictions, and while it is an interesting problem, the terms of reference under which the IERS RS/PC operates has been reconfirmed by the survey results. However, there is a need for increased accuracy and the efforts of the WGP to examine algorithms and incorporate potential new sources of data appears to address that need. In addition there seems to be a growing interest in daily and sub-daily predictions which require more timely measurements of EOP quantities and some increased processing capability.

5. PLANNING CONSIDERATIONS

The second task of the WGP is to examine the fundamental properties of the different input data sets and algorithms. To facilitate this task the WGP consists of two subgroups: one to examine the input data sets and another to examine the algorithms used for doing the prediction. Input data sets used for EOP determination come from geodetic sources such as VLBI, SLR, and GPS and also from geophysical sources such as AAM. Additional data sets are available as a result of recent geophysical research in the modeling of the oceans and the hydrological cycle. The earliest prediction algorithms for EOP were very simplistic but over the years have gotten more complex as measurements have become more precise.

Figure 2: Desired characteristics of the predictions as a function of user application.

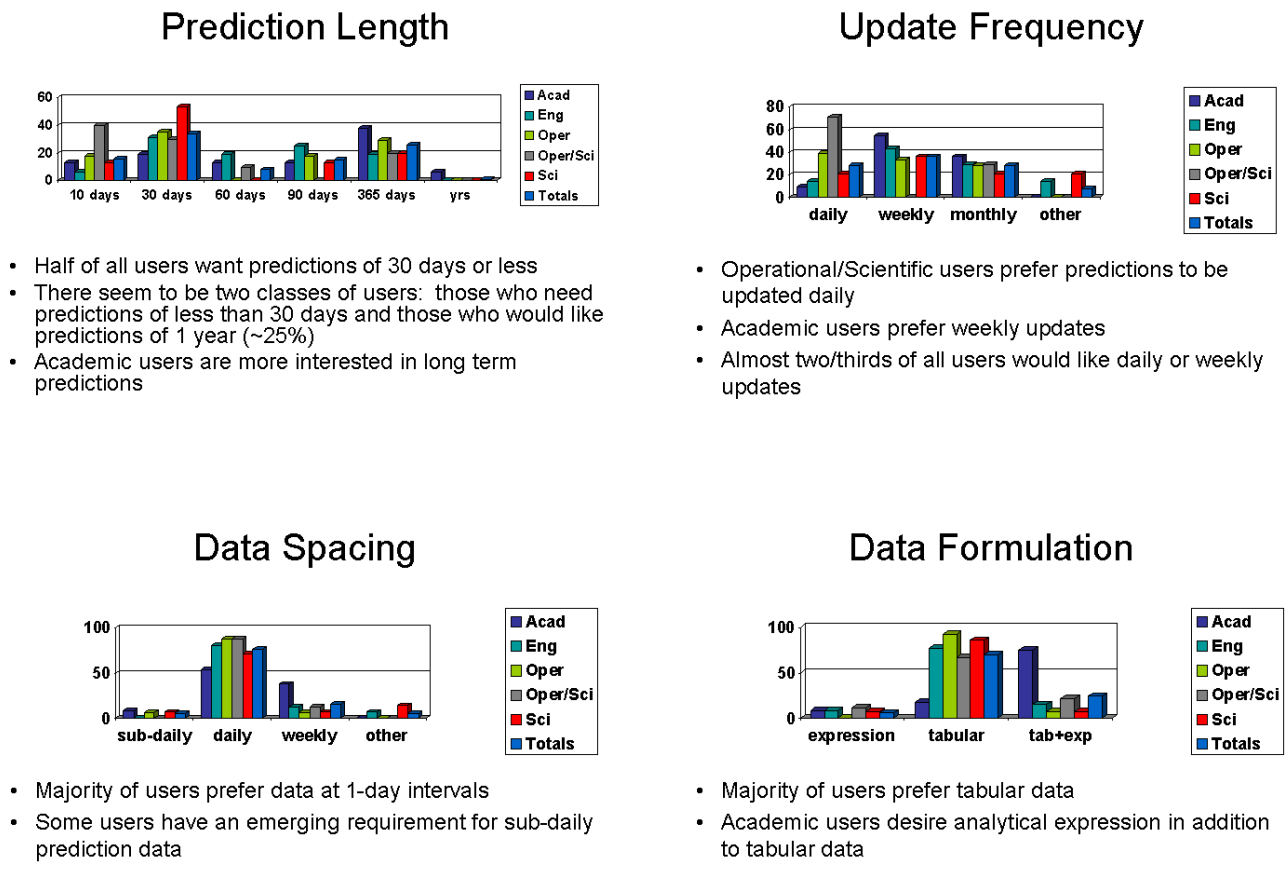

- Half of all users want predictions of 30 days or less
- There seem to be two classes of users: those who need predictions of less than 30 days and those who would like predictions of 1 year (~25%)
- Academic users are more interested in long term predictions

- Operational/Scientific users prefer predictions to be updated daily
- Academic users prefer weekly updates
- Almost two/thirds of all users would like daily or weekly updates

- Majority of users prefer data at 1-day intervals
- Some users have an emerging requirement for sub-daily prediction data

- Majority of users prefer tabular data
- Academic users desire analytical expression in addition to tabular data

Several different algorithms were used in the EOP Prediction Comparison Campaign. Because each participant in that campaign was able to choose what input data to use and also what algorithm to use, it is not possible to ascertain whether the best prediction was due to superior input data or a superior algorithm. Therefore, to determine the strengths and weaknesses of the various algorithms, a multitude of input data sets need to be processed. Additional considerations will be addressed in the next sections.

6. INPUT DATA

WGP goals #2 and #3 will be answered by looking closely at the intrinsic properties of data sets available and how to maximize the geodetic and geophysical information content. The following input data issues need to be addressed:

1. Exploit methods to minimize data latency and reduce extrapolation to current time;
2. Determine loss of information if all data sets were reduced to common epochs;
3. Examine potential geophysical data sets from the IERS Global Geophysical Fluids Center;
4. Examine the geodetic technique services combination data sets resulting from the IERS Combination Pilot Project;
5. Determine sensitivities of missing data sets to the prediction process;
6. Examine pathological data sets from times when the Chandler and annual polar motion destructively interfere;
7. Determine the optimum combination of geophysical signals to create the best predictions;
8. Determine where research is needed to make future improvements in EOP prediction.

A password protected repository for retrieval and analysis has been established at the University of Luxembourg so that the test data sets and results can be tracked and readily available to the WGP. Test cases have been identified for polar motion loops, large amplitude Chandler/annual polar motion, radical UT1 changes, minimal UT1 changes, differences in smoothing, artificial noisier end points, and a general test case for 2000-2006. Input data sets include time series of geodetic data (GPS, SLR, GPS). Additional data sets are being identified in the geophysical fluids data area [AAM, Oceanic Angular Momentum (OAM), Hydrological Angular Momentum (HAM)].

7. ALGORITHMS

WGP goals #4 and #5 will be answered by understanding the intrinsic properties of each algorithm, how each handles the various pathological test cases, and what additional information content is beneficial. The following algorithm issues need to be addressed:

1. Maintain the integrity of effort, the group analyzing the predictions will be different from the group generating the predictions – each group checks the other groups' results;
2. Finalize the specific metric criteria for comparison;
3. Examine time dependency and/or frequency dependency issues with the results;
4. Provide definitive description of each algorithm – characterize the advantages and shortcomings;
5. Determine what the state-of-the-art is in prediction techniques;
6. Determine how robust the algorithms are;
7. Determine suitability for operational setting.

The EOP time series data generally consist of both deterministic and stochastic components. The deterministic component gives rise to trends, seasonal variations, and tidal variations, while the stochastic component causes statistical fluctuations which have a short-term correlation structure. The best prediction results of the EOP are obtained when the deterministic components are predicted by the deterministic method and a stochastic prediction technique is applied to forecast the stochastic component. Combination of deterministic and stochastic predictions improves the prediction accuracy in low and high frequency components.

Prediction methods to be considered include least-squares extrapolation, least-squares collocation, Kalman filter, autoregressive, autoregressive (integrated) moving-average, autocovariance, neural networks, fuzzy logic, and multidimensional. Unfortunately, there are problems associated with each of these methods. However, each has certain advantages under given conditions. The focus of the algorithm group is to characterize the strengths and weaknesses of each of the algorithms on the basis of the various test cases. A recent comparison of different techniques is given by Kosek *et al.* (2007).

8. FUTURE

The future activities of the WGP include adding more data sets to the repository at the University of Luxembourg, finalizing criteria for algorithm comparisons, determining the optimal parameters in combination prediction algorithms, investigating geophysical causes of prediction errors, and investigating new forecast techniques. The expectations of the WGP are to have definitive user requirements, a comprehensive look at prediction methods, a comprehensive look at new data sets, and to produce an IERS Technical Note describing current state-of-the-art EOP prediction including requirements, methods, and data set information content.

9. REFERENCES

Dick, Wolfgang R. and Richter, Bernd, ed., (2007) IERS Annual Report 2005 International Earth Rotation and Reference Systems Service, Central Bureau, Frankfurt am Main: Verlag des Bundesamts für Kartographie und Geodäsie, 2007, 175 p., ISBN 3-89888-838-X

IERS Central Bureau (2004), IERS Message No. 53: Call for Participation in the IERS Combination Pilot Project.

IERS Central Bureau (2005), IERS Message No. 74: Earth Orientation Parameters Prediction Comparison Campaign (EOP PCC): Call for Participation.

IERS Central Bureau (2006), IERS Working Group on Prediction (http://www.iers.org/MainDisp.csl?pid=167-1100082)

Kalarus, M., Kosek, W., Schuh, H. (2007) "Current results of the Earth Orientation Parameters Prediction Comparison", Proc. Journées Systèmes de Référence Spatio-Temporels 2007

Kosek, W., Kalarus, M., Niedzielski, T. (2007) "Forecasting of the Earth Orientation Parameters Comparison of Different Techniques", Proc. Journées Systèmes de Référence Spatio-Temporels 2007

Stamatakos, N., Luzum, B., Wooden, W. (2007) "Recent Improvements in the IERS Rapid Service/ Prediction Center Products", Proc. Journées Systèmes de Référence Spatio-Temporels 2007

Wooden, W.H., Johnson, T.J., Carter, M.S., and Myers, A.E. (2004) "Near Real-time IERS Products", Proc. Journées Systèmes de Référence Spatio-Temporels 2003, pp. 160-163

RIGOROUS COMBINATION TO ENSURE ITRF AND EOP CONSISTENCY

Z. ALTAMIMI[1], D. GAMBIS[2], C. BIZOUARD[2]
[1]Institut Géographique National, LAREG
6-8 Avenue Blaise Pascal, 77455 Marne-la-Vallée, France
e-mail: altamimi@ensg.ign.fr
[2]Observatoire de Paris; 61 Avenue de l'Observatoire, 75014 Paris
e-mail: daniel.gambis@obspm.fr; christian.bizouard@obspm.fr

ABSTRACT. The ITRF2005 is the first rigorous combination ensuring ITRF and EOP consistency, based on time series of station positions and Earth Orientation Parameters (EOPs). The objective of the presentation is the development of a combination strategy allowing to ensure the ITRF2005 and IERS 05 C04 consistency with time. Combining additional input time series after the release of ITRF2005 from the four techniques (VLBI, SLR, GPS and DORIS) allows the assessment of two main procedures: (1) using CATREF combination model and (2) using EOP-only combination method. The main features of the two combination strategies are presented together with numerical application. Comparisons of results obtained by the two procedures will be discussed in an attempt to evaluate the current accuracy of EOP determination by space geodesy techniques and to guide our conclusion for future development.

1. ITRF2005 INPUT DATA

For the first time of the ITRF history, the ITRF2005 input data are under the form of time-series solutions, provided in a weekly production by the IAG International Services of satellite techniques (the International GNSS Service, IGS, the International Laser Ranging Service, ILRS and the International Doris Service,IDS) and in a daily (VLBI session-wise) basis by the International VLBI Service, IVS. Each per-technique time series is indeed a combination, on a weekly basis, of the individual Analysis Center (AC) solutions of the technique, except for DORIS for which two individual analysis center time series were submitted for the ITRF2005 computation. Local tie vectors at about 87 sites were used in the ITRF2005 combination allowing the connection between the four techniques. The ITRF2005 is composed of 608 stations located at 338 sites as illustrated on Figure 1, with an imbalanced distribution between the northern (268 sites) and the southern hemisphere (70 sites).

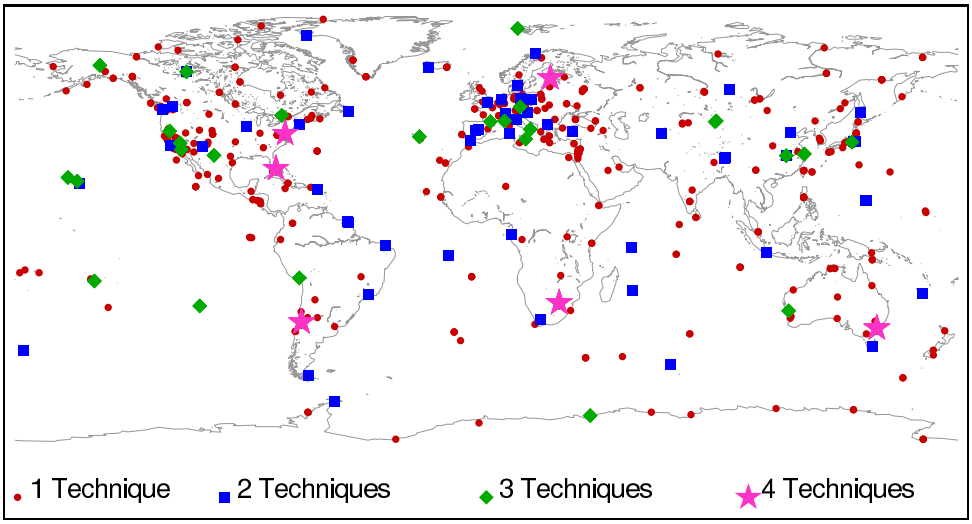

Figure 1: ITRF2005 sites with co-located techniques

2. ADVANTAGES OF USING TIME SERIES

The main advantages of using time series as input data for the construction of the ITRF2005 solutions are:

- to monitor non-linear motion of stations and all kind of discontinuities in the time series. This allows in fact to (1) ensure an optimal velocity field determination and consequently to (2) rigorously define the time evolution of the frame orientation,
- to examine the temporal behavior of the physical parameters of the frame, namely the origin and the scale. The analysis of the temporal behavior of these parameters are of great importance since it helps guiding our choice on how to define the origin and the scale of the ITRF2005 that need to be optimally stable over time, i.e. they should not exhibit temporal discontinuities in order to avoid any internal frame distortion, in order to ensure an optimal temporal stability of a secular frame like the ITRF,
- to ensure a rigorous combination of EOP and ITRF and so to enforce their mutual consistency.

3. ITRF2005 DATA ANALYSIS

The strategy adopted for the ITRF2005 generation follows the following steps:

- Remove original constraints (if any) and apply minimum constraints equally to all solutions
- Use as they are minimally constrained solutions
- Form per-technique combinations (TRF + EOP)
- Identify and reject (de-weight) outliers and properly handle discontinuities using a piece-wise approach
- Combine (if necessary) all solutions of a given technique into a unique solution
- Combine per-technique combination adding local ties in co-location sites

The final step yields the ITRF2005 global solution comprising a full time series of EOPs consistent with the combined frame in addition to the station positions and velocities. For a detailed description of the ITRF2005 data analysis, refer to Altamimi et al. (2007).

4. EOP SERIES ASSOCIATED TO ITRF2005

One of the primary tasks of the IERS is to ensure consistency between the ITRF, the International Celestial Reference Frame (ICRF) and EOPs connecting the two frames. The ITRF2005 provides a major step towards this consistency by providing a consistent series of polar motion and its daily rate, Universal Time (UT1) and Length of Day (LOD). Note that UT1 and LOD values included in the ITRF2005 combination are provided by VLBI only. Biased LOD values from satellite techniques were not included in order to avoid contaminating the VLBI estimates. In a presentation at the GRF2006 Symposium, October 2006, Munich, Germany, J. Ray proposed a multi-step procedure to derive complete UT1/LOD time series consistent with the ITRF2005 making use of UT1 determination from one-hour single-baseline VLBI sessions that were not included in the ITRF2005 combination.

As results from the global ITRF2005 combination, Figure 2 shows Polar Motion differences between the ITRF2005 combination and the IERS C04 series. The mean of these differences indicates a significant bias of about 200 mas in the Y component between the two EOP series. Therefore the ITRF2005 was a good opportunity to reset the IERS C04 to make it consistent with the ITRF2005. The new calibrated series is now called IERS 05 C04 (Bizouard and Gambis, 2008).

In order to evaluate the performance of the solutions used in the ITRF2005 generation in terms of polar motion, Figure 3 illustrates the post fit residuals in x and y components. As an indication of the EOP quality, we computed the WRMS of these residuals resulting in the following approximate numbers: 130μas for VLBI and SLR, 50μas for GPS and 700μas for DORIS.

5. RE-COMPUTATION OF THE EOP 05C04

5.1. Upgrade of the C04 code

For the first time a terrestrial reference frame, i.e. ITRF2005 was available with an associated EOP system. This was a good opportunity to recompute the C04 series since 1962 in a frame consistent with ITRF2005. By the way, the combination code leading to the C04 combined solution was upgraded.

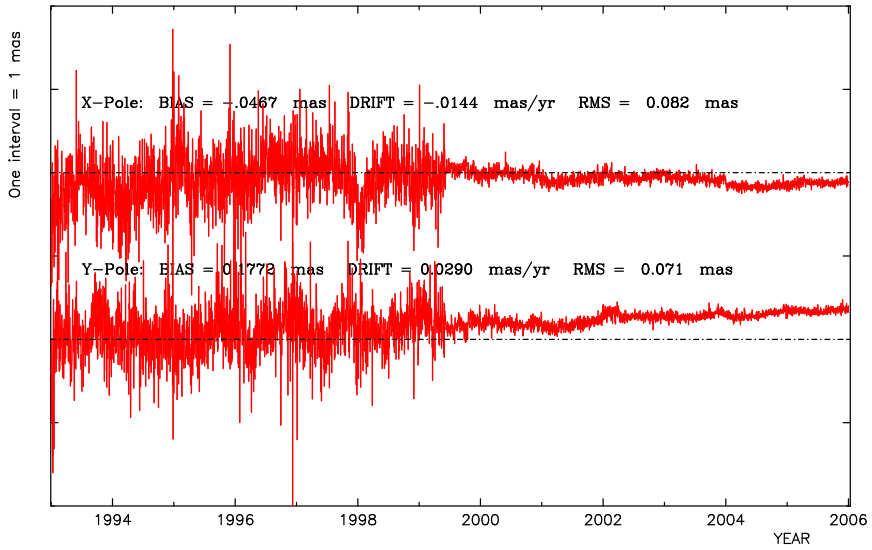

Figure 2: Polar Motion Differences Between ITRF2005 and the IERS C04

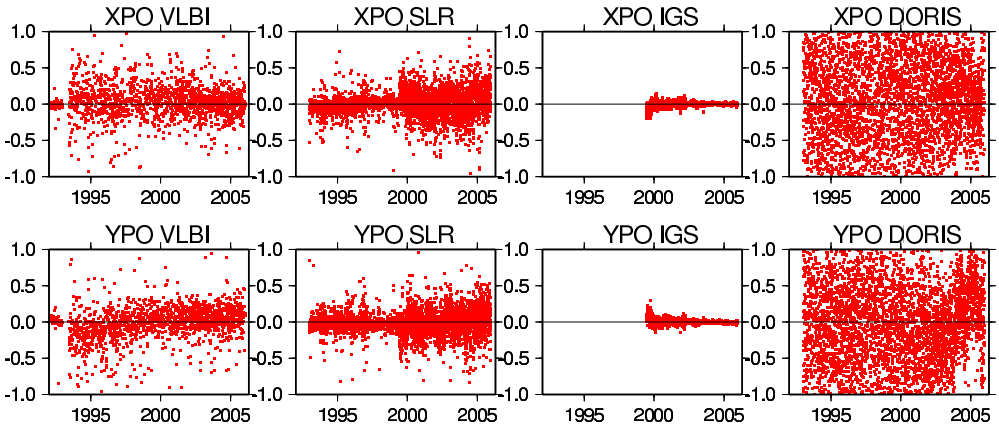

Figure 3: Polar motion residuals per technique resulting from the ITRF2005 combination

The description of the algorithm leading to the combined C04 EOP series is presented in Gambis (2004). The numerical code was recently upgraded to take advantage of the evolution of the precision of EOP derived from the various techniques as well as to benefit of the dramatic improvement of computational resources (Bizouard and Gambis, 2008). The nutation model IAU 2000 was implemented. Solution can now be performed over 20 years in one run. Formal errors associated with the computed EOPs are estimated.

5.2. Performance of the new combination code

The C04 solution has been significantly improved : on one hand it is consistent with the current ICRF and ITRF 2005, on the other hand its parameters present an improved accuracy (50 μas for polar motion, 20 μas for LOD). The parameters $UT1$ and $d\psi * \sin\varepsilon_0$ and $d\varepsilon$ are in better agreement with VLBI series than the official IVS official combined VLBI solution, especially for UT1. Their present accuracy is about 5 μs for $UT1$ and 60 μas for nutation offsets.

6. ENSURING THE CONSISTENCY OVER TIME

From the user point of view of the ITRF and EOP results, it is fundamental to ensure the consistency over time between ITRF2005 and the IERS 05 C04. Therefore it is agreed between the two IERS product centers to assess the extension of the series in two ways: using (1) the EOP PC upgraded procedure and (2) CATREF combination incorporating the routinely available SINEX files by the technique services. The procedure of the EOP Product Center at Paris Observatory is routinely performed whereas the CATREF combination is to be done at regular interval (let us say every 6 months). Both results should then be compared on this time scale in order to evaluate the level of their consistency. In order to illustrate the current level of consistency between the two computations, Figure 4 shows the polar motion differences, including the extended period of about two years of data after the end of ITRF2005 series (i.e. epoch 2006.0). A particular feature could easily be seen from Figure 4 that is, the small but distinguishable jump around the end of 2006. This jump curiously coincides with the time where the IGS switched from relative to absolute model of antenna phase center variations which normally impacts mostly station vertical components. Still, this jump is largely within the current GPS polar motion performance estimated to be at the level of 50μas.

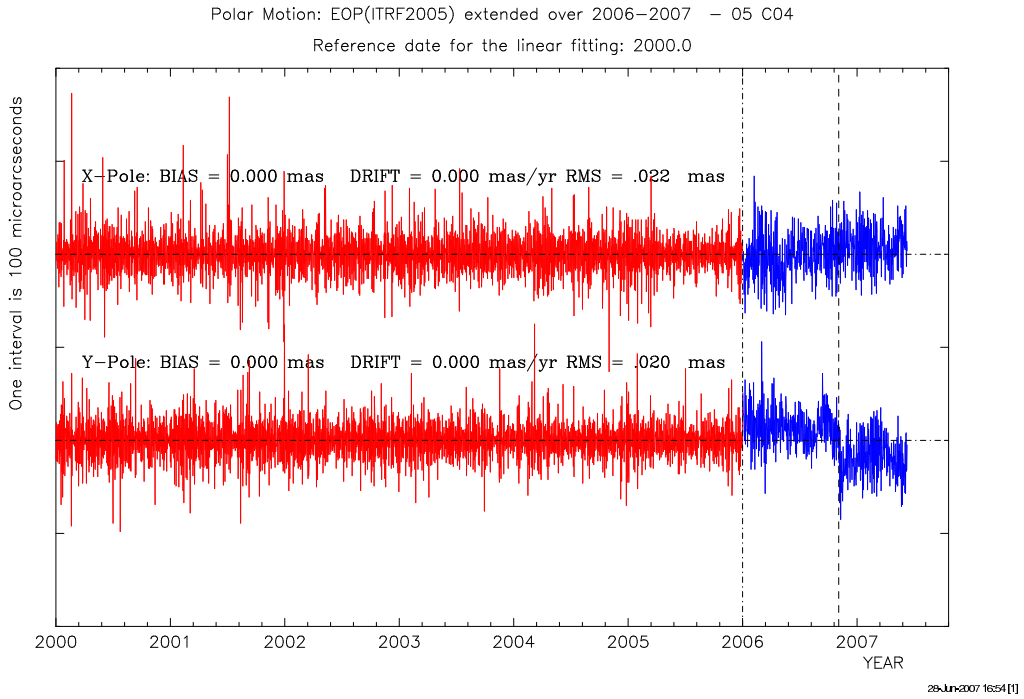

Figure 4: Polar motion differences between ITRF2005 and IERS 05 C04, the time interval was extended over 2 more years after epoch 2006.0

7. CONCLUSION

The ITRF history and evolution demonstrates the continuous improvement of the ITRF solutions, since the BIH era, in the 1980's. It is now fundamental to use time series analysis for ITRF implementation, a major step for improving quality and consistency. The ITRF2005 is a starting point of rigorous unification of ITRF and EOPs. This paper shows that the overall consistency between ITRF2005 and the IERS EOP series 05 C04 is now ensured at the level of 20-30 μas.

8. REFERENCES

Altamimi, Z., Collilieux, X., Legrand, J., Garayt, B. and C. Boucher, 2007, ITRF2005: A New Release of the International Terrestrial Reference Frame based on time series of station positions and Earth Orientation Parameters, J. Geophys. Res., DOI: 10.1029/2007JB004949.

Bizouard, C. and D. Gambis, 2008, The combined solution C04 for Earth Orientation Parameters, recent improvements, in print in Springer Verlag series.

Gambis, D., 2004, Monitoring Earth orientation using space-geodetic techniques: state-of-the-art and prospective, J. of Geodesy, Volume 78, Issue 4-5, pp. 295-303, doi 10.1007/s00190-004-0394-1.

FORECASTING OF THE EARTH ORIENTATION PARAMETERS - COMPARISON OF DIFFERENT ALGORITHMS

W. KOSEK[1], M. KALARUS[1], T. NIEDZIELSKI[1,2]
[1]Space Research Centre, Polish Academy of Sciences
Bartycka 18A, 00-716 Warsaw, Poland
e-mail: kosek@cbk.waw.pl, kalma@cbk.waw.pl, niedzielski@cbk.waw.pl
[2]Institute of Geography and Regional Development, University of Wrocław
pl. Uniwersytecki 1, 50-137 Wrocław, Poland
e-mail: niedzielski@geom.uni.wroc.pl

ABSTRACT. The Earth orientation parameters (EOP) are determined by space geodetic techniques with very high accuracy. However, the accuracy of their prediction, even for a few days in the future, is several times lower and still unsatisfactory for practical use. The main problem of each prediction technique is to predict simultaneously long and short period oscillations of the EOP. It has been shown that the combination of the prediction methods which are different for deterministic and stochastic components of the EOP can provide the best accuracy of prediction. Several prediction techniques, e.g. combination of the least-squares with autoregressive and autocovariance methods as well as combination of wavelet transform decomposition and autocovariance prediction, were used to predict x, y pole coordinates in polar coordinate system and $UT1-UTC$ or length of day (Δ) data. Different prediction algorithms were compared considering the difference between the EOP data and their predictions at different starting prediction epochs as well as by comparing the mean EOP prediction errors.

1. INTRODUCTION

Predictions of Earth orientation parameters (EOP): x, y pole coordinates, universal time ($UT1-UTC$) and nutation-precession corrections dX, dY provide real-time transformation between celestial and terrestrial reference frames. They are required in the process of tracking and navigation of interplanetary spacecrafts by the Deep Space Network. The other precision applications, for instance astronomy, geodesy, communication and time-keeping also need EOP predictions (e.g., Schuh et al. 2002). The EOP predictions are published by the International Earth Rotation and Reference Systems Service (IERS) Rapid Service/Prediction Centre (RS/PC) (e.g. Wooden et al. 2004). Many efforts were made within the IERS RS/PC to improve pole coordinates data (e.g. Kosek et al. 2004) and $UT1-UTC$ data (e.g. Johnson et al. 2005) prediction accuracy.

2. DATA

The following data sets were used in the analysis: (1) x, y pole coordinates data from EOPC01 solution in 1846 to 2000, (2) x, y pole coordinates, $UT1-UTC$ data from the EOPC04_05 solution (IERS 2007), (3) χ_3 component of the atmospheric angular momentum from ncep.reanalysis which is the sum of mass and motion terms.

3. ANALYSIS

In this work the following prediction techniques were used: (1) least-squares (LS) extrapolation, (2) autocovariance (AC) prediction, (3) autoregressive (AR) prediction, (4) multivariate autoregressive (MAR) prediction. Some of these techniques - when combined - enable forecasting the EOP data with a better accuracy than a single prediction technique. The following combinations of at least two prediction techniques called prediction algorithms were used: (1) combination of the LS extrapolation and AR prediction denoted as LS+AR, (2) combination of the LS and MAR denoted as LS+MAR, (3) combination of the discrete wavelet transform (DWT) (Popiński and Kosek 1995) and AC prediction (Kosek et al. 1998) denoted as DWT+AC.

In the LS+AR prediction algorithm first the LS model is fit to x, y pole coordinates data. The

differences between the x, y pole coordinates data and their LS models are equal to LS residuals. Prediction of x, y pole coordinates data is the sum of the corresponding LS extrapolation models and the AR predictions of the LS residuals. The LS model consists of the trend, Chandler circle as well as annual and semi-annual ellipses. The length of the LS residuals fit to the autoregressive model is equal to 850 days which is approximately equal to twice of the period of the Chandler oscillations. The autoregressive order was estimated by Akaike's Information Criterion (AIC) and empirically by looking at the minimum prediction errors (Kalarus 2007).

Absolute values of the difference between x, y pole coordinate and their predictions computed by the LS method and by the LS+AR combination, as a function of starting prediction epoch from 1980 till 2007.6 and from one day to one year in the future, are shown in Figure 1. The LS model is fit to different data span of pole coordinates data equal to 5, 10 and 15 years. The prediction errors computed by the LS method are greater than by the LS+AR combination. The increase of the pole coordinates data length fit to the LS model cause increase of the prediction errors in the LS method but their decrease in the LS+AR combination (Fig. 1).

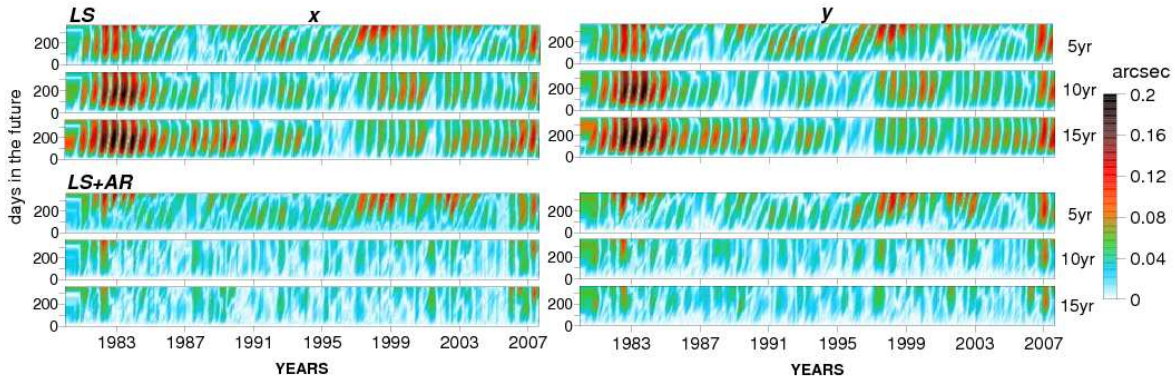

Fig. 1. Absolute differences between x, y pole coordinates data and their predictions computed by the LS and LS+AR combination methods.

The influence of the length of the autoregressive order on prediction errors of EOP data in the AR prediction method was investigated by Kalarus (2007). Empirically computed autoregressive order values for which the prediction errors from 1 to 500 days in the future were minimum are shown in Figure 2. The length of the autoregressive order usually increases with the length of prediction but it should not exceed about 6 years for the EOP data. The mean LS and LS+AR prediction errors of x, y pole coordinates data computed over time span 1980 to 2007 are shown in Table 1. The LS model was fit to 10 years of x, y pole coordinates data and in the LS+AR algorithm the autoregressive order was estimated by the AIC or its empirical value was adopted for longer term predictions. The mean prediction errors of x, y pole coordinates data are smaller for the LS+AR prediction than for the LS one. Longer term prediction accuracy can be improved when the autoregressive order was empirically obtained, however at the same time this autoregressive order is not good for shorter term predictions (Tab. 1).

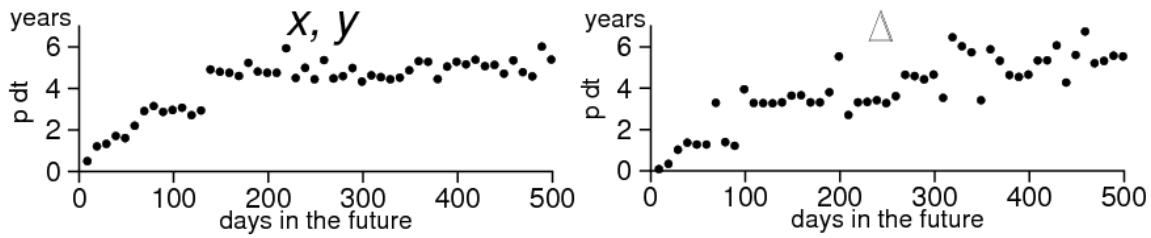

Fig. 2. Empirically computed autoregressive order for which the AR prediction errors of the EOP data have minimum values (Kalarus 2007).

The prediction of x, y pole coordinates data can be also computed in polar coordinate system (Kosek 2002) in which the radius and angular velocity are predicted by the DWT+AC prediction (Kosek 2003, Kosek and Popiński 2006). The radius can be computed from x, y pole coordinates and mean pole

computed by the Orsmby low pass filter and prolonged into the future using extrapolation of the LS model. In the DWT+AC method the radius and angular velocity is decomposed by the DWT into frequency components and each frequency component is predicted by the AC prediction (Kosek 2002). The prediction of the radius and angular velocity is the sum of AC predictions of all the frequency components. Afterwards, the predictions of x, y pole coordinates data are computed from the prediction of the radius, angular velocity and the mean pole using linear intersection formulae (Kosek 2002). The DWT+AC mean prediction errors of x, y pole coordinates data computed from October 2006 to August 2007 have reasonable accuracy in comparison with the results of other prediction algorithms (Tab. 1).

	days in the future	5	10	20	30	60	120	180	360
x pole coordinate	time span								
LS	Jan.1980-Jan.2007	3.7	7.0	13.1	18.8	33.7	54.0	60.4	45.8
LS+AR (AIC)	Jan.1980-Jan.2007	1.4	3.1	6.0	8.5	14.3	20.9	23.5	33.1
LS+AR (emp)	Jan.1980-Jan.2007	3.8	8.4	12.0	11.8	15.4	20.6	23.8	29.5
DWT+AC	Oct.2006-Aug.2007	3.2	5.0	8.2	12.7	-	-	-	-
y pole coordinate	time span								
LS	Jan.1980-Jan.2007	3.2	6.3	12.1	17.7	32.8	54.0	61.4	46.8
LS+AR (AIC)	Jan.1980-Jan.2007	0.9	1.9	3.5	5.1	9.7	19.0	26.9	34.0
LS+AR (emp)	Jan.1980-Jan.2007	2.9	6.4	9.5	9.8	13.7	20.6	25.3	30.6
DWT+AC	Oct.2006-Aug.2007	2.5	4.3	7.7	10.2	-	-	-	-

Table 1: Mean prediction errors of x, y pole coordinates data [in mas] computed by the LS, LS+AR and DWT+AC methods.

Prediction of $UT1-UTC$ data are usually computed from prediction of length of day (Δ) data from which tidal model $\delta\Delta$ described in the IERS Conventions (McCarthy and Petit 2004) is subtracted. The $\Delta-\delta\Delta$ data were obtained after subtracting leap seconds from $UT1-UTC$ to derive $UT1-TAI$, next computing time derivative of $UT1-TAI$ to get length of day Δ data and finally subtracting tidal model from Δ data. In this paper, in order to compute $\Delta-\delta\Delta$ prediction the LS, LS+AR, LS+MAR and DWT+AC algorithms were used. After adding tide model to $\Delta-\delta\Delta$ prediction, then integrating prediction of Δ data and adding leap seconds the predictions of $UT1-UTC$ were computed.

In the LS, LS+AR and LS+MAR prediction algorithms the LS model consists of the trend and 18.6, 9.3, 1.0 and 0.5 year oscillations and it is fit to $\Delta-\delta\Delta$ data from January 1962 to starting prediction epoch moving from January 1990 to January 2007. The LS prediction of $\Delta-\delta\Delta$ data is simply extrapolation of the LS model. The LS+AR and LS+MAR prediction of $\Delta-\delta\Delta$ data is the sum of LS extrapolation model and AR and MAR predictions of $\epsilon(\Delta-\delta\Delta)$ residuals obtained as a difference between $\Delta-\delta\Delta$ data and their LS models, respectively (Niedzielski and Kosek 2007). The autoregressive orders in the AR and MAR predictions of $\epsilon(\Delta-\delta\Delta)$ residuals were estimated by AIC and Schwarz Bayesian criterion (SBC), respectively. In the LS+MAR prediction algorithm χ_3 component of atmospheric angular momentum was used as an explanatory variable, i.e. the residuals computed as the difference between the atmospheric angular momentum χ_3 data and LS models consisted of 1.0 and 0.5 year oscillations are considered concurrently with the $\Delta-\delta\Delta$ residuals. The autoregression matrices are estimated by means of a stepwise LS estimation for MAR models (Neumaier and Schneider 2001). Combination LS+MAR provides $UT1-UTC$ predictions with better accuracy than the combination LS+AR which provides smaller mean prediction errors than the LS extrapolation (Tab. 2).

In the DWT+AC algorithm first, $\Delta-\delta\Delta$ data were decomposed into frequency components by the DWT band pass filter and each frequency component was predicted using AC prediction. The prediction of $\Delta-\delta\Delta$ was computed as the sum of DWT+AC predictions of all the frequency components. The mean prediction errors of $UT1-UTC$ data computed from October 2006 to August 2007 are of the same order as those computed by other prediction algorithms (Tab. 2).

4. CONCLUSIONS

The LS+AR combination of x, y pole coordinates data provides their prediction with the highest accuracy. The minimum prediction errors for particular number of days in the future depends on the

autoregressive order. Prediction of x, y pole coordinates data with reasonable accuracy can be computed also in the polar coordinate system by forecasting the mean pole, radius and angular velocity using DWT+AC algorithm. Decomposition of time series by the DWT band pass filter solves the problem of forecasting them in different frequency bands. Prediction of $UT1-UTC$ data can be improved by using LS+MAR combination, which takes into account axial component of the atmospheric angular momentum.

	days in the future	5	10	20	30	60	120	180	360
	time span								
LS	Jan.1990-Jan.2007	0.29	0.99	2.90	4.95	10.5	21.0	31.3	66.9
LS+AR (AIC)	Jan.1990-Jan.2007	0.29	0.97	2.66	4.34	8.8	18.0	27.6	62.4
LS+MAR (SBC)	Jan.1990-Jan.2007	0.29	0.99	2.68	4.32	8.4	16.3	24.4	53.8
DWT+AC	Oct.2006-Aug.2007	0.49	1.25	2.84	4.44	-	-	-	-

Table 2: Mean prediction errors of $UT1-UTC$ data [in ms] computed by the LS, LS+AR, LS+MAR and DWT+AC prediction algorithms.

Acknowledgements. Attendance of co-authors M. Kalarus and T. Niedzielski at the Journees 2007 were supported by a conference grant within 'Descartes-nutation project'. T. Niedzielski is supported by the Foundation for Polish Science within the Start Programme (stipends for young researchers). The paper was supported by the Polish Ministry of Education and Science under the project No 4 T12E 039 29.

5. REFERENCES

IERS, 2007, ftp://hpiers.obspm.fr/iers/eop/eopc04_05/eopc04_IAU2000.62-now.

Johnson T., Luzum B.J., Ray J.R., 2005, Improved near-term Earth rotation predictions using atmospheric angular momentum analysis and forecasts. J Geodyn 39: 209221.

Kalarus M., 2007, Analiza metod prognozowania parametrów orientacji przestrzennej Ziemi, PhD thesis (*in Polish*), Warsaw Technical University.

Kosek, W., McCarthy, D.D., Luzum, B.J., 1998, Possible improvement of Earth orientation forecast using autocovariance prediction procedures, Journal of Geodesy 72, 189–199.

Kosek W., 2002, Autocovariance prediction of complex-valued polar motion time series, Advances of Space Research, Vol. 30, No. 2, 375–380.

Kosek W., 2003, Polar motion prediction by different methods in polar coordinate system. Proc. Journees 2002, Systemes de Reference Spatio-Temporels, Bucarest, 125–131.

Kosek W., McCarthy D.D., Johnson T.J., Kalarus M., 2004, Comparison of polar motion prediction results supplied by the IERS Sub-bureau for Rapid Service and Predictions and results of other prediction methods. Proc. Journees 2003, Systemes de Reference Spatio-Temporels, St. Petersburg, 164–169.

Kosek W., Kalarus M., Johnson T.J., Wooden W.H., McCarthy D.D. and Popiński W., 2005, A comparison of LOD and UT1-UTC forecasts by different combination prediction techniques" Artificial Satellites Vol. 40, No. 2, 2005, 119–125.

Kosek W. and Popinski W., 2006, Forecasting of pole coordinates data by combination of the wavelet decomposition and autocovariance prediction. Proc. Journees 2005 Systemes de Reference Spatio-Temporels, 139–140.

McCarthy, D.D., Petit, G. (eds.), 2004. IERS Conventions, IERS Technical Note 32.

Neumaier, A., Schneider, T., 2001, Estimation of parameters and eigenmodes of multivariate autoregressive models, ACM Transactions on Mathematical Software 27, pp. 27–57.

Niedzielski, T., Kosek, W., 2007, Prediction of UT1-UTC, LOD and AAM χ_3 by combination of the least-squares and multivariate stochastic methods, Journal of Geodesy, doi: 10.1007/s00190-007-0158-9.

Popiński W., Kosek W., 1995. Discrete Fourier and Wavelet Transforms in Analysis of Earth Rotation Parameters. Proc. Journees 1995 "Systemes de Reference Spatio-Temporels", Warsaw, 121–124.

Schuh, H., Ulrich, M., Egger, D., Mueller, J., Schwegmann, W., 2002, Prediction of Earth orientation parameters by artificial neural networks, Journal of Geodesy 76, pp. 247–258.

Wooden W.H., Johnson T.J., Carter M.S., Myers A.E., 2004, Near Realtime IERS Products. Proc. Journees 2003, Systemes de Reference Spatio-Temporels, 160-163.

CURRENT RESULTS OF THE EARTH ORIENTATION PARAMETERS PREDICTION COMPARISON CAMPAIGN

M. KALARUS[1], W. KOSEK[1], H. SCHUH[2]
[1] Space Research Centre, Polish Academy of Sciences
ul. Bartycka 18A, 00-716 Warsaw, Poland
e-mail: kalma@cbk.waw.pl, kosek@cbk.waw.pl
[2] Institute of Geodesy and Geophysics, Vienna University of Technology
Gußhausstraße 27-29, A-1040 Vienna, Austria
e-mail: harald.schuh@tuwien.ac.at

ABSTRACT. The precise transformation between the celestial (ICRF) and terrestrial (ITRF) reference frames is needed for many advanced geodetic and astronomical tasks. To perform this transformation for the time moment of observation the precise EOP predictions have to be known. This paper presents the current status of the Earth Orientation Parameters Prediction Comparison Campaign (EOP PCC), which started in October 2005 under the umbrella of the IERS (International Earth rotation and Reference systems Service). The ultra-short term, short term and medium term EOP predictions submitted since then by different groups were evaluated by means of the same statistical analysis. The mean prediction errors of the EOP with respect to IERS C04 data for each proposed algorithm were computed to show the performance in each prediction category. In October 2006 the EOP PCC rules were slightly changed, however all prediction results before this moment were transformed according to the new conventions.

1. OBJECTIVES

The main objective of the EOP PCC is to compare the various methods, models, techniques and strategies which can be applied for EOP predictions. We use the same statistical method for all results, and what is different from many other studies we collect predictions before any EOP observations are available. Our main goal is to investigate the EOP time series as well as other data strongly correlated with the EOP (e.g. AAM and OAM). We also expect the final conclusions to be useful for the operational computation of the EOP.

2. MAIN RULES

The EOP PCC provides three categories of the predictions: ultra short-term (for 10 days), short-term (for 30 days) and medium-term (for 500 days). This is a consequence of our assumption that in general short and long term predictions require different strategies and techniques. In that case each participant can submit any type of the prediction of any EOP except ultra short-term and short-term predictions of dX, dY or $d\psi$, $d\varepsilon$. Various prediction techniques can be applied by the same participant. This allows to provide different and very specific algorithms adjusted to each category. After joining the EOP PCC a participant is asked to submit the specified predictions every Thursday with one day delay. Then all the submissions are being processed and the current results are available on the official EOP PCC website: `http://www.cbk.waw.pl/EOP_PCC/`.

3. ANALYSES

Thanks to the EOP PCC participants (Tab. 1) we received a few thousands of predictions. Such a valuable collection give us an opportunity to perform many unique statistical analysis. Unfortunately, a reliable comparison of the submissions cannot be performed directly since very often predictions sent by different participants are referred to different prediction epochs. The detailed investigation of predictions also shows that some of them have unexpected high errors mostly caused by human mistake rather than by the applied prediction technique. The substantial reduction of mentioned problems is performed by means of the median absolute prediction error ($MDAE$) computed for all predicted EOP. For i^{th} day in

ID	Participant	Institute/Organization
011 012	Sergey Kumakshev	IPM RAS, Russia
021	Orhan Akyilmaz Hansjoerg Kutterer	ITU, Turkey University of Hannover, Germany
031	Richard Gross	NASA JPL, USA
051 052 053	Wiesław Kosek	Space Research Centre PAS, Poland
061	Maciej Kalarus	Space Research Centre PAS, Poland
071	EOP Product Center	Paris Observatory, France
072 073 074 075	Daniel Gambis	Paris Observatory, France
091 092 093	Leonid Zotov	SAI, Moscow State University, Russia
101	Sergey Pasynok	SAI, Moscow State University, Russia
111	Paulo Jorge Mendes Cerveira	IGG, Vienna University of Technology, Austria
121	Bora Jovanovic	Astronomical Observatory, Belgrade, Serbia

Table 1: List of participants (status as of Dec. 2007)

the future $MDAE$ is defined as follows:

$$MDAE_i = median\left(|\varepsilon_{i,1}|, |\varepsilon_{i,2}|, ..., |\varepsilon_{i,P}|\right), \qquad i = 1, 2, ..., N_p, \tag{1}$$

where $\varepsilon_{i,j}$ is the difference between the EOP data (IERS C04) and its j^{th} prediction for i^{th} day in the future, P is the number of all available predictions of a given EOP and N_p is a prediction length (10, 30 or 500 days). Then, a coefficient β_n is computed (Eq. 2) in order to get the relative quality of each prediction. Finally we exclude predictions with $\beta_n < 0$, while $\alpha = 10$ is deduced empirically to preserve a representative set of data.

$$\beta_n = \sum_{i=1}^{N_p} \left(\alpha \cdot MDAE_i - |\varepsilon_{i,n}|\right) \tag{2}$$

In practice we accepted about 98.6% of the predictions and then performed the main statistical analysis based on the Mean Absolute Error (MAE) expressed by equation

$$MAE_i = \frac{1}{N_{Acc}} \sum_{k=1}^{N_{Acc}} |\varepsilon_{i,k}|, \qquad i = 1, 2, ..., N_p, \tag{3}$$

where N_{Acc} is a number of accepted predictions related to the given EOP and prediction technique.

4. COMBINED PREDICTIONS

This part of our work is devoted to the combined solution and its relative quality with respect to the individual solutions provided by the participants. The final combined prediction CP is computed as a weighted mean of all submissions available at a given prediction epoch. The weights W are referred to the global quality factor Q and the number of accepted N_{Acc} submissions of a given prediction technique which can simply be described as follows:

$$W \sim [Q^2 \cdot N_{Acc}], \qquad Q = \left(\sum_{i=1}^{N_p} MAE_i\right)^{-1}. \tag{4}$$

In that case small weight (Fig. 1) is caused by low quality factor and/or small number of submitted predictions. On the other hand significant contributions clearly say about good quality factor of the given predictions which can also be seen in the final comparison presented in the next section.

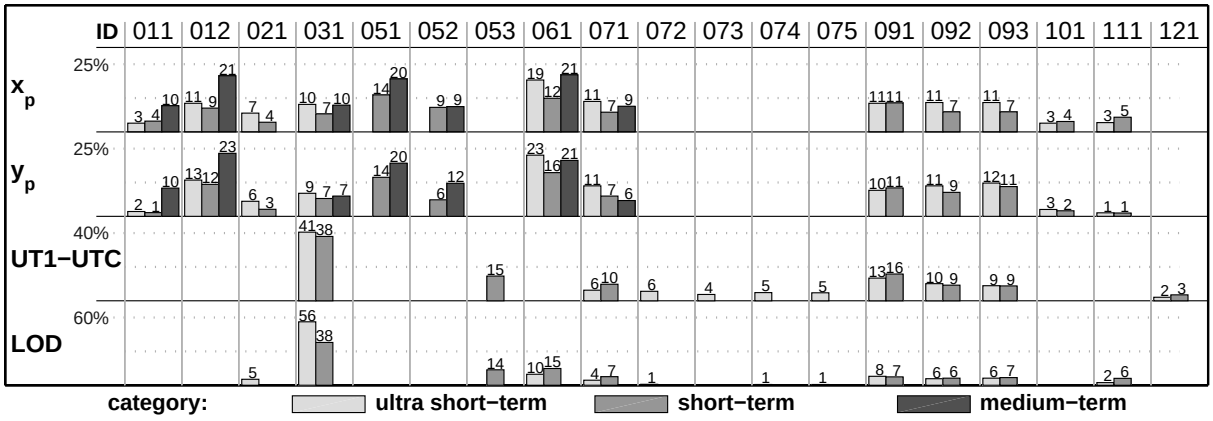

Figure 1: Contributions to the combined solution (weights [%])

5. RESULTS

The most important results of the EOP PCC are presented in Fig. 2 and for more information we refer to the EOP PCC website. Here we would like to underline that a brief comparison of those results can lead to wrong conclusions. In order to express the reliability figures are supplemented by the bar plot related to the number of predictions used to compute MAE. Therefore a small bar means that a given result is less reliable and in fact the direct comparison can be performed between results with maximal or at least significant reliability. The MAE of combined predictions is included as well with the exception of medium-term statistics of $UT1 - UTC$ where too few individual predictions are available. It is also worth to notice that due to lack of the future EOP data the medium-term statistics were computed from 8 submissions only.

6. CONCLUSIONS

Although we did not present the full results of the EOP PCC it is clearly visible that combined predictions are superior to most individual predictions, a fact which can also be seen when combining weather forecast. Nevertheless in order to increase the reliability of the results we need more submissions as well as more observed EOP data especially for medium-term category. It can be noticed that the short-term category of x_p, y_p is the most popular one within our campaign. In this case the combined solution provides the best accuracy.

7. PROSPECTS

The termination of the EOP PCC is foreseen in March 2008, however we hope its achievements will be very useful for the IERS Working Group on Prediction, which is going to find the best prediction algorithm for computing operational predictions of EOP. The first summary of the EOP PCC will be presented at the EGU General Assembly 2008. We plan to compute statistics with respect to different input data used by participants as well as to compare different types of algorithms.

Acknowledgements. Maciej Kalarus would like to express his sincere thanks for the travel grant provided by the "Descartes-Nutation" consortium. This paper was supported by the Polish Ministry of Education and Science Project No 4T12E 039 29.

8. REFERENCES

Kalarus M., Kosek W., Schuh H., 2007, "Current Results of the Earth Orientation Parameters Prediction Comparison Campaign", Geophysical Research Abstracts, Vol. 9, 02779, 2007, European Geosciences Union.

Schuh H., et al., 2006, "First Results of the Earth Orientation Parameters Prediction Comparison Campaign", Geophysical Research Abstracts, Vol. 8, 01228, 2006, European Geosciences Union.

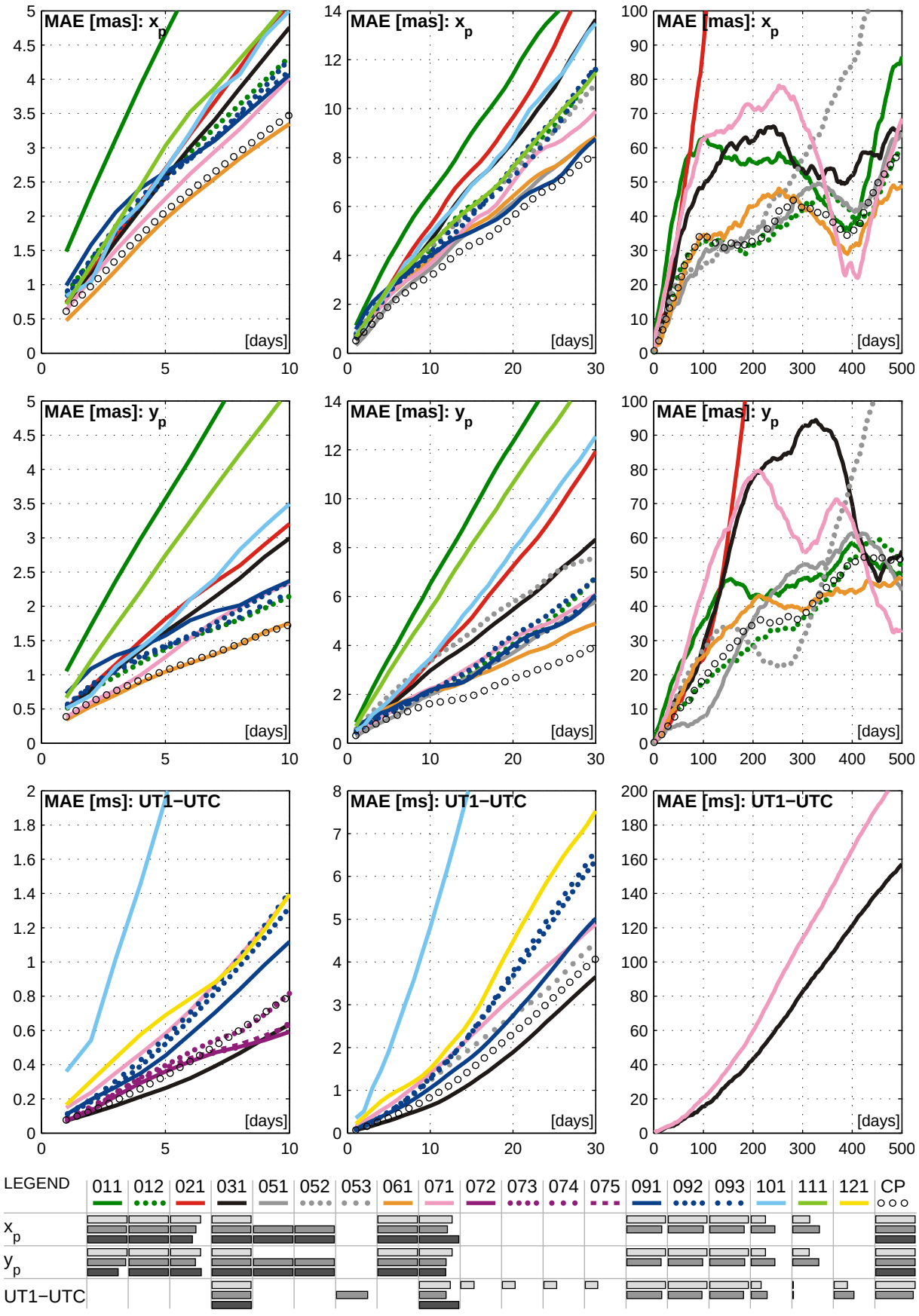

Figure 2: Mean Absolute Prediction Errors of x_p, y_p, and $UT1-UTC$ computed for all categories. Colors of the bars are related to different categories (like in Fig. 1)

RECENT IMPROVEMENTS IN IERS RAPID SERVICE/PREDICTION CENTER PRODUCTS

N. STAMATAKOS[1], B. LUZUM[2], W. WOODEN[3]
USNO, 3450 Massachusetts Avenue, N. W., Washington, D. C. 20392
[1] e-mail: Stamatakos.Nick@usno.navy.mil
[2] e-mail: Brian.Luzum@.usno.navy.mil
[3] e-mail: Wooden.William@usno.navy.mil

ABSTRACT. The International Earth Rotation and Reference System Service (IERS) Rapid Service/Prediction Center (RS/PC) at USNO has made several improvements to its combination and prediction products. These improvements are due to the inclusion of new input data sources as well as modifications to the combination and prediction algorithms. These changes and their impact on the users of the RS/PC data are presented.

1. INTRODUCTION

A review of the data provided for and users of IERS RS/PC combination and prediction solutions is presented. Recent improvements to the combination process, including using electronic Very Long Baseline Interferometry (e-VLBI) for faster data transfer of intensives, replacing extrapolated International GNSS Service (IGS) Rapid with IGS Ultra determined polar motion data, and adding one and removing two Satellite Laser Ranging (SLR) data series, is discussed. Recent improvements to the prediction process, which includes using e-VLBI, a least-squares, autoregressive algorithm (LS-AR) for polar motion determination, and an extended atmospheric angular momentum (AAM) forecast data is also discussed. Finally, an overview of the IERS RS/PC AAM process for determining Length-of-Day (LOD) is given.

2. OVERVIEW OF EOP RS/PC SOLUTION

The daily Earth Orientation Parameters (EOP) combination and prediction solution is produced at approximately 1700 UTC each day; the weekly is produced on Thursday at approximately 1700 UTC. The EOP data include polar motion, UT1, and celestial pole offsets. Observations of past data are combined with appropriate weighting factors and then used, along with some provided forecast data, to predict the EOP solutions into the future. Data from VLBI, Global Positioning System (GPS), SLR, and AAM are used in these EOP solutions, (Wooden et al., 2005). The International VLBI Service (IVS), the National Aeronautics and Space Administration (NASA) Goddard Space Flight Center, and the US Naval Observatory (USNO) periodically provide VLBI data observed over a 24 hour interval; while 1 hour long intensive solutions are also provided by NASA and USNO. The SLR data are provided by the International Laser Ranging Service (ILRS), the Russian Mission Control Center (MCC), and the Institute of Applied Astronomy (of the Russian Academy of Sciences) (IAA). The AAM information comes from two analysis centers: the U. S. Navy Operational Global Atmospheric Prediction System (NOGAPS) and from the National Oceanographic and Atmospheric Administration (NOAA). The GPS solutions, of various kinds, are provided by the IGS; Geodetic Survey Division, Natural Resources Canada (NRCan, formerly EMR Canada); and USNO. The EOP RS/PC combination solution is compared daily to the 05C04 series provided by the EOP Prediction Center (PC) in Paris. The 05C04 series is the 2005 realization of the C04, which is regarded as the EOP reference system. It is estimated there are 1500 users of the IERS RS/PC data. Most uses of the data are for practical, non-research purposes with many users – 85 to 90 % – having limited technical skills.

3. RECENT IMPROVEMENTS IN THE COMBINATION

The IERS RS/PC switched to the system of the 05C04 IERS reference series on June 14, 2007. Electronic transfer of VLBI intensives data (e-VLBI) are decreasing the turnaround time for processing since the data arrive sooner at the RS/PC than they did in the past. The Int1 intensive observations (which use

the Wetzell, Germany to Kokee, Hawaii baseline) are typically made Monday through Friday. Starting in August 2005, Wetzell has transferred their data electronically to a location near the USNO, reducing data transfer to about 1 day, allowing Int1 experiments to be reduced with only 2 days of latency. The Int2 intensive, using the Wetzell, Germany to Tsukuba, Japan baseline, also benefited from e-VLBI. The observations collected on Saturday and Sunday are correlated at Tsukuba, Japan via e-VLBI, and the weekend solutions are usually available on Monday.

The ILRS series A and IGS Ultras were added, and two other series were dropped (the Center for Space Research (CSR) and the Delft University of Technology (DUT) SLR) as inputs to the combination software. Note, only IGS Ultra polar motion data which are more recent than the IGS Rapid data are included in the combination. Previously, extrapolated IGS Rapids were used to estimate polar motion beyond the last IGS Rapid point.

As shown in Figure 1, IGS Rapid data are produced daily, and the epoch is at noon UTC the day before the IERS RS/PC daily solution is run. Previously, pseudo-points were created by the RS/PC ± 6 hours from noon UTC using the rate and polar motion value at noon. However, starting in July 2007, the IGS Ultra data replaced these extrapolated Rapid values, since the accuracy of the Ultras is better than the pseudo-points. As shown in Figure 3, for close to 4000 days both extrapolated Rapid and Ultra polar motion were compared with the IGS Finals data. The resulting residuals computed using Ultra are significantly lower than the residuals using extrapolated Rapid data. Note, to simplify the analysis, the extrapolated Rapids used to produce Figure 3 were not computed at the 6 and 18 hour epochs, shown in Figure 1; they were computed at epochs to match the Finals data epochs (e.g., at D0 + 12 and D1 + 12). The possibility of using Ultra LOD in the combination procedure is a continuing topic of research.

4. PREDICTION PROCEDURE

The UT1-UTC predictions benefited from faster turnaround times provided by e-VLBI intensives. The least-squares, autoregressive algorithm for polar motion, which was developed by W. Kosek in the 1990s (and later enhanced by T. Johnson) was implemented. AAM data were improved with the addition of the NOGAPS series; this series was combined with the existing NOAA series for a more robust AAM estimation. Also, the NOGAPS and NOAA recently extended the predictions from 5 to 7.5 days potentially increasing the accuracy of the RS/PC UT1 short-term predictions. Lastly, improved AAM diagnostics, in the form of LOD residuals, will be implemented in the future.

5. PREDICTIONS OF POLAR MOTION DATA USING LS-AR

As shown in Figure 2, the polar motion prediction algorithm uses polar motion data from the C04 series, from 1962 to 1973, and the USNO combination data from 1973 to the present. From this data, a median linear fit is created, thus determining a long-term bias and slope. The median fit (as opposed to least squares) is used because of its robust characteristics regarding odd outlier points. It determines the line coefficients which minimize the 1-norm of the error, i.e., finds the minimum of the merit function

$$\Sigma_{i=1}^{N} |y_i - a - bx_i| \tag{1}$$

where, in this case, y_i is the polar motion from the C04 and USNO combination data, a is y-intercept of the line, and b is the slope. The least squares approach would minimize the following merit function,

$$\Sigma_{i=1}^{N} (y_i - a - bx_i)^2. \tag{2}$$

In the least squares case, the odd outlier would have a squared contribution to the merit function of equation (2), as opposed to the non-squared contribution to the merit function in (1). This line is then subtracted from the data, and the resulting residuals are the input to a least-squares (LS) routine to determine significant periodic signals, namely, the Chandler period (433 days), annual (365.2442 days), semiannual, terannual, and $\frac{1}{4}$ annual. These periodic signals are then also subtracted from the residuals, yielding a polar motion minus median fit and periodic signals. The result contains primarily stochastic characteristics, which are fed into an autoregressive forecasting process to generate a predicted signal. The Chandler, annual, and semiannual, bias and slope signals are then added back to the predicted signal, yielding a prediction of the polar motion.

6. IMPROVED PREDICTIONS WITH RECENTLY EXTENDED AAM DATA

The flowchart in Figure 4 illustrates the RS/PC process of obtaining, analyzing, and combining AAM analysis and forecast data from both the NOGAPS and NOAA $\chi_3^{(w)}$ and $\chi_3^{(p)}$ values to estimate the LOD. These χ_3 values are the effective wind and pressure AAM functions related to Earth rotation. First, analysis and forecast files are obtained from Navy and NOAA ftp sites. Preliminary checks on data quality are performed, and for any data files that are missing or corrupt, estimates are created based on the previous day's set of analysis and forecast files. Note that the estimated data files would, of course, be less accurate than the computed versions from the Navy and NOAA. Fifteen days of past analysis and 7.5 days of forecast data are read into each of the RS/PC processing software for the Navy and NOAA data. The 15 analysis and 7.5 forecast days are combined into a continuous series and then filtered twice with a 5 point Hanning window to filter out high frequency noise.

Once the filtered Navy and NOAA χ_3 values are created, if both are determined to be valid and not estimated values, they are simply averaged together to get a combined χ_3 . If any of the Navy or NOAA values are estimated, then that value is de-weighted by 50%. For example if some of the Navy data were estimated over the 15 analysis and 7.5 forecast days, and the NOAA data were not estimated, then the equation for the averaging would be

$$\chi_{3comb} = 0.25 * \chi_{3Navy} + 0.75 * \chi_{3NOAA}. \tag{3}$$

In rare cases when neither estimate nor provided values (from Navy or NOAA) are available, then that missing value will result in a weight of 0.0. For example if no NOAA data were available, then the overall χ_3 value would be computed as follows:

$$\chi_{3comb} = 1.0 * \chi_{3Navy} + 0.0 * \chi_{3NOAA}. \tag{4}$$

If both Navy and NOAA values are estimated, the weighting is slightly toward the NOAA data:

$$\chi_{3comb} = 0.4 * \chi_{3Navy} + 0.6 * \chi_{3NOAA}. \tag{5}$$

The combined χ_3 values are then integrated to form a UT1 estimate, which is used in the combination and prediction software. The AAM data receive a low weight in the combination calculations, but form the basis for UT1 predictions out to 7 days.

7. INTERFACE WITH USERS

The archive notes available through the web pages (http://maia.usno.navy.mil/ser7/archive.notes) have been reinstated. The archive notes are intended to document all changes in data sets and algorithms that are made to the combination and prediction software. These should give a summary of all changes that could potentially impact the quality and reliability of the RS/PC solution. They provide the date and a description of the event so that users of RS/PC data can determine when significant changes were made. The RS/PC has continued to maintain close contact with contributors to and users of the RS/PC solution. On a daily basis, the input data sets are scrutinized and any unusual feature examined to ensure data quality; potential problems are reported to the appropriate contributor in a timely fashion. Communication with RS/PC users is encouraged so that their changing needs are understood. To ensure the reliability of the RS/PC solution, a plan to expand our redundant off-site computer capability is being implemented; it currently includes the acquisition and setup of off-site hardware. There is also a need to rewrite the combination and prediction software to maximize its portability. It is estimated that the hardware and software will be ready for remote operations in the next calendar year.

8. FUTURE DIRECTIONS

In the near future, the EOP RS/PC will be working toward establishing an operational backup at a remote location, establishing increased version control of the combination and prediction software, creating more helpful diagnostics of AAM inputs, and upgrading and enhancing its web pages. Further into the future, using additional AAM data sets in the predictions, IGS Ultra data in the determination of LODs, AAM data in the polar motion predictions, and more extensive e-VLBI use to reduce latency in EOP combinations, are on the agenda.

9. REFERENCES

Wooden, W.H., Johnson, T.J., Kammeyer, P.C., Carter, M.S., Myers, A.E., (2005) "Determination and Prediction of UT1 at the IERS Rapid Service/Prediction Center," Journées Systèmes de Référence Spatio-Temporels 2004, pp 260-264.

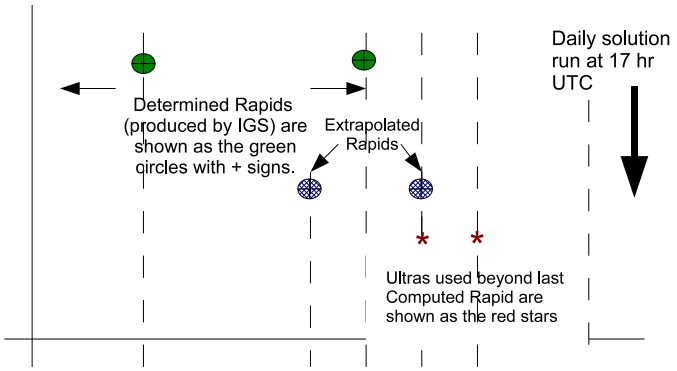

Figure 1: Replacement of Extrapolated Rapid with IGS Ultra Data

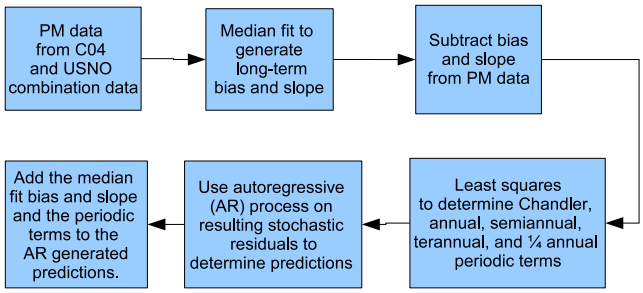

Figure 2: Polar Motion Least Squares / Auto Regression (LS/AR) Polar Motion Prediction Algorithm

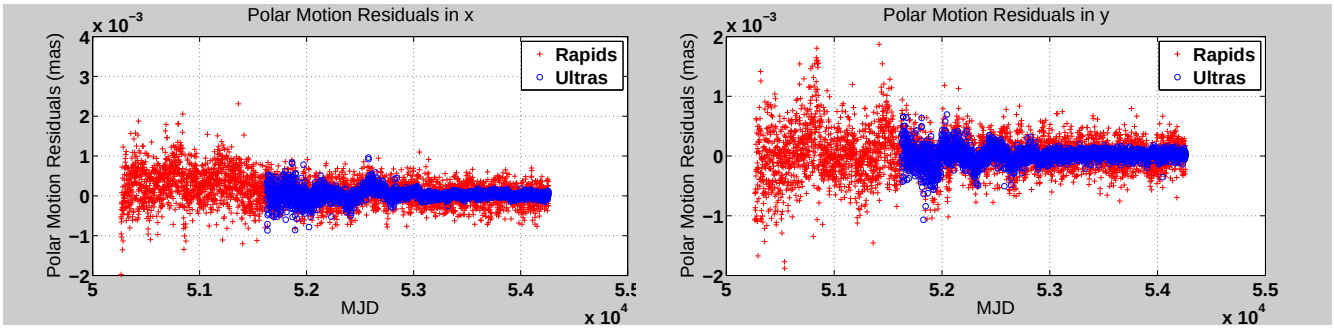

Figure 3: Polar Motion X and Y Residuals – Extrapolated IGS Rapid vs. Ultra data

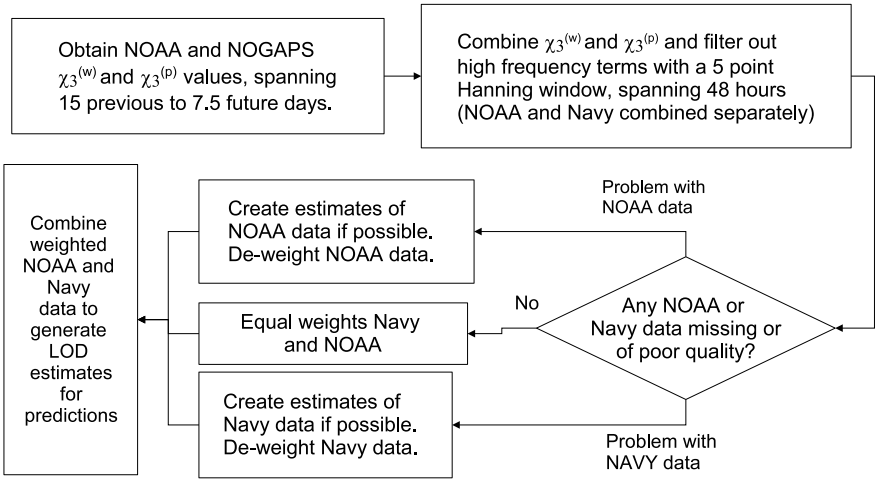

Figure 4: LOD Estimation Details

GGOS-D: A GERMAN PROJECT ON THE INTEGRATION OF SPACE GEODETIC TECHNIQUES

A. NOTHNAGEL[1], M. ROTHACHER[2], D. ANGERMANN[3], T. ARTZ[1], S. BÖCKMANN[1], W. BOSCH[3], H. DREWES[3], M. GERSTL[3], R. KELM[3], M. KRÜGEL[3], D. KÖNIG[2], R. KÖNIG[2], B. MEISEL[3], H. MÜLLER[3], B. RICHTER[4], N. PANAFIDINA[2], S. RUDENKO[2], W. SCHWEGMANN[4], P. STEIGENBERGER[2], V. TESMER[3], D. THALLER[2]
[1] Institut für Geodäsie und Geoinformation der Universität Bonn (IGGB)
Nußallee 17, D-53115 Bonn, Germany
e-mail: nothnagel@uni-bonn.de
[2] GeoForschungsZentrum (GFZ)
Telegrafenberg D-14473 Potsdam, Germany
[3] Deutsches Geodätisches Forschungsinstitut (DGFI)
Alfons-Goppel-Straße 11, D-80539 München
[4] Bundesamt für Kartographie und Geodäsie (BKG)
Richard-Strauß-Allee 11, D-60598 Frankfurt am Main, Germany

1. INTRODUCTION

Since September 2005 the German Ministry for Research and Education has been funding a group of scientists at GeoForschungsZentrum (GFZ Potsdam), Deutsches Geodätisches Forschungsinstitut (DGFI Munich), Bundesamt für Kartographie und Geodäsie (BKG Frankfurt am Main) and Institut für Geodäsie und Geoinformation der Universität Bonn (IGGB Bonn) in a project related to the integration of space geodetic techniques. These groups comprise experience in GPS, SLR, and VLBI observing techniques as well as in satellite altimetry, global gravity field investigations and large scale combinations. They cooperate with the aim to investigate the production of reference frames and related time series which are consistent across techniques by adapting software packages to common standards and by refining combination procedures. Since the aims of the project closely resemble the general ideas of the GGOS initiative (Global Geodetic Observing System) by the International Association of Geodesy (IAG), the group has gathered under the acronym GGOS-D.

Parameter Type	VLBI	GPS/GLON.	SLR	Altimetry
Quasar Positions (CRF)	x			
Nutation	x	(x)	(x)	
Polar Motion	x	x	x	
UT1	x			
Length of Day	x	x	x	
Ionosphere	x	x		x
Troposphere	x	x		x
Coord. & Velocity (TRF)	x	x	x	(x)
Geocenter		x	x	x
Satellite Orbits		x	x	x
Gravity Field		x	x	x

Table 1: Recent parameter space for rigorous combination.

2. CURRENT STATUS

Space geodetic observing techniques like GPS, SLR, and VLBI, as well as satellite altimetry and satellite gravity missions are sensitive to a certain set of parameters and in this have strengths as well as limitations. Combining these techniques and their results will ultimately lead to a consistent set of

parameters which will be superior to one from individual techniques alone. In Table 1 all techniques and their sensitivities to the respective parameters are depicted linking the inertial reference frame of the quasar positions via the satellite orbits to the low degree harmonics of the gravity field through a cascading of the information through intermediate levels of observations.

In order to prepare for a consistent and rigorous combination across techniques a number of organisational issues had to be decided on first. Since the group possesses expertise in several space geodesy analysis software packages it was decided that two packages each for VLBI, GPS and SLR be used in this project. The other techniques are represented just once each (see Tab. 2). The set of parameters to be combined has been selected to include whatever is supposed to be identical. For this, most of the analysis software packages had to be augmented so that each of them is able to generate datum-free normal equations in SINEX format with the full parameter space at pre-defined reference epochs. This is of particular importance for quickly changing effects like the atmosphere where non-identical epochs would require interpolations which introduce an additional level of noise.

The identification of systematic errors of the individual techniques is a necessary step towards optimal results which has to be done before the observations of all techniques can be combined consistently. The first step here is that all techniques are analysed on the basis of the same geophysical models. For this reason a catalogue has been established listing all models which are to be used in the different software packages. When the combination will have been carried out other systematic effects may become obvious and will have to be taken care of.

Technique (Software)	Site Coord.	UT1/ LOD	Nut.	C_{nm}/ S_{nm}	Geo-center	Trop. ZD	Trop. Grad.	Range Bias	Radio Source Positions
VLBI (OCCAM)	x	x	x			x	x		x
VLBI (Calc/Solve)	x	x	x			x	x		x
GPS (Bernese)	x	x	x		x	x	x		
GPS (EPOS)	o	o	o		(o)	o	o		
SLR (DOGS-OC)	x	x		x	(x)			x	
SLR (EPOS)	x	x		x	(x)			x	
LEO	x	o		x	(o)				
Altimetry	(x)	(o)		(x)	(x)				

Table 2: GGOS-D Extended Parametrization (x: realized; o: planned); C_{nm}/S_{nm} = Low degree harmonics of the gravity field, ZD = Zenith Delay, LEO = Low Earth Orbiters.

Some of the analysis software packages are being modified specifically for this very purpose since the extended list of parameters is normally not foreseen for standard use. In some cases the solution setup is heavily over-parametrized which leads to singularity of the normal equation system. However, since the SINEX files are only generated for further combination steps, singularity in the stand-alone files are not critical. The full strength of each technique will only be activated when the combination is carried out and datum information will be carried over from the technique most sensitive to the respective datum parameter.

3. OUTLOOK

In the next few months, a consistent terrestrial reference frame will be generated from a rigorous combination of all software packages in use by the collaborators. This will be the basis to compute consistent time series of all parameters which will be analyzed in further detail. We expect that these time series will show a much better agreement than any other existing combination products because models and parametrizations have been laid out specifically for the purpose of combination. The GGOS-D project will, thus, produce some very valuable insights in the processes and requirements necessary for the establishment of a Global Geodetic Observing System.

THREE-YEAR SOLUTION OF EOP BY COMBINATION OF RESULTS OF DIFFERENT SPACE TECHNIQUES

V. ŠTEFKA[1], I. PEŠEK[2], J. VONDRÁK[1]
[1] Astronomical Institute, Academy of Sciences of the Czech Republic
Boční II, 14131 Prague 4, Czech Republic
e-mail: stefka@ig.cas.cz, vondrak@ig.cas.cz
[2] Dept. of Advanced Geodesy, Faculty of Civil Engineering, CTU in Prague
Thákurova 7, CZ-16629 Prague
e-mail: pesek@fsv.cvut.cz

ABSTRACT. The method of non-regular combination of results of different techniques, namely GPS, VLBI, SLR and Doris, to obtain unique values for both the Earth orientation parameters (EOP) and the station coordinates needs the EOP at the adjacent epochs to be suitably constrained to each other. Modified smoothing algorithm was used as this constraint. Weighting controls smoothness of the combined EOP, so that it can also be used to filter out undesirable frequencies from the solution. To do it, a transfer function was empirically estimated from two combinations of EOP and used to compute three-year solution. The result is compared with IERS c04 series and presented here.

1. INTRODUCTION

Orientation of the Earth's body in space is described by five angles, called Earth orientation parameters, EOP, which tie the Earth-fixed coordinate system ITRF to the celestial reference frame. The EOP are two coordinates of the intermediate pole with respect to the ITRF, x_p, y_p, a time correction $UT1-UTC$, which characterizes irregularity of the Earth's proper rotation and, finally, two components of the celestial pole offset, dX, dY, which denote the observed corrections to the adopted precession-nutation model (they are not considered in the present paper because they are measured only by one technique, VLBI). International reference frame ITRF is realized by geocentric rectangular coordinates of reference points of a set of stations (observatories) equipped by one or more high precision observation techniques.

The space geodesy techniques used to produce the EOP and station coordinates are Global Position System (GPS), Very Long-Baseline Interferometry (VLBI), Satellite Laser Ranging (SLR), and recently also Doris, all of them working with a high internal accuracy. The individual techniques, though, are referred to different standards and constants, and use different mathematical models, so that their results suffer form mutual systematic differences and biases.

For deriving a function from scattered data, a smoothing (Vondrák, 1977) is widely used. The method is designed to find the most probable function values as a compromise between the least squares fit and the demanded function's smoothness. We implemented this smoothing to the non-rigorous combination (Štefka and Pešek, 2007) as a more sophisticated approach to tie EOP at the adjacent epochs. Before using the method with real observations, we tested it with simulated data in order to derive a transfer function.

2. NON-RIGOROUS COMBINATION

The basic idea of the method is to combine station position vectors, x_C, in the celestial reference frame (Pešek and Kostelecký 2006). These vectors are functions of both the Earth orientation parameters and the station coordinates x_T,

$$x_C = PN(t)R_3(-GST)R_1(y_p)R_2(x_p)x_T, \tag{1}$$

where $PN(t)$ is precession-nutation matrix and R_i is the matrix of rotation around the i-th axis. Input data for the combination consist of M sets of EOP $(x_p, y_p, UT1-UTC, dX, dY)_m$ and corresponding sets of station coordinates $x_m, m = 1, ...M$, as derived by analysis centers for individual techniques.

To make the combination more stable, parameters $p = p_1, ...p_7$ of a individual seven-parametric transformation formula are derived for each technique, instead of corrections to the station coordinates themselves.

The partial derivative of the formula (1) with respect to U, which stands for any unknown parameter (EOP and p), yields observation equations of the form

$$\sum_{m=1}^{m=M} \frac{\delta x_C}{\delta U_m} dU_m = x_{C|obs} - x_{C|0} + v, \tag{2}$$

where the "observed" vectors $x_{C|obs}$ are calculated from the respective input solution, $x_{C|0}$ are functions of adopted a priori values of the unknowns.

To remove singularity of the system (2), a no net-rotation constraint, minimizing mutual shifts and preserving the system as a whole, has to be introduced,

$$\sum p^T p = min, \tag{3}$$

which stabilizes calculating the station coordinates. On the other hand, Earth orientation parameters are calculated for each individual epoch independently of the others. As a consequence, errors in the input data, including station coordinates, are transferred to the EOP and increase their scatter substantially. The effect can be reduced by including constrains, in the form of additional observation equations (pseudo-observations), that tie the values of the respective EOP at adjacent epochs, here denoted generally as E. In the original method they were used

$$dE_i - dE_{i-1} = E_{i-1} - E_i + v. \tag{4}$$

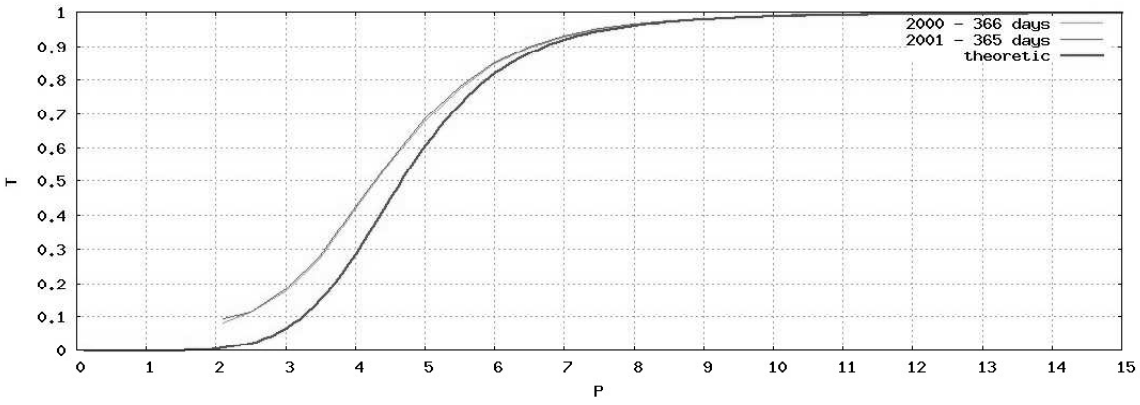

Figure 1: The comparison of the computed transfer functions with the theoretic one. The choice of the numerical value of ϵ was calculated by the formula (7), where $P_{0.99} = 10$ days and $p = 1$

3. AN IMPROVEMENT IN THE LATTER METHOD

The improvement was done by implementation of a method of smoothing (Vondrák 1977). It consists of replacing constraints (4) by the third derivatives of third-order Lagrange polynomial $L_i(x)$ running through the four adjacent points i, $i+1$, $i+2$, $i+3$, i.e.

$$L_i''' = \sum_{k=0}^{3} \left(6 \prod_{j=0, j\neq k}^{3} \frac{1}{(x_{i+k} - x_{i+j})} \right) E_{i+k}. \tag{5}$$

By assigning a weight w to these constrains (5), we can control a smoothness of each series of unknowns x_p, y_p and $UT1 - UTC$, respectively. The following rule applies: the bigger the weight w, the smoother is the solution. That means that we can use three different values of w (w_1, w_2, w_3), for the three EOP´s, but here we use simply $w = w_1 = w_2 = w_3$.

4. CHOICE OF WEIGHT OF SMOOTHING

To study a relation between the weight and smoothness, we supposed that the observation equations (2) can be expressed as a sum of several periodic functions. Each term can then be smoothed separately and the resulting smoothed function expressed as the sum of individual smoothed terms. Then, by changing values on the RHS of the observation equations in order to simulate a signal with a known period P and amplitude A, we can compute a transfer function T (i.e., the ratio between the amplitude of the smoothed curve and the observed amplitude of a periodic function with frequency f).

Two solutions of transfer functions were computed from independent data sets, each covering a year period, 2000 and 2001, respectively. Both solutions are displayed in Fig. 1 and compared with a modified analytical formula proposed by (Huang&Zhou 1981, 1982) as

$$T = \frac{\epsilon P^6}{61529p + \epsilon P^6}, \tag{6}$$

where p is an average weight of E_i. Alternatively, different formula holds for calculating both coeficients (ϵ and w) if we wish to pass 99% of the amplitude of the periodic process with period $P_{0.99}$ (corresponding to $T = 0.99$):

$$\frac{1}{w(P_{0.99})} = \epsilon(P_{0.99}) = 99p \left(\frac{2\pi}{P_{0.99}}\right)^6. \tag{7}$$

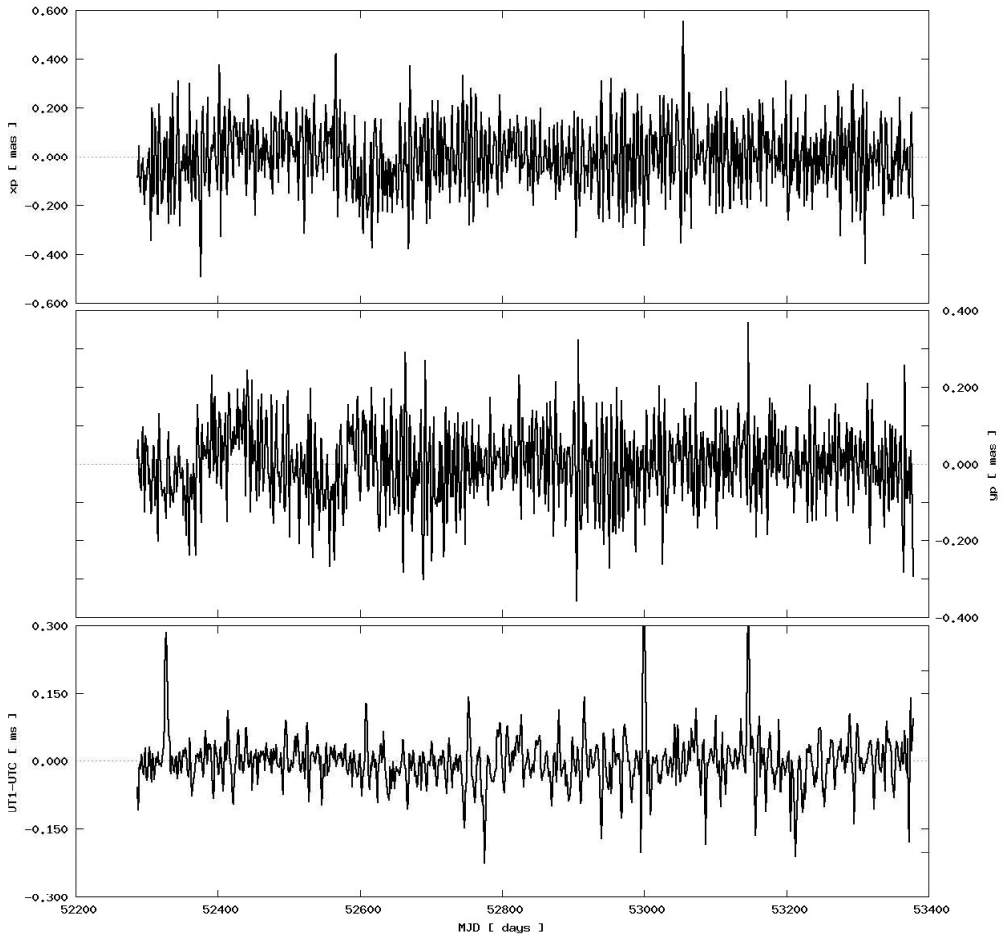

Figure 2: Three-year solution was computed, using $w = 150$, and compared with IERS c04 series. Differences are 0.129 mas, 0.102 mas and 0.0536 mas for the polar motion x_p (top), y_p (center), and the time correction $UT1 - UTC$ (bottom), respectively.

5. DATA AND NUMERICAL SOLUTION

The latter method was tested with the following data: GPS and VLBI data were taken from the IERS Combination Pilot Project database. For SLR, the constrained *ilrsb* solution was used, as published by ILRS analysis centre. Both GPS and SLR are weekly Sinex solutions, from which the EOP and station coordinates were extracted. VLBI data consists of per seance singular normal equation matrices. They were regularized by constraining the station coordinates to the VTRF 2005 frame (Nothnagel, 2005) with the a priori precision of 5 mm. As none of the techniques currently provides the database with the celestial pole offset, only the x_p, y_p, and $UT1-UTC$ are solved for. The techniques enter the combination with the following weights: 1.44 for GPS, 0.8 for SLR, and 1.0 for VLBI. Out of these weights, we used the weight of the constraints for smoothness (5) equal to $w = 150$, assuming there is 99% signal with period greater than 4 days. Three-year solution produced by this method was compared with the IERS c04 series, and the results are displayed in Fig. 2.

6. CONCLUSION

A method for non-rigorous combination of the results of different space geodesy techniques to obtain representative sets of the Earth orientation parameters was modified by implementing the Vondrák´s smoothing. This was done by replacing a simple formula (4) by a more complex one (5), in the level of observation equations. Transfer functions of our method, which was empiricaly computed from two combination of EOP, is in good agreement with the theoretical one. Finally, three-year solution of combination of EOP was calculated, using $w = 150$ to ensure that there is 99% signal with a period greater than 4 days in the solution, and compared with IERS c04 series. The rms differences are 0.129 mas, 0.102 mas and 0.0536 mas for the polar motion x_p, y_p, and the time correction $UT1 - UTC$, respectively.

Acknowledgements. This study was supported by the grant LC506 awarded by the Ministry of Education, Youth and Sports of the Czech Republic.

7. REFERENCES

Huang Kun-Yi; Zhou Xiong: "On the essentiality of the Whittaker-Vondrák method as a filter, and estimations of standard deviations and correction for digital computer", Acta Astron. Sinica 22 (1981), 120.

Huang Kun-Yi; Zhou Xiong: "A new definition in the design of digital filter and the variational solution about extended Whittaker problem", Asta Astron. Sinica 23 (1982), 280.

Nothnagel, A., 2005: VTRF2005 – "A combined VLBI Terrestrial Reference Frame". `http://miro.geod.uni-bonn.de/vlbi/IVS-AC/`

Pešek, I. and Kostelecký J., 2006: "Simultaneous determination of Earth orientation parameters and station coordinates from combination of results of different observation techniques", Stud. Geophys. Geod., 50 (2006), pp. 537–548.

Štefka V. and Pešek I., 2007: "Implementation of the Vondrák's smoothing in the combination of results of different space geodesy techniques", Acta Geodyn. Geomater., Vol. 4, No. 4 (148), 129-132.

Vondrák, J., 1977: "Problem of smoothing observational data II", Bull. Astron. Inst. Czechosl., 28, pp. 84–89.

ADVANCES IN INERTIAL EARTH ROTATION MEASUREMENTS - NEW DATA FROM THE WETTZELL G RING LASER

T. KLÜGEL[1], U. SCHREIBER[2], W. SCHLÜTER[1], A. VELIKOSELTSEV[2]
[1] Bundesamt für Kartographie und Geodäsie
Fundamentalstation Wettzell, Sackenrieder Str. 25, D-93444 Bad Kötzting
e-mail: thomas.kluegel@bkg.bund.de, wolfgang.schlueter@bkg.bund.de
[2] Forschungseinrichtung Satellitengeodäsie, TU München
Fundamentalstation Wettzell, Sackenrieder Str. 25, D-93444 Bad Kötzting
e-mail: schreiber@fs.wettzell.de, alex@fs.wettzell.de

1. INTRODUCTION

Ring lasers are a new type of instrument in geodesy to measure variations in Earth rotation. The scope is to obtain complementary measurements to the geodetic space techniques like VLBI (Very Long Baseline Interferometry), SLR (Satellite Laser Ranging), or GNSS (Global Navigation Satellite Systems). Employing a completely different type of measurement, they yield different components of the Earth's rotation. While the geodetic space techniques perform a relative measurement to determine the rotation matrix between the Earth and the observed objects, ring lasers measure the absolute spin rate and are sensitive to motions of the rotation axis with respect to the Earth. They are not sensitive to motions of the rotation axis in space. Thus ring lasers give direct access to polar motion. Other aspects comprise the high temporal resolution for a better sampling of subdaily variations, the continuous operation and the real time availability of the data.

2. THE WETTZELL RING LASER G

The Wettzell ring laser "G" is in operation since 2001. The basic principle and the technical realisation is described in Klügel et al. (2005) or at http://www.fs.wettzell.de/LKREISEL/G/LaserGyros.html. The unique resolution and stability was reached by a vastly expanded cavity size of 4 m x 4 m, an extreme mechanical and thermal stability resulting from the use of the glass ceramic Zerodur as base material, the use of low-loss dielectric supermirrors, and the operation in an underground installation.

However it was found that the long term stability of the Sagnac frequency suffered from a variable gain of the laser medium by outgassing of impurities like hydrogen or water from the inner stainless steel surfaces of the laser cavity enclosure. As a consequence the vacuum system has been modified in 2006 by replacing the old 50 mm tubes by 150 mm tubes in order to increase the ratio between gas volume an steel surface. In addition a getter tank has been installed to absorb gas impurities. Further modifications include the replacement of a rubidium frequency standard by a reference frequency coming from a hydrogen maser, and the stabilisation of the control loop steering the power of the laser excitation by installing it in a thermally stable environment.

3. THE NEW TIME SERIES

After the thermal perturbation due to the construction had died out, a continuous time series from August 2006 till March 2007 of outstanding quality was obtained. Varying drift rates and unregular excursions of the Sagnac signal, as could be observed in the former time series, are now strongly reduced (figure 1). The instrumental drift now changes gradually mostly due to thermal relaxation. The amplitude spectrum reveals a noise reduction in the entire spectral range (figure 2). The periodic signals around 1 and 2 cycles per day (cpd), being an effect of diurnal polar motion and local tidal tilts, come out with a much better signal to noise ratio.

For the acquisition and processing of the new time series, the following steps had been performed:

- Data acquisition using a frequency counter integrating over 30 minutes

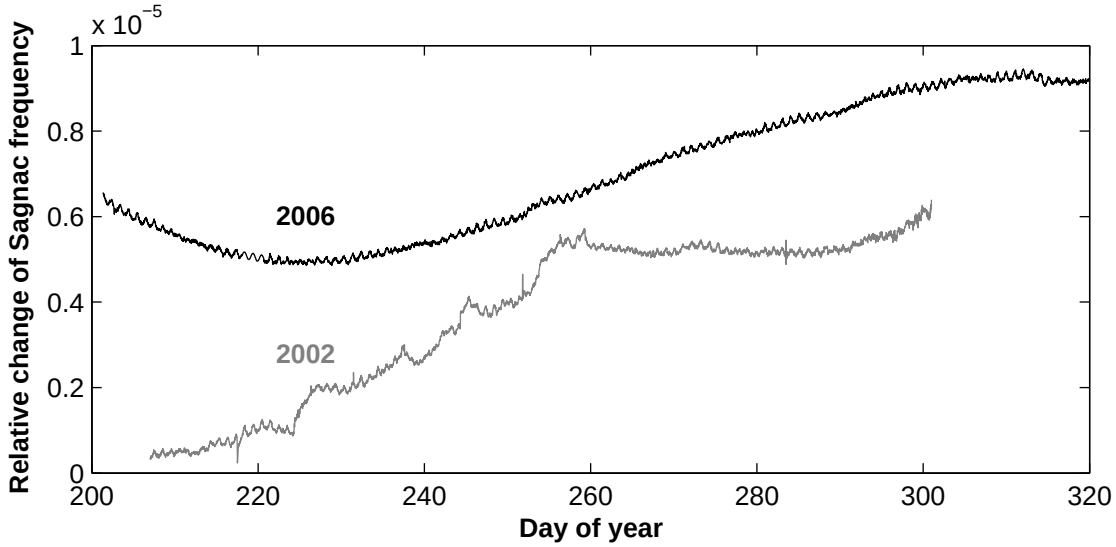

Figure 1: Ring laser time series before and after the modifications

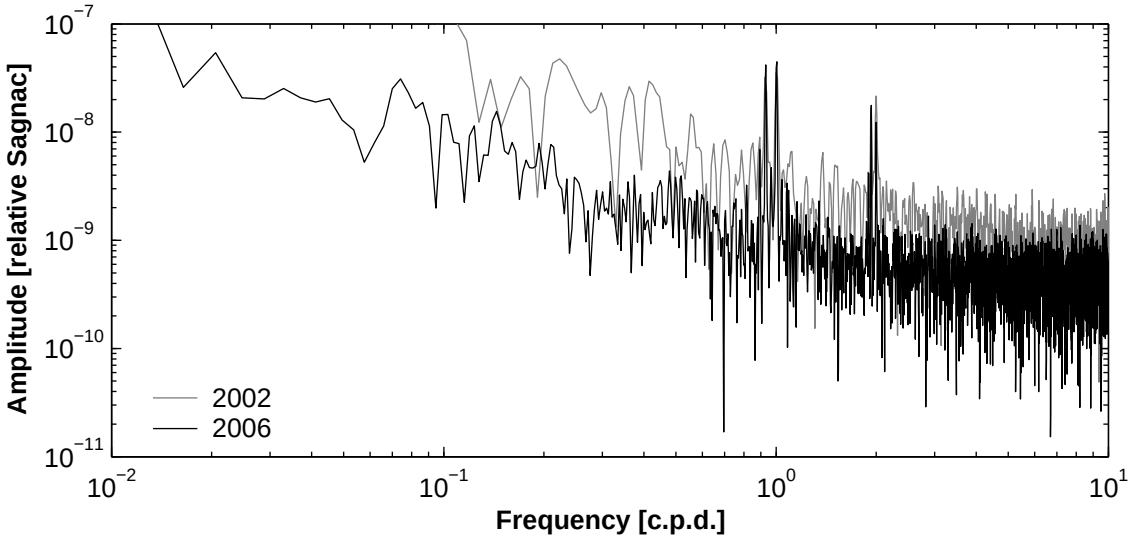

Figure 2: FFT amplitude spectrum demonstrates significant noise reduction in the entire spectral range

- Removal of outliers and resampling to 30 minutes
- Correction for local tilts using tiltmeters on top of the ring laser having a resolution of less than 0.1 mas, which themselves are corrected for tidal attraction and thermal effects
- Correction for instrumental effects like drifts due to pressure-induced temperature variations
- Spectral analysis using multiple Fourier transformations in order to increase frequency resolution
- Correction for diurnal polar motion, using the 21 largest terms from Brzezinski (1986), or
- Amplitude estimation of diurnal polar motion terms using (1) Matlab least square fit, (2) routine ERPEST of Bernese GPS software, (3) Eterna Earth tide analysis program

The amplitude spectrum of the raw time series (figure 3, left) shows that the 7 tidal components Q1, O1, M1, P1, K1, J1 and OO1 can be identified in the diurnal band. The amplitudes are generally somewhat bigger than the values taken from the Brzezinski (1986) polar motion model (plus signs). This is mainly an effect of local tidal tilts being responsible for the tidal signals in the semidiurnal band and

a fraction of the signals in the diurnal band. After removing the tidal tilt by applying the tiltmeter correction, the tidal signals in the semidiurnal band nearly completely vanish, and the amplitudes in the diurnal band are reduced close to the model values (figure 3, right). The signal at exactly 2 cpd is assumed to be of atmospheric origin (see below and Schreiber et al. 2003). The reason for the remaining signal at 1.932 cpd (M2 tidal wave) is not yet clear; it can be either due to an incomplete tidal tilt correction, or an effect of the ocean tides on polar motion or rotation speed.

Another signal is visible at exactly 3 cpd (8 hours). Signals having a period of 8 hours have also been reported in VLBI observations (e.g. Schuh 2007) or in GPS observations (e.g. Steigenberger 2007). Although there is strong evidence for air pressure effects (VLBI) or artefacts due to 24h binning (GPS), the origin of these signals is not definitely resolved. In the case of the ring laser the 8 hour signal can be removed by subtracting the ring laser temperature record, multiplied by an arbitrary factor, from the ring laser time series. As the air pressure is the main source of temperature variations in the ring laser lab, the 12 hour atmospheric oscillation and its harmonics (8 hours, 6 hours,..) are prominent in the temperature records. The local air pressure record however is not suitable to correct the ring laser time series due to the phase lag between air pressure and temperature. Hence the 8 hour signal is identified as an instrumental thermal effect of the ring laser.

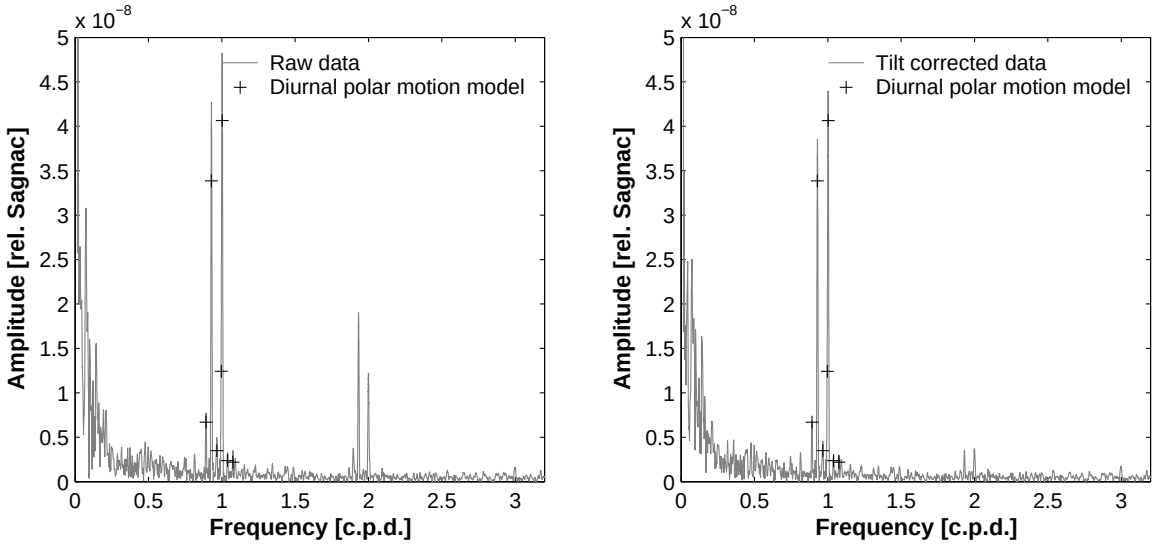

Figure 3: FFT amplitude spectrum of raw (left) and tilt corrected data (right), time series over 243 days

4. ESTIMATION OF DIURNAL POLAR MOTION TERMS

Because ring lasers are not sensitive to nutations in space, they have the unique capability to directly measure the quasi-diurnal motions of the instantaneous rotation axis with respect to the Earth's body due to the torques of Sun and Moon (Schreiber et al. 2004). The amplitude estimation of the 7 identified diurnal polar motion constituents (see above) has been done in terms of least squares fits of sinusoidal functions of given frequencies using different software tools. First the MatLab least square fit of Fourier type has been used. The resulting amplitudes of the tilt corrected time series are closer to the model values than those of the raw data (table 1). A previously injected signal having an amplitude of 1 mas and a frequency of 1.5 cpd came out with an amplitude of 1.01 mas after the fitting routine. This indicates that the fitting process works reliable. Second the Earth rotation parameter estimation routine ERPEST of the Bernese GPS software 5.0, which had been modified in order to process ring laser data, was applied. Third the Earth tide analysis package Eterna 3.4 has been used for the estimation of amplitudes and phase lags. For this purpose the ring laser time series was treated like a tidal potential just to get the amplitude and phase information, neglecting effects of tidal deformation.

All three kinds of fitting procedures give similar results. The Eterna fit yields somewhat smaller amplitudes, but the estimated errors are bigger and seem to be more realistic than the formal Bernese errors. With the exception of the tidal wave O1, all model amplitudes are within the 2σ error bar of the

estimated polar motion amplitudes. The model amplitudes represent not the denoted constituent alone, but comprise the sum of all model amplitudes within +/- 0.002 cpd around the constituent frequency. The reason is that the frequency resolution of the time series is 0.004 cpd, being the sampling interval (48 per day) divided by the number of samples (11664). Thus all constituents within this interval contribute to the estimated amplitude.

Astronomical arguments						Darwin	Frequency	MatLab		Bernese		Eterna		Model
l	l'	F	D	Ω	Θ	symbol	[c.p.d.]	raw data ampl.	tilt cor. ampl.	tilt corrected ampl.	rms	tilt corrected ampl.	stdev	
1	0	2	0	2	-1	Q1	0.8932	1.82	1.61	1.53	0.07	1.24	0.16	1.59
0	0	2	0	2	-1	O1	0.9295	9.78	8.83	8.65	0.07	7.51	0.16	8.08
1	0	0	0	0	-1	M1	0.9664	1.32	1.24	1.19	0.07	0.84	0.12	0.83
0	0	2	-2	2	-1	P1	0.9973	3.18	2.87	2.94	0.07	2.70	0.19	2.96
0	0	0	0	0	-1	K1	1.0027	10.60	9.66	10.06	0.07	9.28	0.17	9.69
-1	0	0	0	0	-1	J1	1.0390	0.78	0.63	0.66	0.07	0.89	0.16	0.57
0	0	-2	0	-2	-1	OO1	1.0759	0.89	0.78	0.67	0.07	0.45	0.09	0.52
Synthetic signal (1 mas)							1.5000	1.03	1.01					

Table 1: Estimated amplitudes in milliarcseconds of 7 diurnal polar motion terms

5. SUMMARY AND OUTLOOK

The performance of the Wettzell ring laser has been significantly improved in 2006. The average noise level at subdaily frequencies is less than 10^{-9}. The recent detection limit for subdaily signals is 0.4 milliarcseconds (2 nanorad) for polar motion or 0.15 milliseconds for length of day. The amplitudes of the 7 diurnal polar motion terms Q1, O1, M1, P1, K1, J1 and OO1 has been reliably determined with formal errors less than 0.1 mas (Bernese) or 0.2 mas (Eterna).

Regarding the technical feasibility for further improvements like the stabilization of the optical frequency, there is still potential for an increase in resolution and stability, that the determination of diurnal polar motion terms with higher precision and the detection of high frequency UT1 variations due to ocean tides or atmosphere might be possible in future.

6. REFERENCES

Brzezinski A., 1986, "Contribution to the theory of polar motion for an elastic earth with liquid core", Manuscripta Geodaetica, 11, pp. 226–241.

Klügel T., Schlüter W., Schreiber U., and Schneider M., 2005, "Grossringlaser zur kontinuierlichen Beobachtung der Erdrotation", Zeitschrift für Vermessungswesen, 130(2), pp. 99–108.

Schreiber, U., Klügel, T., Stedman, G. E., 2003, "Earth tide and tilt detection by a ring laser gyroscope", J. Geophys. Res. , 108 (B2), 10.1029/2001JB000569.

Schreiber U., Velikoseltsev A., Rothacher M., Klügel T., Stedman G.E., and Wiltshire D.L., 2004, "Direct measurement of diurnal polar motion by ring laser gyroscopes", J. Geophys. Res. , 109 (B6), 10.1029/2003JB002803, B06405.

Schuh H., 2007, "The intricacies of high-frequency polar motion and universal time variations: status report of the SPEED project", Status seminar Earth Rotation and Global Dynamic Processes, Dresden.

Steigenberger, P., 2007, "GPS-derived long time series of sub-daily Earth rotation parameters", Status seminar Earth Rotation and Global Dynamic Processes, Dresden.

ATMOSPHERIC EXCITATION OF EARTH ROTATION/ POLAR MOTION AT HIGH TEMPORAL RESOLUTION

D.A. SALSTEIN[1], J. NASTULA[2], K. QUINN[1], D. MACMILLAN[3], P.J. MENDES CERVEIRA[4]
[1] Atmospheric and Environmental Research, Inc
131 Hartwell Ave., Lexington, MA 02468 USA
e-mail: salstein@aer.com, kquinn@aer.com
[2] Space Research Center of the PAS
Bartycka 18a, 00-716 Warsaw, Poland
e-mail: nastula@cbk.waw.pl
[3] NASA Goddard Space Flight Center
Greenbelt, MD 20771, USA
e-mail: dsm@leo.gsfc.nasa.gov
[4] Vienna University of Technology
Gushausstrasse 27-29,Vienna, 1040, Austria
e-mail: mendes@mars.hg.tuwien.ac.at

ABSTRACT. We have calculated atmospheric effective angular momentum functions of Earth rotation/polar motion with hourly resolution based on the NASA Goddard Earth Observation System (GEOS-4) atmospheric model. Such excitations are based on model forecasts at five of the six hours, and a mixture of model and observations at the sixth hour. This heterogeneous procedure can cause discontinuities if not mitigated by special approaches. The wind-based polar motion terms have a strong diurnal signal related to tidal fluctuations, though the phase appears to vacillate. October 2002 encompassing the intensive CONT02 Earth rotation-observing period was selected here. Time-spectra of wind-based, pressure-based, and geodetic terms reveal diurnal and semidiurnal signals with additional sub-daily spectral peaks. NASA is currently introducing the d́2Modern Era Retrospective-Analysis Research and Applications system, which should eliminate the 6-hour discontinuities. This MERRA system will give us the opportunity to investigate high temporal resolution excitation for more recent CONT campaigns.

1. ATMOSPHERIC ANGULAR MOMENTUM (AAM) AND EARTH ROTATION

The values of AAM are closely related to the excitations of variability of Earth rotation and polar motion due to conservation of angular momentum in the Earth system. Changes in winds and the atmospheric mass are responsible for the AAM variability, with winds dominating the variations in the axial (length-of-day) terms, and the pressure dominating the polar motion terms on frequencies other than the very rapid sub-daily ones.

The wind-based excitation terms have a strong diurnal signal due to the atmospheric thermal tides. These signals are, however, modulated seasonally (Zhou et al. 2006) so that signals determined at particular hours (example only at 00 UTC) are relatively smooth. The mean diurnal signals of the wind-based polar motion excitation changes phase throughout the months of the year, so for example, large diurnal amplitudes occur in the solstitial seasons, in mid-summer and mid-winter, and smaller amplitudes occur in the equinoctial seasons.

2. HIGH TEMPORAL RESOLUTION ANGULAR MOMENTUM ANALYSIS WITH NASA SYSTEM

GEOS-4 data assimilation system is run on a 1.25 degree longitude by 1 degree latitude resolution. Although it is formally updated every 6 hours by means of a data assimilation step at that epoch, we have worked with the Global Model and Assimilation Office at NASA Goddard Space Flight Center to save winds and surface pressure as well on an hourly basis during the course of the model integration in between the 6-hourly analyses. Thus the 5 hourly values in between the formal six-hour analyses are based on the forecast model results. We chose one month, October 2002, to determine the hourly excitation functions

from the GEOS-4 model, during the Very Long Baseline Interferometry (VLBI) CONT02 campaign in which high temporal resolution Earth Orientation Parameter data would be available for comparisons with the atmospheric high-resolution data.
Meteorological data assimilation systems are composed of an analysis step and a forecast step, with raw observations from instruments including rawinsondes, aircraft and satellite sensors. They are combined in an optimal fashion with the results from a forecast initialized 6 hours prior. Then a new forecast is started, during which excitations may be calculated at any time step. Here we access hourly values.
The chi-1, chi-2, and chi-3 data from both winds and pressures have been computed hourly. The biggest signals occur in the chi-1 and chi-2 wind terms, with different periods during the month having a strong value, and appear sometimes to be about 1/4 day apart in phase. (Fig. 1) All fields have some visible discontinuities in the graphs that occur before all hours divisible by 6, indicating the data assimilation step. We are reasonably confident in the solution because it matches fairly well the values computed from the NCEP-NCAR reanalyses (not shown). We noted that the wind based-excitation terms diurnal signals vacillate considerably in amplitude and partly in phase throughout the month.
We address the issues of the 6-hour discontinuities evident in the data, and we have derived two methods to deal with it, one by linear removal (LDLIN) of the jumps that occur then, and the other by a statistical spectral analysis (SSA3) approach (Fig. 2). Time spectra of the rapid fluctuations up to the order of a day were computed and we note that the peaks that existed at some of the harmonics of a day in the new data have decreased but not fully disappeared in the processed data (Fig. 3). The atmosphere may thus be related, though weakly to the 8-hour fluctuations that have been detected in the geodetic series, though their amplitudes are considerably larger.
Estimates of the spectra of excitations of polar motion from geodetic measurements are given below for CONT02 and a later period of intense examination by the VLBI technique in 2005 (Fig. 4). We can see peaks around 6, 8, 9 and 12 hours, though these are strong for the CONT02 period, though less so for the CONT05 period.

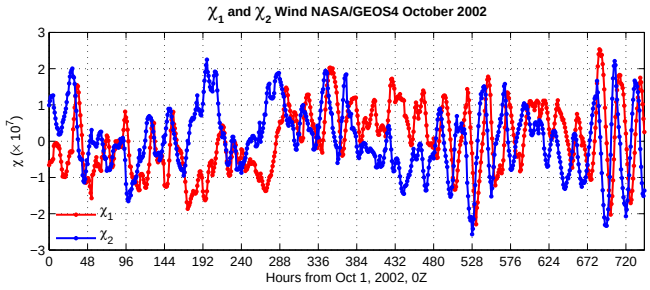

Figure 1: Hourly values of the wind-based excitations for polar motion from the GEOS-4 simulations.

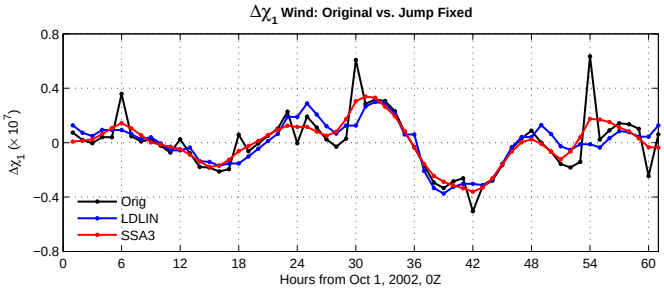

Figure 2: Time series in the first 60 hours of the chi-1 wind term with jumps removed by two methods.

3. MERRA MODERN ERA RETROSPECTIVE ANALYSIS FOR RESEARCH AND APPLICATIONS

The MERRA system is being developed at NASA Goddard Space Flight Center to be run as a reanalysis, and it is designed to make special use of remote sensing on satellites. It will have smoother transitions because of an Incremental Analysis Update technique. Although 3-dimensional and two-dimensional fields are regularly output on 6- and 3-hour intervals, respectively, we are preparing for

hourly fields from the model, as we did for the GEOS-4 series, when they are available to be able to calculate the atmospheric excitation term for polar motion.

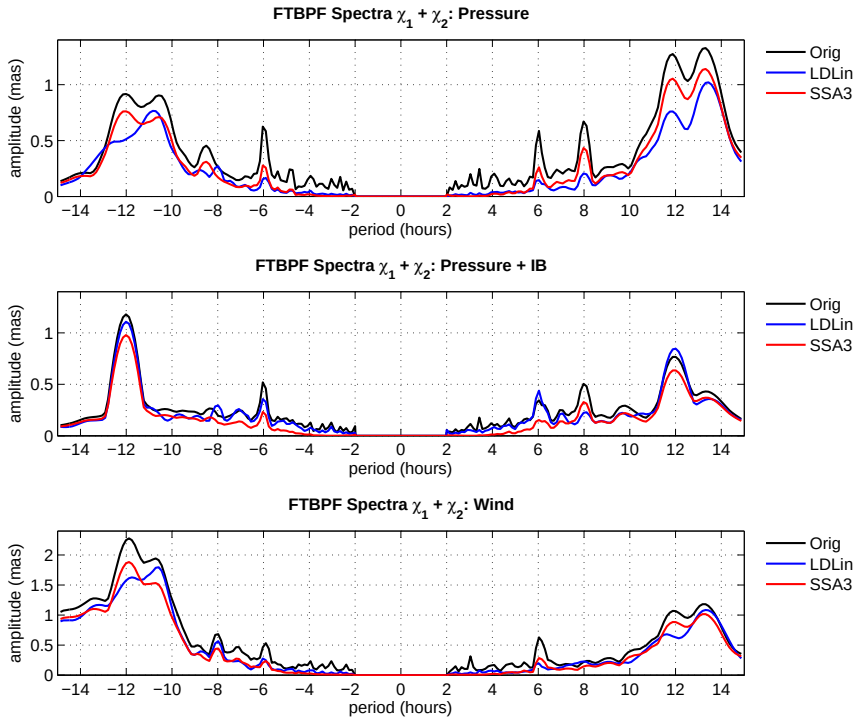

Figure 3: Power spectra of complex chi-1, chi-2 with and without jump removal.

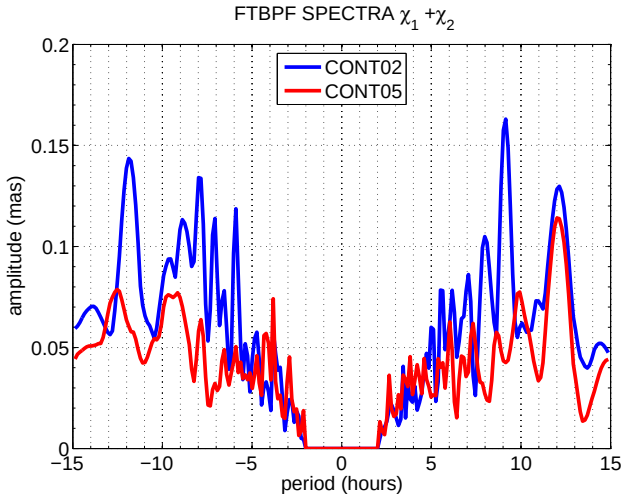

Figure 4: Power spectra of complex polar motion excitations from the CONT02 and CONT05 periods.

Acknowledgements. U.S. National Science Foundation Grant ATM-0429975. NASA Center for Computational Sciences provided computation. We acknowledge the assistance of Siegfried Schubert and Rob Lucchesi of NASA GSFC in preparing the hourly model values.

4. REFERENCES

Zhou, Y.H., D.A. Salstein, and J.L. Chen, 2006, Revised atmospheric excitation function series related to Earth rotation under consideration of surface topography, J. Geophys. Res. (Solid Earth), 1111, D12108, doi:10.1029/2005JD006608.

ON THE INFLUENCE OF DIURNAL ATMOSPHERIC TIDES ON EARTH ROTATION

A. BRZEZIŃSKI
Space Research Centre, Polish Academy of Sciences
Bartycka 18A, 00-716 Warsaw, Poland
e-mail: alek@cbk.waw.pl

ABSTRACT. We give a general description of the perturbations of Earth rotation caused by diurnal thermal tides in the atmosphere and the oceans, and briefly overview the observation and modeling efforts. We also report on own estimation using the available high resolution atmospheric and oceanic excitation data and the space-geodetic observations of Earth rotation. Parameters of the S1 component of excitation, estimated from geophysical models and observations, are compared to each other.

1. INTRODUCTION

Diurnal atmospheric tides are global-scale waves excited by the differential heating of the Sun (thermal tides) and, to a much lesser extent, by the gravitational lunisolar tidal force; for detailed description see the review paper by Volland (1997) and the references therein. The basic frequency is 1 cycle per solar day (cpd). But the departures from the sinusoidal pattern (e.g. the diurnal cycle in solar heating is close to a slightly smoothed 2-valued step function) and the differences near the ground (due to irregular ocean-continent distribution, topography, cloudiness, ice coverage, vegetation, etc.) produce additional harmonics with frequencies k cpd, where k is integer. According to Volland (1997), only harmonics with k=1,2,3 are significant. The atmospheric tides are coherent with gravitational tides therefore it is generally accepted to label them using the standard notation introduced to the tidal research by George Darwin. Hence, components with frequencies 1, 2, and 3 cpd are designated S_1, S_2, S_3, respectively.

The main diurnal and subdiurnal harmonics of thermal origin subject to seasonal modulations (annual, semiannual) producing side lobes shifted in frequency by ± 1, ± 2 cycles per year (cpy) with respect to the main spectral line. Hence, the annual modulation of S_1 gives rise to the P_1 and K_1 harmonics, while the semiannual modulation produces the π_1 and Ψ_1 terms. The side lobes of S_2 are the R_2, T_2 components (annual modulation) and the K_2, P_2 components (semiannual modulation).

The time variation of the atmospheric angular momentum (AAM) exhibits a similar spectral structure as the contributing meteorological quantities, that is the surface pressure and the wind velocity (Bizouard et al., 1998; Brzeziński et al., 2002; Brzeziński et al., 2004). But it is important to note that the standard sampling of AAM is 6 hours which is sufficiently short for estimation in the diurnal band, but not short enough for resolving the semidiurnal band where only rough overall estimate is possible. Of course, this sampling is not adequate for studying the terdiurnal variations.

The large-scale variations in the atmosphere influences the oceans giving rise to the nontidal diurnal and subdiurnal signals. Such signals can be estimated from the available time series of nontidal ocean angular momentum (OAM) evaluated using the outputs of the numerical ocean general circulation models with subdiurnal resolution (e.g., Brzeziński et al., 2004). A more sophisticated hydrodynamic ocean models have been also developed to estimate the diurnal and subdiurnal components of OAM (e.g., Ray and Egbert, 2004). Such an approach is expected to provide more realistic results than from the OAM series; on the other hand this model expresses only the harmonic components neglecting the effects of seasonal modulations. Again, as the atmospheric fields used to force the ocean models are sampled 4-times daily, the same limitations for the use of OAM apply as in case of the AAM data.

It follows from the conservation law of angular momentum that diurnal and subdiurnal signals in AAM and OAM influence all components of Earth rotation vector, including polar motion, nutation and UT1 variation. For each harmonic component the observed effect is a mixture of thermal influence expressed by AAM+OAM, and the ocean tide contribution directly related to gravitational forcing. The ratio of contributions from the thermal and ocean tide forcings is about 10/1 for S_1 and 1/20 for S_2

(Brzeziński et al., 2004); in case of S_3 the gravitational signal is negligible therefore any possible observed effect should be entirely of thermal origin. The side lobes of S_1 and S_2 appear to be dominated by the ocean tide contributions.

Our purpose here is to estimate from geophysical models the influence of diurnal atmospheric tides on Earth rotation and compare this result to the observations by space geodesy. We neglect the terdiurnal variations which cannot be estimated from standard geophysical models. When considering the diurnal and semidiurnal variations it appears that in most cases the thermal contributions can hardly be separated from much larger ocean tide influences. The only exclusion is the S_1 Sun-synchronous term of excitation which will be considered in details below.

2. DATA ANALYSIS AND RESULTS

The equatorial retrograde component of S_1 contribute to prograde annual nutation while its prograde counterpart influences diurnal polar motion. The S_1 term in the axial component of excitation gives rise to a 24-hours component in UT1.

The estimation of the contribution of S_1 from the space-geodetic observations of Earth rotation is possible, though difficult for the following two reasons: 1) the signal is relatively small, the maximum peak-to-peak size is only 200 to 300 microarcseconds (μas); and 2) the estimation can be corrupted by different Sun-synchronous errors, e.g. those due to the thermal deformation of the VLBI antennas. We use in comparisons the following estimates of the S_1 contribution to prograde polar motion and to UT1

VLBI1: (Bolotin and Brzeziński, 2006), input data span 1984–2005;

VLBI2: (Gipson, 1996), input data span 1979–1994;

GPS: (Rothacher et al., 2001), data span 1995–1998.1.

We also use the VLBI observation of prograde annual nutation and the geophysical contributions derived by Mathews et al. (2002).

The parameters of the S_1 harmonic in the atmospheric angular momentum and the corresponding contributions to Earth rotation have been estimated from the following AAM data sets which are available from the International Earth Rotation and Reference Systems Service Special Bureau for the Atmosphere (IERS SBA):

AAM1, AAMIB1: NCEP-NCAR reanalysis data (Kalnay et al., 1996; Salstein and Rosen, 1997), period 1948–2006; sampling interval 6 hours;

AAM2: ERA-40 reanalysis model (Uppala et al., 2004)), period 1948–2004, sampling interval 6 hours;

AAM2′: ECMWF operational data, period 1993.0–1996.5, sampling interval 6 hours with gaps;

AAM3, AAMIB3: JMA operational data, period 1993.3–2000.5, sampling interval 6 hours with gaps.

The corresponding contributions of the S_1 harmonic in nontidal oceanic angular momentum have been estimated from the following models

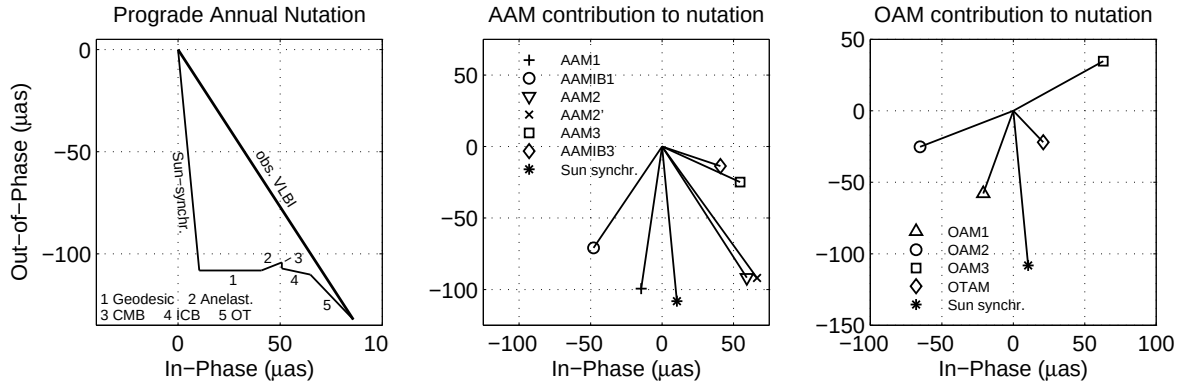

Figure 1: Atmospheric and oceanic contributions to prograde annual nutation: model MHB 2000 (left) vs. modeled geophysical contributions, atmospheric (middle) and oceanic (right).

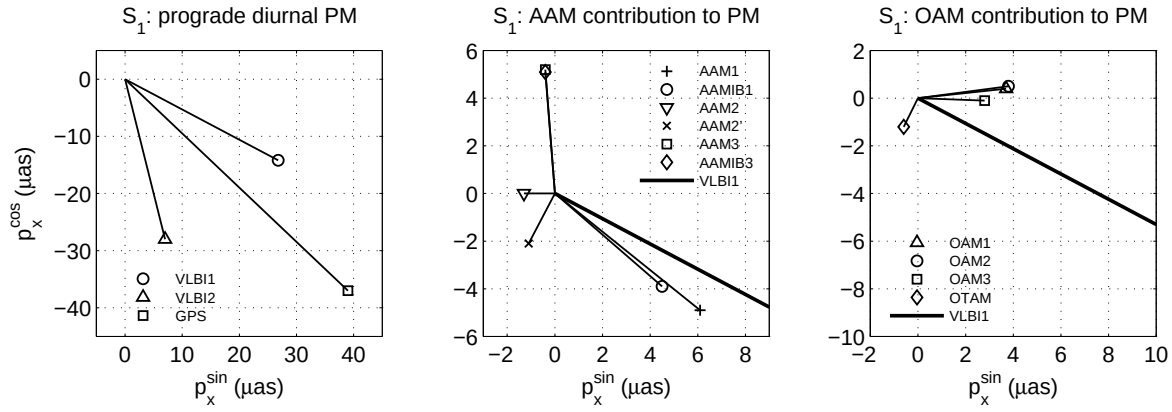

Figure 2: Atmospheric and oceanic contributions to prograde diurnal polar motion, S1 term: space-geodetic observations (left) vs. modeled geophysical contributions, atmospheric (middle) and oceanic (right).

OAM1: hydrodynamic model of the S1 component (Ray and Egbert, 2004);

OAM2: barotropic model (Ponte and Ali, 2002; Brzeziński et al., 2004) forced by wind and atmospheric pressure fields from the NCEP-NCAR reanalysis model, period 1993.0–2000.5, sampling interval 1 hour;

OAM3: ocean model for circulation and tides (OMCT) (Thomas et al., 2001) forced by wind and pressure fields from the model ERA-40, period 1963–2001, sampling interval 30 minutes.

Parameters of the S_1 term estimated from the atmospheric and oceanic models are compared to the parameters derived from observations in Figures 1, 2 and 3.

Precession-nutation (Fig.1). The left diagram shows the correction to the amplitude of the prograde annual nutation together with the theoretical contributions from 1) geodesic nutation, 2) mantle anelasticity, 3) coupling at the core-mantle boundary, 4) coupling at the inner core boundary, and 5) ocean tide (Mathews et al., 2002, Table 2). The remaining part denote "Sun-synchronous" is expected to express the combined influence of the S_1 harmonic in AAM and OAM. There is a rough agreement between the estimated contributions of AAM. The best agreement with observation is obtained the non-IB NCEP-NCAR reanalysis series. The contributions from OAM are only slightly smaller than those from AAM, but there are large differences in phase. Particularly surprising is that the OMCT and barotropic OAM yield almost opposite results. The best agreement with observations is found for the hydrodynamic model of OAM combined with ERA-40 AAM.

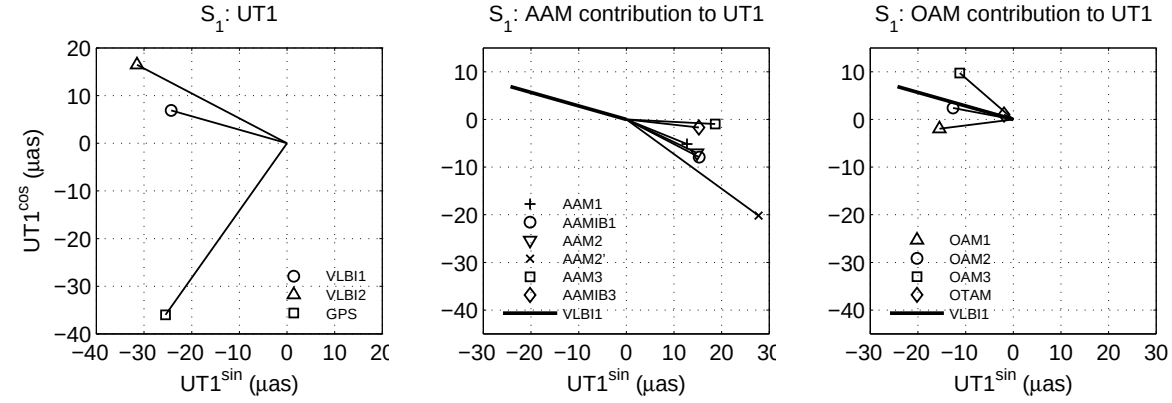

Figure 3: Atmospheric and oceanic contributions to diurnal variation of UT1, S1 term: space-geodetic observations (left) vs. modeled geophysical contributions, atmospheric (middle) and oceanic (right).

Prograde polar motion (Fig.2). The amplitudes estimated from the VLBI data are of the order of 30 μas while the analysis of data from GPS yields almost 2 times larger value. The estimated total contribution from the atmosphere and ocean is only about 8 μas, about 4 times less than the VLBI value. The OAM results are coherent while there are large differences between the estimated contributions of AAM. The best agreement with observations is found for the barotropic OAM combined with the NCEP-NCAR reanalysis AAM.

UT1 (Fig.3). The 2 estimates from VLBI are of the order of 30 μas and agree with each other, while the amplitude from GPS is larger than 40 μas and its argument differs from VLBI results by about 90 degrees. There is a good agreement between the estimated contributions of AAM with exception of the value derived from the operational ECMWF data which is of poor quality. There is also quite a good agreement between different values of OAM. Unfortunately, the contributions of AAM and OAM tend to cancel each other and the total effect does not agree with the observation.

3. SUMMARY AND CONCLUSIONS

The diurnal cycle in solar heating give rise to variations in AAM and OAM with main components S1, S2 of periods 24 and 12 hours, and their side lobes due to seasonal modulations. These variations of AAM and OAM excite small perturbations in all three components of Earth rotation, including precession-nutation, polar motion and UT1. So far, only the S1 contributions to Earth rotation could be detected in both geophysical models and space-geodetic observations. However, comparison done in this work revealed significant differences between estimates from different models and different observation techniques, as well as between the models and observation. Investigations should be continued using improved geophysical models and space-geodetic data derived by improved reduction procedures.

Acknowledgements. This research was supported by the Polish national science foundation 2007-2009 under grant No. N526 037 32/3972. I thank Mike Thomas for providing the OMCT and ERA-40 data and Anna Korbacz for preparing the figures.

4. REFERENCES

Bizouard, Ch., Brzeziński, A., and Petrov, S. D., 1998, "Diurnal atmospheric forcing and temporal variations of the nutation amplitudes", J. Geodesy 72, pp. 561–577.

Bolotin, S., and Brzeziński, A., 2006, "A search for geophysical signals in diurnal and semidiurnal polar motion from analysis of the routine VLBI observations", Geophys. Res. Abstracts, Vol.8, abstract No. EGU06-A-01665.

Brzeziński, A., Ponte, R. M., and Ali, A. H., 2004, "Non-tidal oceanic excitation of nutation and diurnal/semidiurnal polar motion revisited", J. Geophys. Res. 109(B11407), doi: 10.1029/2004JB003054.

Gipson, J. M., 1996, "Very long baseline interferometry determination of neglected tidal terms in high-frequency Earth orientation variations", J. Geophys. Res. 101(B12), pp. 28,051–28,064.

Kalnay, E., et al., 1996, "The NMC/NCAR 40-year reanalysis project", Bull. Amer. Met. Soc. 77(3), pp. 437–471.

Mathews, P. M., Herring, T. A., and Buffet B. A., 2002, "Modeling of nutation-precession: New nutation series for nonrigid Earth, and insights into the Earth's interior", J. Geophys. Res. 107 (B4), doi:10.1029/2001JB000390.

Ray, R. D., Egbert, G. D., 2004, "The Global S_1 Tide", J. Phys. Oceanogr. 34, pp. 1922–1935.

Rothacher, M., Beutler, G., Weber, R., and Hefty J., 2001, "High-frequency variations in Earth rotation from Global Positioning System data", J. Geophys. Res. 106(B7), pp. 13,711–13,738.

Salstein, D. A., and Rosen D., 1997, "Global momentum and energy signals from reanalysis systems", Proc. 7th Conf. on Climate Variations, American Met. Soc., Boston, Massachusetts, pp. 344–348.

Ponte, R. M., and Ali, A. H., 2002, "Rapid ocean signals in polar motion and length of day", Geophys. Res. Lett. 29, doi:10.1029/2002GL015312.

Thomas, M., Sündermann, J., and Maier-Reimer, E., 2001, "Consideration of ocean tides in an OGCM and impacts on subseasonal to decadal polar motion excitation", Geophys. Res. Lett. 28(12), pp. 2457–2460.

Uppala, S. M., et al., 2005, "The ERA-40 re-analysis", Q. J. R. Meteorol. Soc. 131, pp. 2961–3012.

Volland, H., 1997, "Atmospheric Tides", in. H. Wilhelm, W. Zürn and H.-G. Wenzel (eds.), Tidal Phenomena, Lecture Notes in Earth Sciences 66, Springer Verlag, Berlin-Heidelberg, pp. 221–246.

EMPIRICAL VALIDATION OF THE CONVENTIONAL MODEL FOR LENGTH OF DAY VARIATIONS DUE TO ZONAL TIDES

S. ENGLICH, R. WEBER, H. SCHUH
Institute of Geodesy and Geophysics, Advanced Geodesy
Vienna University of Technology
Gusshausstrasse 27-29, 1040 Vienna, Austria
e-mail: sigrid.englich@tuwien.ac.at

ABSTRACT. The deformations of the Earth caused by the zonal part of the tidal potential induce fluctuations in the rotational speed of the Earth with periods from about 5 days to 18.6 years. Measures for the deviation of the Earth rotation from a uniform motion are the parameter dUT1 (defined as the difference between Universal Time UT1 and atomic time UTC) and its time derivative the length of day (LOD). LOD variations were derived from 23 years of VLBI observations, using the VLBI software package OCCAM61E. We also calculated a second LOD series of two years with the Bernese GPS Software 5.0 for the years 2005 and 2006, analysing data of 113 stations of the global IGS network. The atmospheric influence on LOD was computed from atmospheric angular momentum functions provided by the NCEP and subtracted from the original series. Different sets of tidal terms were estimated in a least squares adjustment introducing the remaining LOD variations as pseudo-observations. The resulting amplitudes were compared with the values of the model recommended in the IERS Conventions 2003 (Defraigne and Smits, 1999).

1. ZONAL TIDAL POTENTIAL

The response of the Earth to the zonal tidal potential results in a periodic change of the principal moments of inertia. According to the conservation of angular momentum this leads to a periodic change of the rotation rate and consequently to variations in dUT1 or LOD, respectively. The tidal potential V_G in a point A can be expanded into spherical harmonics, using Legendre polynomials.

$$V_G(A) = GM \sum_{n=2}^{\infty} \frac{R^n}{r^{n+1}} P_n cos(\psi) \tag{1}$$

with G = gravitational constant, M = mass of the celestial body, r = geocentric distance of the celestial body and R = Earth radius. When the geocentric zenith angle ψ is expressed by geocentric spherical coordinates of the station (θ, λ) and of the tracing point of the celestial body (p, Λ) the tidal potential (limited to second order) can be split up into three families of spherical harmonics (e.g. Melchior, 1978).

$$V_{G,20} = GM \frac{R^2}{r^3} P_{20}(cos\theta) P_{20}(cosp) \tag{2}$$

$$V_{G,21} = \frac{1}{3} GM \frac{R^2}{r^3} P_{21}(cos\theta) P_{21}(cosp) cos(\Lambda - \lambda) \tag{3}$$

$$V_{G,22} = \frac{1}{12} GM \frac{R^2}{r^3} P_{22}(cos\theta) P_{22}(cosp) cos2(\Lambda - \lambda) \tag{4}$$

The equations (3) and (4) are denoted sectorial and tesseral functions and describe the short period tides with semi-diurnal and diurnal variations. Function (2) is called zonal function. It depends on the slowly varying latitude of the tracing point of the celestial body only and therefore describes the medium and long period tides. Major periods are fourteen and twenty eight days for the moon and six months for the sun. Accordingly these are the periods of the largest terms of the LOD variations induced by the zonal tidal deformations.

2. LOD TIME SERIES FROM VLBI AND GPS

We processed 23 years of VLBI observations using the VLBI software package OCCAM Version 6.1 (least squares approach, Gauss-Markov model). The so-called VLBI Intensive sessions, as well as all geodetic 24-hour experiments, except those, which are not suitable for the estimation of Earth orientation parameters due to their limited extension in one or more components, were included in the solution (time span: 1984-2006). Coordinates of stations and sources were fixed to the ITRF2005 resp. ICRF Ext.2 reference frames. Hence the estimates are Earth orientation, troposphere and clock parameters. Nutation offsets, polar motion and dUT1 were set up once per session, as regards the 24-hour experiments. In the analysis of Intensive sessions, nutation and polar motion have to be fixed to a priori values and solely one dUT1 value is estimated per session. LOD was not directly estimated as dUT1-rate, but the generated dUT1 time series was converted to LOD after processing. The a priori models applied in VLBI analysis are listed in Table 1.

For the generation of the GPS-based LOD series observation data of 113 stations, which belong to the IGS05 reference frame sites, was processed by means of Bernese GPS Software Version 5.0. The selected observation period was 2005-2006. Hence we derived a two-years LOD time series. Due to the enormous computing time expenditure of GPS data processing, the generation of a longer time series was not feasible so far. LOD was estimated in 6-hour intervals. The geodetic datum was defined, imposing a no-net-rotation condition on the IGS05 station coordinates. The satellite positions were fixed to the final orbits provided by CODE (Center for Orbit Determination in Europe). All calculations were performed using absolute antenna phase center corrections. The applied a priori models correspond to those introduced in VLBI processing (Table 1).

Parameter	Model
Nutation	IAU2000A
Ocean loading	FES2004
sub-daily ERP variations	IERS2003

Table 1: A priori models applied in VLBI/GPS processing

3. ESTIMATION OF TIDAL TERMS

Before the LOD time series can be analysed to extract the tidal signals of interest, it is necessary to eliminate other geophysical signals from the observed LOD variations. The largest impact, to be considered, is atmospheric excitation. The LOD variations induced by the atmosphere are calculated from atmospheric angular momentum functions provided by the NCEP (U.S. National Centers for Environmental Prediction; Salstein and Rosen, 1997). Short period variations in LOD with diurnal and semi-diurnal periods are induced by ocean tides. These fluctuations were already considered within the VLBI/GPS processing by applying the conventional model. The series were additionally "cleaned" by subtracting linear trends and very low frequency variations. From the remaining signal the main zonal tidal terms were estimated at predefined periods. The periods are in principle waves of the tidal potential, which are very well known from the orbital motion of the moon and sun (and planets). The amplitudes of the tidal terms were determined in a least squares adjustment, introducing the LOD variations as pseudo-observations. As observation equations we employed a spectral representation of the tidal variations $\delta LOD(t)$ as follows

$$\delta LOD(t) = \sum_{i=1}^{n} [A_i cos\xi_i(t) + B_i sin\xi_i(t)] \quad with \quad \xi_i(t) = \sum_{j=1}^{5} N_{ij} F_j(t) \tag{5}$$

A_i and B_i denote the cosine and sine amplitudes belonging to the tidal wave i, while n specifies the number of tides considered. The angle argument $\xi_i(t)$ is built as a linear combination of the five fundamental arguments F_j. Each period is specified by a sequence of integer multipliers N_{ij}, where the subscript i labels the tide (Simon et al., 1994). The so-called out-of-phase terms, which are represented by the sine terms here, were in fact neglected in this study, because their expected magnitude is close to zero, according to the IERS conventional model.

In terms of VLBI-derived LOD we solved for 10 major terms, 20 sideband terms and one test term, with periods from 6.85-365.26 days. For the test term we chose the period 16.63 days, where no tidal signal is expected. The magnitude of the test term should give an estimate of the noise level of the observed variations. In case of GPS-based LOD, where the time series covers just two years, only the amplitudes of periods below 35 days were estimated, i.e. 8 major terms, 17 sideband terms and the same test term were determined. Since it is impossible to separate the sideband terms from the major terms with only two years of data, we imposed additional constraints on the estimated amplitudes in order to account for the contribution of the sidebands. To specify, the sideband contribution was considered in the adjustment as a fraction of the main terms, assuming that the relative size of the excitation A is proportional to the relative size of the amplitude V of the waves in the tidal potential: $A_i^{'} = \frac{V_i^{'}}{V_i} A_i$. Since the sideband terms were introduced as additional conditions for the main terms, they were not estimated directly within the adjustment, but calculated a posteriori from the condition equations. Hence no formal errors can be given for the sideband terms, determined in this way. Figure 1 shows the amplitude spectra of the LOD variations after the signal processing steps.

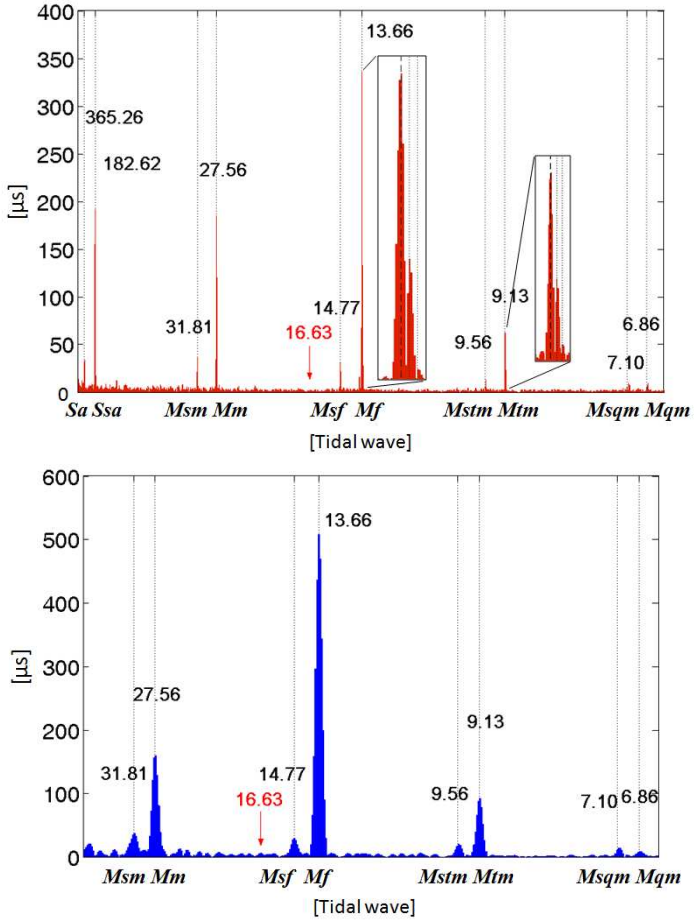

Figure 1: Amplitude spectra of δLOD VLBI (top) and δLOD GPS (bottom)

The main tidal terms are marked with the corresponding periods in days and the names for the tidal waves in Darwin's notation. The upper spectrum (VLBI-derived LOD variations) reveals that it is possible to separate the adjacent sidebands from the main terms with a time series of over 20 years. Most of the very close periods differ by only one cycle in 18.6 years (period of the lunar ascending node), which implicates that an observation period of at least this length is necessary to separate these terms. For example two distinct peaks at the fortnightly band are magnified, demonstrating the separability of the *Mf'* tidal wave (13.63 d) from the main tidal wave *Mf* (13.66 d). The lower picture, which is the spectrum of the GPS-based LOD variations, shows on the contrary, that these terms cannot be separated using a time span of two years. Examining again the *Mf* tidal band, exhibits that the two terms accumulate

to one single peak with increased amplitude in the spectral analysis. Thus the results of the frequency analysis support the previously introduced approach of estimating the contribution of the sideband terms with additional conditions in the adjustment, in case they are not resolvable. This applies for all sideband terms estimated from GPS-derived LOD variations and also for the sideband of the annual tidal wave *Sa* (365.26 d) determined from VLBI-derived LOD variations. The final amplitudes determined in the least squares adjustment are compared to the amplitudes of the IERS Conventions model in Figure 2.

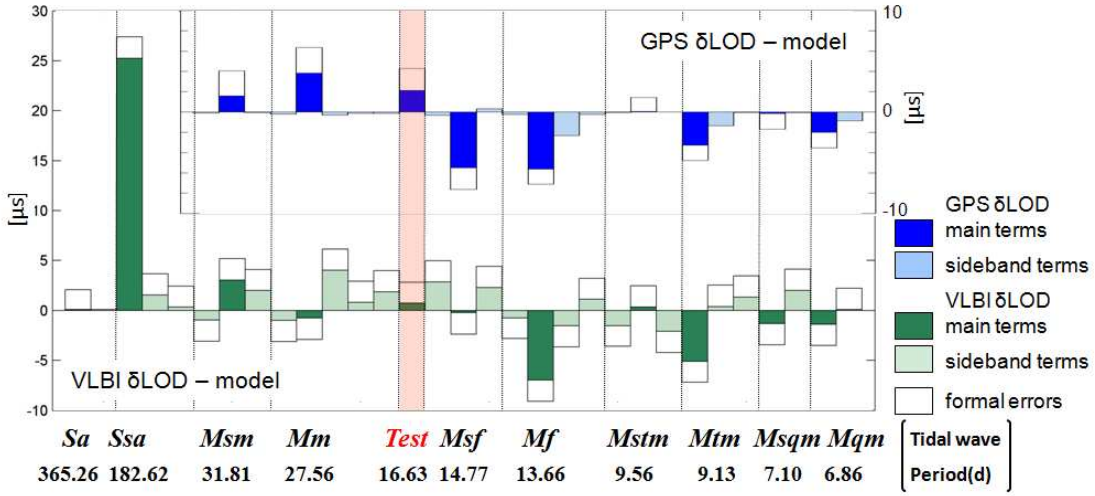

Figure 2: Comparison of tidal amplitudes: observed - IERS model

4. DISCUSSION

The magnitude of the major part of the estimated terms agrees with the amplitudes specified in the IERS model. The values differ less than 5 μsec and the differences are well within the range of three times the formal errors of the adjustment. The agreement is slightly worse for the *Msf* and *Mf* tidal waves in terms of GPS-derived LOD variations and for the *Mf* and the *Mtm* tidal waves determined from VLBI-based LOD variations. For the semi-annual *Ssa* wave, which was estimated from VLBI δLOD only, we found a remarkable discrepancy of 25 μsec between the observed and the theoretical amplitude. In general the two solutions (VLBI/GPS), which are obtained independently, confirm each other and show a very similar pattern regarding the sign of the differences; this is particularly true for the Mf and Mtm tidal waves. As for the difference in *Msf* we can state that periods in the fortnightly band are always critical in GPS analysis, because they are possibly affected by aliasing due to imperfect reduction of the influence of short period ocean tides and processing characteristics. The reasons for the differences in the other terms mentioned are suspected to be either insufficient modelling of the atmospheric influence or inexact consideration of medium and long period ocean tides in the theoretical model, or even a combination of both.

5. REFERENCES

Defraigne, P., Smits, I., 1999, "Length of day variations due to zonal tides for an inelastic earth in non-hydrostatic equilibrium", Geophys. J. Int. 139, pp. 563-572.

IERS Conventions (2003), IERS Technical Note 32, D.D. McCarthy and G. Petit (eds), Frankfurt am Main: Verlag des Bundesamts für Kartographie und Geodäsie, 2004.

Melchior, P., 1978, "The tides of the planet Earth", Pergamon Press, Oxford.

Salstein, D.A., Rosen, R.D., 1997, "Global momentum and energy signals from reanalysis systems", 7th Conf. on Climate Variations, American Meteorological Society, Boston, MA, pp. 344-348.

Simon, J.L., Bretagnon, P., Chapront, J., Chapront-Touze, M., Francou, G., Laskar, J. ,1994, "Numerical expressions for precession formulae and mean elements for the Moon and the planets", A&A 282, no. 2, pp. 663-683.

GEOPHYSICAL EXCITATION OF LOD/UT1 ESTIMATED FROM THE OUTPUT OF THE GLOBAL CIRCULATION MODELS OF THE ATMOSPHERE - ERA-40 REANALYSIS AND OF THE OCEAN - OMCT

A. KORBACZ[1], A. BRZEZIŃSKI[1], M. THOMAS[2]
[1] Space Research Centre, Polish Academy of Sciences
Bartycka 18a, 00-716 Warsaw, Poland
e-mail: akorbacz@cbk.waw.pl
[2] GeoForschungsZentrum
Telegrafenberg, D-14473 Potsdam, Germany

ABSTRACT. We use new estimates of the global atmospheric and oceanic angular momenta (AAM, OAM) to study the influence on LOD/UT1. The AAM series was calculated from the output fields of the atmospheric general circulation model ERA-40 reanalysis. The OAM series is an outcome of global ocean model OMCT simulation driven by global fields of the atmospheric parameters from the ERA-40 reanalysis. The excitation data cover the period between 1963 and 2001. Our calculations concern atmospheric and oceanic effects in LOD/UT1 over the periods between 20 days and decades. Results are compared to those derived from the alternative AAM/OAM data sets.

1. INTRODUCTION

The axial component of Earth rotation which is expressed by the length of day (LOD) or universal time (UT1), is subject to changes with periods ranging from a fraction of a day to decades. According to the principle of conservation of angular momentum, changes in the LOD are excited by mass redistributions and angular momentum exchanges between the solid Earth and geophysical fluids: atmosphere, oceans, land hydrosphere and fluid core. It has been proven that variations with decadal and longer periods are excited mainly by the interactions between the core and the mantle (Gross et al., 2005). Changes with shorter periods are driven mostly by the dynamically coupled system atmosphere-oceans.

Our earlier investigations of excitation of the equatorial components of Earth rotation (Korbacz et al., 2007) revealed significant differences between the effective angular momentum functions derived from the ERA-40 reanalysis and nontidal OMCT (Ocean Model for Circulation and Tides) and from other atmospheric and oceanic models. These differences were found smaller at shorter periods while increasing towards the longer periods. Current research is an extension of the previous work by considering the axial component of rotation expressed as changes of the length of day (LOD). The combination ERA-40 + OMCT will be compared to other available models of the atmospheric and oceanic excitation and to the observations of the LOD over a broad band of frequencies: from decadal through interannual and seasonal, up to intraseasonal. Comparison between geophysical excitation data and geodetic observations of LOD is much simpler than in case of polar motion because there is a linear relationship between the χ_3 component of the atmospheric and oceanic angular momenta (AAM, OAM) and LOD.

2. DATA DESCRIPTION AND ANALYSIS

We used in our analysis two atmospheric angular momentum time series. The first one, estimated from the NCEP/NCAR reanalysis model, is available from the website of the IERS Special Bureau for Atmosphere. The second one was estimated from output fields of the ERA-40 reanalysis model (Uppala et al., 2005). Both series have the same temporal resolution of 6 hours and long, but slightly different data spans. In our combinations we used the standard AAM series and that with the "inverted barometer" correction, denoted AAMIB. The AAM series is based on the full variability of the pressure fields, while AAMIB assumes an isostatic ocean response to the atmospheric pressure fluctuations and thus only include effects of variability in the average atmospheric pressure over the ocean.

The description of the oceanic angular momentum time series used in our analysis is shown in Table 1. Each data set is designated by the code containing 3 characters. The first character is an abbreviation of

OAM code	description	ocean model	forcing atmosphere model	temporal resolution	data span
T06	Thomas et al., 2001	OMCT	ERA-40	30 min.	1963-2001
P01	Ponte, 2001	MOM + assimil.	COADS/NCEP	1 month	1950-2000
G05	Gross et al., 2005	ECCO-MITgcm	NCEP	10 days	1949-2002
G03	Gross et al., 2004	ECCO-JPL	NCEP	1 day	1980.0-2002.2
Pas	Ponte et al., 2001	ECCO-Scripps + assim.	NCEP	1 day	1992.8-1998.0

Table 1: Oceanic angular momentum time series.

the name of the author, who computed or described the series, the last two characters express the year of publication and "as" means data assimilation. Besides the new T06 series, we use four different OAM estimates. In computations, the T06 OAM series will be combined with the ERA-40 AAM, while all other OAM series with the NCEP/NCAR reanalysis AAMIB. The difference between AAM and AAMIB is important when considering the influence on polar motion, but in case of the axial component of rotation the difference is negligible, because the atmospheric pressure term plays only a minor role in the excitation of the LOD.

The time series of OAM: P01 and G05 cover long data span, but have lower temporal resolution. They are capable for investigation of the seasonal and longer variations. The next two time series G03 and Pas are with diurnal sampling, but are significantly shorter, therefore cannot be applied for investigation of long periods. The new data set T06 has a high temporal resolution and covers a long time span enabling estimation over the entire band of frequencies considered in this work.

We use for comparison the LOD time series COMB2002 (Gross, 2000), which is combined solution derived by the Kalman filter. This series is denoted here **obs**.

The first step of data analysis consists in converting the time series AAM and OAM into the effective angular momentum function χ_3 and then into LOD using a linear transformation (Gross et al., 2004). Then we split up all the LOD series into the model comprising the first order polynomial and seasonal harmonics with periods 1, 1/2 and 1/3 year, and the residuals, that is the difference between the original series and the model. These two components of the LOD are treated separately. First we estimate amplitudes and phases of the seasonal harmonics and compare them in the phasor diagrams. Then we apply the band-pass filter to split up the residual series into four components: decadal ($T > 8$ years), interannual ($2 < T < 8$ years), seasonal ($1/2 < T < 2$ years) and intraseasonal (20 days $< T < 1/2$ year). Finally we compare the estimated oceanic and atmospheric LOD to the observed one in each of the selected spectral bands.

Figure 1 shows the atmospheric LOD calculated from the ERA-40 reanalysis data, wind term and pressure term, and the corresponding oceanic LOD from the OMCT model, currents and mass term. All plots are shown in the same scale. It can be seen that the dominant part of LOD is that due to the zonal winds. The oceanic contribution to LOD is almost negligible. The annual signal is clearly visible in all components. Significant part of the power disappear from data after subtracting the seasonal harmonic model.

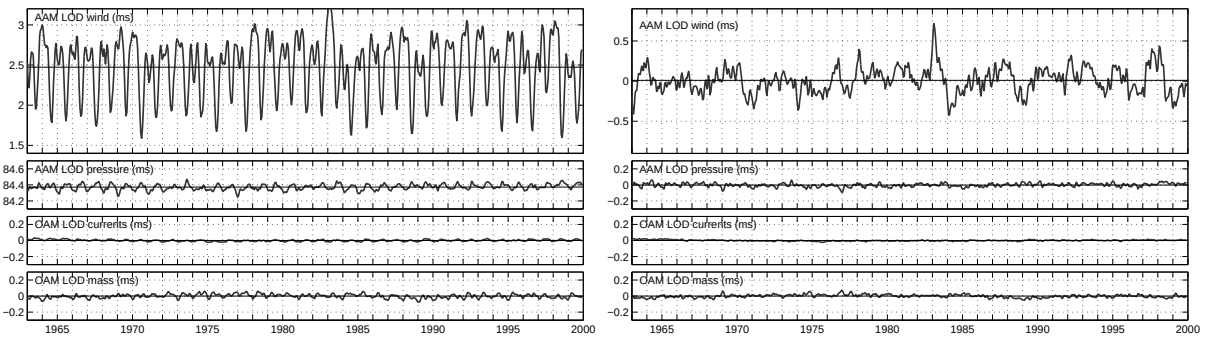

Figure 1: Atmospheric and oceanic LOD from ERA-40 and OMCT. Variations with period $T < 20$ days have been removed by smoothing. The right panel shows the data after subtracting the model.

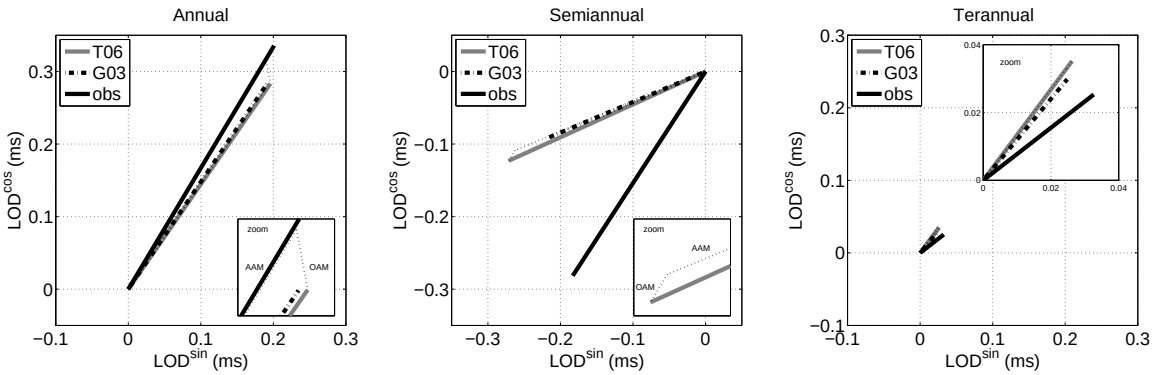

Figure 2: Comparison of the seasonal harmonics estimated from the series T06, G03 and **obs**.

3. RESULTS

The seasonal harmonics estimated from the G03 and T06 series are compared to each other and to observations, in phasor diagrams of Figure 2. In case of T06 shown are additionally separate contributions from AAM and OAM (dotted line). For each component there is a very good agreement in phase between the geophysical models, and slightly worse in amplitude. In case of the annual harmonic the AAM+OAM combination based on the T06 model yields good agreement in phase and amplitude with the observations. However, from the decomposition into the atmospheric and oceanic contributions it can be seen that atmosphere alone gives better agreement in amplitude and phase. In case of the semiannual oscillation we detected phase difference about 30^o between geophysical models and observations, which is probably caused by land hydrology which is not taken into account in this comparison. It appears that adding the ocean OMCT to the ERA-40 makes the amplitude and phase a little closer to the observed. The terannual oscillation is very weak in comparison to other terms considered, nevertheless the zoom shows quite good agreement between geophysical models and observations.

Figure 3 illustrates the analysis of the residual part. On the left-hand side there are plots showing decadal, interannual, seasonal and intraseasonal components of LOD computed from geophysical and observed time series. The tables on the right show the correlation coefficient between the modeled and observed LOD and the reduction of variance when subtracting the modeled excitation from the observed one. The reduction is negative when the variance increases after this operation. The last part of table contains standard deviations of each excitation series (wind, pressure, current and mass terms), giving the measure of their contribution to the observed LOD.

For each component of residual part there is a very good agreement of T06 series with other AAM+OAM estimates. Standard deviation shows that atmospheric winds are the most important in the excitation of LOD.

In case of decadal component changes in observed LOD are not significantly influenced by the atmosphere and the ocean, as could be expected. For the interannual component of LOD there is much better agreement between geophysical models and observations than for decadal band. The correlation coefficients are about 0.6 for each series, the reduction of variance is always positive and has similar value. The analysis of the seasonal component of LOD shows almost perfect agreement between the AAM+OAM series and observations. In case of the intraseasonal component the correlation coefficients are still high, but lower than in the seasonal band.

4. CONCLUSIONS

Unlike equatorial component of Earth rotation, the axial component of T06 combination AAM+OAM does not differ significantly from other geophysical models. In case of annual and terannual harmonics in LOD there is an excellent agreement in amplitude and phase between models and observations. For semiannual oscillation there is a high agreement in amplitude, but a large phase difference ($\sim 30^o$) occurs. An obvious candidate to explain this difference is the land hydrology. At decadal periods, the AAM and OAM are much smaller than the observed LOD, as could be expected from earlier works. For periods shorter than 8 years the atmospheric/oceanic excitation plays an important role with the highest

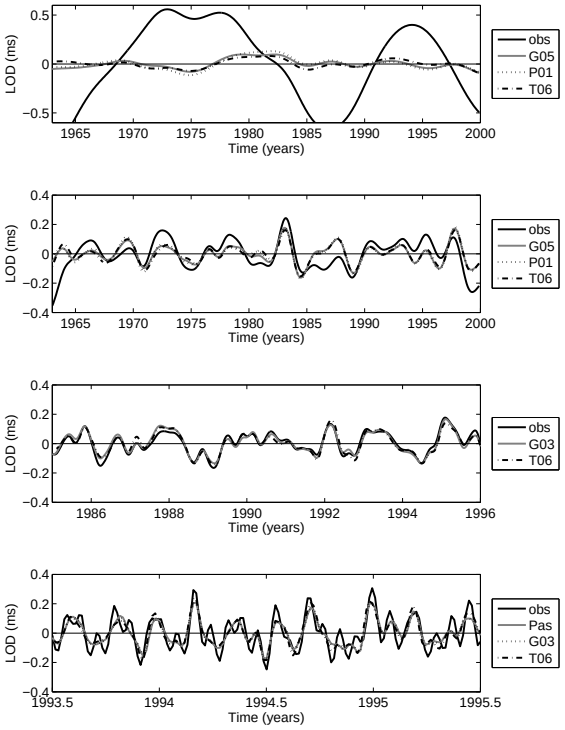

	Corr. with **obs**	Var. reduct. (%)	Standard deviation (μs)			
Series	(1963.0→1999.9)		wind	pres.	curr.	mass
P01	-0.104	-4.970	40	8	2	1
G05	0.151	2.144	40	8	2	1
T06	0.071	0.423	41	7	6	11
				obs	413	

Series	(1963.0→1999.9)		wind	pres.	curr.	mass
P01	0.588	34.038	61	6	2	2
G05	0.631	39.854	61	6	2	2
T06	0.608	37.002	60	5	1	4
				obs	102	

Series	(1980.0→2001.9)		wind	pres.	curr.	mass
G03	0.958	91.733	81	8	3	3
T06	0.963	92.538	84	9	3	7
				obs	84	

Series	(1992.9→1997.9)		wind	pres.	curr.	mass
Pas	0.858	73.059	96	15	6	
G03	0.858	73.028	96	15	6	6
T06	0.870	75.174	100	20	6	17
				obs	195	

Figure 3: Comparison of data after removal of the seasonal model and trend. From up to down shown are the results for decadal, interannual, seasonal and intraseasonal bands.

agreement with observations in the seasonal band. The dominating contribution to the excitation of LOD at periods shorter than 8 years comes from zonal winds. Variations of the atmospheric pressure and the ocean play a minor role.

Acknowledgements. Anna Korbacz would like to express her sincere thanks for the travel grant provided by the "Descartes-Nutation" consortium. This work has been supported by the Polish Ministry of Science and Higher Education under grant No. N526 037 32/3972.

5. REFERENCES

Gross R. S., 2000, "Combinations of Earth Orientation Measurements: SPACE97, COMB97 and POLE97", J. Geodesy, Vol. 73, 627-637.

Gross R. S., Fukumori I., Menemenlis D., 2004, "Atmospheric and oceanic excitation of length-of-day variations during 1980-2000", J. Geophys. Res. , Vol. 109, B01406.

Gross R. S., Fukumori I., Menemenlis D., 2005, "Atmospheric and oceanic excitation of decadal-scale Earth orientation variations", J. Geophys. Res. , Vol. 110, B09405, doi:10.1029/2004JB003565.

Korbacz A., Brzeziński A., Thomas M., 2007, "Atmospheric and nontidal oceanic excitation of polar motion estimated from the output of the models ERA-40 and OMCT", Geophysical Research Abstracts, Vol. 9, 09625, European Geosciences Union.

Ponte R. M., 2001, "A 50-year time series of ocean angular momentum for Earth rotation studies", unpublished manuscript.

Ponte R. M., Stammer D., Wunsch C., 2001, "Improving ocean angular momentum estimates using a model constrained by data", Geophys. Res. Lett., Vol. 28, 9, 1775-1778.

Thomas M., Sündermann J., Maier-Reimer E., 2001, "Consideration of ocean tides in an OGCM and impacts on subseasonal to decadal polar motion excitation", Geophys. Res. Lett., Vol. 28, 12, 2457-2460.

Uppala S. M., et al., 2005, "The ERA-40 re-analysis", Q. J. R. Meteorol. Soc., Vol. 131, 612, 29613012.

GEOPHYSICAL EXCITATION OF DIURNAL PROGRADE POLAR MOTION DERIVED FROM DIFFERENT OAM AND AAM DATA

M.V. KUDRYASHOVA
Sobolev Astronomical Institute of St. Petersburg University
Universitetskii pr.28, Petrodvorets, St. Petersburg, 198504, Russia
kudryashova@astro.spbu.ru

ABSTRACT. Short period variations in polar motion are mostly caused by the system atmosphere-ocean impact. In this work we compare the geodetic and geophysical excitation. Geodetic excitation have been estimated on the basis of polar motion series with sub-diurnal temporal resolution obtained from VLBI observations. For our comparison we used two sets of geophysical data: first one is that of atmospheric and oceanic angular momenta (AAM, OAM) calculated during ERA-40 reanalysis project; second one contains AAM series derived from NCEP/NCAR reanalysis project and corresponding OAM series from the barotropic OGCM (Oceanic Global Circulation Model) model. Our analysis covers prograde diurnal frequency band.

1. GEODETIC EXCITATION OF POLAR MOTION DERIVED FROM VLBI OBSERVATIONS

VLBI observations obtained in the period from 1989 till 2004 have been used for estimating of polar motion by the least square collocation method (LSCM) as it is realized in OCCAM 6.1 software. The distinctive feature of this method is that the Earth rotation parameters (ERP) are estimated as stochastic process with known covariance matrix. Elements of this matrix (q_{ERP}) are calculated in according to the following formula (see Titov,2000):

$$q_{ERP}(\tau) = \frac{\sigma^2_{ERP}}{\cos(\varphi)} e^{-\alpha|\tau|} \cos(\omega\tau + \varphi), \quad (1)$$

where σ^2_{ERP} is a priori variance of stochastic process, τ — time shift (in parts of day) $0 \leq \tau \leq 1$; $\alpha = 50\,day^{-1}$ — damping parameter, $\omega = 1$ cpd — cyclic frequency; $\varphi = 0.3$ rad — initial phase. All these parameters except a priori variance of ERP can be estimated from VLBI observations during iterative process. The value of σ^2_{ERP} should be derived from some a priori information on process. We obtain two solutions under different values of a priori variance: series SPU_1 ($\sigma^2_{ERP} = 4.4cm^2$) and series SPU_2 ($\sigma^2_{ERP} = 0.44cm^2$).

Note that in both of this series the model of the diurnal and sub-diurnal variations in polar motion due to oceanic tides has already been taken into account (corresponding model is provided by the International Earth Rotation Service (IERS) Conventions 2003). Based on this series we calculated the geodetic excitation.

The resulting geodetic excitation series are unevenly sampled with time resolution 3-5 min within one 24-hours session. The method of complex demodulation has been applied in order to extract from the series mentioned above a signal in the prograde diurnal frequency band. It have been shown by Brzezinski et al. (2002), Kudryashova and Petrov (2005) that an application of complex demodulation method for such a series yields meaningful results. This procedure can be described by the following equation:

$$\chi' = -\chi e^{-in\phi},$$

where $\phi \approx \Omega(t - t_0) + \phi_0$ is the Greenwich mean sidereal time, χ, χ' are the initial and demodulated excitation series, and $n\Omega$ — frequency of demodulation (which equals $+\Omega$ in this study). In the frequency domain such a transformation just shifts spectrum of the initial series along the frequency axis in such a way that $n\Omega$ becomes 0. This procedure was followed by Gaussian filtering.

After applying the complex demodulation, frequencies of those diurnal tides which play the main role in AAM and OAM (S1, P1, π1, K1), have been changed for $\nu_1 = -1$ cycle per year (cpy) (annual

retrograde), $\nu_2 = -2$ cpy (semiannual retrograde), $\nu_3 = -3$ cpy (terannual retrograde) and $\nu_0 = 0$ (constant term), respectively.

As a next step we estimated the best least square fit of the model, which contains first-order polynomial and sum of complex sinusoids:

$$f = a + bt + \sum_{k=1}^{3}(A_k \exp^{(i2\pi t\nu_k)} + B_k \exp^{(-i2\pi t\nu_k)}) \tag{2}$$

Components of this model either correspond to the thermal tide S1 or are caused by its seasonal modulation.

2. GEOPHYSICAL EXCITATION OF POLAR MOTION

In the subsequent analysis two sets of geophysical excitation, provided us by R. Ponte and M. Thomas, have been used. Let us briefly describe theses data.

R. Ponte

Atmospheric excitation is expressed by the AAM estimates calculated on the basis of the NCEP/NCAR (U.S. National Center for Environmental Prediction/National Center for Atmospheric Research) reanalysis project results (see for details Kalnay E., et al., 1996). The series is now available from the web-site of the IERS Special Bureau for the Atmosphere. This series is sampled four-times daily and covers the period from 1948.0 till now.

The oceanic excitation series OAM used in the present study are based on the barotropic ocean model by Ponte and Ali (2002). The model is driven by the atmospheric surface wind and pressure fields from the NCEP/NCAR reanalysis project. The series spans the period from 1993.0 till 2000.5 and has one-hour temporal resolution.

M. Thomas

Atmospheric excitation is expressed by AAM estimates calculated on the basis of atmospheric global circulation model. These estimates have been obtained during data reanalysis project ERA-40 carried out in European Center for Medium-Range Weather Forecast (ECMWF).

For consistency oceanic excitation has been estimated on the basis of the Ocean Model for Circulation and Tides(OMCT), driven by the ERA-40 wind and surface pressure fields (Seitz et.al., 2004).

Procedure of the complex demodulation with subsequent Gaussian filtration have been applied to both sets of geophysical data, as well as estimation of coefficients of the model (2). Comparison of demodulated data revealed that matter terms of OAM and AAM, as well as motion terms of OAM from both sets are comparable. However, AAM motion term from ERA-40 estimations is about twice more powerful then that one from NCEP/NCAR estimations.

3. RESULTS AND CONCLUSIONS

Figures 1 and 2 show a comparison of the geodetic and geophysical excitation of diurnal polar motion, assuming different models of the ocean response to atmospheric forcing:

- the non-IB model which assumes rigid ocean, with excitation expressed by AAM;
- the IB model which implies static ocean response, with excitation expressed by AAMIB;
- the dynamic model of ocean response with excitation expressed by the sum of AAMIB+OAM.

Comparison of Figure 1 and 2 shows that the best agreement between geodetic and geophysical excitation is achieved when estimation of the ERP is performed with an a priori dispersion $\sigma = 0.44\,cm^2$. From Table 1 it could be seen that amplitude and phase of the S1 term as they seen from SPU1 solution and AAM (matter term) reveal very good agreement. Moreover, the agreement became better after 1996. This is the case for both sets of geophysical data.

In case of estimation of the ERP with a larger a priori dispersion ($\sigma = 4.4\,cm^2$), geodetic excitation is highly overestimated with respect to geophysical excitation (Figure 2). However, comparison (Kudryashova M. et. al., 2007) of VLBI series obtained in Astronomical Institute of St. Petersburg University and that one calculated in GSFC reveals that these series are in better agreement if the former series is calculated with a larger a priori dispersion ($\sigma = 4.4\,cm^2$).

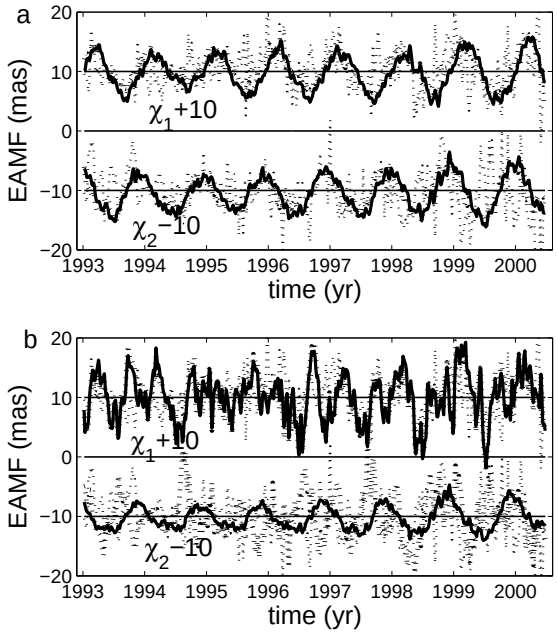

Figure 1: Comparison of the geodetic (SPU1) and geophysical excitation of diurnal polar motion: a — AAM and OAM from data, provided by R. Ponte; b — AAM and OAM from data, provided by M. Thomas. Geodetic excitation is denoted by dotted grey line; rigid ocean responce — dotted black line; dynamic model of ocean response — solid black line.

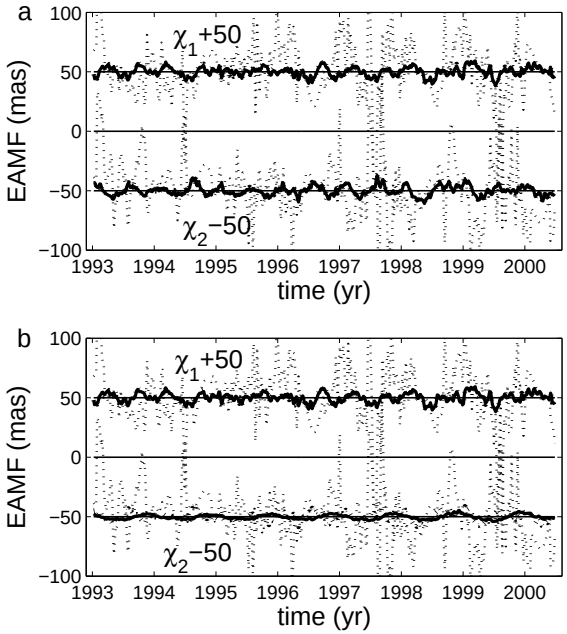

Figure 2: Comparison of the geodetic (SPU2) and geophysical excitation of diurnal polar motion: a — AAM and OAM from data, provided by R. Ponte; b — AAM and OAM from data, provided by M. Thomas. Geodetic excitation is denoted by dotted grey line; rigid ocean responce — dotted black line; dynamic model of ocean response — solid black line.

term	EAMF		polar motion	
	ampl.(mas)	phase[°]	ampl.(μas)	phase[°]
data provided by R. Ponte				
geodetic excit.(SPU2)	14.1	16.3	33.3	−163.7
geodetic excit.(SPU1)	2.04	12.8	4.8	−167.2
AAM(matter)	2.03	12.6	4.9	−169.7
AAM(motion)	2.24	90.8	5.2	−91.5
AAMIB(motion)	1.58	−8.9	3.8	168.8
OAM(mater)	3.28	66.6	7.9	−115.8
OAM(motion)	2.26	−137.7	5.2	40.0
data provided by M. Thomas				
geodetic excit.(SPU2)	14.1	16.3	33.3	−163.7
geodetic excit.(SPU1)	2.04	12.8	4.8	−167.2
AAM(matter)	2.1	17.7	5.0	−162.3
AAM(motion)	1.2	−87.9	2.8	92.1
OAM(matter)	1.4	59.1	3.3	−120.9
OAM(motion)	0.8	−175.3	1.9	5.0

Table 1: Parameters of S1 component derived from atmospheric and nontidal oceanic contribution as well as from different VLBI solution (SPU1 and SPU2).

Acknowledgements. Author is very grateful to Rui Ponte and Maik Thomas for provided geophysical data. This work has been partly supported by the grant in frame of 'Descartes-Nutation' Project.

4. REFERENCES

Brzezinski A., Bizouard Ch., Petrov S.D., 2002, "Influence of the atmosphere on Earth rotation: what new can be learned from the recent atmospheric angular momentum estimates?", Surveys in Geophisics, 23, pp. 33-69.

Kalnay E., et al., 1996, "The NCEP/NCAR 40-year reanalysis project", Bull. Amer. Met. Soc., Vol.77, 437–471.

Kudryashova M.V., Petrov S.D., 2006, "Diurnal polar motion from VLBI observations", Proc. Journées Systèmes de Référence Spatio-Temporels 2005, eds. A. Brzeziński, N. Capitaine and B. Kołaczek, Space Research Centre of Polish Acad. of Sciences, Warsaw, pp.117-120.

Kudryashova M., MacMillan D., Titov O., 2007, "A commparison of intraday variations of the Earth orientation parameters from different VLBI solutions", Proc. of the 18th European VLBI for Geodesy and Astrometry Working meeting, eds. J. Bohm, A. Pany, H. Schuh, Vienna, pp.196-200.

Ponte R.M., Ali A.H., 2002, "Rapid ocean signals in polar motion and length of day", Geophys. Res. Lett., Vol.29(15), doi: 10.1029 / 2002GL015312.

Salstein D.A., Rosen R.D., 1997, "Global momentum and energy signals from reanalysis systems", Preprints, 7th Conf. on Climate Variations, American Meteorological Society, Boston, MA, pp. 344–348.

Seitz F., Stuck J., Thomas M., 2004, "Consistent atmospheric and oceanic excitation of the Earth's free polar motion", Geophys.J.Int., v.157, p.25-35.

Titov O.A., 2000, "Estimation of the subdiurnal UT1-UTC variations by least squares collocation method", Astron. and Astrophys. Transactions, pp. 779-792.

POLAR MOTION INTERPRETATION USING GRAVIMETRIC OBSERVATIONS

L. SEOANE, C. BIZOUARD, D. GAMBIS
Observatoire de Paris, SYRTE, UMR 8630/ CNRS,
61 avenue de l'Observatoire, 75014 Paris, France.
e-mail: lucia.seoane@obspm.fr; christian.bizouard@obspm.fr; daniel.gambis@obspm.fr

ABSTRACT. Polar motion is interpreted as the effect of i) the Earth's inertia moment changes associated with the so-called mass term of the Earth's angular momentum ii) the Earth's relative angular momentum in the terrestrial frame. Thanks to the GRACE mission and in a lesser extent to LAGEOS missions, the mass term is determined since 2002, independently from any geophysical model. Besides the modeled excitations of the polar motion, *i.e* the atmospheric angular momentum (AAM), the Oceanic Angular Momentum (OAM), the Hydrological Angular Momentum (HAM), this gravimetric mass term is a new kind of information which can be matched to the observed excitation of the polar motion after removal of the effect of the relative angular momentum, mostly caused by the wind and the oceanic currents. Such comparison, already performed by various authors, is updated for the last releases (RL04) of the gravity field changes *i.e.* those of the GFZ, CSR, JPL and explored for the mixed LAGEOS-GRACE solution of the GRGS. We confirm that a fair general agreement, especially for the y-component of the equatorial excitation. After removing the modeled oceanic and atmospheric excitations from the signals, we obtain the non-modeled excitation, mostly of hydrological nature; this allows us to compare them to the existing hydrological models, differences might comes from others Earth's phenomena, for example, earthquakes.

1. INTRODUCTION

The primary cause of the Earth's polar motion is the mass transport occurring in the Earth. In the terrestrial frame (Oxyz) off-diagonal inertia moments (I_{xz}, I_{yz}) of the Earth undergoes permanent changes, and relative motion takes place. Thus a time-variable equatorial angular momentum is created, composed by a *matter term* $\Delta\overline{I}\underline{\omega}$ where $\underline{\omega}$ represents the terrestrial components of the Earth's angular velocity vector, and a relative angular momentum (*motion term*). But according to the angular momentum conservation, that increment is balanced by motion of the rotation pole with respect to the crust. By estimation of the matter term and relative angular momentum, it is possible to provide an interpretation of the polar motion. So far those quantities are determined partially and commonly approached by ground observations, especially for the atmosphere and the oceans, which are known as the main source of angular momentum changes at seasonal and sub-seasonal scale. The assimilation of ground pressure and wind into Global Circulation Model allows to estimate the atmospheric angular momentum (AAM) on a routine basis. The determination of the oceanic angular momentum (OAM) is less easy, because oceanic observations are not so widespread. Whereas AAM explains 90% of the length-of-day variations at seasonal and sub-seasonal scales, combined AAM and OAM series fit up to 80% of the excitation found in polar motion at those periods. That might be due to the defect of OAM model or to the neglect of some other geophysical excitation, like the one linked to hydrological processes.

The advent of the Gravity Recovery and Climate Experiment (GRACE) mission shed light on the polar motion excitation. It has been monitoring the variability of the gravity field with unprecedented accuracy and spatial resolution since March 2002. As the inertia moments (I_{xz}, I_{yz}) are directly related to the spherical harmonics coefficients C_{21} and S_{21} of the geopotential, we can assume that GRACE mission permits to observe the equatorial part of the variable matter term, independently from any geophysical model. The GRACE's matter term has to be compared to the excitation found in the observed polar motion, mainly at seasonal and sub-seasonal time scales, since we have at hand 4 years of observations. It is interesting to know to which extent mass redistribution observed by GRACE is compatible with the Earth's rotation observations.

Such study has already be initiated by Chen and Wilson (2003), Chen et al. (2004), and revisited by

Nastula et al. (2007) for the previous GRACE products releases. We shall reproduce their study for the updated release, and complete it by an analysis of the hydrological signal. We shall see that our results differ significantly.
The analysis of GRACE satellites data is carried out by four centres: the Centre for Space Research (CSR), the GeoForschungsZentrum (GFZ), the Jet Propulsion Laboratory (JPL) and the Groupe de Recherche de Géodésie Spatiale (GRGS). Each Centre has provided updated solutions in several releases, not only the time span lengthens, but the data processing, especially the background models are revised. Recently, in April 2007, CSR, GFZ and JPL have updated their GRACE products in the Release 04. Our investigation uses this latest version of the gravity field solution in the form of normalized spherical harmonic coefficients for each centre.

2. METHOD

Polar motion excitation is deduced from the relation between the (2,1) Stokes coefficients of the gravity field and off-diagonal inertia moments of the Earth in the terrestrial frame. We have used Chen et al. (2003) formulation for computing excitation from GRACE solutions. For each Centre we have time series of the (2,1) normalized spherical harmonic coefficients of the gravity field $\Delta\overline{C}_{21}$ and $\Delta\overline{S}_{21}$ are tide free and also corrected from non tidal atmospheric and oceanic effects using ECMWF model and OMCT baroclinic model respectively, except for the GRGS that uses a barotropic ocenic model, MOG2D (Biancale et al. 2007). The degree 2 coefficients of the GRGS solution are determined by a combined analysis of the LAGEOS and GRACE observations. The non-tidal models have to be added back, in order to compare C_{21} and S_{21} variations to polar motion excitation deduced from Earth rotation observations.
The International Earth rotation and Reference systems Service (IERS) provides combined time series of the Earth Orientation Parameters (EOP) at daily interval (Gambis 2004, Bizouard and Gambis 2007), in particular the pole coordinates x and y, which allows us to compute the "geodetic" polar motion excitation according to:

$$\chi_G = \chi_1 + i\chi_2 = p + i\frac{\dot{p}}{\sigma_c} \tag{1}$$

where $p = x - iy$ is the complex pole coordinate and σ_c is the Chandler pulsation ($2\pi/433$ rad/days) with an adopted quality factor of 175. Geodetic excitation are corrected from oceanic tides using FES-2004 model (Lefevre et al. 2005).
GRACE or LAGEOS excitation only reflects mass redistribution, we have then to remove the motion part from the geodetic excitation associated with atmospheric winds and ocean currents. Wind term is computed by the National Center for Environmental Predictions (NCEP) (Salstein et al. 1993) and provided by the IERS Special Bureau for Atmosphere (SBA); current term is computed from ECCO model (Gross et al. 2003) provided by the IERS Special Bureau for Oceans (SBO).
On the other hand latitude-longitude grids providing the charge of continental water by surface unit at monthly intervals are available for the period 2002-2006. By integrating the grids of the CPC hydrological model we have reconstituted the hydrological excitation function or hydrological angular momentum - HAM - reduced to its mass term. Adding the HAM to the mass term of the atmospheric and oceanic excitations computed from NCEP and ECCO series we obtain an Earth's modelled mass redistributions that we labelled PAOH.
Time series of the CSR, GFZ and JPL solutions present common sampling of about 30 days, but the GRGS solution is given at approximately 10-day intervals. On the other hand our geodetic excitation function presents variations up to 2 days. Applying Vondrak smoothing (Vondrak 1977), which transmits 95% of the signal at 121 days (1% transmitted at 34 days, 22% transmitted at 60 days) we make both GRGS, geodetic series and modelled mass excitation spectrally consistent with the CSR, GFZ and JPL solutions. All those solutions are then interpolated at common dates at 30 day intervals.

3. RESULTS

The correlation coefficients between each "gravity" excitation and the geodetic excitation computed labelled here-after "G-WC" (that is from geodetic excitation with winds and currents effects removed) are reported in table 1. Also we shows correlation between the modeled mass excitation "PAOH" and the geodetic excitation. There is generally a good correlation for the component χ_2 (0.8-0.9). In the case of χ_1 function, which is mainly associated with mass transport over oceanic regions, correlation drops

to 0.4-0.6. That points out the defect of the modelling of the coupled oceanic-atmospheric influence on the oceans. We also compare the standard deviation of the GRACE excitation with that one of the geodetic excitation (restricted to its mass term). As shown also in table 1 there is globally more power in GRACE excitation (0%-50% more) for χ_1 component, and less power in GRACE excitation for χ_2 component (10-20% less). As for correlation the agreement in standard deviation is globally better for χ_2 component. Generally modeled mass excitation are better correlated with geodetic excitation than gravimetric excitation. But series are short, only 39 points, according to Nastula et al. (2007) formulation

	Standard deviation ratio		Correlation			
					$\chi_1 + i\chi_2$	
	χ_1	χ_2	χ_1	χ_2	Magnitude	Phase degree
CSR/G – WC	1.6	0.9	0.6	0.8	0.8	7
GFZ/G – WC	1.5	0.9	0.4	0.8	0.8	-1
JPL/G – WC	1.9	1.0	0.6	0.9	0.8	14
GRGS/G – WC	1.6	0.9	0.4	0.8	0.7	-11
PAOH/G – WC	0.8	0.9	0.8	0.9	0.9	1

Table 1: Correlation coefficients between the *gravimetric* excitation (CSR, GFZ, JPL, GRGS, GRGS) and the mass term of the *geodetic* excitation, labelled G-WC. Also the table shows the correlation between the modeled mass excitation PAOH computed from geophysical fluids models (NCEP, ECCO, CPC) and the *geodetic* excitation.

90% significance level of correlation for 39 points is 0.26 and only a difference of 0.24 in the correlations is significant.
From the GRACE solutions we remove the modeled influence of the atmosphere and the oceans using NCEP data and ECCO. Hence those signals should reflect the mass term of "exotic" nature, like the one caused by hydrological processes and geodynamic processes like earthquakes. Therefore we have also a precious information on the non-modeled causes of the polar motion. That residual excitation can be compared to the geodetic excitation, after removing not only the motion term but also the mass term caused by the atmosphere and the oceans.
They are large discrepancies in time timing, and amplitudes (up to 10 mas) which are also reflected by the spectra shown in Figure 1. Corresponding correlation coefficients up to 0.7 and standard deviation ratios are given in table 2. Residual geodetic excitation G-WC-PAO is also compared to hydrological excitation computed from CPC model. Correlation is better what shows that the models seems to better reflect the hydrological angular momentum than the GRACE observation. Note that the solutions are all referred to the same atmospheric data (NCEP) and oceanic model (ECCO).

	Standard deviation ratio		Correlation			
					$\chi_1 + i\chi_2$	
	χ_1	χ_2	χ_1	χ_2	Magnitude	Phase degree
CSR – PAO/G – WC – PAO	1.9	1.3	0.5	0.4	0.4	5
GFZ – PAO/G – WC – PAO	1.9	1.8	0.3	0.7	0.5	-3
JPL – PAO/G – WC – PAO	2.3	1.0	0.4	0.5	0.4	8
GRGS – PAO/G – WC – PAO	1.9	1.3	0.2	0.4	0.3	-18
CPC/G – WC – PAO	0.4	1.2	0.7	0.7	0.7	-24

Table 2: Correlation coefficients between the hydrological excitation from *gravimetric* data (CSR, GFZ, JPL, GRGS, GRGS) or models (CPC) and hydrological signal from geodetic data. Note that atmospheric and oceanic effects are removed: motion term is labelled "WC" and mass term is labelled "PAO".

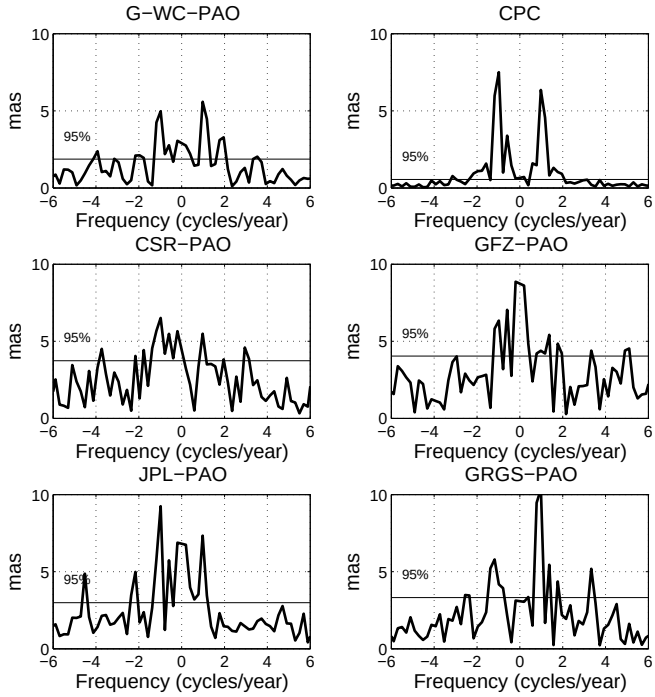

Figure 1: Spectrum of complex residual excitation functions computed from gravimetric data (JPL,CSR,GFZ,GRGS) and geodetic data by removing the atmospheric and oceanic signals, and also from global water storage model (CPC)

4. REFERENCES

Biancale, R., Lemoine, J. M., Balmino, G., Bruinsma, S., Perosanz, F., Marty, J.C., Loyer, S., Bourgogne, S. & Gégout, P., 2007. 4 years of gravity variations from GRACE and LAGEOS data at 10-day intervals over the period from July 29th, 2002 to October 25th, 2006, http://bgi.cnes.fr:8110/geoid-variations/README.html.

Bizouard, C. & Gambis, D., 2007. The combined solution C04 for Earth Orientation Parameters consistent with International Terrestrial Reference Frame 2005, Technical Note of IERS Earth Orientation Center, http://hpiers.obspm.fr/iers/eop/eopc04_05/C04_05.guide.pdf.

Chen, J.L. & Wilson, C.R., 2003. Low degree gravitational changes from earth rotation and geophysical models, Geophys. Res. Lett., 30(24), 2257, doi:10.129/2003GL018688.

Chen, J.L., Wilson, C.R., Tapley, B.D. & Ries, J.C., 2004. Low Degree Gravitational Changes from GRACE: Validation and Interpretation, Geophys. Res. Lett., 31, L22607,doi:10.1029/2004GL021670.

Gambis D., 2004. Monitoring Earth Orientation at the IERS using space-geodetic observations, J. of Geodesy, 78, pp 295-303, state-of-the-art and prospective, J Geod 78(4-5):295-303, doi: 10.1007/s00190-004-0394-1.

Gross, R.S., Fukumori, I. & Menemenlis, D., 2003. Atmospheric and oceanic excitation of the Earth's wobbles during 1980-2000. J. Geophys. Res., 108(B8), 2370, doi:10.1029/2002JB002143.

Lefevre, F., Letellier, T. & Lyard, F., 2005. FES2004 Model (realization FES2004_r190105).

Nastula, J., Ponte, R.M. & Salstein, D.A., 2007. Comparison of polar motion excitation series derived from GRACE and from analyses of geophysical fluids, J. Geophys. Res. vol. 34, L11306, doi: 10.1029/2006GL028983.

Salstein, D. A., Kann, D. M., Miller, A. J. & Rosen, R. D., 1993. The sub-bureau for atmospheric angular momentum of the International Earth Rotation Service: A meteorological data center with geodetic applications, Bull. Am. Meteorol. Soc., 74, 67-80.

Vondrak, J., 1977. Problem of smoothing observational data II, Bull. Astron. Inst. Czech, 28, p. 84-89.

SUMMARY OF THE DISCUSSION ON THE PREDICTION OF EARTH ORIENTATION PARAMETERS

W. WOODEN
USNO Naval Observatory
3450 Massachusetts Avenue, N. W.
Washington, D. C. 20392, USA
e-mail: william.wooden@usno.navy.mil

This panel discussion took place after Session 4 entitled "Prediction, Combination, and Geophysical Interpretation of Earth Orientation Parameters." The panel, drawn from the membership of the IERS Working Group on Prediction (WGP), represented a broad cross section of the Earth Orientation Parameter (EOP) prediction community. W. Wooden, the chairperson of the WGP, served as moderator for the discussion. He introduced the panel members and explained that the purpose was to solicit input and suggestions from the conference attendees on the topics that are being considered by the working group. To stimulate subsequent discussion, each panel member gave their view on critical issues that need to be resolved for progress to be made in EOP prediction.

H. Schuh (Univ.Tech.Vienna) summarized the EOP Prediction Comparison Campaign and the interest generated by that activity. The primary conclusion was that prediction algorithms are extremely sensitive to the length of prediction required, i.e., there was no single algorithm that was best for all lengths of prediction. Additional conclusions were that a combination of deterministic and statistical components should be used, that predictions are better when geophysical fluid information is included, and that they also will improve when EOP measurements are obtained in near real-time.

W. Kosek (Space Research Centre, PAS), chairperson of the algorithms subgroup, summarized what we know about EOP data and their prediction. Namely, that EOP data have deterministic and stochastic components, that prediction accuracy is dependent on starting prediction epochs due to irregularities in the motion of the pole and the Earth's rotation, that prediction accuracy decreases with increasing prediction length, that prediction errors are much larger than the observational errors of the input data, that good approximation does not guarantee a good prediction, and that incorporating fluid excitation functions and forecasts improve prediction accuracy. Issues to be considered are how to best characterize differences between algorithms and what should be included in an algorithm for best results.

R. Gross (JPL), the head of the IERS Special Bureau of Oceans, spoke of his experience using a Kalman filter for EOP estimation in support of operational tracking and navigation of interplanetary spacecraft. The Kalman filter is particularly well suited to the task because of the stochastic nature of EOP. Frequently taken and rapidly processed measurements are necessary to meet stringent accuracies of spacecraft navigation. Results are greatly enhanced by incorporating atmospheric angular momentum data from weather models and somewhat improved from also including oceanic angular momentum.

T. van Dam (Univ.Luxembourg), chairperson of the input data subgroup, is head of the IERS Global Geophysical Fluids Center (GGFC) and spoke of her role in providing multiple new sources of potentially useful data and model information from the GGFC that can improve EOP prediction. It appears that there is significant unmodeled signal content in the time series of EOP, and the mass transport of geophysical fluids is a likely source. A better understanding/modeling of this process could reduce EOP prediction errors.

D. Salstein (Atmos.Environ.Research), the head of the IERS Special Bureau for the Atmosphere, has done extensive research of dynamical predictions of geophysical fluids (esp., atmosphere) angular momentum, for which connections to the EOP predictions may be made. He reviewed the model-based

analyses and forecasts of atmospheric angular momentum (AAM), talked about the components of AAM and the relationship to EOP, and gave an outlook of forecast skill as it relates to EOP prediction.

After the summaries by each panel member, the following list of questions was presented to solicit comments and suggestions from the attendees of the meeting:

1. How far into the future are predictions needed?
2. How often are updates needed?
3. Is precession/nutation modeling good enough to forget about celestial pole offset predictions?
4. What can be done to minimize data latency?
5. Are there other data sets with geophysical information that can be used in prediction?
6. What criteria should be used for comparing algorithms?
7. Should we focus on improving polar motion or UT1-UTC?
8. What criteria define a good algorithm?
9. Are there dynamical predictions of geophysical fluids angular momentum connections to EOP?
10. What other improvements are needed?
11. What statistics should be used for comparisons?

There was lively participation from the audience. Some questions were asked about accuracies of predictions and members of the audience suggested other models should also be considered. Unfortunately, time was short so not all of the listed questions could be considered by the audience. W. Wooden thanked the audience for their comments and suggestions and invited them to share any additional comments or suggestions with the panel members after the closing of the session. The reader is directed to other papers in this session for more detail on some of the work by the panel and others involved in EOP prediction activity.

ESTIMATION OF COEFFICIENTS OF DIFFERENTIAL EQUATIONS MODELING THE POLAR MOTION

Y. AKIMENKO, E. SPIRIDONOV, E. TSURKIS
Schmidt's Institute for Physics of the Earth RAS, Moscow, Russia
spiridonov@ifz.ru

ABSTRACT. We dealt with Liouville equations which describes the polar motion and presents a system of first-order equations with coefficients depending on T (period of free nutation) and Q (mantle quality factor). The actual problem is to evaluate these coefficients (i.e. T and Q) by:1) excitation functions series used for constructing right hand-side of Liouville equations and 2) polar coordinates series which one can interpret as a solution of the equations. Validity of this task which is typical inverse problem is shown. Practically we solved a number of "direct" ones under different meanings of T and Q. The preferred values of parameters to be estimated are: T=425-440 days and Q=20-60. Disagreement between our model based on Liouville equations and data series is conditioned by physical reasons, as far as mathematical problem is valid. Possible causes of such disagreement are discussed. In this work, we attempted to find optimal values T and Q as parameters fitted by the numerical integration of the Liouville equations with simultaneous modeling of the yearly and Chandlerian components of the pole motion. Also, the stability of values (T and Q) depending on time, length of data sets and different variants of excitation functions (right-hands sides of equations) was investigated.

1. MODELS

Five classes of models were examined. They differ one from another by excitation functions and length of data sets. The calculations of each model were carrying out in two variants: without and with variation of initial conditions (Models 1_1-5_1 and Models 1_2-5_2 accordingly). The free nutation period T and the quality factor Q at the resonance frequency were varied from 400 to 500 days (a step 2.4 h) and from 1 to 500 (a step of 0.1) accordingly. For each model we calculate the dispersion values D_{opt} for the chosen optimum model parameters (T and Q) and the correlation coefficient r between the optimum model and the observed pole motion series (in percent). The value D_{opt} was determined by the formula: $D_{opt} = 1 - D_{res}/D_{pm}$, where D_{res} is the dispersion of the residual series defined above and D_{pm} is the dispersion of the observed pole motion series.

Model 1. The right-hand sides of equations of motion (1) formed by excitation functions based on sum of OAM derived from R.Gross data sets an AAM (NCEP/NCAR, 2005).

Model 2 = Model 1, but the data here averaged by 10-days sinusoidal window (step 10 days). D_{opt} of this models accounts for more than 60-70%. The optimum quality factor here equal about 30 ± 10 and free nutation period T=435-439 days.

Model 3. As distinct from Models 1 and 2 the length of OAM and AAM excitation functions series in this model is twice as many (1962-2002). The excitation functions are the same. (Step = 10 days.) This model describes the least part of the pole motion sets dispersion. After initial condition selection Model 3_2 give $D_{opt} = 55 - 58\%$. Without this selection the model describes only 25-30% of dispersion. This model describes about 50% pole motion dispersion if $Q = 40 \pm 20$ (for Y-component) and $Q = 20 - 130$ (for X-component) in the range of period about $T = 432 - 438$ days. As a whole the Model describes the observed pole motion unsatisfactorily. In order to look into this fact we analyzed the changes of T and Q values in time. For that we calculate the values of parameters over the sequential short data sets chosen from sets of Model 3. We select seven 10-years sequential intervals with 5-years overlapping from 1962 till 2002. Lowest values of Q and D% correspond to period of time from 1962 till 1977. In time interval from 1972 till 1982 the Q value (for y-component) tends to infinity. Most likely it is a consequence of the best phase agreement of excitation functions and observed pole motion data sets. Following years

(1977-2002) the Q's values lies as a rule within the limits from 20 to 70. Optimum values of T lies in the range from 420 to 450 days.

Model 4. In contrast to previous models we use in this model the OAM mass terms were calculated by us from TOPEX/POSIEDON satellite altimetry data. Then we added these mass terms data sets with Gross's OAM motion terms and AAM excitation functions. The value of Dopt% obtained in the Model 4_2 for x- and y-components greater by 10% than one for Models 1_2 and 2_2. At the same time, we have here the greater uncertainty of Q values, calculated in Model 4_2, in comparison with previous models. Apparently it is a consequence of the short length of the TOPEX/POSEIDON project data sets. Thus, the use of the TOPEX data for calculation of OAM leads to adequate results in process of the pole motion modeling. However, short lengths of sets don't allow evaluate the quality factor value.

Model 5 constructed by excitation functions of Model 1 (OAM+AAM) plus water storage hydrology excitation functions(HAM, Jianli Chen). The Dopt% values of Model 5_1 obtain only 50% after initial conditions variation. It indicates to still insufficient quality of water storage excitation function data sets. (T=434-438 days, Q=30-40).

2. REFERENCES

Spiridonov, Eugene and Tsurkis, Elias. Modeling of the Earth's Pole Motion from Data on the Atmospheric and Oceanic Angular Momenta over 1980-2002, Izvestiya, Physics of the Solid Earth, 2006, Vol. 42, No 2, pp 149-155.

COMBINATION OF DIFFERENT SPACE GEODETIC TECHNIQUES: ALGORITHM OF PARAMETERS ESTIMATION

O. BOLOTINA[1], S. BOLOTIN[1], O. KHODA[1], Ch. BIZOUARD[2]
[1] Main Astronomical Observatory National Academy of Sciences of Ukraine
27, Akad. Zabolotnoho str., 03680, Kiev, Ukraine
e-mail: olga@mao.kiev.ua, bolotin@mao.kiev.ua, oleg@mao.kiev.ua
[2] Observatoire de Paris
61, avenue de l'Observatoire, 75014, Paris, France
e-mail: christian.bizouard@obspm.fr

ABSTRACT. Main principles of organization of parameters estimation for combination analysis are listed. Algorithm for estimation of parameters with an arbitrary time interval are described. Program realization of the algorithm are illustrated.

1. PARAMETERS ESTIMATION FOR COMBINATION ANALYSIS

The organization of parameters estimation is one of the main problem of the combination analysis. It is divided on three basic tasks: organization of recursive data analysis; combination of different types of parameters in one solution; estimation of parameters which are defined on an arbitrary time intervals.

A new algorithm for estimation of parameters with an arbitrary time interval was developed. It presents the following main features: least squares method realized with the square-root information filter are used for parameters estimation; forward pass of data processing is used for formation of normal equations system; then global parameters are estimated and on the backward pass local and stochastic parameters are evaluated.

2. IMPLEMENTATION

The presented algorithm for estimation of parameters was implemented in the software SteelBreeze.

As an example, we present an estimation of Earth orientation parameters (EOP) on the interval January 12–24, 1994. Here three VLBI networks performed observations, CONT-94, NAVex and R&D. One VLBI session of NEOS-A network also observed during this period.

The data analysis was performed using the IERS Conventions (2003) models. For the whole set of observations the coordinates of stations and sources were estimated. Their values were used as a priori for further tests. Then the EOP for separate networks and common set of observations were estimated (figure 1).

3. CONCLUSIONS

Proposed algorithm of parameters estimation has the following advantages. First, proposed algorithm is suitable for combined analysis of different space geodetic techniques. Second, this algorithm of parameters estimation allows to decrease sizes of working matrices, which leads to improving of data processing performance.

Acknowledgements. The work was supported by the Ministry of Education and Science of Ukraine (grant No M/102-2007 "High precise and consistent determination of the Earth Rotation and Terrestrial/Celestial Reference System") and French Government in the framework of the French-Ukrainian cooperation program DNIPRO.

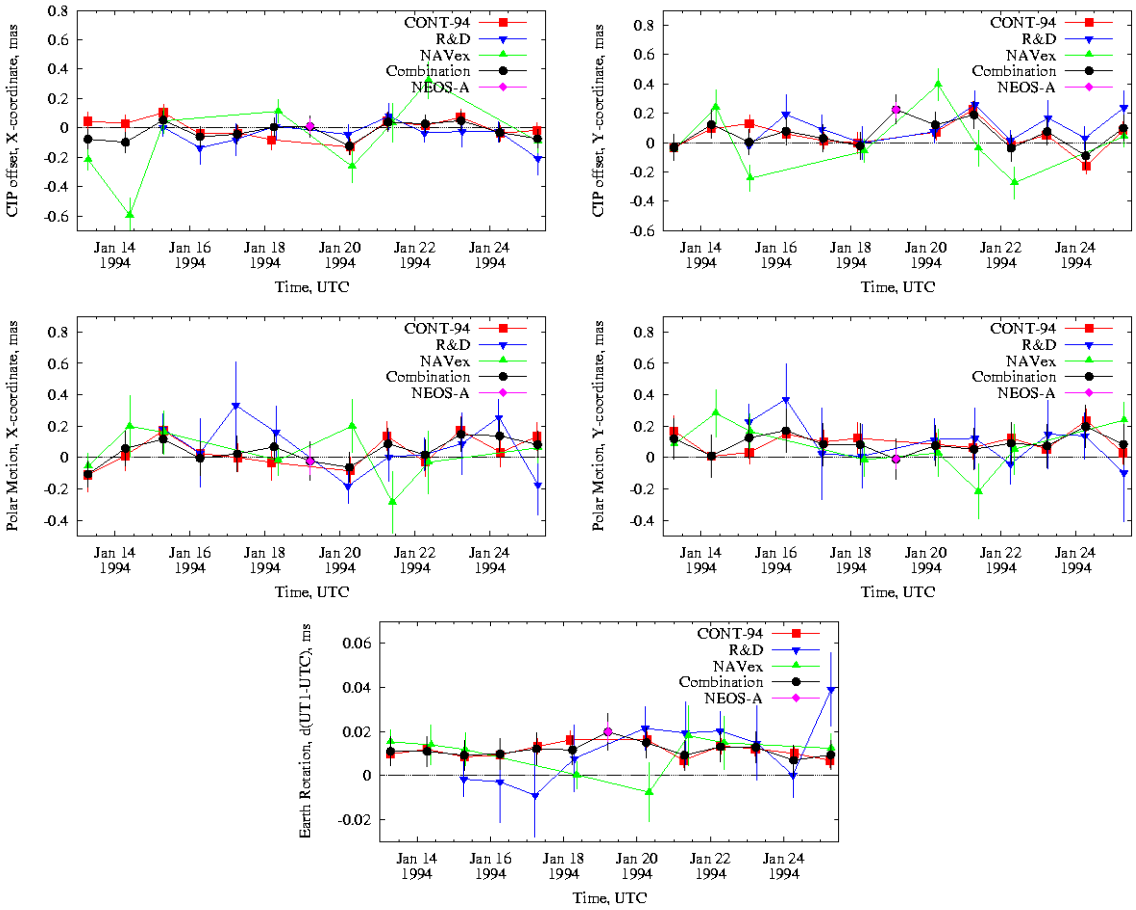

Figure 1: Estimations of EOP on separate VLBI networks and combined solution

4. REFERENCES

Bolotin, S., Bolotina, O., Khoda, O., 2005, "Methods of the combined VLBI, SLR and GPS data processing", Preprint MAO-05-1U, 18 p.

CORRELATION BETWEEN THE SOLAR ACTIVITY CYCLES AND THE EARTH ROTATION

Ya. CHAPANOV[1], D. GAMBIS[2]
[1] Central Laboratory for Geodesy of Bulgarian Academy of Sciences
Acad. G. Bonchev Str., Bl.1, 1113 Sofia, Bulgaria
e-mail: astro@bas.bg
[2] IERS EOP PC, Observatoire de Paris 61,
Avenue de l'Observatoire, 75014 Paris, France
e-mail: daniel.gambis@obspm.fr

ABSTRACT. The correlation between the solar activity cycles and the Earth rotation is investigated by means of UT1 series from the solution C04 of the IERS. The different oscillations of the Earth rotation are separated by an approximation of the difference UT1-TAI for the period 1962-2006, which includes power polynomials of degree up to 3, main oscillations with periods 22a, 18.6a, 12a, 6.75a, 1a and their harmonics. The UT1-TAI oscillations at solar activity frequencies are approximated with step-variable periods as follow: 11.1a for UT1 data before 1977.5; 10.3a for data between 1977.5 and 1987.8; 9.7a for data between 1987.8 and 1997.5; and 10.0a for data after 1997.5. The step-variable periods yield better approximation of the Earth rotation response to different solar activity cycles. The estimated UT1-TAI oscillations at solar activity frequencies are highly-correlated with the smoothed values of the Wolf's numbers with mean delay of about 1.5a.

1. MODELS OF EARTH ROTATION RESPONSE TO SOLAR ACTIVITY CYCLES

The most popular combination of all UT1-TAI observations comes from the solution C04 of the IERS, which is determined daily since the epoch 1962.0. This solution gives a good opportunity to study long-term variations of the Earth rotation and their relationships with some natural phenomena. A model of the Earth rotation variations is

$$\Delta UT1 = \sum_{m=0}^{3} p_m (t-t_0)^m + \sum_{k=1}^{6} \sum_{i=1}^{n_k} a_{ik}\mathbf{sin} i\omega_k (t-t_0) + b_{ik}\mathbf{cos} i\omega_k (t-t_0) + \sum_{j=1}^{44} B_j \mathbf{sin}\xi_j + C_j \mathbf{cos}\xi_j \quad (1)$$

where ΔUT1 is the difference UT1-TAI, the mean epoch t_0 is 1984.0, p_m are polynomial coefficients, n_k - the harmonics number of the frequencies $\omega_k = 2\pi/P_k$, which correspond to six periods P_k, and the coefficients B_j and C_j represent 44 zonal tidal terms ξ_j. The model of universal time response to the solar activity cycles includes oscillations with the following periods and their harmonics (Table1).

Table 1: Periods and harmonics numbers of the oscillations, included in the model of UT1 response to the solar activity.

Oscillations	Periods P_k	Harmonics number n_k
Solar activity (magnetic cycles)	22.06a	1
Lunar node	18.61295a	8
Empirical oscillation	11.94a	5
Solar activity (spot cycles)	10.47a	4
Gravity oscillations	6.75a	10
Seasonal oscillations	1a	10
Zonal tides	5.64d to 177.84d	44 waves

The model (1) approximates the UT1-TAI variations for the period 1962.0-2006.0 with accuracy about 1.5ms and maximal residuals between 4ms and 6ms, when the maximal number of used harmonics is 40. Here the model of universal time variations is truncated, so the quasi-biennial UT1 oscillations stay in the residual part of the approximation.

The Earth rotation response to solar activity cycles is determined by the UT1 residuals plus the oscillations with fixed period 10.47a (first case) and with step-variable periods 11.1a, 10.3a, 9.7a, 10.0a (second case, Table2). The correlation coefficients between the UT1 response to solar activity and the monthly mean Wolf's numbers W_n are +0.86 and +0.90 (Fig.1).

Table 2: Step-variable periods of UT1 response to the solar activity.

Time interval	Period P_k	Time interval	Period P_k
1962.0 – 1977.5	11.1a	1977.5 – 1987.8	10.3a
1987.8 – 1997.5	9.7a	1997.5 – 2006.0	10.0a

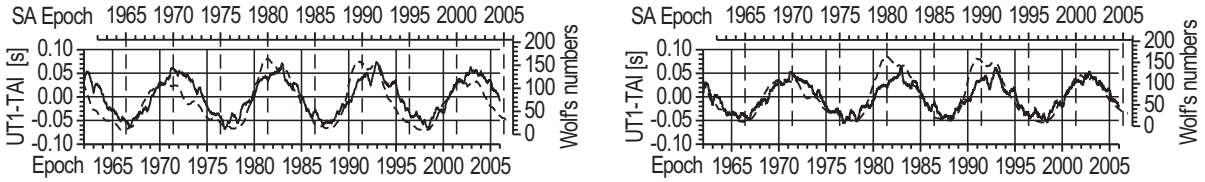

Figure 1: Comparison between the Earth rotation responses to the solar activity cycles and monthly mean Wolf's numbers. The time delay is 1.5a. The correlation coefficient is +0.86 in case of fixed period 10.47a (left) and +0.90 in case of step-variable periods (right).

2. REGRESSION MODELS OF SOLAR ACTIVITY INFLUENCE ON EARTH ROTATION VARIATIONS

Linear regression models of Earth rotation response to solar activity cycles are determined.

$$\begin{aligned} \Delta UT1_f &= 0.71W_n - 48.67, \\ \Delta UT1_v &= 0.59W_n - 42.06, \end{aligned} \tag{2}$$

where $\Delta UT1_f$ and $\Delta UT1_v$ are in [ms], the index f means the case of fixed period of 10.47a and the index v - the case of step-variable periods (Fig.2). The case of step-variable periods provides better linear fitting.

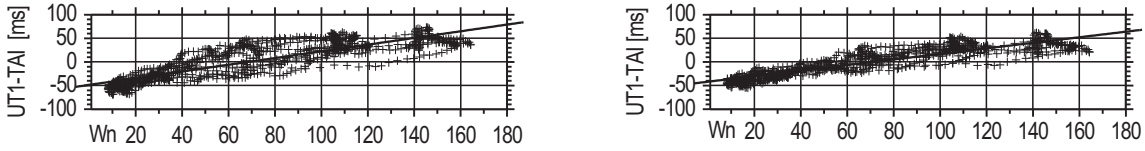

Figure 2: Linear regressions between the Earth rotation responses to the solar activity cycles and monthly mean Wolf's numbers W_n. The regression coefficients are 0.71ms per unit W_n in case of fixed period of 10.47a (left) and 0.59ms per unit W_n in case of step-variable periods (right).

3. CONCLUSIONS

The decadal variations of the Earth rotation are strongly affected by 11-year cycles of the solar activity. The Earth rotation response to the solar activity cycles is delayed by 1.5a. The correlation coefficient between 11-year UT1 variations and monthly mean Wolf's number is 0.86, when mean period of solar cycles 10.47a is used. The UT1 response to solar cycles, determined by step-variable periods, provides a better fit to the monthly mean Wolf's number, which increases the correlation coefficient to 0.90 and allows significant improvement of the linear regression model.

ESTIMATION OF THE SHORT-TERM ZONAL TIDES FROM UT1 OBSERVATIONS

Ya. CHAPANOV[1], C. RON[2], J. VONDRÁK[2]
[1] Central Laboratory for Geodesy of Bulgarian Academy of Sciences
"Acad. G. Bonchev" Str., Bl.1, 1113 Sofia, Bulgaria
e-mail: astro@bas.bg
[2] Astronomical Institute of Academy of Sciences of the Czech Republic
Boční II/1401a, 141 31 Prague, Czech Republic
e-mail: ron@ig.cas.cz; vondrak@ig.cas.cz

ABSTRACT. Zonal tides with periods shorter than 35d, according to the latest IERS model, are estimated by means of UT1-TAI series from the solution C04 of the IERS. Corrections of AAM and OAM influences on UT1 variations are applied. The accuracy of the estimated amplitudes of the fortnightly and monthly zonal tides is about 4μs. After removing the estimated zonal tides from UT1-TAI variations, the residual time series contain significant oscillations with periods below 35d. New 56 terms are involved and proposed here 97-term model of fortnightly and monthly zonal tides yields estimation of tidal amplitudes with accuracy of about 2.1μs and residuals below 13μs.

1. AAM INFLUENCE ON UT1-TAI VARIATIONS

Atmospheric Angular Momentum (AAM) function excites Length of Day (LOD) variations and provides strong disturbances at frequencies of short-term zonal tides, which should be removed before the tide estimation. AAM influence on UT1 periodical oscillations are determined by a numerical integration of AAM / LOD function after removing the AAM constant part. The resulting series still contain significant linear trends for time intervals 1962.0-1977.3; 1977.3-1995.8; 1995.8-2007.0 (Fig. 1, left graph). The final UT1 corrections for AAM are determined after removing of these trends (Fig. 1, right graph). Similar corrections of UT1 variations, due to Ocean Angular Momentum (OAM) are determined and applied.

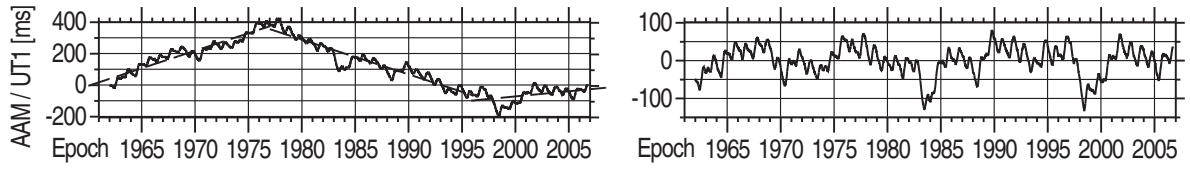

Figure 1: AAM influence on UT1 determined by numerical integration of AAM/LOD function (left) and UT1 corrections for AAM after removing the linear trends (right).

2. ESTIMATION OF MONTHLY AND FORTNIGHTLY ZONAL TIDES

The filtration of long-term UT1 variations is made by Fourier approximation of UT1 data between 1962.0-2007.0 with number of used harmonics equal to 470. The residuals of this approximation contain short-term UT1 oscillations with periods below 35d only. The UT1 data before 1983.0 contain relatively high level of noise, so the data after 1983.0 will be used in the next computations. The spectrum of tidal residuals according Yoder's model contain signals with significant amplitudes above 10μs. Additional zonal tide terms are used in (Schastok et al., 1994) and 6 of them are recognized here. Their values are marked by asterisks in Table 1. Additional 50 terms with amplitudes above 9μs are included in the estimation, so the original Yoder's model is expanded to 97-term model of fortnightly and monthly zonal tides. The periods of additional tidal terms are chosen to be close to the spectral peaks of the residuals and their fundamental arguments should be defined more accurately after comparison of the estimated and theoretical tidal amplitudes. The new model yields certain decrease of tidal residuals for

UT1 data before 1983.0 and excellent behavior of UT1 residuals after 1983.0 (Fig. 2). The estimated tidal amplitudes are in range 9–37μs with accuracy of about 2.1μs and residuals below 13μs (Fig. 2).

Table 1: Periods and estimated amplitudes of new tidal terms, added to original model of zonal tides.

l	l'	F	D	Ω	Period [d]	A[μs]	l	l'	F	D	Ω	Period [d]	A [μs]
2	1	0	0	4	13.381	13.3	4	-1	-2	-1	-1	28.396	13.9
4	1	-2	0	-1	13.413	22.4	4	-2	-1	-2	2	28.635	15.8
0	0	2	0	-4	13.498	17.5	-1	-1	2	0	-2	28.767	14.1
-2	2	2	2	1	13.519	25.9	0	0	0	1	-4	29.026	9.6
0	0	2	0	-1	13.54 *	36.7	0	0	0	1	-1	29.40 *	23.1
2	1	-1	1	4	13.918	16.0	1	-1	0	0	-1	29.673	13.9
2	-4	-2	2	4	18.092	12.7	1	-1	0	0	1	29.934	10.4
0	-4	-2	4	1	19.663	11.8	0	1	-1	2	4	30.186	12.8
4	4	-2	-1	0	20.509	9.4	1	-1	0	0	4	30.335	27.4
1	2	2	-2	0	21.036	10.3	-2	0	1	2	-4	30.788	20.3
-2	2	4	-1	-1	21.660	9.8	4	-2	-2	-1	-3	30.513	8.6
-4	4	4	1	4	21.715	14.2	-2	0	1	2	-2	31.070	18.9
2	1	1	-2	0	22.552	16.5	-1	0	0	2	-4	31.227	10.1
-2	1	4	-1	-1	23.025	11.9	-2	0	1	2	1	31.501	23.4
1	2	0	0	2	24.112	15.1	-1	0	0	2	2	32.112	17.1
2	1	0	-1	1	24.207	12.3	0	0	-1	2	0	32.281	9.7
1	2	0	0	4	24.284	21.0	1	-2	0	0	0	32.45 *	23.0
-2	2	2	1	-1	24.753	19.7	1	-1	-1	1	1	32.763	21.9
-1	1	2	0	1	25.13 *	23.2	1	0	-2	2	2	33.082	32.5
-1	2	1	1	4	25.506	16.5	2	-1	-2	1	1	33.261	34.2
2	1	-1	0	4	26.327	12.1	1	0	-2	2	4	33.408	11.5
-4	1	4	1	4	26.428	18.9	-2	-1	1	2	-4	33.623	35.7
4	0	-2	-1	1	26.553	20.7	-4	1	1	4	1	33.755	21.4
-1	0	2	0	-1	26.77 *	13.6	-4	1	1	4	2	33.927	26.1
-1	0	2	0	4	27.310	15.6	-2	-1	1	2	-1	34.129	17.2
0	2	-1	2	4	27.882	19.8	-1	-2	1	1	-2	34.319	31.4
4	-1	-2	-1	-4	28.045	34.3	-1	-2	1	1	0	34.669	14.5
-3	0	2	0	1	−28.15 *	22.0	-1	-1	0	2	1	35.026	19.2

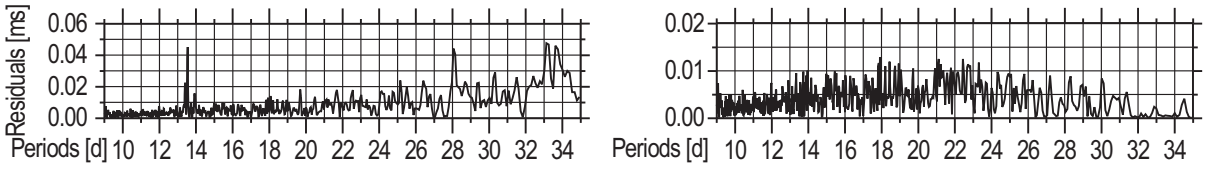

Figure 2: Residual spectra of fortnightly and monthly zonal tides determined by UT1 observations after 1983.0, according to the original model (left) and expanded 97-term model (right).

3. CONCLUSIONS

The UT1 time series from the solution C04 of the IERS contain high-accuracy data after 1983, which is possible to use for zonal tides estimation. The AAM affects various UT1 oscillations with periods below 35 days. The corrected UT1 series for AAM influence are useful for estimation of zonal tides. The estimation accuracy of fortnightly and monthly zonal tides increases significantly when new terms are added to the classical Yoder's model. The 97-term model of fortnightly and monthly zonal tides proposed here yields estimation of tidal amplitudes with accuracy of about 2.1μs and residuals below 13μs. The fundamental arguments and exact periods of the new terms should be defined more accurately after comparison of the estimated and theoretical tidal amplitudes.

4. REFERENCES

Yoder, C.F., Williams, J.G., Parke, M.E., 1981, "Tidal variations of Earth rotation", J. Geophys. Res., Vol. 86, pp. 881–891.

Schastok, J., Soffel, M., Ruder, H., 1994, "A contribution to study of fortnightly and monthly zonal tides in UT1", A&A 283, pp. 650–654.

USE OF ATMOSPHERIC ANGULAR MOMENTUM FOR UT1 PREDICTIONS

D. Gambis[1], J.Y. Richard[1], D. Salstein[2]
[1] Observatoire de Paris/SYRTE/UMR 8630-CNRS, Paris, France
[2] Atmospheric and Environmental Research, Inc, Lexington, MA , USA

ABSTRACT. Real-time orbitography and interplanetary navigation require accurate predictions of Universal Time UT1. On time scales of up to 10 days, variations in earth rotation are mostly due to dynamic effects of the atmosphere. Therefore, the axial Atmospheric Angular Momentum (AAM) series can be used as a proxy index to predict UT1 (Feissel et al., 1988; Gambis, 1990) . In the present work, we have been using AAM forecasts derived by three independent centres, i.e. the U.S. National Centers for Environmental Prediction (NOAA/NCEP, formerly NMC), the Japanese Meteorological Agency (JMA) and the United Kingdom Meteorological Office (UKMO). An adaptive procedure is being applied on a real-time basis in the frame of the EOP Prediction Campaign (Kalarus et al; 2007, same issue). We give the statistics concerning the prediction performances obtained in the process. They are in the range of respectively 300 and 600 microseconds for a forecast lead time of 5 and 10 days roughly twice better than the current predictions directly based on statistical procedures applied onto the earth orientation C04 time series.

1. ATMOSPHERIC ANGULAR MOMENTUM FUNCTIONS

Atmospheric Angular Momentum (AAM) fluctuations are due to the variability of the atmospheric circulation. It is well known that these fluctuations are compensated by opposite ones in the solid Earth, a process accomplished by the dynamical interactions between the atmosphere and the underlying planet. The Atmospheric Angular Momentum (AAM) functions can be expressed as excitation functions of Earth rotation because of conservation of angular momentum between Earth and atmosphere due to a pressure-term related to the redistribution of the air masses and a wind-term related to the relative angular momentum of the atmosphere. The length-of-day variation can be directly expressed as:

$$\frac{\Delta LOD}{LOD} = \chi_3$$

2. IMPROVEMENT OF ATMOSPHERIC FORECASTS

Forecasts made at weather centers are based on equations that advance the state of the atmosphere in time, which including those of motion, energy, and moisture as well as the detailed description of atmospheric physical interactions. The sophistication of the various models contained within the weather forecast systems, as well as the quality of the initial and boundary conditions, dependent upon a mixture of meteorological observations, both in situ and remotely sensed, are of paramount importance to the quality of the forecasts. For example latest improvements at NCEP include new radiation schemes within the model physics. A three-dimensional variation approach and an improved vertical coordinate system are in place, and new observing systems are available. Such developments are relevant to the predictions related to winds and surface pressure, and hence, AAM. Information concerning how the skill of wind forecasts decrease with lead time during a recent period is given by the Heidke Skill Score, which is the percentage improvement of successful forecasts over those due to random chance.

Data sets used

We have used the following data sets: JMA: Since early 1993, the AAM functions computed from the JMA global analysis data at 00h UTC, 06h UTC, 12h UTC and 18UTC have been provided operationally. Forecasts are out to 8 days. NCEP: AAM forecasts are computed at 12 hour intervals over 5 days; since October 2007 they have been extended to 7 days. UKMO: AAM forecasts are computed at 24 hour intervals over 6 days

Procedure used

1 - Predicted values of AAM are transformed into an equivalent LODR series using both pressure and wind terms

2 - The AAM-derived LODR is then integrated into a 10-day UT1R prediction

3 - The method is adaptive, i.e. the bias error on LOD (linear drift on UT1) computed on the previous 10-day interval is used for the following real time forecast

4 - The process is done each week on Thursdays for each series JMA, NCEP and UKMO in the frame of the EOP Prediction Campaign (Kalarus et al., 2007)

5 - Since the individual AAM series are given for different time spans (5 to 8 days depending on the AAM Analysis Center) a linear extrapolation is made to give a 10-day forecast required by the EOP Prediction Campaign.

6 - A combined mean solution based on the three independent solutions then performed

7 - Every week the difference between this atmospheric based UT1R series and the reference 05C04 series is made

8 - Absolute mean errors of differences are given from 1 to 10 days for the 4 series. This mean error give the quality of the forecasts performances.

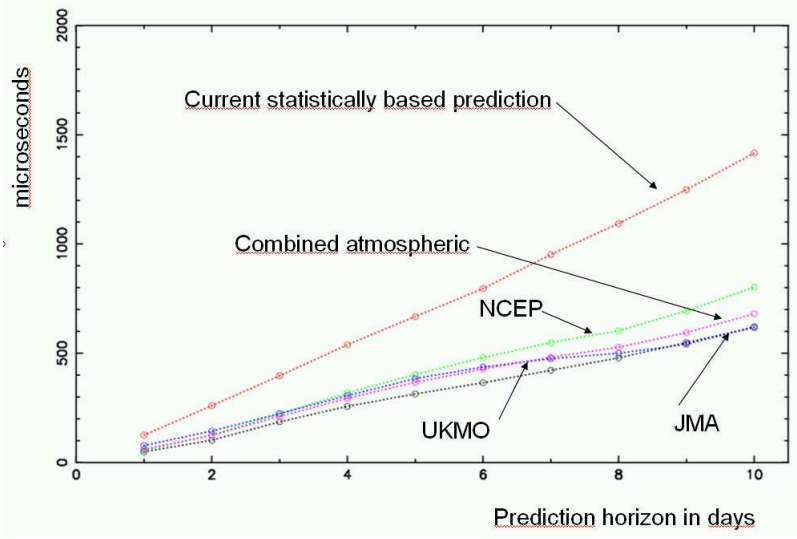

Figure 1: - UT1-UTC mean prediction skill based on the integration of the axial angular momentum prediction derived from various centers, i.e; JMA, NCEP (NMC), UKMO , their mean. The current prediction based on purely statistical processes has errors twice as large as those using the AAM forecast approach.

3. CONCLUSIONS

The Prediction Comparison Campaign is a good opportunity to check the performance of the procedure of used AAM-based UT1 on a real-time basis. Mean errors over a time span of 6 months are in the range of 300 and 600 microseconds for a horizon of 5 and 10 days, respectively. All centers' forecasts have approximately the same quality and that of the combined solution is not significantly better than that of any individual. The use of AAM can lead to on the order of a factor of 2 improvement compared to statistical predictions just related to the EOP series themselves.

4. REFERENCES

Feissel M., D. Gambis and T. Vesperini, 1988,Predicting Weeks to Months Variations of the Earth Rotation Parameters, Babcock and Wilkins (eds), Reidel, pp269-273.

Gambis D., 1990, Universal Time prediction using both geodetic and atmospheric Angular Momentum, data, Springer-Verlag (ed.), New-York Publishers.

Kalarus M., Kosek W. and Schuh, H, 2007, Current results of the Earth Orientation Parameters Prediction Comparison Campaign, Pres. at Journes JSR2007, Paris, France, 17-19 September 2007.

THE IMPACT ON EOP PREDICTIONS OF AAM FORECASTS FROM THE ECMWF AND NCEP

R. S. GROSS[1], O. DE VIRON[2], T. VAN DAM[3]
[1] Jet Propulsion Laboratory, California Institute of Technology
4800 Oak Grove Drive, Pasadena, CA 91109, USA
e-mail: Richard.Gross@jpl.nasa.gov
[2] Institut de Physique du Globe de Paris et Université Paris 7
4, Place Jussieu, 75252 Paris, France
e-mail: deviron@ipgp.jussieu.fr
[3] University of Luxembourg
162a, avenue de la Faïencerie, L-1511 Luxembourg
e-mail: tonie.vandam@uni.lu

1. INTRODUCTION

Predictions of UT1 are improved when dynamical model-based forecasts of the axial component of atmospheric angular momentum (AAM) are used as proxy length-of-day (LOD) forecasts (Freedman et al. 1994; Johnson et al. 2005). For example, the accuracy of JPL's predictions of UT1 are improved by nearly a factor of 2 when AAM forecast data from the National Centers for Environmental Prediction (NCEP) are used. Given the importance of AAM forecasts on the accuracy of UT1 predictions, other sources of AAM forecasts should be sought. Here, the angular momentum of the forecasted wind fields from the European Centre for Medium-Range Weather Forecasts (ECMWF) are computed and used to predict UT1. The results are compared to those obtained using NCEP forecasts.

2. UT1 PREDICTION ERROR

In support of spacecraft navigation, JPL's Kalman Earth Orientation Filter was run 73 times during 19 March 2004 to 22 July 2004 to predict polar motion and UT1. These runs have been re-processed here using the ECMWF forecasts instead of the NCEP forecasts that were used then. Since the angular momentum of only the 5-day wind forecasts from NCEP are used at JPL to predict UT1, only the 5-day wind forecasts from ECMWF are used here. Table 1 gives the error in the resulting predictions of UT1 out to 7 days in the future. This error was determined by comparing the predictions to measurements that were taken at the time the predictions were generated but that were not available until later. As seen in Table 1, if no AAM forecasts are used to predict UT1, the error in the predictions grows rapidly, becoming 33.7 cm after just 7 days. But when AAM forecasts are used, the error is dramatically reduced, becoming only 19.2 cm after 7 days with the NCEP forecasts, and 20.1 cm with the ECMWF forecasts.

To assess the potential impact of oceanic angular momentum (OAM) forecasts on UT1 predictions, an OAM series has been added to the AAM forecasts and the predictions re-generated. Since actual OAM forecasts are not currently available, analyses from the ECCO/JPL data assimilating ocean model kf066b were treated here as if they were forecasts. As seen in Table 1, adding the OAM to the AAM forecasts improves the UT1 predictions, reducing the error of the 7-day prediction from 19.2 cm to 17.9 cm when added to the NCEP AAM forecasts, and from 20.1 cm to 19.4 cm when added to the ECMWF forecasts.

3. DISCUSSION AND SUMMARY

Both the NCEP and ECMWF 5-day wind AAM forecasts agree extremely well with LOD during 19 March 2004 to 22 July 2004, with respective correlations of 0.9879 and 0.9914, and with 97.565% and 96.931% of the observed LOD variance being explained by the NCEP and ECMWF AAM forecasts, respectively. This high degree of agreement allows AAM forecasts to be used as proxy LOD forecasts when predicting UT1.

NCEP and ECMWF 5-day wind AAM forecasts are found to have similar impact on UT1 predictions.

Table 1: UT1 Prediction Error

Forecast Series	Prediction Interval, days							
	0	1	2	3	4	5	6	7
No forecasts	4.1	4.7	5.8	8.5	12.9	18.7	25.7	33.7
NCEP 5-day wind forecasts	4.2	4.7	5.5	6.9	9.0	11.7	15.0	19.2
ECMWF 5-day wind forecasts	4.1	4.7	5.6	7.2	9.6	12.4	15.9	20.1
NCEP 5-day wind forecasts & OAM	4.2	4.7	5.5	6.8	8.7	11.1	14.1	17.9
ECMWF 5-day wind forecasts & OAM	4.1	4.7	5.6	7.2	9.5	12.1	15.4	19.4

Prediction day 0 is the epoch of the last polar motion measurement. The epoch of the last UT1 measurement is typically a few days earlier. Units of UT1 prediction error are cm. 46.3 cm = 1 ms.

ECMWF AAM forecasts would therefore be a valuable additional source of AAM forecasts for predicting UT1 if they could be made available as routinely and rapidly as are the NCEP forecasts. Furthermore, since the ECMWF forecasts extend out to 10 days in the future, whereas the NCEP forecasts extend out to only 7.5 days, using the ECMWF forecasts would improve UT1 predictions beyond 7.5 days.

Adding OAM to AAM forecasts improves the accuracy of the UT1 predictions only slightly. This is to be expected given the high degree of agreement that already exists between LOD and AAM. But adding OAM to AAM forecasts should greatly improve polar motion predictions since the oceans are known to be a major source of polar motion excitation.

Acknowledgements. The work of one of the authors (RSG) described in this paper was performed at the Jet Propulsion Laboratory, California Institute of Technology, under contract with the National Aeronautics and Space Administration.

4. REFERENCES

Freedman, A.P., Steppe, J.A., Dickey, J.O., Eubanks, T.M., Sung, L.-Y., 1994, "The short-term prediction of universal time and length of day using atmospheric angular momentum", J. Geophys. Res. (Solid Earth), 99(B4), pp. 6981–6996.

Johnson, T.J., Luzum, B.J., Ray, J.R., 2005, "Improved near-term Earth rotation predictions using atmospheric angular momentum analysis and forecasts", J. Geodyn., 39, pp. 209–221.

REPORT ON THE FENNOSCANDIAN-JAPANESE PROJECT FOR NEAR REAL-TIME UT1-OBSERVATIONS WITH E-VLBI

R. HAAS[1], J. WAGNER[2], J. RITAKARI[3], A. MUJUNEN[4], M. SEKIDO[5], H. TAKIGUCHI[6], Y. KOYAMA[7], T. KONDO[8], S. KURIHARA[9], D. TANIMOTO[10], M. POUTANEN[11]
[1] Chalmers University of Technology, Department of Radio and Space Science,
Onsala Space Observatory, SE-439 92 Onsala, Sweden
e-mail: rudiger.haas@chalmers.se
[2−4] Helsinki University of Technology, Metsähovi Radio Observatory,
Metsähovintie 114, FIN-02540 Kylmälä, Finland
e-mail: [2] jwagner@kurp.hut.fi, [3] jr@kurp.hut.fi, [4] amn@kurp.hut.fi
[5−8] National Institute of Information and Communications Technology,
Kashima Space Research Center, 893-1, Hirai Kashima Ibaraki, 314-8501 Japan
e-mail: [5] sekido@nict.go.jp, [6] htaki@nict.go.jp, [7] koyama@nict.go.jp, [8] kondo@nict.go.jp
[9−10] Geographical Survey Institute,
Kitasato 1, Tsukuba, Ibaraki, 305-0811 Japan,
e-mail: [9] skuri@gsi.go.jp, [10] tanimoto@gsi.go.jp
[11] Finnish Geodetic Institute,
Geodeetinrinne 2, FIN-02430 Masala, Finland
e-mail: Markku.Poutanen@fgi.fi

ABSTRACT. The Fennoscandian-Japanese project for near real-time UT1-observations with e-VLBI is a collaboration between the VLBI research groups at the telescopes Onsala (Sweden), Metsähovi (Finland), Kashima (Japan) and Tsukuba (Japan). Several UT1-sessions were observed during 2007 and the e-VLBI data technology was applied to send in real-time the Fennoscandian data to software correlators in Japan where the data were correlated with the Japanese data in near real-time. The final UT1 estimates were available in the best cases already within 30 minutes after the end of a one hour long observing session. The latency of the UT1 measurement could thus be improved dramatically compared to the regular Intensive sessions (INT) of the International VLBI Service for Geodesy and Astrometry (IVS). The accuracy of the derived UT1 values was confirmed to be as accurate as the combined solution of International Earth Rotation Service (IERS).

1. MOTIVATION AND INTRODUCTION

Geodetic Very Long Baseline Interferometry (VLBI) is one of todays most important geodetic space technique for the determination of Earth orientation parameters (EOP). It is of major importance in particular for UT1 and nutation. The International VLBI Service for Geodesy and Astrometry (IVS) organizes daily UT1 observations in the so-called Intensive-series (INT). These sessions are usually observed during one hour with two stations that form a long east-west baseline. However, the final UT1 results from these INT sessions are usually not available before several hours to days after observation, mainly due to delays in data transfer and data correlation. Thus, any application that demands accurate close to real-time UT1 values, e.g. space navigation, suffer from this high latency and so far depends on UT1 predictions, e.g. the IERS Bulletin-A predictions.

In order to improve the latency of UT1 results and to study systematic influences on the VLBI derived UT1 results, the VLBI research groups at the Kashima Space Research Center (Japan), the Geographical Survey Institute at Tsukuba (Japan), the Onsala Space Observatory (Sweden) and the Metsähovi Radio Observatory (Finland) started a project in early 2007 to measure UT1 with e-VLBI.

The four research groups operate VLBI telecopes that are used for geodetic VLBI and have access to international high-speed optical fibre networks at data rates of at least 1 Gbit/sec. Furthermore, operate the two Japanese groups software-correlators that were developed at Kashima and allow near real-time correlation. These pre-requisites make it possible to perform e-VLBI experiments.

2. OBSERVATIONS AND RESULTS

The Fennoscandian-Japanse e-VLBI UT1 measurements were started in April 2007 using the VLBI network shown in the left graph of Figure 1. Between April and December 2007 more than 20 sessions were observed, and different observing setups with data rates of 128 Mbps, 256 Mbps and 512 Mbps were tested. In all sessions the observational data from Onsala and/or Metsähovi were sent in real-time or close to real-time with the data transfer protocol "Tsunami" via high-speed optical fibre networks to Kashima and/or Tsukuba where the data were correlated with software-correlators. After the near real-time correlation, the data were analyzed with a VLBI data analysis software. For several of the sessions, the final UT1 results were derived already 30 minutes after the end of the observations. This is a new record for ultra-rapid UT1 measurements.

The derived UT1 results have formal errors on the order of a few microseconds to several tens-microsecond. The agreement between the e-VLBI derived UT1 results and the final IERS EOPC04 values is on the order of a few microseconds to several tens-microsecond, too. The right graph in Figure 1 shows as an example the e-VLBI UT1 results obtained during the first half of 2007 together with IERS Bulletin-A predictions and IERS EOPC04 final results. The e-VLBI UT1 results agree well with the final IERS EOPC04 values, while the prediction values degrade rapidly.

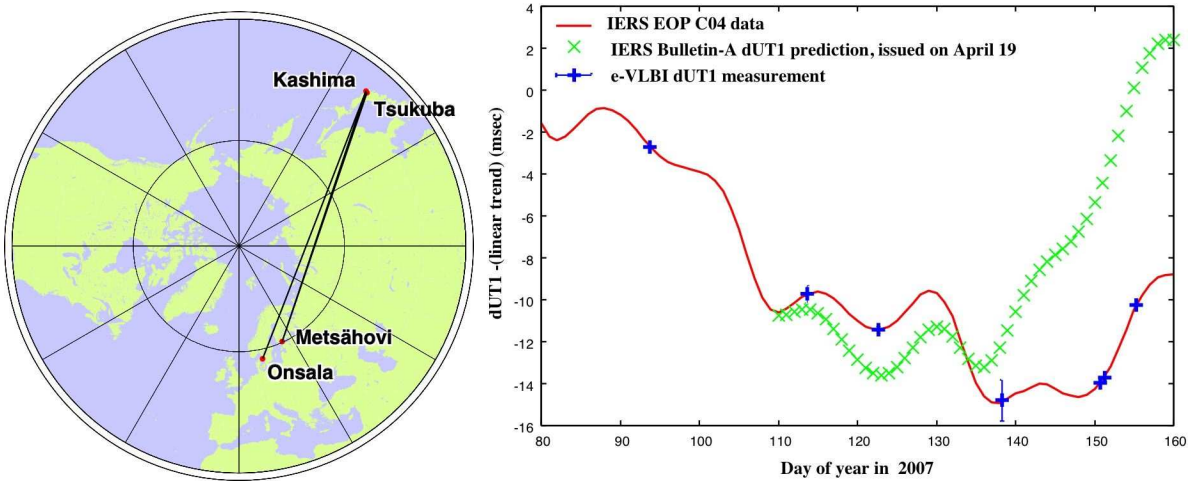

Figure 1: Left: VLBI-network for the Fennoscandian-Japanese project for near real-time UT1-observations with e-VLBI. Right: e-VLBI UT1 results (blue dots with error bars) during the first half of 2007 compared to IERS EOPC04 values (green crosses) and IERS Bulletin-A predictions (red line).

3. CONCLUSIONS AND OUTLOOK

The Fennoscandian-Japanese e-VLBI UT1 project is very successful and provides accurate UT1 results with low latency. We demonstrated that e-VLBI UT1 results can be derived within 30 minutes after an observing session of one hour. Observing data rates of 128 Mbps, 256 Mbps and 512 Mbps have been applied successfully. The agreement between the e-VLBI derived UT1 values and the IERS EOPC04 values is within several tens-microsecond. Thus, our e-VLBI results provide the same level of accuracy as IERS EOPC04 already with observations on just a single baseline.

We will continue this successful project and focus in the future on:

1. the investigation of systematic errors in UT1 estimation by inter-comparison of results derived on parallel baselines as well as other IVS routine session
2. the consistency of ultra-rapid UT1 results with standard IVS results
3. the impact of different data rates and scheduling options on the UT1 results

METEOROLOGICAL INTERPRETATION OF TRANSIENT LOD CHANGES

Y. MASAKI
Geographical Survey Institute
1, Kitasato, Tsukuba, Ibaraki, 305-0811, JAPAN
e-mail: ymasaki@gsi.go.jp

ABSTRACT. The Earth's spin rate is mainly changed by zonal winds. For example, seasonal changes in global atmospheric circulation and episodic changes accompanied with El Niños are clearly detected in the Length-of-day (LOD). Sub-global to regional meteorological phenomena can also change the wind field, however, their effects on the LOD are uncertain because such LOD signals are expected to be subtle and transient. In our previous study (Masaki, 2006), we introduced atmospheric pressure gradients in the upper atmosphere in order to obtain a rough picture of the meteorological features that can change the LOD. In this presentation, we compare one-year LOD data with meteorological elements (winds, temperature, pressure, etc.) and make an attempt to link transient LOD changes with sub-global meteorological phenomena.

1. INTRODUCTION

The Earth's spin rate is sensitive to atmospheric zonal motion at a global scale. In observed LOD excess, various types of transient signals which are superimposed on seasonal variations are detected. LOD changes associated with El Niño events are famous examples on episodic LOD signals occurred by meteorological phenomena. The southern oscillation index (SOI) is a good indicator for such LOD changes because the SOI is strongly correlated with activity of El Niños (e.g., Chao (1984), Dickey et al.(1999)).

Then, what are other transient LOD signals attributable to? Do other meteorological indices can also explain LOD changes? Since such transient changes are also detected in the atmospheric angular momentum (AAM) functions, they must reflect atmospheric phenomena.

Geodetic observation may have potential tasks on monitoring Earth's climate changes in near future. It is important to know what becomes detectable through geodetic observation.

We compare one-year-data of the LOD excess for 2005 with meteorological data or meteorological indices which describe the atmospheric circulation status at a sub-global scale. These indices are expected to have close relations to the zonal flow of the atmosphere.

2. ANALYSIS METHOD

Meteorological data used in this study is the NCEP-DOE reanalysis data. Since episodic signals produced by transient atmospheric phenomena are overwhelmed by seasonal signals, mean seasonal variation averaged over 25-year-data (1979-2003) is subtracted from the original time-series data.

Since seasonal variation of UT1 is well approximated by the UT2 function, we subtract UT2 from UT1. The Earth's spin rate is expressed in the LOD excess.

3. RESULTS AND DISCUSSION

We show meteorological data (wind velocity anomalies from the mean value and meteorological indices which represent the atmospheric status at a sub-global scale) for 2005 in Fig. 1.

So far, some events in the LOD can be explained by meteorological indices, however, no strong relations between meteorological indices (except for the SOI) and the LOD excess have been found. A brief summary on the results for two meteorological indices is shown below:

Blocking index: A blocking index represents blocking activity in the westerlies at mid- or high latitudes. When a strong blocking occurs, we can see the negative zonal wind anomaly at high latitudes

(Figure 1 (a)). However, its effect on the Earth's spin rate is small (Figure 1 (b)) because of the smaller effect on the angular momentum change by winds blowing at higher latitudes.

Arctic Oscillation: In theory, a positive Arctic Oscillation (AO) index intensifies the polar jet and weakens the subtropical jet. In early spring of 2005, the AO index turns negative. Around the same time, the SOI also turns negative. Both indices intensify increase in the LOD excess, the opposite case of 1989 (de Viron et al.(2001)) but for a shorter duration.

Meteorological indices used in this study mainly describe the atmospheric status at mid- or higher latitudes. Therefore, even if they certainly affect the wind field at higher latitudes in Figure 1 (a), their effects on the LOD become smaller (Figure 1 (b) and (c)) because excitation efficiency depends on the latitude. The well-known index, SOI, describes the atmospheric status at low latitudes where the atmosphere efficiently excites the Earth's spin rate variation, the index strongly correlates with the LOD changes.

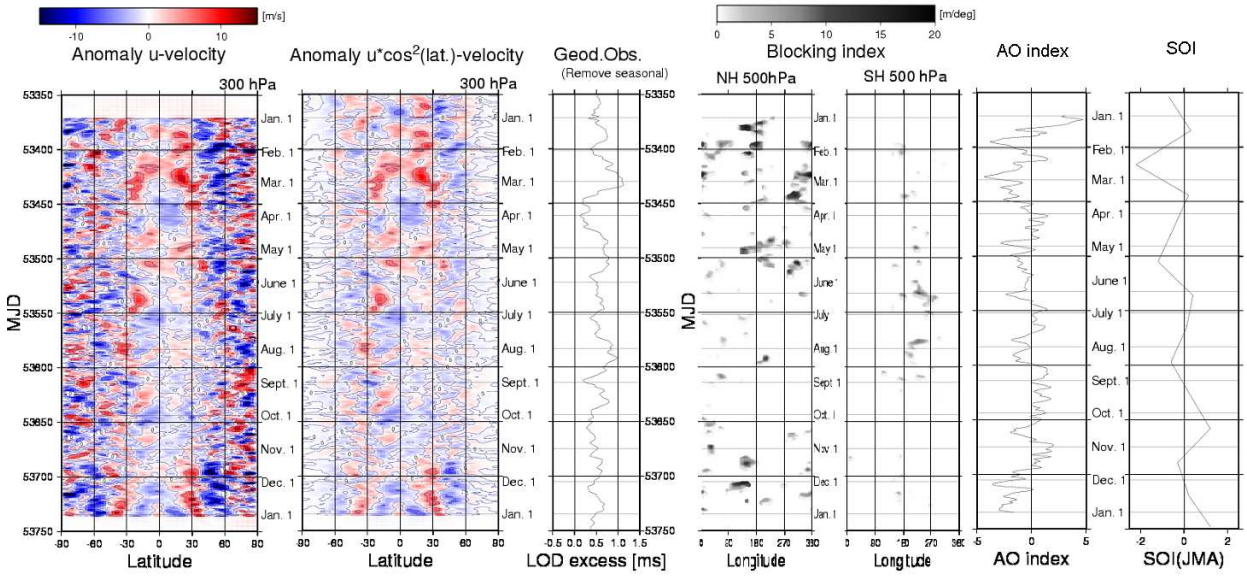

(a) (b) (c) (d) (e) (f) (g)

Figure 1: Meteorological data and the Earth's spin rate (converted into the LOD excess) for 2005. In the left three panels, seasonal variations are removed from the original data. Wind data are zonally averaged. From left to right: (a) latitude dependence of zonal wind velocity anomaly at 300 hPa (b) same as (a), but multiplied by $\cos^2$(latitude), in order to easily read contribution to the axial AAM function from the plot (c) LOD excess (seasonal (UT2) contribution is removed). The right four panels show meteorological indices which describe the atmospheric circulation status at a sub-global scale. (d/e) the NH/SH blocking index (f) the arctic oscillation (AO) index (calculated by the CPC/NCEP) (g) the southern oscillation index (SOI) (calculated by the JMA).

4. REFERENCES

Chao, B.F., 1984, "Interannual Length-of-day Variation with Relation to the Southern Oscillation/El Nino", Geophys. Res. Lett., 11(5), 541–544.

de Viron, O., S.L. Marcus and J.O. Dickey, 2001, "Atmospheric Torques during the Winter of 1989: Impact of ENSO and NAO positive phases", Geophys. Res. Lett., 28(10), 1985–1988.

Dickey, J.O., P. Gegout and S.L. Marcus, 1999, "Earth-atmosphere Angular Momentum Exchange and ENSO: The Rotational Signature of the 1997-98 Event", Geophys. Res. Lett., 26(16), 2477–2480.

Masaki, Y., 2006, "Estimation of UT1 Variations from Atmospheric Pressure Data", submitted to the Proceedings of 'Geodetic Reference Frames 2006' (Oct. 9-14, 2006, Munich, Germany).

THE POLAR MOTION AND THE DRACONITIC PERIOD

G. MORCOV
Faculty of Geodesy
B-dul Lacul Tei, nr. 124, sector 2, Bucharest, Romania
e-mail: georgemorcov@yahoo.com

ABSTRACT. The main topic of this paper is to study how an average of the periods belonging to the circular components of the polar motion (Chandler's wobble) can be determined and its supervision through a connection with the period of the lunar precession. There is an average period of the polar circular periods, well determined, using the synodic polar periods as weights. These ones are offering to the determined medium polar period, precision and stability. There is an empirical connection between the equation of the eclipses' year (the draconitic year) and the medium circular polar period, determined on the basis of the polar synodic periods, whose accuracy is offered by the proximity of its value to 435.4 days. We propose the following equation: 1/T = 1/435.42 z + 4/T2 and 1/T1 = 1/435.42z + 3/T2, derived from the equation of the draconitic year (the eclipses' year) 1/T= 1/T1 + 1/T2.

1. GOAL, METHODS AND EXAMPLES

The goal of this paper is to determine a medium circular polar period (Chandler's wobble) stable and accurate and to supervise the circular polar periods through a connection between the medium circular polar period and the lunar precession period. For determining the medium circular period we have introduced the indirect usage as weights of the synodic periods of the circular polar periods. We are taking in consideration the following: Pi= the polar circular periods; Si= the polar synodic periods. For each polar period we can determine the synodic period related to it, adjusted to a Pm period, closed to the average: 1/Si = | 1/Pi ± 1/Pm | (1).

Making determinations of synodic polar periods' sum for different Pm values, the medium circular polar period can be defined as being that Pm value for which the sum of the synodic periods is minimal. The advantages are: 1) the synodic polar periods of the extreme spires (related to the circular polar periods that are very small or very big) are going to have quite small weights as compared with the average, while the synodic polar periods of the medium spires (with small errors) are going to have quite big weights, as compared also with the average; 2) the average of the polar motion that is calculated in this way, is very stable, remaining unchanged even in the case of eliminating some terms, especially the extreme ones (because they have an insignificant share to the creation of the average). In this way, there can be diminished, without affecting the average, the circular polar periods with extreme values (and not only), bearers of the deviations with the greatest values. For the surveillance of the circular polar periods, the empirical connection between the average circular polar period and the lunar precession can be used. The known equation of the eclipses' year is: 1/T= 1/T1 + 1/T2 (2), where: T = 346.62 days (the eclipses' year) T1=365.24 days (the tropical medium year) and T2=18.6128 x 365.25 days (the period of the lunar precession). Decomposing equation (2) into two other equations (3) and (4), the value of 435.42 days close to that of the medium polar period there is underlined:

1/T = 1/435.42 z + 4/T2 (3) and

1/T1 = 1/435.42z + 3/T2 (4).

We can observe the fact that if we decrease term by term, equation (3) and (4), we get the known equation of the eclipses' year or of the draconitic year (1). Equation (3) shows us that the eclipses' year (T) is synodic combined with the period of 435.42 days and with a quarter (1/4) from the lunar precession period. In equation (4) there can be seen that the tropical medium year (T1) is synodical combined with a period of 435.42 days and with a third (1/3) from the lunar precession period.

Making some practical determinations of the spires belonging to polar motion, having as references for the circular polar periods the EOP (IERS) C04 data, between the years of 1962-2006, it resulted a polar medium period with values between 435 and 436 days, slightly different from Chandler's wobble. There is an empirical connection between the medium circular polar period and the period of 435.42

days, because in the previous examples that medium circular polar period is closed to the period of 435.42 days. But when it is slightly different from this one, the difference is reduced by eliminating some terms that are generally related to very small circular polar periods. That is why in the example above mentioned, the average of 435.7 was diminished to 435.4 days, through the elimination of the smallest circular synodic periods. The same method was applied to other examples. It should be underlined that by eliminating these circular synodic periods with quite small weights, the deviation with quite big values is also eliminated. This leads to an improved accuracy and to a potential of using it within the field of predictability. The coincidence between the average of the polar circular components with the period of 435.42 days allows the usage of the synodic combination from equations (3) and (4).

2. REFERENCES

http://hpiers.obspm.fr/iers/eop/eopC04_new/eopC04‘_IAU2000.62-now
http://www.jgiesen.de/planets/index.html

COMPARISON OF HYDROLOGICAL AND GRACE-BASED EXCITATION FUNCTIONS OF POLAR MOTION IN THE SEASONAL SPECTRAL BAND

J. NASTULA[1], B. KOLACZEK[1], D.A. SALSTEIN[2]
[1] Space Research Center of the PAS
Bartycka 18a, 00-716 Warsaw, Poland
e-mail: nastula@cbk.waw.pl, kolaczek@cbk.waw.pl
[2] Atmospheric and Environmental Research, Inc.
131 Hartwell Avenue, Lexington, MA 02421
e-mail: dsalstei@aer.com

ABSTRACT. Understanding changes in the global balance of the Earths angular momentum due to the mass redistribution of geophysical fluids is needed to explain the observed polar motion. The impact of continental hydrologic signals, from land water, snow, and ice, on polar motion excitation (hydrological angular momentum-HAM), is still inadequately known. Although estimates of HAM have been made from several models of global hydrology based upon the observed distribution of surface water, snow, and soil moisture, the relatively sparse observation network and the presence of errors in the data and the geophysical fluid models preclude a full understanding of the HAM influence on polar motion variations. Recently the GRACE mission monitoring Earths time variable gravity field has allowed us to determine the mass term of polar motion excitation functions and compare them with the mass term derivable as a residual from the geodetic excitation functions and geophysical fluid motion terms on seasonal time scales. Differences between these mass terms in the years 2004 - 2005.5 are still on the order of 20 mas. Besides the overall mass excitation of polar motion comparisons with GRACE (RL04-release), we also intercompare the non-atmospheric, non-oceanic signals in the mass term of geodetic polar motion excitation with hydrological excitation of polar motion.

1. DATA AND ANALYSES

Three different sets of degree-2, and order-1 harmonics of the gravity field, derived from Gravity Recovery and Climate Experiment (GRACE) data, processed at the GeoforschungsZentrum (GFZ-RL04), Jet Propulsion Laboratory (JPL-RL04), and Center for Space Research (CSR-RL04), http://grace.jpl.nasa.gov, are used to compute the polar motion excitation functions (Fig.1).

The geodetic mass excitation function (G - WC) is obtained by a time domain deconvolution formula applied to the IERS C04 series of polar motion, based on a combination of geodetic observing techniques. The mass term of the geodetic excitation function is estimated by removing the atmospheric winds (W) and oceanic currents (C) terms (Figs. 1, 2).

Atmospheric excitation function (AAM) is from the U.S. NCEP-NCAR reanalysis [Kalnay et al., 1996], including pressure with inverted barometer correction (PIB) and wind terms. ECCO_kf049f series - oceanic excitation function (OAM) [Gross et al., 2003] – the modification of the MIT ocean model forced by atmospheric surface wind stress, heat flux, and freshwater flux data based on the NCEP-NCAR reanalyses, with 1 day sampling, January 1993 - March 2006. The OAM series, mass and motion terms, are based on the distribution of bottom pressure and currents, respectively.

Hydrological excitation function (HAM) are computed using the Chen and Wilson [2005] formulation from the three hydrological models: CPC, GLDAS, and LaD. Two total series are analysed: PAO series is the sum of the atmospheric (PIB) and oceanic pressure terms of polar motion excitation functions, PAOH series is the sum of the atmospheric (PIB) and oceanic pressure terms of excitation functions of polar motion and the average of the CPC and GLDAS and LaD hydrological excitation functions.

To ensure consistent availability at the same set of time steps, all series were interpolated by applying a Gaussian smoother [Feissel and Lewandowski, 1984] with output step 30 days, FWHM = 30 days and least squares (LSQ) fit of the model comprising the 1st order polynomial and sum of complex sinusoids with periods $1, 1/2$ and $1/3$ years. Each of the three GRACE-based polar motion excitation functions

(RL04) is compared with the mass term of geodetic excitation function of polar motion (G-WC) in Fig. 1.

The mass term of the geodetic excitation function G-WC is compared with the mean GRACE-RL04 and the total PAOH excitation functions of polar motion, showing some agreement of the annual oscillation in χ_1, especially for GRACE RL04, and good agreement in χ_2 (Fig. 2). The differences of these curves are of the order of 10 mas. Next the annual oscillations were isolated by filtering from the mass term of the geodetic excitation functions G-WC, GRACE(RL04) and geophysical excitation functions (PAO, PAOH). Residuals obtained after removing seasonal oscillations (annual, semiannual, terannual) from these series reach maxima of about 20 mas (Fig. 3)

2. CONCLUSIONS

Differences between mass term of the geodetic excitation function G - WC and the three GRACE polar motion excitation functions (JPL - RL04, GFZ - RL04, CSR - RL04) as well as their mean in the years 2004 - 2005.5 are still on order of 20 mas (Fig. 1).

There are distinct annual oscillations in variations of χ_2 of all considered series (Figs. 1,2). Differences between mass term of geodetic excitation function (G - WC) and the total geophysical excitation functions PAOH and the mean GRACE RL04 are on order of a few mas (Fig. 2).

Residuals obtained after removing seasonal oscillations (annual, semiannual, terannual) from the considered series reach in maximum about 20 mas (Fig. 3).

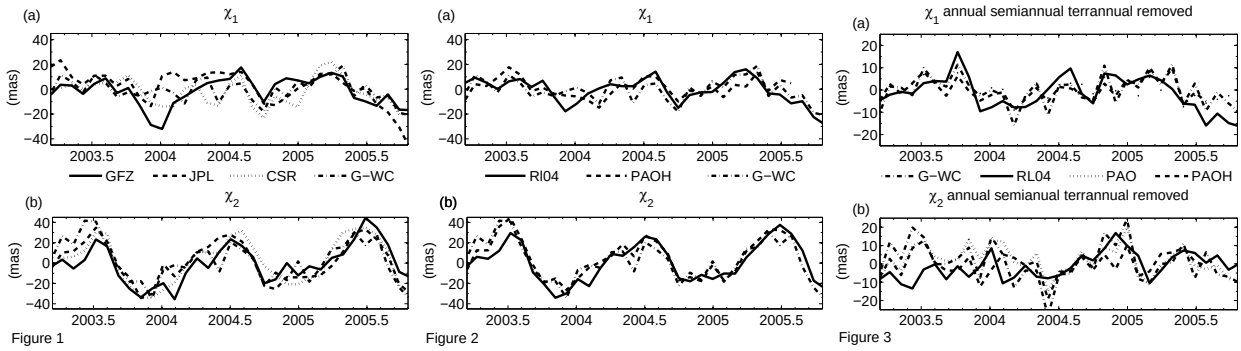

Figure 1: Comparison of mass term of the geodetic excitation function (G-WC; dash-dotted), with three GRACE-RL04 polar motion excitation functions (GFZ solid, JPL dashed, CSR dotted).

Figure 2: Comparison of mass term of the geodetic excitation function (G-WC; dash-dotted), with the mean GRACE polar motion excitation function (GRACE RL04 dotted) and the total series (PAOH dashed).

Figure 3 : Comparison of mass term of the geodetic excitation function (G-WC; dash-dotted), with the mean GRACE polar motion excitation function (GRACE RL04 dotted line) and the total series (PAOH dashed).

Acknowlegements. U.S. National Science Foundation Grant ATM-0429975 and under the Polish Ministry of Science and Higher Education through project N526 037 32/3972.

3. REFERENCES

Chen, J.L., and C.R. Wilson (2005), Hydrological excitations of polar motion, 1993 -2002, Geophys. J. Int., 160, 833-839.

Feissel, M., and W. Lewandowski (1984), A comparative analysis of vondrak and Gaussian smoothing techniques Bull.Geod., 58, 464.

Gross R. S. Fukumori, I. and Menemenlis, D., (2005) , Atmospheric and Oceanic Excitation of Decadal-Scale Earth : Orientation Variations, J. Geophys. Res., vol. 110, B09405.

Kalnay, E., et al.(1996), The NMC/NCAR 40-year reanalysis project, Bull. Am. Meteorol. Soc., 77(3), 437-471.

FORECASTING IRREGULAR VARIATIONS OF UT1-UTC AND LOD DATA CAUSED BY ENSO

T. NIEDZIELSKI[1,2], W. KOSEK[1]
[1]Space Research Centre, Polish Academy of Sciences
Bartycka 18A, 00-716 Warsaw, Poland
e-mail: niedzielski@cbk.waw.pl, kosek@cbk.waw.pl
[2]Institute of Geography and Regional Development, University of Wrocław
pl. Uniwersytecki 1, 50-137 Wrocław, Poland
e-mail: niedzielski@geom.uni.wroc.pl

ABSTRACT. The research focuses on prediction of LOD and UT1-UTC time series up to one-year in the future with the particular emphasis on the prediction improvement during El Niño or La Niña events. The polynomial-harmonic least-squares model is applied to fit the deterministic function to LOD data. The stochastic residuals computed as the difference between LOD data and the polynomial-harmonic model reveal the extreme values driven by El Niño or La Niña. These peaks are modeled by the stochastic bivariate autoregressive prediction. This approach focuses on the auto- and cross-correlations between LOD and the axial component of the atmospheric angular momentum. This technique allows one to derive more accurate predictions than purely univariate forecasts, particularly during El Niño/La Niña events.

1. INTRODUCTION

Variations of Universal Time (UT1-UTC) and its first derivative Length-of-Day (LOD) are driven by various geophysical processes and contain oscillations ranging from decades to hours. There are irregular fluctuations, which are directly associated with El Niño/Southern Oscillation (ENSO). El Niño events are always preceded by weakening of zonal winds, which causes the increase of the axial component of atmospheric angular momentum (AAM χ_3) and LOD. There exist relationships between LOD fluctuations and indices which quantitatively describe ENSO (Southern Oscillation Index, Niño indices) (e.g. Gross et al., 1996). As a result, extreme irregular variations of zonal winds preceding ENSO decrease the accuracy of LOD predictions. The multivariate stochastic approach to predict LOD/UT1-UTC is proposed by Niedzielski and Kosek (2007).

2. DATA AND METHODS

For the analysis the two time series are selected. First, we process the nontidal LOD time series denoted as $\Delta - \delta\Delta$, where Δ is the LOD time series and $\delta\Delta$ is the tidal correction (McCarthy and Petit, 2004). The time span of data is January 1, 1962 – October 22, 2006. Second, the AAM χ_3 time series is analysed. The AAM χ_3 data being the sum of wind (motion) and pressure (mass) terms modified by inverted barometer (IB) correction were smoothed and interpolated at 1-day sampling interval.

The polynomial-harmonic least-squares (LS) model is fit to $\Delta - \delta\Delta$ data. This model consists of annual, semi-annual, 9.3-year, 18.6-year harmonic oscillations and the linear trend. The similar model, however with annual, semi-annual oscillations and the mean, is applied to AAM χ_3 time series. The polynomial harmonic LS models are used to compute the residual time series $\varepsilon(\Delta - \delta\Delta)$ and $\varepsilon(\mathrm{AAM}\chi_3)$, for LOD and AAM χ_3, respectively. Furthermore, the polynomial-harmonic LS model for $\Delta - \delta\Delta$ is extrapolated in order to compute the deterministic prediction of these data.

In order to capture both causal and temporal relations between $\varepsilon(\Delta - \delta\Delta)$ and $\varepsilon(\mathrm{AAM}\chi_3)$ time series the multivariate autoregressive (MAR) technique is adopted. This method allows one to fit vector time series model to the multivariate data by estimating the memory of the process (autoregressive order p) and the autoregressive coefficient matrices. The matrices say about the structure of the relations in question. The computationally efficient method for fitting the autoregressive models is proposed by Neumaier and Schneider (2001). The prediction of $\Delta - \delta\Delta$ time series is the sum of the polynomial-harmonic LS model

extrapolation and the stochastic MAR prediction of $\varepsilon(\Delta - \delta\Delta)$ residuals. This prediction scheme is denoted as LS+MAR. The predictions of UT1-UTC are computed by integrating predictions of $\Delta - \delta\Delta$ and adding the tidal model together with leap seconds.

3. RESULTS AND DISCUSSION

The results indicate that the application of the LS+MAR technique allows one to derive the LOD/UT1-UTC predictions with the acceptable accuracy. For instance, root mean square errors (RMSEs) of UT1-UTC prediction are: 1.15 ms, 2.85 ms, 24.51 ms, and 53.96 ms, for 10-day, 20-day, 180-day, and 360-day in the future, respectively (Niedzielski and Kosek, 2007). For short-term predictions, these values are slightly greater than those computed by Schuh et al. (2002). However, 90-day predictions computed by the technique presented in this paper are more accurate than those obtained by Schuh et al. (2002). In contrast, the MAR solution presented herein provides one with the predictions exhibiting smaller RMSE values than those computed using the autocovariance technique by Kosek et al. (1998).

The predictions obtained by the LS+MAR method are more accurate than forecasts derived by the pure polynomial-harmonic LS model extrapolation. In particular, the improvement is well seen during the periods when El Niño or La Niña events occur. This significant improvement may be noticed in the case of El Niño 1994/1995, La Niña 1998/1999, and El Niño 2002/2003. This can be seen from maximum absolute differences between UT1-UTC data and their predictions (Tab. 1). However, the maximum reduction in the RMSE for one-year predictions may reach even 20 % in respect to the RMSE of predictions computed using the polynomial-harmonic LS model.

The results allow one to infer the multivariate approach combined with the polynomial-harmonic LS modelling to be a promising method for LOD/UT1-UTC prediction. In fact, the proposed method may lead to the improved UT1-UTC predictions during the ENSO periods, hence when there are extreme fluctuations of the Earth's rotation rate.

	10-day	90-day	180-day	360-day
LS	4.45	58.60	115.55	197.20
LS+MAR	3.70	36.56	56.27	121.59

Table 1: Maximum absolute values of differences between UT1-UTC data and their predictions for different prediction lengths.

Acknowledgements. The paper is supported by the Polish Ministry of Education and Science under the project No 4 T12E 039 29 under leadership of Wiesław Kosek. Tomasz Niedzielski is supported by the Foundation for Polish Science within the Start Programme (stipends for young researchers). Tomasz Niedzielski has been awarded a conference grant within 'Descartes-nutation project'. The first author is also supported by European Union within the Marie-Curie Actions. We are indebted to Maciej Kalarus who provided us with his tide model program for UT1 and LOD time-series. The analyses are performed in R 2.0.1.

4. REFERENCES

Gross, R.S., Marcus, S.L., Eubanks, T.M., Dickey, J.O., Keppenne, L., 1996, Detection of an ENSO signal in seasonal length-of-day variations, Geophysical Research letters 23, pp. 3373–3376.

Kosek, W., McCarthy, D.D., Luzum, B.J., 1998, Possible improvement of Earth orientation forecast using autocovariance prediction procedures, Journal of Geodesy 72, pp. 189–199.

McCarthy, D.D., Petit, G. (eds.), 2004. IERS Conventions, IERS Technical Note 32.

Neumaier, A., Schneider, T., 2001, Estimation of parameters and eigenmodes of multivariate autoregressive models, ACM Transactions on Mathematical Software 27, pp. 27–57.

Niedzielski, T., Kosek, W., 2007, Prediction of UT1-UTC, LOD and AAM χ_3 by combination of the least-squares and multivariate stochastic methods, Journal of Geodesy, doi: 10.1007/s00190-007-0158-9.

Schuh, H., Ulrich, M., Egger, D., Mueller, J., Schwegmann, W., 2002, Prediction of Earth orientation parameters by artificial neural networks, Journal of Geodesy 76, pp. 247–258.

THE INFLUENCE OF VARIABLE AMPLITUDES AND PHASES OF THE MOST ENERGETIC OSCILLATIONS IN THE EOP ON THEIR PREDICTION ERRORS

A. RZESZÓTKO[1], W. KOSEK[1], W. POPIŃSKI[2]
[1] Space Research Centre, Polish Academy of Sciences, Warsaw, Poland
[2] Central Statistical Office, Warsaw, Poland
e-mail: alicja@cbk.waw.pl

ABSTRACT. The Discrete Wavelet Transform (DWT) based on the Morlet wavelet was applied to determine the variable amplitudes and phases of the dominant oscillations in the Earth Orientation Parameters (EOP) data. Next, the model EOP data were constructed using constant amplitudes and phases computed by the LS method as well as variable amplitudes and phases computed by the DWT. The model data and the original EOP data were then predicted using forward and backward prediction by the combination of the least–squares model extrapolation (LS) and the autoregressive prediction (AR) denoted as LS+AR. Comparison of the forward and backward predictions of the EOP data and the model data, computed at different starting prediction epochs has enabled examination of irregular variations in the EOP data as well as influence of variable amplitudes and phases of the most energetic oscillations in the EOP data on their prediction errors.

1. DATA

In the analysis x, y pole coordinates and length of day Δ data of IERS EOPC04 in 1962.0-2007.6 were used. The Δ–$\delta\Delta$ data were obtained from Δ data by subtracting the tidal model $\delta\Delta$.

2. COMPUTATION TECHNIQUES APPLIED

Coefficients of the DWT can be obtained by the formula:

$$W(T_j, t_k) = \frac{1}{C_{jk}} \sum_{i=1}^{N} x_i \overline{\psi}\left(\frac{t_i - t_k}{T_j}\right), \tag{1}$$

where $C_{jk} = \sum_{i=1}^{N} |\psi\left(\frac{t_i - t_k}{T_j}\right)|$ and $\psi(t) = e^{-\frac{t^2}{2\sigma^2}} e^{-2\pi i t}$ is the Morlet wavelet function. Instantaneous DWT amplitudes and phases of the oscillations with periods T_j can be determined from the DWT coefficients by the following formulae (Kosek et al. 2006):

$$A_j(t_k) = \mathrm{abs}[W(T_j, t_k)],\ \phi_j(t_k) = \arg[W(T_j, t_k)] - \frac{2\pi t_k}{T_j} \tag{2}$$

In the LS+AR method, the LS residuals of the EOP data are determined as the difference between these data and their fitted LS models (Kosek et al. 2004). Next, the AR prediction method is applied to the LS residuals of the EOP data. The final prediction of the data is the sum of the LS model extrapolation and the AR prediction of the LS residuals.

3. RESULTS

To find the contribution of variable amplitudes and phases of the most energetic oscillations in the EOP data to their LS+AR prediction errors, the models of the EOP data were constructed using constant LS amplitudes and phases and variable DWT amplitudes and phases of the most energetic oscillations. The model data consists of the Chandler (Ch), Annual (An) and semi-annual (Sa) oscillations in case of x, y data and An and Sa oscillations in case of $\Delta - \delta\Delta$ data. Next, the LS+AR predictions of different model data were computed. The UT1–UTC forecasts were computed by summing the Δ–$\delta\Delta$ predictions and adding tidal model together with leap seconds. The absolute values of the difference between the

EOP data and their LS+AR predictions are shown in Fig. 1. The mean prediction errors of the EOP data are shown in Fig. 2.

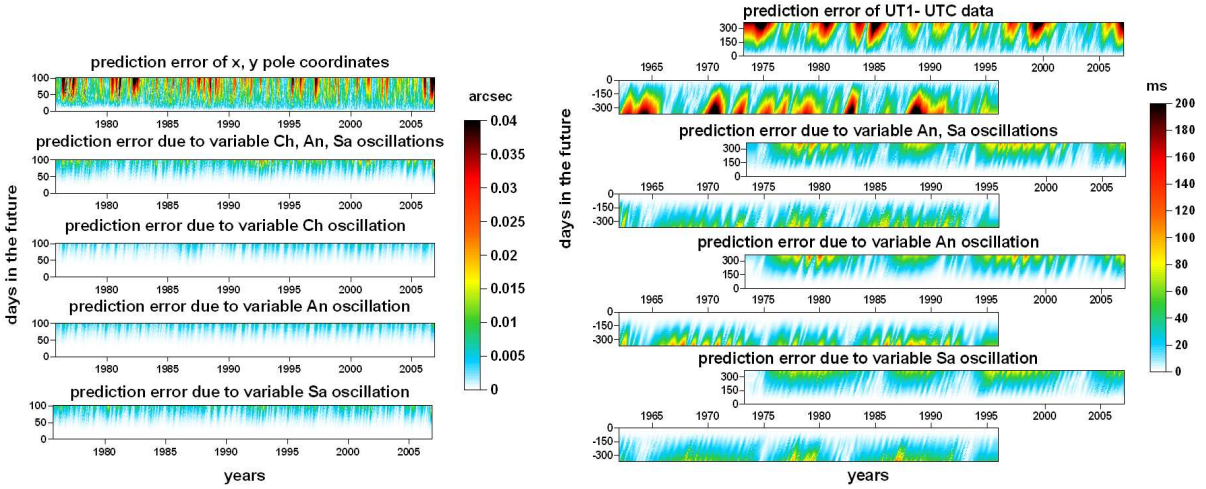

Figure 1: The LS+AR prediction error of x, y pole coordinates (left) and the LS+AR backward and forward prediction errors of UT1-UTC (right) data and of model data constructed with the use of constant LS and variable DWT amplitudes and phases.

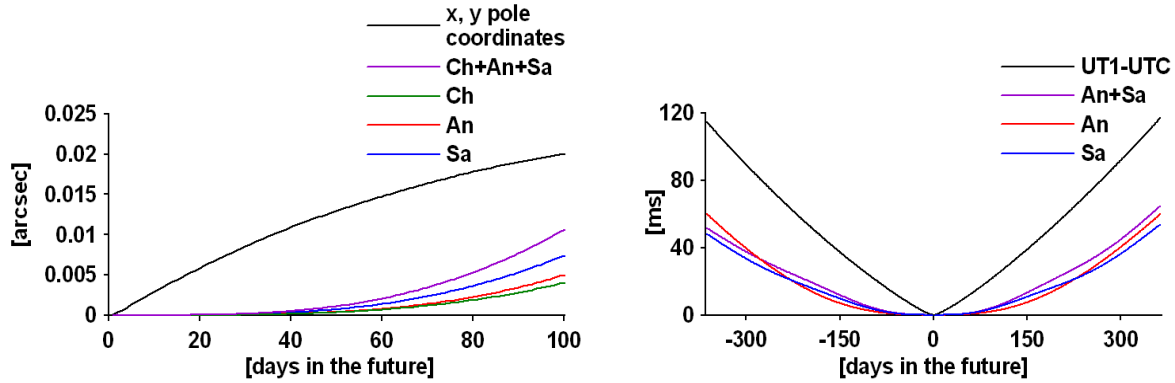

Figure 2: The LS+AR prediction error of x, y pole coordinates (left) and UT1–UTC (right) data and of the model data constructed with the use of variable amplitudes and phases computed by the DWT.

4. CONCLUSIONS

It has been shown that influence of the variable semi–annual oscillation in EOP data up to 100 days in the future is greater than influence of the annual (and Chandler) oscillations. Considering UT1–UTC data, the greatest prediction errors occur at almost the same moments of time independently of the prediction direction. The prediction errors of x, y pole coordinates and UT1–UTC data cannot be explained by the most energetic monochromatic oscillations in these data with variable amplitudes and phases.

5. REFERENCES

Kosek, W., McCarthy, D.D., Johnson, T.J., Kalarus, M., 2004, "Comparison of polar motion prediction results supplied by the IERS Sub-bureau for Rapid Service and Predictions and results of other prediction methods", Proc. Journées 2003, pp. 164-169.

Kosek, W., Rzeszótko, A., Popiński, W., 2006, "Phase variations of oscillations in the Earth Orientation Parameters detected by the wavelet technique", Proc. Journées 2005, pp. 121-124.

CORRESPONDENCE OF *EOP* AND GEOMAGNETIC FIELD

P. VARGA[1], Z. BUS[1], B. SÜLE[1], Ch. BIZOUARD[2], D. GAMBIS[2], K. KIS[3], A.A. SCHREIDER[4]
[1] Geodetic and Geophysical Research Institute, Seismological Observatory
H-1112 Meredek u. 18., Budapest, Hungary
e-mail: varga@seismology.hu
[2] International Earth Rotation Service, Observatoire de Paris, Paris, France
[3] Eötvös University, Geophysical Department, Budapest, Hungary
[4] Shirshov Institute of Oceanology, Moscow, Russia

ABSTRACT. Connection of *EOP* with centred and eccentric geomagnetic dipole fields is described (with the use of Gaussian coefficients) for the epoch 1880-2000. The main tools of statistical investigation carried out were Laplace-type robust estimation (in case of ΔLOD) and the non-linear regression analysis (for PM). On the basis of computations carried out it can be concluded that the statistical comparison of temporal variation of earth magnetic and *EOP* data shows significant correlation.

1. DECADAL VARIATIONS OF LOD AND GEOMAGNETIC DIPOLE FIELD

Dependence of LOD from processes of the liquid outer core is especially strong in case of periods between 20 and 60 years. This phenomenon determined first of all by core mantle interactions. These interactions can be of different kind. Bloxham (2000) and Gubbins et al. (2003) describe the sensitivity of the axial geomagnetic dipole to thermal interactions at the CMB. Mound and Buffett (2006) detected gravitational oscillations in the LOD. Yukutake (1972) and Yokohama and Yukutake (1992) explain the connection between sixty-year variation in length of day and magnetic field with the electromagnetic core-mantle coupling. Extension of the range of the link between variations of geomagnetic field and LOD in direction of shorter than 20 year periods is problematic because the worldwide geomagnetic data are available recently with a time step of 5 years. More principal difficulty is related to the strong influence of the atmospheric angular momentum on LOD in case of annual/sub-annual periods (Abarca del Rio, 2003), what hides the possibly existing core-mantle interactions. In case of longer, secular, periods one meet the problem of sparse LOD data and indefinability of dating both the magnetic (archeomagnetic) and LOD data. For the aims of present investigation in case of decadal variations the geomagnetic data were obtained from IAGA global spherical expansion database for the time-interval 1880-2000 with a five-year step. Length of day variation data for the same time-interval (and digitalization) are given in form of mean annual values derived from long-term data set of IERS.

2. STATISTICAL BACKGROUND

For the study of correlation of geomagnetic and *EOP* data the robust estimation technique were used together with well-known non-linear regression analysis. The robust estimation is a generalization of least-squares method which reduces the influence of outliers and allows optimal solution in case of different error distribution. According to authors numerous mathematical tests for correlation of LOD and geomagnetic dipole moment the best fit is in case of use of Laplace robust modelling (Laplace type modelling means: the central part of the distribution curve is normal while the wings are linear). In case of correlation of PM and geomagnetic dipole moment the non-linear regression analysis of degree n=6 was in use. In Table 1 the correlation coefficients both for three components of central geomagnetic dipole and for the four components of eccentric dipole field are collected together. The connection of X and Y components of PM are shown and described by Figs. 1a and 1b.

3. CONCLUSIONS

Statistical dependence was detected between the geomagnetic dipole moment M_0 and ΔLOD (Table 1). The orientation and eccentricity of the geomagnetic dipole show also somewhat weaker correlation with variations of axial rotation speed. In case of polar motion the X and Y components of PM have

	M_0	θ	ϕ	δ
Central dipole	0.928	0.210	0.361	0.000
Eccentric dipole	0.808	0.612	0.740	0.703

Table 1: Correlation of LOD and components of geomagnetic field. M_0 is the dipole moment, the angle between the geomagnetic dipole and geographic axes is θ, the azimuthal angle is ϕ, while the distance of the dipole from the Earth centre is given by δ.

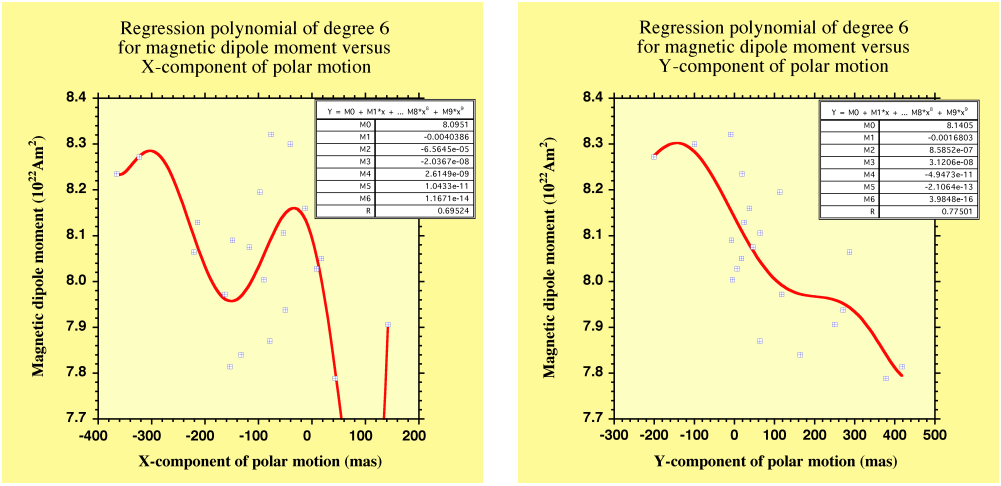

Figure 1: Relationship of X, Y components of PM and M_0 (the reliability factors are 0.69 and 0.77)

also statistical connection with M_0.

The physical meaning of above described results is: the interrelation between the variation of ΔLOD and the geomagnetic field in decadal time-scale can be explained with toroidal circulation in the liquid outer core which leads to the temporal variations of the core angular momentum through frictional processes at the core mantle boundary. The dependence of ΔLOD on temporal variations of orientation of geomagnetic dipole and also correlation of PM and M_0 suggest that beside the toroidal flow in the liquid outer core there are also spheroidal flows present what leads to the radial mass redistribution within the outer core.

Acknowledgements. Research activity described in this presentation was supported in frame of French-Hungarian bilateral project of Centre National de la Recherche Scientifique and Hungarian Academy of Sciences. Hungarian participants enjoyed help of Hungarian Science Foundation (OTKA K60394).

4. REFERENCES

Abarca del Rio, R., Gambis, D., Salstein, D., Nelson, D., Dai, A., 2003, "Solar activity and Earth rotation variability", J. of Geodyn., 36, pp. 423-443.

Bloxham, J., 2000, "Sensitivity of the axial dipole to thermal core-mantle interactions", Nature, 405, pp. 63-65.

Gubbins, D., Alfé, D., Masters, G., Price, G.D., Gillan, M.J., 2003, "Can the Earth dynamo run on heat alone?", Geophys. J. Int. , 155, pp. 609-622.

Mound, J.E., Buffett, B.A., 2006, "Detection of gravitational oscillation in the length-of-day", Earth and Planet. Sci. Lett., 243, pp. 383-389.

Varga, P., Bus, Z., Süle, B., Schreider, A.A., Bizouard, Ch., Gambis, D., Denis, C., 2007. "Variation in the rotation rate of the Earth and the geomagnetic field", Acta Geod. Geoph. Hung., 42(4), pp. 433-448.

Yokohama, Y., Yukutake, T., 1992, "The sixty-year variation in the rate of rotation of the Earth and the geomagnetic field", J. Geomag. Geoelectr., 44, pp. 555-560.

Yukutake, T., 1972, "The effect of change in the geomagnetic dipole moment on the rate of the Earth's rotation", J. Geomag. Geoelectr., 24, pp. 19-26.

VERIFICATIONS FOR MULTIPLE SOLUTIONS OF EARTH ROTATION

W.-J. WANG[1], W.-B. SHEN[2], H.-W. ZHANG[1]
[1] School of Surveying, Henan Polytechnic University, Jiaozuo, China
[2] School of Geodesy and Geomatics, Wuhan University, Wuhan, China
[1] email: wwj@asch.whigg.ac.cn, [2] email: wbshen@sgg.whu.edu.cn

ABSTRACT. In this study, we provide several approaches to the solution of the rotation of an arbitrary rigid body with triaxial principal moments of inertia. We found multiple solutions for the triaxial Earth rotation with two stable periodic trajectories and an unstable hyperbolic one. Data series filtering approach also shows explicit period of about 14 year in polar motion as well as in LOD.

1. EARTH'S SHAPE

The Earth has an anisotropic shape according to gravity or the geoid.

Table 1: Comparison of the polar and equatorial ellipticity for several planets

	Earth	Mars	Moon	Hyperion	Eros433
H_0	3.28475×10^{-3}	5.38×10^{-3}	5.2×10^{-4}	0.799	0.278?
H_1	2.1946×10^{-5}	5×10^{-4} or 6.896×10^{-4}	5.5669×10^{-5}	0.158	0.158?
e	0.00382	0.06463	0.214	0.978	0.723

In this paper, we discuss the rotation of triaxial Earth starting from the triaxial rigid body; a discussion of pear-shaped Earth rotation can be found in Wang Wen-Jun [2004].

2. EXACT SOLUTION

Euler dynamical equations for rigid body rotation can be written equivalently as algebraic equations:

$$\begin{array}{lll} A\dot{\omega}_1 + (C-B)\omega_2\omega_3 = 0 & \dot{\omega}_1 + \sigma_1\omega_2\omega_3 = 0 & \sigma_2\omega_1^2 + \sigma_1\omega_2^2 = C_{12} \\ B\dot{\omega}_1 + (A-C)\omega_3\omega_1 = 0 \longrightarrow & \dot{\omega}_2 - \sigma_2\omega_3\omega_1 = 0 \longrightarrow & \sigma_3\omega_2^2 + \sigma_2\omega_3^2 = C_{23} \\ C\dot{\omega}_1 + (B-A)\omega_1\omega_2 = 0 & \dot{\omega}_3 + \sigma_3\omega_1\omega_2 = 0 & \sigma_1\omega_3^2 - \sigma_3\omega_1^2 = C_{31} \end{array}$$

where C_{ij} are constants to be determined. The latter one gives two ellipses and a hyperbola. The solution of Euler equations is:

$$\omega_1 = \mu\sqrt{\frac{D(C-D)}{A(C-A)}}\mathrm{cn}u \qquad \omega_2 = -\mu\sqrt{\frac{D(C-D)}{B(C-B)}}\mathrm{sn}u \qquad \omega_3 = \mu\sqrt{\frac{D(D-B)}{C(C-B)}}\mathrm{dn}u$$

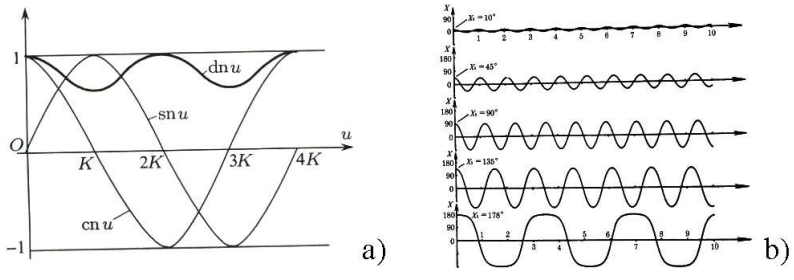

Figure 1: a) Graphs of elliptic functions b) cn$u$ compared with trigonometric $\cos u$

3. MOMENTUM CONSERVATION

Conservative momentum approach to the components of rotation angular velocity ω_i, $i = 1, 2, 3$, results in the conservation for the angular momentum H and for the potential energy $T \propto m^2$.

$H = \frac{1}{2}M(\omega_1^2/A + \omega_2^2/B + \omega_3^2/C), \quad \omega_1^2 + \omega_2^2 + \omega_3^2 = m^2 \quad (1)$

Let $x_i = \omega_i/m$, $(i = 1, 2, 3)$ and $\lambda_1 = 1/A$, $\lambda_3 = 1/C$, $A < B < C$, $1/A > 1/B > 1/C$, here $1/C$ is the least. The first equation of (1) is changed to a quadratic polynomial of variables x_i in which the respective coefficients λ_i satisfy (+, +, +).

$H = \frac{1}{2}m^2M(\lambda_1 x_1^2 + \lambda_2 x_2^2 + \lambda_3 x_3^2) = \frac{1}{2}m^2M[(\lambda_1 - \lambda_3)x_1^2 + (\lambda_2 - \lambda_3)x_2^2 + \lambda_3] \quad (2)$

$H = \frac{1}{2}m^2M[\lambda_1 + (\lambda_2 - \lambda_1)x_2^2 + (\lambda_3 - \lambda_1)x_3^2] \quad (3)$

Theory of quadratic polynomial tells us that if and only if the determinant of the last formula of (2) is positively definite, then it has stable elliptic solution, otherwise it has instable saddle point solution. For the case of $A \leq B$ and $A \leq C$, the quadratic polynomial (3) satisfies the positive definite condition (+, -, -). There must be another stable elliptic solution for the triaxial Earth rotation.

4. ALGEBRAIC CURVE EQUATIONS

Let σ_1, σ_2 and σ_3 be small quantities, defined by following equations

$\alpha = \sigma_1 = (C - B)/A \quad \beta = \sigma_2 = (C - A)/B \quad \gamma = \sigma_3 = (B - A)/C \quad (4)$

5. EIGEN VALUE APPROACH

(4) allows us writing the Euler equations as vector form:

$$\begin{pmatrix} \dot{\omega_1} \\ \dot{\omega_2} \\ \dot{\omega_3} \end{pmatrix} = \begin{pmatrix} -\sigma_1\omega_2\omega_3 \\ \sigma_2\omega_3\omega_1 \\ -\sigma_3\omega_1\omega_2 \end{pmatrix} \longrightarrow \dot{\omega} = F(\omega)$$

with equilibrium for the nonlinear vector equation of Taylor expansion.

$$\dot{\omega} = F(\omega_0) + \dot{F}(\omega_0)(\omega - \omega_0) + O(\omega^2)$$

The derivative operator of the vector is obtained in Jacobian matrix.

$$\dot{F}(\omega) = \begin{pmatrix} 0 & -\sigma_1\omega_3 & -\sigma_1\omega_2 \\ \sigma_2\omega_3 & 0 & \sigma_2\omega_1 \\ -\sigma_3\omega_2 & -\sigma_3\omega_1 & 0 \end{pmatrix}$$

$$\dot{F}(\omega) = \begin{pmatrix} 0 & 0 & 0 \\ 0 & 0 & \sigma_2 \\ 0 & -\sigma_3 & 0 \end{pmatrix} \omega_1 + \begin{pmatrix} 0 & 0 & -\sigma_1 \\ 0 & 0 & 0 \\ -\sigma_3 & 0 & 0 \end{pmatrix} \omega_2 + \begin{pmatrix} 0 & -\sigma_1 & 0 \\ \sigma_2 & 0 & 0 \\ 0 & 0 & 0 \end{pmatrix} \omega_3$$

This provides decomposed theorem for triaxial rotation with each matrix describing the torque on a principal axis. By solving the eigen values of each matrix the behavior of the solution on each principal axis may be obtained. There are two stable solutions with elliptic orbits with the first and the third matrices for the minimum and the maximum axes of inertia as well as an unstable hyperbolic trajectory with the medium matrix appearing as a one-way inverted pendulum deemed as the secular wander in Goldreich & Toomre (JGR 1969: 10, 2555-2567).

6. CONCLUSION

According to the authors of this study, Earth rotation theory would need a new convention in which the two free wobbles should be added with similar consequences as Chandler wobble. The new convention may not be contradicted in the case of that of biaxial rotation.

POSTFACE

JOURNÉES 2008 SYSTÈMES DE RÉFÉRENCE SPATIO-TEMPORELS
"Astrometry, Geodynamics and Astronomical Reference Systems"

Dresden (Germany), 22-24 September 2008

Scientific Organizing Committee
M. Soffel, Germany (Chair); A. Brzeziński, Poland; N. Capitaine, France (co-Chair); P. Defraigne, Belgium; T. Fukushima, Japan; S. Klioner, Germany; D.D. McCarthy, USA; J. Vondrák, Czech R.; Ya. Yatskiv, Ukraine

Local Organizing Committee
A. Theuser (Chair), L. Graefe, R. Langhans, S. Zschocke

Scientific objectives

The Journées 2008 "Systèmes de référence spatio-temporels", with the sub-title "Astrometry, Geodynamics and Astronomical Reference Systems", will be organized at the Lohrmann Observatory, Technical University in Dresden, Germany, from to 22 to 24 September 2008.

These Journées will be the nineteenth conference in this series whose main purpose is to provide a forum for researchers in the fields of Earth rotation, reference frames, astrometry and time. Nine years after the Journées 1999, these Journées will be held again in Dresden. The conference will be organized in cooperation between the TU Dresden and the Department "Systèmes de Référence Temps Espace" (SYRTE) of Paris Observatory.

The Journées 2008 will be focused on the issues related to the recent developments in astronomical reference systems, interrelation of modern astrometry and Earth orientation, numerical standards and their relativistic aspects, and modelling and observations of global geodynamical processes.

There will be presentations and discussions related to the Division 1 Commission 52 "Relativity in Fundamental astronomy" and IAU Working Groups, such as "Numerical standards in Fundamental astronomy" and "The second realization of the ICRF".

Scientific programme

The preliminary list of sessions is the following:

Session I : Modern astrometry and Earth orientation

Session II : Relativity and numerical standards in fundamental astronomy

Session III : Global geodynamic modelling

Session IV : Observations of global geodynamics

Session V : Developments in astronomical reference frames

Contact : Journées 2008
Dresden Technical University
Institut fuer Planetare Geodaesie
Lohrmann-Observatorium
01062 Dresden, Germany

phone: +49-351-463-34097; fax: +49-351-463-37019
e-mail: journees2008@astro.geo.tu-dresden.de
or: Prof.Michael Soffel: Michael.Soffel@mailbox.tu-dresden.de

or see : http://astro.geo.tu-dresden.de/journees2008/